Eva Morava
Matthias Baumgartner
Marc Patterson
Shamima Rahman
Johannes Zschocke
Verena Peters *Editors*

JIMD Reports

Volume 30

SSIEM

Springer

JIMD Reports
Volume 30

Eva Morava
Editor-in-Chief

Matthias Baumgartner · Marc Patterson · Shamima Rahman · Johannes Zschocke
Editors

Verena Peters
Managing Editor

JIMD Reports
Volume 30

Springer

SSIEM

ISSN 2192-8304 ISSN 2192-8312 (electronic)
JIMD Reports
ISBN 978-3-662-53680-3 ISBN 978-3-662-53681-0 (eBook)
DOI 10.1007/978-3-662-53681-0

This Springer imprint is published by Springer Nature
The registered company is Springer-Verlag GmbH Germany
The registered company address is: Heidelberger Platz 3, 14197 Berlin, Germany

Contents

JIMD Reports
DOI 10.1007/8904_2016_527

CASE REPORT

Multidisciplinary Team Approach Is Key for Managing Pregnancy and Delivery in Patient with Rare, Complex MPS I

J. Troko • Y. Poonawala • T. Geberhiwot • B. Martin

Received: 30 June 2015 / Revised: 30 November 2015 / Accepted: 04 December 2015 / Published online: 27 February 2016

Abstract A 23-year-old primiparous lady (Ms S) was referred to preconception clinic with known Hurler–Scheie syndrome (mucopolysaccharidosis 1). Ms S had been under the care of the adult inherited metabolic disorder physicians prior to becoming pregnant. She and her partner received prenatal counselling and following spontaneous conception was closely managed by a multidisciplinary team involving foetomaternal obstetricians, anaesthetists, cardiologists, geneticists and endocrinologists in two tertiary referral hospitals throughout her pregnancy. She went on to deliver a live male child at 37/40 by elective caesarean section. As far as we are aware, this is the first case report of a term pregnancy in a woman with moderate to severe mucopolysaccharidosis 1 (MPS 1).

Introduction

A literature search was performed to identify any publications on pregnancy management in patients with MPS 1. The databases MEDLINE, CINAHL, Cochrane Library, DUETs, NHS Evidence and DynaMed were reviewed with the MeSH terms 'treatment AND/OR management', 'pregnant females' and 'mucopolysaccharidosis'. One case report described a 32-year-old lady with attenuated MPS 1 who had been on laronidase replacement therapy for 3 years prior to conception of her second child. She went on to have a live male child who was breastfed for 3 months. No laronidase was detected in her breast milk, and the infant did not develop any adverse drug-related events by 2.5 years of age (Castorina et al. 2015). There were no further papers documenting management of pregnant patients with moderate to severe MPS 1. Eleven patients with MPS 1 on the specialist registry are also known to have become pregnant to date, but their outcomes and management have not been disclosed.

Hurler–Scheie syndrome (MPS 1) is a rare autosomal recessive condition affecting 1.07/100,000 births in the UK (Mooreetal.2008). It occurs in individuals with a lysosomal enzyme alpha-L-iduronidase deficiency secondary to a defective iduronidase alpha (IDUA) gene (4p16.3) on chromosome 4. Alpha-L-iduronidase catalyses the metabolism of glycosaminoglycans (GAGs), and its deficiency leads to GAG accumulation in the cells and connective tissues of sufferers. With time it causes irreversible damage to tissues throughout the body and, depending upon the degree of severity, impedes on the functioning of the bones, corneas, skin, cartilage, tendons and vital organs. MPS 1 clinically manifests as a continuous spectrum of symptoms but can be divided into three broad types with overlapping features as follows:

Communicated by: John H Walter, MD FRCPCH

Competing interests: None declared

J. Troko (✉) · Y. Poonawala · B. Martin
Birmingham Women's Hospital, Mindelsohn Way, Birmingham B15 2TG, UK
e-mail: jtroko@googlemail.com

T. Geberhiwot
University of Birmingham and Queen Elizabeth Medical Centre, Mindelsohn Way, Birmingham B15 2GW, UK

Type	Severity	Age of onset	Presentation
Scheie syndrome	Mild	5 years	Normal intelligence/ mild learning disability, corneal opacification, glaucoma, retinal degeneration, carpal tunnel syndrome, deformed hands/feet, short neck, valvular heart disease and obstructive and restrictive airway disease. Patients usually survive to adulthood (Campos and Monaga 2012; Saudubray et al. 2012)
Hurler–Scheie syndrome	Moderate	3 years	Moderate learning disability, hearing loss, corneal opacification, coarse facial features, short stature, small jaw, progressive joint stiffness, compressed spinal cord, valvular heart disease, umbilical hernia, recurrent respiratory tract infections, obstructive and restrictive airway disease and sleep apnoea. Patients may survive to adulthood (Campos and Monaga 2012; Saudubray et al. 2012)
Hurler syndrome	Severe	1 year	Progressive mental decline, loss of physical skills, speech impairment, hearing loss, enlarged tongue, corneal opacification and retinopathy, carpal tunnel syndrome, restricted joint movement, inguinal or umbilical hernia, short stature, distinct facies (flat face, low nasal bridge, prominent forehead), hepato-/ spleno-/cardiomegaly, recurrent ear and respiratory tract infections and obstructive airway disease. Mean survival time 9 years (Moore et al. 2008)

Enzyme replacement therapy slows the progression of MPS 1, but there is currently no cure. Those with milder forms such as Scheie syndrome may consider starting families should they reach adulthood. Yet the physiological changes associated with pregnancy render the patients high risk obstetrically. The collaborative input of multiple medical specialties is important therefore to counsel and monitor progression of these patients throughout pregnancy.

Background

Ms S was diagnosed in childhood with moderate to severe Hurler–Scheie syndrome. She had a short stature with a BMI of 27, coarse facial features, a restricted airway and contracted pelvis. She had asthma, mild to moderate mitral and aortic regurgitation and stenosis and occasionally suffered from migraines. As a child Ms S required the insertion of a right grommet and left ventilation tube to manage recurrent episodes of non-suppurative otitis media and sensorineural hearing loss. She also had surgery for decompression of her wrist for carpal tunnel syndrome, an umbilical hernia repair, tonsillectomy and adenoidectomy and a cervical spine fusion using a morphogenic bone graft. She had received a weekly enzyme infusion of Aldurazyme 5,500 international units through a portacath to slow the progression of her condition for over 10 years. Ms S was blood group A positive and had no known drug allergies.

Prior to becoming pregnant, Ms S had been under the care of the adult inherited metabolic disorder physicians. Together with her husband (who was diagnosed with retinoblastoma as a child), she received robust prenatal counselling following multidisciplinary team input from foetomaternal obstetricians, anaesthetists, cardiologists, geneticists and endocrinologists regarding the following:

1. *Grown-up congenital heart disease in pregnancy*

   Cardiac output increases 30–50% (increase in blood volume and heart rate principally peaking in the second trimester) in pregnancy, and patients with congenital heart disease (CHD) are at 5% risk of mortality, 3–5% risk of CHD (albeit in Ms S's case, her cardiac disease was part of the constellation of symptoms associated with her autosomal recessive condition) and growth restriction in the offspring. Ms S had a satisfactory echocardiogram preconceptually therefore upon review with the cardiologist and obstetrician; plans were made for a repeat echocardiogram and foetal echocardiogram at 24/40, serial foetal growth scans from 28/40 and regular reviews to check for signs of cardiac decompensation (Steer et al. 2006; Guyton and Hall 2005).

2. *Uncertainty of teratogenicity of enzyme replacement therapy*

   Ms S was counselled regarding the unknown effects of laronidase on the foetus, although there are amassing reports of no overt harm to foetuses (Castorina et al. 2015; Wendt et al. 2005; Giannubilo et al. 2015). What's more, given the risk of her condition worsening without treatment, the decision was made to continue on medication and have regular foetal surveillance.
3. *Contracted pelvis and hip joints*

   The rise of oestrogen and relaxin cause remodelling of connective tissues resulting in increased laxity of joints (particularly sacroiliac and pubic symphysis) (Ostgaard et al. 1991). However, as Ms S had a contracted pelvis, she was at high risk of an obstructed labour. Consequently following discussion with the multidisciplinary team, it was agreed Ms S should have an elective caesarean section (CS) at 37/40 after receiving steroids.
4. *Anaesthetic difficulties due to her previous cervical vertebra fusion and difficult airway*

   Ms S previously had a grade 4 laryngoscopy when requiring general anaesthesia. Her risk of a difficult intubation would be further compounded by pregnancy-induced weight gain, breast enlargement, progesterone-associated respiratory tract mucosal oedema and capillary engorgement (Jouppila et al. 1980). Hence, a decision was made for a combined spinal and epidural (CSE) anaesthetic for rapid onset and sustained pain relief if surgery was prolonged. In the event of failure or complications of regional anaesthesia, an awake fibreoptic intubation (AFOI) was planned to secure her airway for general anaesthesia for the CS.
5. *Increased risk of respiratory impairment*

   Forced vital capacity (FVC) and peak expiratory flow rate (PEFR) normally increase by the second trimester (Grindheim et al. 2012). However, as in a study majority of gravid patients with restrictive lung disease had a stable FVC (and Ms S did not require NIV preconceptually) (Lapinsky et al. 2014); Ms S was managed expectantly for her respiratory symptoms.
6. *Her husband had retinoblastoma*

   Upon advice from the paediatricians and geneticists, a plan for cord blood samples at delivery and having an early eye examination by an ophthalmologist was decided to check for the autosomal dominant condition retinoblastoma in the neonate (Ms S's condition is a rare autosomal recessive condition therefore highly unlikely to be passed on).

Case Presentation

At 7 + 5/40, Ms S, a 23-year-old primiparous lady with Hurler–Scheie syndrome, presented to a tertiary women's hospital following spontaneous conception. She was subsequently seen by a foetomaternal specialist every 4 weeks from 12 + 5/40 until delivery. She had a baseline sinus tachycardia of 130 beats per minute, a mild soft pansystolic murmur, and signs of restrictive lung disease. Bedside tests of her airway revealed poor mouth opening but with a natural inter-incisor gap, large tongue and inability to protrude her lower jaw due to a receding chin. There was no neck extension as a result of previous cervical spine fusion. She complained of worsening snoring as the pregnancy progressed. At 26 + 5/40 she had symptoms suggestive of symphysis pubic dysfunction for which she took simple analgesia but declined physiotherapy. In the last week of her pregnancy, she developed a lower respiratory tract infection which was treated with oral amoxicillin.

Investigations

Ms S had normal routine booking bloods. Her cardiac output and size remained stable upon repeat echocardiogram at 24/40, so no further specialist cardiologist input was required antenatally.

Nasoendoscopy confirmed a good sized laryngeal inlet and flattened epiglottis. Spinal MRI revealed that she had effacement of the anterior and posterior CSF column in the cervical spine region but normal anatomy of the thoracolumbar spine.

The foetal Down's risk was 1:44,000 (through quadruple testing) and had a normal echocardiogram and mid-trimester anomaly scan. Its growth from 26 + 5/40 was above the 50th centile.

Treatment

At 37/40, Ms S was admitted for an elective CS. Two units of blood were crossmatched and intraoperative cell salvage

set up as a prophylactic measure given the uncertain effect of uterotonics in MPS 1 patients. An intensive care (ITU) bed at a neighbouring tertiary hospital was booked to provide post-operative ventilatory support in the event of general anaesthesia. She was initially anaesthetised via CSE using 300 micrograms of diamorphine and 2.2 ml of 0.5% hyperbaric bupivacaine. The initial spinal attempt produced a sensory block level to L1. This was inadequate for surgery so the epidural component was topped up over 10 min to try and achieve the necessary block height to T4. Thirty-five minutes after commencing the epidural top-ups, the block height remained at T10. A second spinal anaesthetic was performed using 1 ml of 0.5% hyperbaric bupivacaine and achieved a block to T4. A consultant maxillofacial surgeon was present during the surgery in case the AFOI failed, and an emergency tracheostomy was necessary. The CS proceeded, and a live male child was delivered with no intraoperative complications. Biosynthetic sutures were used to close the uterus in two layers for adequate haemostasis, and cord blood samples were taken at delivery.

Outcome

Ms S was managed on a high dependency unit for 2 days following CS and was then transferred to a postnatal ward. She had a successful trial without urinary catheter 48 h post-surgery and was discharged on prophylactic oral antibiotics for 7 days and low molecular weight heparin for 6 weeks.

Learning Points

- Multidisciplinary team management of patients with MPS 1 is crucial for successful pregnancies and is best managed by a team with expertise in their fields. The successful outcome of pregnancy in this complicated patient was facilitated by the medical, obstetric and anaesthetic teams with input from the patient.
- If patients with MPS 1 require surgery, input from the ear, nose and throat surgeons, anaesthetists and ITU physicians is advised during the planning stage as induction of anaesthesia, intubation and post-operative respiratory recovery can be problematic.
- Pre-pregnancy counselling for women with MPS 1 should include detailed discussion of the potential complications of each stage of pregnancy and delivery, taking into account the stage of disease and the availability and technical abilities of the medical teams involved.

Acknowledgements Many thanks to Tony Whitehouse and Katherine Pearce for their help with this paper.

Compliance with Ethics Guidelines

Conflict of Interest

Joy Troko, Yasmin Poonawala, and Bill Martin declare that they have no conflict of interest. Tarekegn Geberhiwot has served on the Genzyme advisory board and has received service development and travel grants. All procedures followed were in accordance with the ethical standards of the responsible committee on human experimentation (institutional and national) and with the Helsinki Declaration of 1975, as revised in 2000 (5).

Informed Consent

The patient gave consent for her information to be published.

Contribution of the Authors

Mr Bill Martin was the lead obstetrician involved in the patient's antenatal care and delivery. Dr Tarekegn Geberhiwot was the primary physician for the patient prenatally and was involved in the decision making throughout the patient's pregnancy. Dr Yasmin Poonawala was the consultant anaesthetist who anaesthetised the patient for surgery and was involved in the planning of delivery for the patient. Dr Joy Troko is a trainee obstetrician who assisted in the delivery of the patient and submitted the case for publication. All authors listed were involved in writing the report.

References

Campos D, Monaga M (2012) Mucopolysaccharidosis type I: current knowledge on its pathophysiological mechanisms. Metab Brain Dis 27(2):121–129. doi:10.1007/s11011-012-9302-1

Castorina M, Antuzzi D, Richards SM et al (2015) Successful pregnancy and breastfeeding in a woman with mucopolysaccharidosis type I while receiving laronidase enzyme replacement. Therapy. Clin Exp Obstet Gynecol 42(1):108–113

Giannubilo SR, Pasculli A, Tidu E, Ciavattini A (2015) Replacement therapy for Gaucher disease during pregnancy: a case report. J Reprod Infertil 16(1):53–57

Grindheim G, Toska K, Estensen M-E, Rosseland LA (2012) Changes in pulmonary function during pregnancy: a longitudinal cohort study. BJOG 119(1):94–101

Guyton AC, Hall JE (2005) Textbook of medical physiology, 11th edn. Saunders, Philadelphia, 103g. ISBN 81-8147-920-3

Jouppila R, Jouppila P, Hollmen A (1980) Laryngeal oedema as an obstetric anaesthesia complication: case reports. Acta Anaesthesiol Scand 24:97–98

Lapinsky SE et al (2014) Restrictive lung disease in pregnancy. Chest 145(2):394–398. doi:10.1378/chest.13-0587

Moore D, Connock MJ, Wraith E et al (2008) The prevalence of and survival in Mucopolysaccharidosis I: Hurler, Hurler-Scheie and Scheie syndromes in the UK. Orphanet J Rare Dis 3:24 (ISSN: 1750–1172)

Ostgaard HC, Andersson GB, Karlsson K (1991) Prevalence of back pain in pregnancy. Spine (Phila Pa 1976) 16(5):549–552

Saudubray JM, van den Berghe G, Walter JH et al (2012) Mucopolysaccharidoses and oligosaccharidoses. In: Inborn metabolic diseases: diagnosis and treatment. http://www.nlm.nih.gov/medlineplus/ency/article/001204.htm. August 2014

Steer PJ, Gatzoulis MA, Baker P (eds) (2006) Heart disease and pregnancy. RCOG, London

Wendt S, Whybra C, Kampmann C, Teichmann E, Beck M (2005) Successful pregnancy outcome in a patient with Fabry disease receiving enzyme replacement therapy with agalsidase alfa. J Inherit Metab Dis 28(5):787–788

JIMD Reports
DOI 10.1007/8904_2016_530

RESEARCH REPORT

Clinical Evolution After Enzyme Replacement Therapy in Twins with the Severe Form of Maroteaux–Lamy Syndrome

M. Pineda • M. O'Callaghan • A. Fernandez Lopez • M.J. Coll • R. Ullot • G. Garcia-Fructuoso

Received: 05 September 2015 / Revised: 27 November 2015 / Accepted: 10 December 2015 / Published online: 27 February 2016

Abstract Mucopolysaccharidosis type VI (MPS VI) is a progressive, autosomal, recessive lysosomal disorder. This disorder, due to a deficiency in *N*-acetylgalactosamine-4-sulfatase (ASB), results in an accumulation of glycosaminoglycan (GAG), causing multiple organ failures. In this study, monochorionic biamniotic twins with the severe form of MPS VI underwent enzyme replacement therapy (ERT) with weekly infusions of recombinant human ASB (galsulfase) at 1 mg/kg. After 9 years of ERT, a comprehensive clinical examination was performed. Several types of biochemical, immunological, and genetic investigations were also conducted. Both twins showed the typical symptoms and signs of MPS VI at baseline, including short stature, progressive dysmorphic facial features, and dysostosis multiplex. Twin 2 presented stronger multisystemic involvement, with marked musculoskeletal, neurological, and odontological components. She also developed an ischemic spinal cord lesion after surgery, which is the first case described in the literature in Maroteaux–Lamy syndrome. However, the extent of disease was found to be equally stabilized in the two sisters, concretely the cardiac and respiratory functions and body length. The early diagnosis and treatment of MPS VI are critical for an optimal clinical outcome, and further evidence for the new treatment strategies is needed.

Communicated by: Olaf Bodamer, MD PhD

Competing interests: None declared

M. Pineda (✉) · M. O'Callaghan
Fundación y Servicio de Neuropediatría, Hospital Universitario Sant Joan de Déu, CIBERER, Barcelona, Spain
e-mail: pineda@hsjdbcn.org

A. Fernandez Lopez
Servicio de pediatría, Hospital Sant Joan de Déu, Universidad de Barcelona, Spain

M.J. Coll
Sección Errors Congènits, Servei de Bioquímica i Genètica Molecular, Hospital Clinic, CIBERER, Barcelona, Spain

R. Ullot
Servicio de Traumatología y Ortopedia, Hospital Universitario Sant Joan de Déu, Barcelona, Spain

G. Garcia-Fructuoso
Servicio de Neurocirugía, Hospital Universitario Sant Joan de Déu, Barcelona, Spain

Introduction

Maroteaux–Lamy syndrome (also known as mucopolysaccharidosis type VI, MPS VI, or polydystrophic dwarfism) is a form of mucopolysaccharidosis that was first described by Pierre Maroteaux and his mentor, Maurice Emil Joseph Lamy, in 1963 (Maroteaux et al. 1963). Estimates of MPS VI incidence range from 1 in 238,095 to 1 in 1,300,000 in the Netherlands (Poorthuis et al. 1999); even higher rates have been reported in Portugal and Brazil (Valayannopoulos et al. 2010). This lysosomal disorder, caused by a deficiency in the enzyme *N*-acetylgalactosamine-4-sulfatase (arylsulfatase B, ASB; EC 3.1.6.12), is a result of mutations in the arylsulfatase B gene (*ASB*) located on chromosome 5 (5q13–5q14) (Litjens et al. 1989). The pathogenic mutations of this gene reduce the activity of the ASB enzyme, leading to an accumulation of glycosaminoglycans (GAGs). In particular, there is a marked accumulation of dermatan sulfate in the lysosomes, producing irreversible cellular and tissue damage, with the consequent multiple organ system dysfunctions.

Patients with the most severe and rapidly progressing disease often show short stature, coarse facial features, and joint deformities. They also suffer from skeletal dysplasia,

myelopathy, compromised cardiovascular function, corneal clouding, upper airway obstruction, and recurrent ear infections. Death usually occurs in the early teenage years due to respiratory and cardiac problems (Neufeld and Muenzer 2001; Valayannopoulos et al. 2010). Symptoms may appear later; in such cases, mortality is expected in the third to fifth decade of life (Thümler et al. 2012).

The international management guidelines for MPS VI have been drafted based on the evidence from randomized, controlled trials and recommend galsulfase (recombinant human ASB; rhASB; Naglazyme®) enzyme replacement therapy (ERT) as the first-line, long-term therapy for treating this disease (Giugliani et al. 2007). In this report, we describe the clinical evolution of Spanish monochorionic biamniotic twins with the severe form of MPS VI after galsulfase treatment.

Material and Methods

Patient Characteristics

The monochorionic biamniotic twins were born to non-consanguineous Spanish parents after 36 weeks of gestation. No family history of genetic disease was found, and the sister of the twins was healthy. At birth, both twins presented normal birth parameters (Twin 1: weight, 2,650 g; length, 49 cm; occipitofrontal circumference (OFC), 34.5 cm; Twin 2: weight, 2,265 g; length, 44 cm; cephalic perimeter, 28.0 cm). Both showed coarse facial features with hypertelorism and a cranial perimeter of 48.5 cm (percentile 70) at 11 months of age. They suffered from frequent otitis. The twins started walking at 16 months of age, both showing a slight lumbar kyphosis.

Twin 1

MPS VI was diagnosed at 18 months of age. The child had elevated urinary GAGs of 45.8 mg/mmol of creatinine (normal values: 0.9–5.5 mg/mmol of creatinine), and dermatan sulfate was identified. The activity of *N*-acetylgalactosamine-4-sulfatase was diminished in the leukocytes (79.6 μmol/g of protein/min; normal value: 950.0 μmol/g of protein/min) and in cultured fibroblasts (63.7 nmol/mg of protein/h, i.e., 15.8% of the parallel normal value of 403.2 nmol/mg of protein/h). The genetic analysis showed the mutations c.1142+2T>A and c238delG in the *ARSB* gene.

At the age of 3, the growth of Twin 1 decelerated. A year later, she underwent ventriculoperitoneal shunt implantation to treat her progressive hydrocephalus and papilledema. The implant was replaced with a programmable shunt after 3 months and required three later revisions. Inguinal hernia surgery was also required. Gingival hyperplasia, increased lumbar lordosis with dragging of the forefoot, weakened right lower limb, increased osteotendinous reflexes, and clonus in the right Achilles tendon were observed. Surgical decompression of the foramen magnum, occipitocervical fixation with autologous bone grafts up to C2, and halo jacket were required at 4.5 years of age to treat the progressive cervical stenosis myelopathy.

Twin 2

MPS VI was diagnosed at 18 months of age with elevated urinary GAGs (39.6 mg/mmol of creatinine; normal values: 0.9–5.5 mg/mmol) and significantly increased levels of dermatan sulfate. We found diminished activity of *N*-acetylgalactosamine-4-sulfatase in leukocytes (38.7 μmol/g of protein/min; normal value: 950.0 μmol/g of protein/min) and in cultured fibroblasts (5.2 nmol/mg of protein/h, i.e., 1.7% of the parallel control normal value of 403.2 μmol/g of protein/min). As expected, the genetic studies showed the same mutations, c.1142+2T>A and c238delG, in the *ARSB* gene.

At the age of 4, a ventriculoperitoneal shunt was placed to treat the progressive increase in cephalic perimeter caused by hydrocephalus, a decrease in visual acuity (0.6), and papilledema. The shunt required conversion to a programmable implant, as in the case of Twin 1, due to a bilateral subdural collection. The patient developed early progressive tetraparesis (4/5) and showed the signs of pyramidal tract dysfunction. Similarly to her twin sister, decompression of the foramen magnum was also required, with occipitocervical fixation with autologous bone grafts up to C2. A halo jacket was placed for the cervical stenosis myelopathy.

Biochemical and Molecular Determinations

GAGs were quantified in urine using a dimethylmethylene-blue spectrophotometric assay, as previously described (Panin et al. 1986). Qualitative analysis for the identification and characterization of dermatan sulfate was performed using thin-layer chromatography after cetylpyridinium chloride precipitation. The normal values for GAGs range from 0.9 to 5.5 mg/mmol of creatinine.

N-acetylgalactosamine-4-sulfatase activity in leukocytes and fibroblasts was determined in vitro by spectrophotometric quantification of the *p*-nitrocatechol produced by hydrolysis of the substrate, *p*-nitrocatechol sulfate (Baum et al. 1959). This assay was performed in three different samples to avoid inter-sample variation usually observed in patients.

The isolation of genomic DNA and mutation analysis of the *ARSB* gene were performed as described in a publication by Garrido et al. (2007).

The assay of galsulfase antibody levels for the evaluation of anti-rhASB antibodies was performed at Cambridge

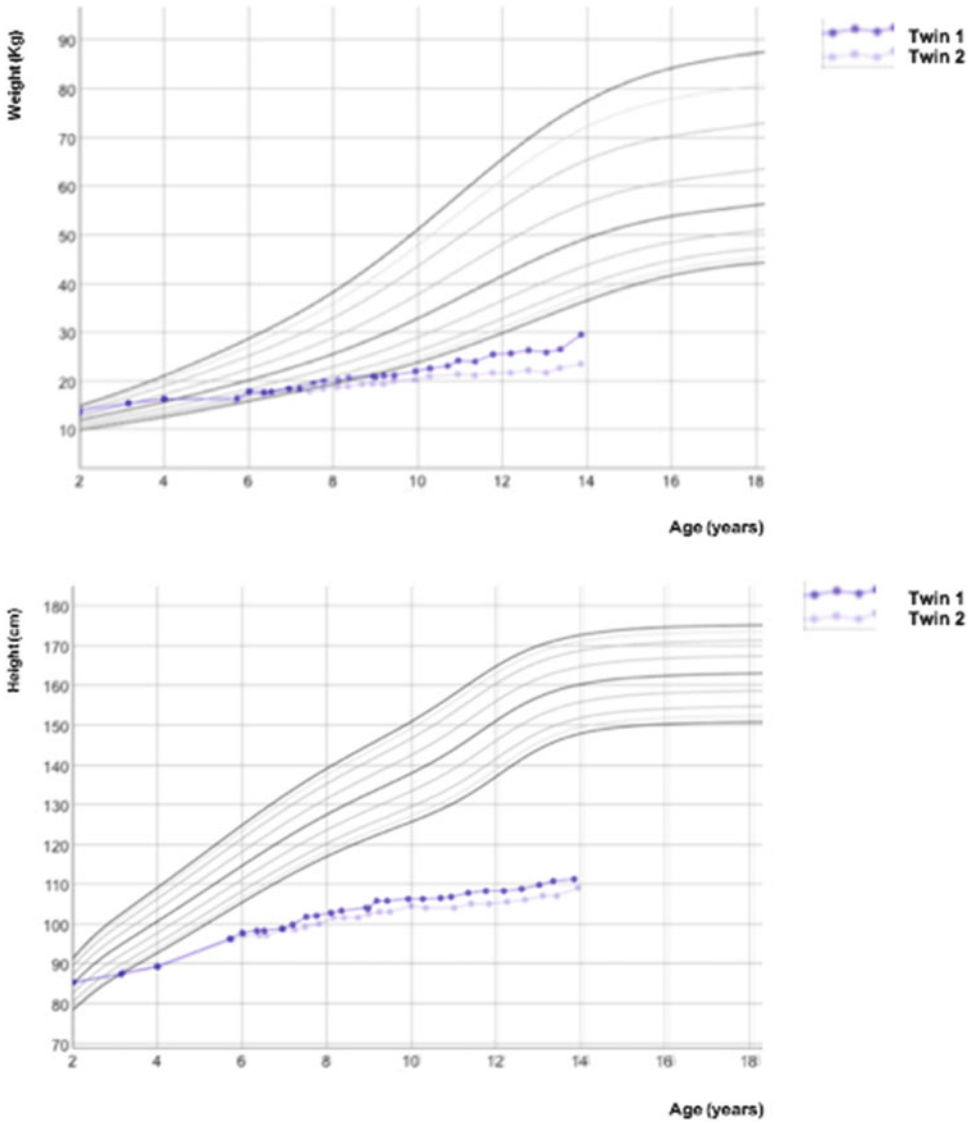

Fig. 1 Growth charts showing weight (kg) and length (cm) from the age of 2 to 14 for dizygotic twins (Twin 1 and Twin 2) with the severe form of MPS VI. Growth was expressed as length-for-age and weight-for-age using currently accepted cross-sectional chart for Spanish children and youth

Biomedical, Inc., Boston (www.cambridgebiomedical.com).

Results

The twins received recombinant human ASB galsulfase (Naglazyme®; BioMarin Pharmaceuticals Inc., Novato, CA) diluted with a physiological saline solution at 1 mg/kg/week, infused over a 4-h period. The ERT was started at 4 years and 9 months of age (Twin 1: length 90 cm, weight 17 kg; Twin 2: length 88 cm, weight 17 kg). By the time of writing, the twins have been treated for 9 years. No adverse events (including infusion-related events) were reported, and the ERT was well tolerated.

After the initiation of ERT, the baseline urinary GAG levels of the twins decreased rapidly, within a few months, to 8.2 mg/mmol of creatinine. The GAG levels remained between 6 and 10 mg/mmol of creatinine up to the time of writing, above the normal values of <4 mg/mmol of creatinine (Braunlin et al. 2013).

Growth charts for the twins showing weight (kg) and length (cm) from the age of 2 to 14 years are presented in Fig. 1. Weight graphs are similar for the two patients, with values within a normal range up to the year 4. The values remained near the lower percentiles until 9 years of age, after which they dropped below clinically normal levels. The decrease in growth rate was easier to see on the length graphs for both twins (Fig. 1); it became clear after the age of 3.

Clinical Manifestations

Twin 1

At the age of 7, Twin 1 was seen by a neurosurgeon due to a worsening of cervical myelopathy. The magnetic resonance imaging (MRI) findings showed a decompensation that produced restenosis in the foramen magnum and a longer cervical area. Therefore, a surgical decompression of the foramen, expansion of the cervical laminectomy, and posterior instrumented arthrodesis were performed. The patient recovered completely, with both upper and lower limbs remaining normal up to the time of writing. When the patient was 9 years old, an exodoncy was performed due to dental caries, ankylosis, and maxillary sinus retention cysts of teeth 73 and 83. The surgery was performed on the tooth 85.

Thickened mucosa in the retromolar pad blocked the eruption of the permanent teeth. At 9 years and 11 months of age, the patient underwent surgery for bilateral carpal tunnel syndrome. One month later, the audiometry examination showed a mild transmission hypoacusis, and ophthalmological tests demonstrated a slight symmetrical opacity of the cornea. An echocardiogram showed a minimal mitral insufficiency; however, the heart and pulmonary functions were normal. Control MRI showed mild stenosis at C5 and C6 without hydrocephalus. The 6-min walk test (6MWT) distance decreased from 460 m (at the age of 10, 6 years after the start of the ERT) to 400 m (age of 13, after 9 years of the ERT). The total antibody response to Naglazyme (galsulfase) showed >1,770,000 anti-rhASB antibodies and 0 neutralizing anti-rhASB antibodies.

Twin 2

Twin 2 was admitted for umbilical hernia surgery at the age of 5; at the same time, a bilateral tenotomy of the Achilles tendon and plantar fasciotomy were performed. One year later, a Gore-Tex mesh was placed by umbilical herniorrhaphy. At 8 years of age, the patient underwent deep anterior lamellar keratoplasty in the right eye, and one month later, in the left eye. Several odontological disorders were observed at the age of 9, including retention of permanent teeth, ectopic teeth, dental cysts, and exodoncy. At the same time, the patient underwent the surgery for carpal tunnel syndrome. During the audiometric evaluation, she showed a hearing loss in both ears at 10 years of age, with mixed hypoacusis in the left ear and conductive hypoacusis in the right. Mitral, tricuspid, and aortic insufficiency were also observed, although the pulmonary function was normal.

At the age of 11, the 6MWT distance was 345 m (7 years under the ERT) and improved to 426 m 2 years later (9 years of the ERT). The severity of the disease was manifest in the musculoskeletal and connective tissue disorders, with sacral hyperlordosis and articular mobility reduced due to mild retractions in the feet, hands, and shoulders. A control MRI showed no symptoms of hydrocephaly. A marked narrowing of the foramen magnum and the cervical spine diameter (C3–C5) was also registered. The imaging examination also showed scoliosis, bilateral valgus knee, and a subtle cavus foot. A hyperreflexia in the left extremities was also observed, which, at 13 years of age, became a progressive spastic tetraparesis, predominantly in the lower extremities.

A surgical decompression of the foramen, expansion of the cervical laminectomy down to C5, and posterior instrumented arthrodesis became necessary. After the surgery, the patient presented with complete paraplegia at the thoracic spine level. The subsequent delayed MRI confirmed that the symptoms were compatible with spinal cord ischemic lesion at the level of the maximum thoracic kyphosis. The results from the coronal plane MRI (T2) before and after ischemic lesion are shown in Fig. 2a and b, respectively. One year later, the patient achieved a good recovery from the thoracic-level paraplegia in the arms.

The total antibody response to Naglazyme showed >2,430 anti-rhASB antibodies and 0 neutralizing anti-rhASB antibodies.

Discussion

Because lysosomal storage disorders such as MPS VI are rare, only limited data are available, and the existing studies cover relatively short periods of observation. The assessment of the cases of rapidly progressive MPS VI reported in this work provides an overview of the clinical evolution during 9 years of therapy with galsulfase. Even though the patients were monochorionic biamniotic twins with the same mutations in the *ASB* gene, their clinical manifestations of this enzymatic deficiency were slightly different. Twin 2 presented stronger multisystemic involvement (with marked musculoskeletal, neurological, and odontological components) than Twin 1.

We found that GAG levels were lower before the infusion than 2 days after the galsulfase infusion treatment. To the best of our knowledge, there are no studies using the levels of antibodies to galsulfase to evaluate the level of anti-rhASB antibodies. In our study, both twins showed negative results, despite higher levels of total antibodies in Twin 1, probably associated with the increased basal levels of the endogenous enzyme. In other lysosomal diseases, the

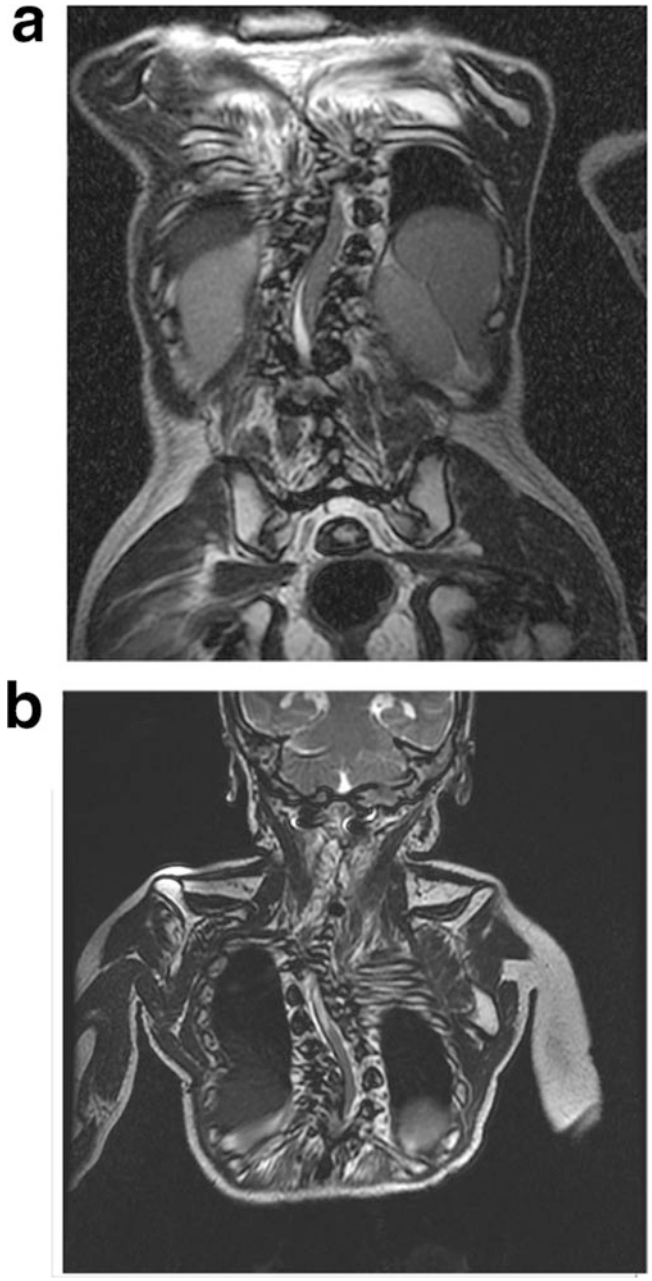

Fig. 2 Results from the coronal plane MRI (T2) before (Fig. 2a) and after (Fig. 2b) ischemic lesion in Twin 2. (**a**) Results from the coronal plane magnetic resonance imaging (T2) were compatible with pronounced scoliosis but showed normal spinal cord image at the mid-dorsal level in Twin 2. (**b**) Results from the coronal plane MRI (T2) showed intramedullary hyperintensity at the D5–6 dorsal level compatible with spinal cord lesion in Twin 2

antibody levels in the blood can affect the efficacy of the ERT by inhibiting the uptake of the enzyme by the target tissues (Brands et al. 2013). Our results show no galsulfase antibodies in MPS VI patients, so the marked signs and symptoms might be only associated with the rapid, progressive form of the disease.

The mean length increase in our patients from the start of the treatment to the last follow-up was 3.3 cm/year. Overall, the length and weight increases remained slightly below normal. Our results are in-line with the previous studies of MPS VI, in which the growth rates are greater in patients below 16 years of age (Decker et al. 2010; McGill et al. 2010; Furujo et al. 2011; Hendriksz et al. 2013). It has been suggested that the improvement in growth is associated with the beneficial effects of the treatment on the bone cells and endocrine gland function, leading to reduced inflammation and a reduction in joint contractures (Decker et al. 2010). However, there is little information on the growth of

MPS VI patients who have not received ERT. Such data are necessary for the understanding of the effect of galsulfase therapy on the disease. Twin 2 in our study displayed progressive musculoskeletal and joint disorders despite being under ERT, but her length evolution was similar to that of her twin sister. In contrast, Twin 1 showed stabilization in the results of the skeletal radiographs and imaging analysis after ERT. Similarly to other cases described in the literature, our patients presented with some of the most common neurosurgical complications, including hydrocephalus and stenosis of the foramen magnum with progressive myelopathy (Lampe et al. 2013). Paraplegia after surgery was described in Twin 2. We have found only three similar cases with thoracolumbar kyphosis reported in patients with MPS who suffered from postoperative spinal cord lesion (2 with Hurler syndrome and 1 with Morquio disease) (Pauchard et al. 2014). In their publication, Pauchard et al. concluded that the narrowing associated with spinal hypermobility may be involved in the origin of this spinal cord damage, but it is not the only determining factor. This view is supported by the two cases of extra-spinal surgery with previously identified kyphosis (Pauchard et al. 2014). Bone dysplasia and spinal involvement are the predominant types of neurological damage in MPS VI patients; the risk of perioperative spinal cord complications must be individually analyzed before any surgery.

Another common clinical manifestation in MPS VI is cardiac involvement, a major cause of mortality. In particular, the left ventricular hypertrophy and functional abnormalities of the mitral and aortic valves are progressive in individuals who are not treated (Braunlin et al. 2013). These abnormalities are stabilized by galsulfase treatment (Brands et al. 2013; Giugliani et al. 2014). We found mild mitral insufficiency in both twins, although mitral valve regurgitation is described in most MPS VI pediatric reports (Azevedo et al. 2004; Scarpa et al. 2009; Fesslova et al. 2009; Lael et al. 2010). However, Twin 2 also presented tricuspid and aortic involvement. Nevertheless, cardiac performance measures were slowed at the age of 13 years in both twins.

A recent pooled long-term data analysis from the clinical ERT trials and the survey study in MPS VI patients showed that the galsulfase therapy partially improved the pulmonary function. The affected parameters are the forced vital capacity, forced expiratory volume in 1 s (FEV1), and the maximum voluntary ventilation (Harmatz et al. 2010). The twins in our study had a stable pulmonary function; the values of the listed parameters were within the normal range during the study period. Some authors have attributed this to the underlying increase in the endurance and the beneficial changes in pulmonary function (Harmatz et al. 2008). These results agreed with the results of 6MWT of Twin 2, which showed an improvement of 81 m (measured at 11 and 13 years of age).

Finally, we reported ophthalmological and audiological outcomes with no tendency to improve after 9 years of the ERT. Almost 80% of patients with MPS VI have reduced visual acuity and 60% have impaired hearing according to the literature. These data are in accord with our results showing that the ERT had no impact on vision or hearing (Hendriksz et al. 2013).

In conclusion, the monochorionic biamniotic twins studied in this work showed typical characteristics of the severe form of MPS VI at the baseline. Even though the younger twin (Twin II) presented stronger clinical symptoms, the progression of the disease was similar in the two sisters; stabilization in the cardiac and pulmonary measures was observed after 9 years of the ERT. There were clear improvements in growth as well as in clinical endurance. In contrast, Twin 2 showed neurological damage with marked perioperative spinal cord complications. Here, we present for the first time the results of the assay of neutralizing anti-rhASB antibodies, which were negative for both twins. The reported spine ischemic kyphosis, a result of surgery in Twin 2, demonstrates the risk of spinal cord damage in MPS VI patients. Overall, we found the ERT to be effective and safe in these two cases. However, improved regimens or schedules might be required to increase the clinical benefits of galsulfase ERT in patients with the rapidly progressing disease.

Acknowledgments Scientific editorial assistance was provided by Irantzu Izco-Basurko and Fernando Rico-Villademoros (Cociente S. L.). The authors thank the family for their collaboration.

Synopsis

Comprehensive description of clinical manifestations in monochorionic biamniotic twins with the severe form of mucopolysaccharidosis type VI under enzyme replacement therapy.

Contributorship

MP analyzed data and drafted the manuscript. MO, GGF, and AF treated and followed up the patients and revised the manuscript. MJC conducted metabolic and genetic studies and revised the manuscript. All authors read and approved the manuscript.

Guarantor

Mercedes Pineda Marfa.

Compliance with Ethics Guidelines

Conflict of Interest

The authors RU, AF, MJC, and LG have no affiliations or financial involvement with any organization or entity with an interest in or conflict with the subject matter discussed in the manuscript. MO has received consulting fees or honoraria from Actelion Pharmaceuticals Ltd for travel, accommodations, or meetings and payment for lectures from BioMarin, Genzyme, and Shire. MP has received consulting fees or honoraria and payment for lectures from Actelion Pharmaceuticals Ltd and BioMarin.

Informed Consent

Informed consent was obtained from the parents of the patients before retrieving the data for the study.

References

Azevedo ACMM, Schwartz IV, Kalakun L, Brustolin S, Burin MG, Beheregaray APC, Leistner S, Giugliani C, Rosa M, Barrios P, Marinho D, Esteves P, Valadares E, Boy R, Horovitz D, Mabe P, de Silva LCA, de Souza ICN, Ribeiro M, Martins AM, Palhares D, Kim CA, Giugliani R (2004) Clinical and biochemical study of 28 patients with mucopolysaccharidosis type VI. Clin Genet 66:208–213

Baum H, Dogson KS, Spencer B (1959) The assay of arylsulphatases A and B in human urine. Clin Chim Acta 4:453–455

Brands MM, Hoogeveen-Westerveld M, Kroos MA, Nobel W, Ruijter GJ, Özkan L, Plug I, Grinberg D, Vilageliu L, Halley DJ, van der Ploeg AT, Reuser AJ (2013) Mucopolysaccharidosis type VI phenotypes-genotypes and antibody response to galsulfase. Orphanet J Rare Dis 8:51

Braunlin E, Rosenfeld H, Kampmann C, Johnson J, Beck M, Giugliani R, Guffon N, Ketteridge D, Sá Miranda CM, Scarpa M, Schwartz IV, Leão Teles E, Wraith JE, Barrios P, Dias da Silva E, Kurio G, Richardson M, Gildengorin G, Hopwood JJ, Imperiale M, Schatz A, Decker C, Harmatz P, MPS VI Study Group (2013) Enzyme replacement therapy for mucopolysaccharidosis VI: long-term cardiac effects of galsulfase (Naglazyme®) therapy. J Inherit Metab Dis 36(2):385–394

Decker C, Yu ZF, Giugliani R, Schwartz IV, Guffon N, Teles EL, Miranda MC, Wraith JE, Beck M, Arash L, Scarpa M, Ketteridge D, Hopwood JJ, Plecko B, Steiner R, Whitley CB, Kaplan P, Swiedler SJ, Conrad S, Harmatz P (2010) Enzyme replacement therapy for mucopolysaccharidosis VI: growth and pubertal development in patients treated with recombinant human N-acetylgalactosamine 4-sulfatase. J Pediatr Rehabil Med 3:89–100

Fesslova V, Corti P, Sersale G, Rovelli A, Russo P, Mannarino S, Butera G, Parini R (2009) The natural course and the impact of therapies of cardiac involvement in the mucopolysaccharidoses. Cardiol Young 19:170–178

Furujo M, Kubo T, Kosuga M, Okuyama T (2011) Enzyme replacement therapy attenuates disease progression in two Japanese siblings with mucopolysaccharidosis type VI. Mol Genet Metab 104:597–602

Garrido E, Chabás A, Coll MJ, Blanco M, Domínguez C, Grinberg D, Vilageliu L, Cormand B (2007) Identification of the molecular defects in Spanish and Argentinian mucopolysaccharidosis VI (Maroteaux–Lamy syndrome) patients, including 9 novel mutations. Mol Genet Metab 92:122–130

Giugliani R, Harmatz P, Wraith JE (2007) Management Guidelines for Mucopolysaccharidosis VI. Pediatrics 120:405–418

Giugliani R, Lampe C, Guffon N, Ketteridge D, Leão-Teles E, Wraith JE, Jones SA, Piscia-Nichols C, Lin P, Quartel A, Harmatz P (2014) Natural history and galsulfase treatment in mucopolysaccharidosis VI (MPS VI, Maroteaux–Lamy syndrome)–10-year follow-up of patients who previously participated in an MPS VI Survey Study. Am J Med Genet A 164(8):1953–1964

Harmatz P, Giugliani R, Schwartz IV, Guffon N, Teles EL, Miranda MC, Wraith JE, Beck M, Arash L, Scarpa M, Ketteridge D, Hopwood JJ, Plecko B, Steiner R, Whitley CB, Kaplan P, Yu ZF, Swiedler SJ, Decker C; MPS VI Study Group (2008) Long-term follow-up of endurance and safety outcomes during enzyme replacement therapy for mucopolysaccharidosis VI: final results of three clinical studies of recombinant human N-acetylgalactosamine 4-sulfatase. Mol Genet Metab 94(4):469–475

Harmatz P, Yu ZF, Giugliani R, Schwartz IV, Guffon N, Teles EL, Miranda MC, Wraith JE, Beck M, Arash L, Scarpa M, Ketteridge D, Hopwood JJ, Plecko B, Steiner R, Whitley CB, Kaplan P, Swiedler SJ, Hardy K, Berger KI, Decker C (2010) Enzyme replacement therapy for mucopolysaccharidosis VI: evaluation of long-term pulmonary function in patients treated with recombinant human N-acetylgalactosamine 4-sulfatase. J Inherit Metab Dis 33(1):51–60

Hendriksz CJ, Giugliani R, Harmatz P, Lampe C, Martins AM, Pastores GM, Steiner RD, Leão Teles E, Valayannopoulos V; CSP Study Group (2013) Design, baseline characteristics, and early findings of the MPS VI (mucopolysaccharidosis VI) Clinical Surveillance Program (CSP). J Inherit Metab Dis 36(2):373–384

Lael GN, de Paula AC, Leone C, Kim CA (2010) Echocardiographic study of paediatric patients with mucopolysaccharidosis. Cardiol Young 20:254–261

Lampe C, Lampe C, Schwarz M, Müller-Forell W, Harmatz P, Mengel E (2013) Craniocervical decompression in patients with mucopolysaccharidosis VI: development of a scoring system to determine indication and outcome of surgery. J Inherit Metab Dis 36(6): 1005–1013

Litjens T, Baker EG, Beckmann KR, Morris CP, Hopwood JJ, Callen DF (1989) Chromosomal localization of ARSB, the gene for human Nacetylgalactosamine-4-sulphatase. Hum Genet 82:67–68

Maroteaux P, Leveque B, Marie J, Lamy M (1963) A new dysostosis with urinary elimination of chondroitin sulfate B. Presse Med 71: 1849–1852

McGill JJ, Inwood AC, Coman DJ, Lipke ML, de Lore D, Swiedler SJ, Hopwood JJ (2010) Enzyme replacement therapy for mucopolysaccharidosis VI from 8 weeks of age—a sibling control study. Clin Genet 77:492–498

Neufeld E, Muenzer J (2001) The mucopolysaccharidoses. In: Valle D, Beaudet A, Vogelstein B, Kinzler K, Antonarakis S, Ballabio A (eds) Scriver's online metabolic and molecular bases of inherited disease. McGraw-Hill Global Education Holdings, LLC, New York, pp 2465–2494

Panin G, Naia S, Dall'Amico R, Chiandetti L, Zachello F, Catassi C, Felici L, Coppa GV (1986) Simple spectrophotometric quantifi-

cation of urinary excretion of glycosaminoglycan sulfates. Clin Chem 32(11):2073–2076

Pauchard N, Garin C, Jouve JL, Lascombes P, Journeau P (2014) Perioperative medullary complications in spinal and extra-spinal surgery in mucopolysaccharidosis: a case series of three patients. JIMD Rep 16:95–99

Poorthuis B, Wevers R, Kleijer W, Groener JE, de Jong JG, van Weely S, Niezen-Koning KE, van Diggelen OP (1999) The frequency of lysosomal storage disease in the Netherlands. Hum Genet 105: 151–156

Scarpa M, Barone R, Fiumara A, Astarita L, Parenti G, Rampazzo A, Sala S, Sorge G, Parini R (2009) Mucopolysaccharidosis VI: the Italian experience. Eur J Pediatr 168:1203–1206

Thümler A, Miebach E, Lampe C, Pitz S, Kamin W, Kampmann C, Link B, Mengel E (2012) Clinical characteristics of adults with slowly progressing mucopolysaccharidosis VI: a case series. J Inherit Metab Dis 35:1071–1079

Valayannopoulos V, Nicely H, Harmatz P, Turbeville S (2010) Mucopolysaccharidosis VI. Orphanet J Rare Dis 5:5

JIMD Reports
DOI 10.1007/8904_2016_531

RESEARCH REPORT

A New Approach for Fast Metabolic Diagnostics in CMAMMA

Monique G.M. de Sain-van der Velden • Maria van der Ham • Judith J. Jans • Gepke Visser • Hubertus C.M.T. Prinsen • Nanda M. Verhoeven-Duif • Koen L.I. van Gassen • Peter M. van Hasselt

Received: 03 June 2015 / Revised: 09 December 2015 / Accepted: 17 December 2015 / Published online: 27 February 2016

Abstract *Background*: The presence of increased urinary concentrations of both methylmalonic acid (MMA) and malonic acid (MA) is assumed to differentiate combined malonic and methylmalonic aciduria (CMAMMA), due to mutations in the ACSF3 gene, from other causes of methylmalonic aciduria (classic MMAemia). Detection of MA in urine, however, is challenging since excretion of MA can be easily missed. The objective of the study was to develop a method for quantification of MA in plasma to allow differentiation between CMAMMA and classic MMAemia.

Methods: Compound heterozygosity for mutations in the ACSF3 gene was detected in two female siblings using diagnostic exome sequencing. Urine (MMA and MA) was analyzed with GC/MS, while plasma was analyzed with UPLC-MS/MS. MA/MMA ratios were calculated.

Results: Both patients had a severe psychiatric presentation (at the age of 6 years and 5.5 years, respectively) after a viral infection. MA excretion in the patients was only just above the highest control value in several samples. MA concentrations in plasma from the two patients were clearly above the highest value observed in control subjects. However, MA concentrations in plasma from patients with classic MMAemia were also elevated. Additional, calculation of MA/MMA ratio in plasma allowed to fully differentiate between CMAMMA and classic MMAemia.

Conclusions: Calculating the MA/MMA ratio in plasma allows differentiation between CMAMMA and classic MMAemia. The full clinical spectrum of CMAMMA remains to be delineated.

Communicated by: Ivo Barić, M.D., PhD, Professor of Pediatrics

Competing interests: None declared

M.G.M. de Sain-van der Velden (✉) · M. van der Ham · J.J. Jans · H.C.M.T. Prinsen · N.M. Verhoeven-Duif · K.L.I. van Gassen
Department of Medical Genetics, UMC Utrecht, PO Box 85090, 3508AB Utrecht, The Netherlands
e-mail: m.g.desain@umcutrecht.nl

G. Visser · P.M. van Hasselt
Department of Pediatric Gastroenterology and Metabolic Diseases, University Medical Centre (UMC) Utrecht, Utrecht, The Netherlands

Introduction

Combined malonic and methylmalonic aciduria (CMAMMA) has thus far been described in two disorders, malonyl-CoA decarboxylase (MCD) deficiency (OMIM #248360) and, recently, acyl-CoA synthetase family member 3 enzyme (ACSF3) deficiency (OMIM #614265). Malonyl-CoA decarboxylase catalyzes the conversion of malonyl-CoA to acetyl-CoA and carbon dioxide, and patients excrete significantly higher malonic acid (MA) than methylmalonic acid (MMA) levels (de Wit et al. 2006). ACSF3 adds a coenzyme A moiety to both MA and MMA, and patients with mutations in ACSF3 excrete more MMA than MA (Alfares et al. 2011). The incidence of CMAMMA due to mutations in the ACSF3 gene has been estimated at approximately 1 in 30,000 (Sloan et al. 2011). However, at present only 11 patients with mutations (missense, in frame deletion, and nonsense mutations) in the ACSF3 gene have been reported in literature (Alfares et al. 2011; Sloan et al. 2011). Patients with mutations in the ACSF3 gene exhibit a highly heterogeneous clinical phenotype, ranging from asymptomatic (Alfares et al. 2011) to severe (Sloan et al. 2011). Symptoms and signs reported thus far in children include coma, ketoacidosis, hypoglycemia, failure to thrive, elevated transaminases, microcephaly, dystonia, axial hypotonia, and/or developmental delay (Sloan et al. 2011). In those who were identified as adults,

symptoms include (mild) memory problems, seizures, and encephalopathy (Sloan et al. 2011).

Here, we describe two sisters who both exhibited an encephalopathic event upon an influenza infection in whom urinary analysis initially revealed repetitive "isolated" methylmalonic aciduria (MMAemia). Diagnostic follow-up for MMAemia (genetic complementation analysis, enzymatic and/or mutation analysis) did not yield a primary defect. Diagnostic exome sequencing – to our surprise – identified compound heterozygosity for mutations in the ACSF3 gene. MA excretion was missed in the routinely performed organic acid analysis since it co-elutes with MMA and was negligible in comparison with the elevated MMA excretion.

Therefore, we developed a simple, fast, sensitive, and robust assay to determine MA in plasma using ultra-performance liquid chromatography-tandem mass spectrometry (UPLC-MS/MS) and applied it to samples of the patients. Clinical data of all of the formerly reported patients were compared.

Material and Methods

Patients

Patient A is the first child of unrelated parents. She had a normal development until the age of 6 years when she was hospitalized because of dehydration and drowsiness thought to be caused by vomiting. Despite rehydration her neurological condition deteriorated. Within a few hours, she exhibited opisthotonus, as well as oculogyric crises. She developed a paresis of both arms. In addition, a Babinski sign was present bilaterally. On suspicion of an encephalitis, she was treated with acyclovir, methylprednisolone, and haloperidol without clear clinical benefits. Catatonia was diagnosed and treated with lorazepam. Viral PCR analysis (nose/throat specimen) was positive for influenza A virus and treatment with oseltamivir was initiated. The initial diagnostic work-up included broad metabolic screening. Urinary organic acid analysis revealed an increased MMA without other overt abnormalities. Metabolic investigations in plasma revealed increased MMA concentrations, while free carnitine, acylcarnitines (including C3DC-carnitine and C4DC-carnitine), amino acids, and total homocysteine were normal. MMA was also quantified in cerebrospinal fluid (CSF) and was found to be increased (13 μmol/L; controls: not detectable). Since some forms of MMAemia respond to cobalamin, vitamin B12 injections were administered, however without a clear clinical or biochemical effect. Initially, brain MRI did not show abnormalities, but a second MRI (performed 3 weeks later) showed increased signal on T2 of the genu of the corpus callosum compatible with demyelination or infection (Fig. 1). In addition, an increased signal was found in the cervical myelum (c2–c7) suggesting edema. She gradually recovered, but upon recovery mutism became evident, which cleared only partially and necessitated revalidation. During follow up she has shown continued improvements. At the age of 10 years, she is visiting a regular elementary school, with higher than average scores.

Patient B, the sister of patient A, developed normally until the age of 5.5 years. She became encephalopathic at the age of 5.5 years after a period of vomiting and fever. Viral PCR (nose/throat specimen) revealed an influenza B infection. She exhibited an opisthotonus and developed oculogyric crises identical to her sister. Likewise there was notable pyramidal tract involvement with bilateral Babinski signs. On examination she had catatonia manifested by stupor, mutism, and flexibilitas cerea. She improved clinically after treatment with lorazepam. MRI investigation showed a diffusely increased T2 signal in the white matter, of note corpus callosum appeared normal. The liver size was slightly increased. At follow-up (age 7.5 years), her development is in the normal range.

Clinical features of the two sisters were compared with formerly reported patients (Table 1).

Samples

Six plasma samples and sixteen urine samples from the two CMAMMA patients were available and were compared with 20 stored plasma samples from a total of six patients with both nonresponsive and responsive MMAs (classic MMAemia) (MMAA or MMAB). Urine samples from 40 females with a similar age were selected as control group.

Reagents

MA, stable isotopically labeled MA ($^{13}C_3$-MA) and dithiothreitol (DTT) were purchased from Sigma (Steinheim, Germany). Formic acid was purchased from Merck (Darmstadt, Germany) and acetonitrile was obtained from Biosolve (Valkenswaard, the Netherlands).

MMA and MA in Urine

Quantification of MMA excretion was performed by GC/MS in standard organic acid analysis. Quantification of MA excretion was performed by GC/MS using selected ion monitoring (SIM) of m/z 233 in the same assay. Prior to analysis the samples were trimethylsilylated.

MMA and MA in Plasma

Sample preparation and chromatographic and mass spectrometric conditions on an UPLC/MS/MS system were used as

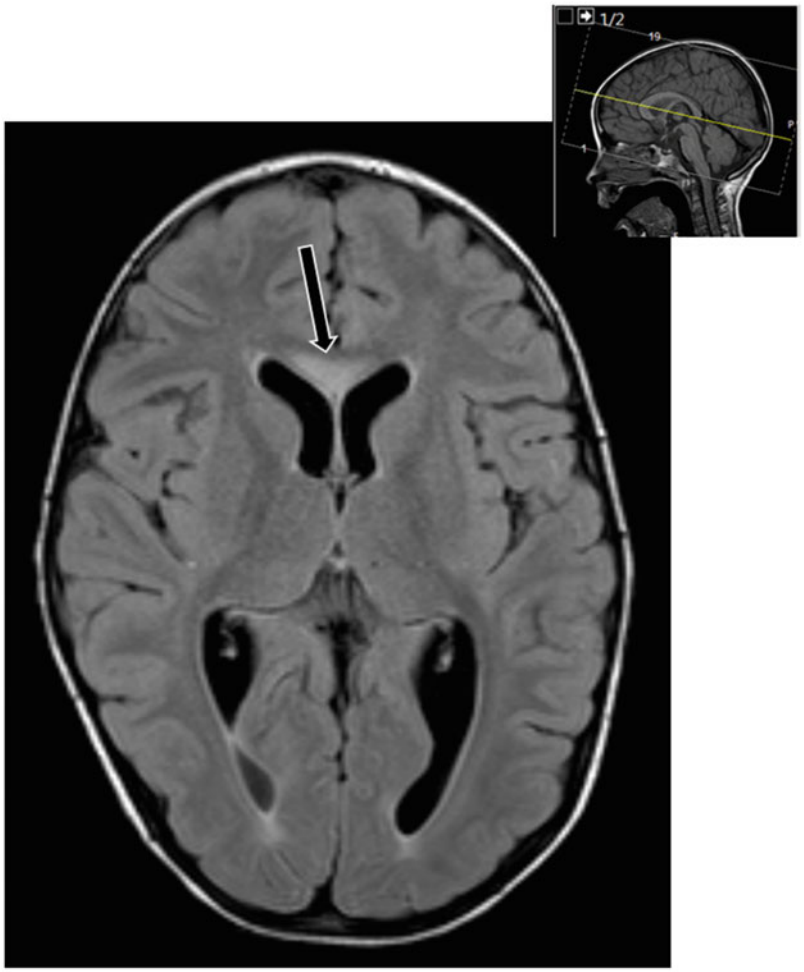

Fig. 1 Sagittal T2 flair showing hyperintense lesion in the genu of corpus callosum

described before (de Sain-van der Velden et al. 2015) with some slight modifications. In short, apart from other internal standards, $^{13}C_3$-MA (12 μmol/L) was added to plasma.

The MS operated in negative electrospray ionization (ESI) mode for MA. Mass transitions *m/z* 102.8 to *m/z* 58.8 (MA) and *m/z* 105.8 to *m/z* 60.8 ($^{13}C_3$-MA) were measured. For quantification a calibration curve of eight standards with spiked concentrations of 0, 0.25, 0.5, 1.0, 2.0, 3.0, 4.0, and 5.0 μmol/L MA was prepared in plasma. For quality control (QC), heparinized blood from a volunteer was used to prepare three QC samples: QC-B (blank, without spiking), QC-L (low, spiked with 1.2 μmol/L MA), and QC-H (high, spiked with 3.7 μmol/L MA). The method was validated for accuracy, process efficiency, carryover, LOD, LOQ, linearity, intra-variation, inter-variation, cross talk, and stability (after preparation of the samples, freeze/thaw cycle) according to recently published guidelines (Honour 2011).

MA in plasma was quantified in control subjects within a wide age range to determine age dependency of this compound. These data were used to set reference ranges for MA.

Results

Genetic Analysis

Diagnostic exome sequencing in both patients identified compound heterozygous missense mutations in ACSF3, a recognized cause of CMAMMA (Alfares et al. 2011). The first mutation c.1075G>A p.(Glu359Lys) has been described before (Alfares et al. 2011). The second mutation c.311A>T p.(Asn104Ile) was not described before in controls (>60,000 controls; Exome Aggregation Consortium (ExAC), Cambridge, MA (http://exac.broadinstitute.org [03–2015]) or patients and concerns a change of an evolutionary highly conserved amino acid. In silico predictions suggest a pathogenic effect for this mutation.

Table 1 Symptoms and signs of patients with known mutation in the ACSF3 gene

Symptoms and signs	Frequency
T2 hyperintensities[a]	4
Increased signal on T2 of the genu of the corpus callosum[b]	1
Diffusely increased T2 signal in the white matter[b]	1
Extrapyramidal tract involvement[a]	3
Oculogyric crises[b]	2
Encephalopathy[a]	3
Loss of speech/mutism[a]	3
Mutism[b]	2
Psychiatric symptoms[a]	3
Catatonia[b]	2
Memory problems	3
Neurodegeneration of the brain and spinal cord[a]	2
Increased T2 signal in the cervical myelum (c2–c7)[b]	1
Pyramidal tract involvement[b]	2
Opisthotonus[b]	2
Acidosis/ketoacidosis	2
Axial hypotonia	2
Psychomotor delay	2
Poor weight gain/failure to thrive	2
Seizure	1
Complex partial seizures	1
Speech delay	1
Elevated transaminases	1
Failure to thrive	1
Hypoglycemia	1
Incontinence	1
Microcephaly	1
Ocular migraine	1

[a] Present in either of the two sisters
[b] Not previously reported

Nomenclature is according to HGVS guidelines and is based upon transcript NM_174917.4.

Quantification of MMA and MA

MMA in plasma ranged from 15.3 to 1,327.4 μmol/L in the group with MMAemia. Urine excretion ranged from 196 to 14,500 μmol/mmol creatinine in this group (Fig. 2).

This group included responsive as well as nonresponsive ($n = 7$ samples) patients for vitamin B12. One sample (from the responsive patients) before starting B12 was included. The other samples from the responsive ones were from the time after B12 application. In both patients, MMA concentrations were consistently elevated in urine as well as plasma (see Fig. 3a and b, respectively). In all urine samples from the CMAMMA patients, excretion of MA was increased. The range of urine MA excretion was 15–201 and 13–226 μmol/mmol creatinine in patient A and patient B, respectively (Fig. 3c). Notably, in some urine samples, this was only just above the upper value (range 0.23–10.0 μmol/mmol creatinine) observed in 40 female control subjects with a mean age of 7.5 years (range 5–11 years). The urinary MA/MMA ratio (ranging from 1.7 to 9.1 in patient A and from 1.1 to 8.2 in patient B) overlapped with those calculated in control subjects (range 0.06–2.4).

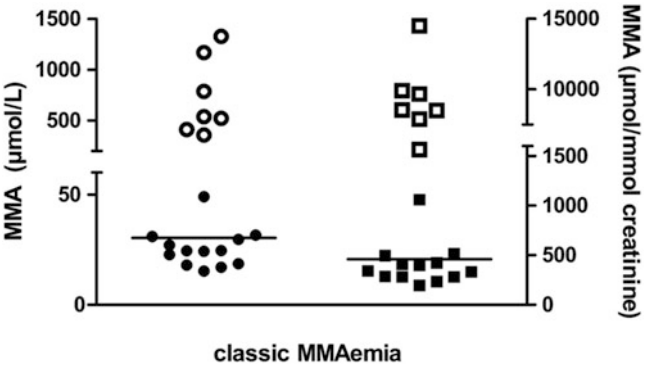

Fig. 2 MMA concentration in plasma (*filled circle*; responders $N = 13$, *open circle*; nonresponders $N = 7$, *left Y*-axis) and in urine (*filled square*; responders $N = 13$, *open square*; nonresponders $N = 7$, *right Y*-axis) from patients with classic MMAemia

General aspects of assay performance for MA in plasma are shown in Table 2. The 95 percentile of MA in plasma was 0.31 (range 0.08–0.79 μmol/L) in 87 control subjects (median age: 13.9 (range 2 months–75 years) and was not age dependent. The range of MA/MMA in plasma was 0.4–5.3 in control subjects. The range of MA was 0.9–3.4 μmol/L in CMAMMA (Fig. 3d) and overlap with those measured in classic MMAemia (0.17–2.12 μmol/L; Fig. 4a). The range of MA was 0.17–0.43 μmol/L in the responders and 0.41–2.12 μmol/L in the nonresponders. In contrast, the MA/MMA ratio in plasma fully discriminates CMAMMA from classic MMAemia (Fig. 4b).

Discussion

Here, we describe two patients with compound heterozygous missense mutations in the ACSF3 gene identified by diagnostic exome sequencing. Both patients presented with a severe psychiatric presentation after a viral infection. Until now 11 patients have been reported in literature with mutations in the ACSF3 gene with various clinical presentations (Table 1). The clinical presentation of the patients described in the present paper was strikingly different from other reports (Table 1). While psychiatric

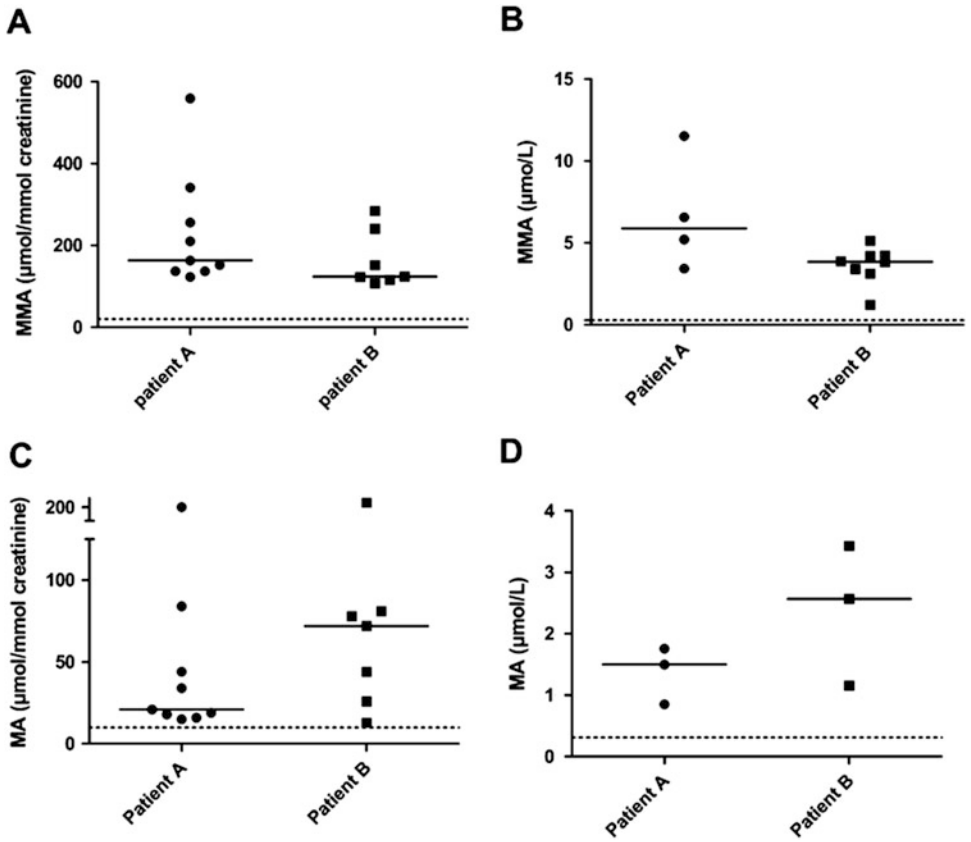

Fig. 3 (**a**) MMA excretion (µmol/mmol creatinine), (**b**) MMA in plasma (µmol/L), (**c**) MA excretion (µmol/mmol creatinine), and (**d**) MA in plasma (µmol/L) in both patients. *Dotted lines* represent 95th percentile of normal

Table 2 General aspects of assay performance and influence of stability for MA in plasma

	MA
Accuracy (%)	91
Process efficiency (%)	57
LOD (µM)	0.02
LOQ (µM)	0.06
Carryover (%)	<0.2
Linearity (µM)	62
Intra-variation (%) ($n = 10$)	6.7
Inter-variation (%) ($n = 10$)	13.4
Cross talk (%)	<0.02
Stability (after sample preparation) (h)	24
Stability (freeze/thaw cycles)	10[a]

[a] Maximum tested

features and neurological problems have been described in adult patients, this was not observed in the younger group (Sloan et al. 2011). Striking features in our patients included mutism (in both) and corpus callosum lesions (in one patient). Interestingly, corpus callosum lesions have been associated with mutism, suggesting a pathophysiological link. However, no clear corpus callosum abnormalities were observed on MRI imaging in the other patient.

CMAMMA is biochemically characterized by elevated concentration of the diagnostic compounds MMA and MA in both urine and plasma. While MMA excretion in patients with mutations in the ACSF3 gene has been reported to be 8–194 (Alfares et al. 2011; Sloan et al. 2011) times normal, MA excretion is typically present at relatively lower levels 3–91 times normal excretion (Alfares et al. 2011; Sloan et al. 2011).

In our laboratory, elevated urinary MA values were initially missed using routinely performed organic acid analysis. Although we successfully increased the sensitivity of our assay for MA – by using selected ion monitoring (SIM) at *m/z* 233 – it should be noted that even then, the elevation of urinary MA concentration may be so subtle that it could easily be missed. Moreover, there was an overlap in urine MA/MMA ratio between control subjects and patients with CMAMMA.

We explored whether – in patients with an elevated MMA excretion – MA concentrations in plasma could allow differentiation. Plasma MA can be easily added to a method for quantification of MMA (and homocysteine) (de

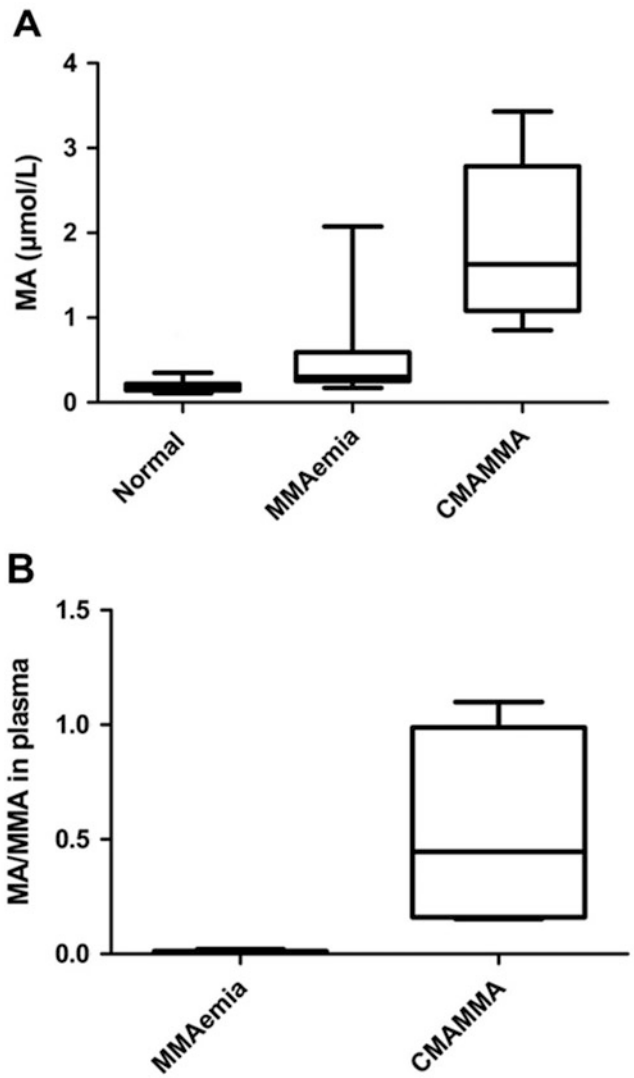

Fig. 4 (**a**) *Box plots* showing MA in plasma (µmol/L) in control subjects, patients with MMAemia and in the two patients with CMAMMA. (**b**) MA/MMA ratio in plasma in both patient groups. Shown are the median and 5th–95th percentile

Sain-van der Velden et al. 2015), allowing no extra material and costs for follow-up. Our upper limit of MA (0.79 µmol/L; $n = 87$) in control subjects quantified by UPLC-MS/MS is in good agreement with the upper limit reported using GC/MS (0.89 µmol/L; $n = 19$) (Sloan et al. 2011). There was a clear increase in MA concentration in patients diagnosed with mutations in the ACSF3 gene in comparison to control subjects (Fig. 4a).

Surprisingly, MA concentrations measured in plasma of patients with CMAMMA overlap with those measured in plasma samples from patients with classic MMAemia (Fig. 4a). Plasma MA concentration in three different samples (from two different patients) with classic MMAemia was above the upper limit of control samples (Fig. 4a).

Of interest is the observation that increased excretion of both MA and MMA is observed in patients with MCD (de Wit et al. 2006). It is speculated that MCD deficiency causes an excess of intramitochondrial malonyl-CoA, leading to the inhibition of methylmalonyl-CoA mutase and, subsequently, an increase in MMA (Alfares et al. 2011). We speculate that the opposite is true in classic MMAemia. Indeed, the plasma samples with the highest MMA concentration showed the highest MA in plasma. When calculating MA/MMA ratio in plasma, it is possible to fully discriminate between CMAMMA and classic MMAemia (Fig. 4b). The MMAemia contained both patients on vitamin B12 (responders) as well as non-responders to stress the discriminatory power of the MA/MMA ratio.

The prevalence of CMAMMA due to mutation in ACSF3 gene is not known. Given the normal concentration of propionyl (C3) carnitine in CMAMMA patients (Alfares

et al. 2011; Sloan et al. 2011), this disorder will not be detected by the current dried blood spot newborn screening. Only when MMA or MA are used as primary screening markers, detection of these patients is feasible. Screening for MCD deficiency is possible on C3DC-carnitine and other acylcarnitine ratios (McHugh et al. 2011). Given the difficulty with diagnosis, we suspect that CMAMMA is an under-recognized condition.

The high calculated incidence and the presence of asymptomatic patients (Alfares et al. 2011) leave room for the possibility that CMAMMA is a biochemical condition rather than a disease (Levtova et al. 2015), similar to SCAD deficiency (Pedersen et al. 2008) and, possibly, 3 methylcrotonylglycinuria (3MCC deficiency) (Lam et al. 2013), and screening for this disorder is then not justified. Alternatively, CMAMMA may be perceived as a risk factor rather than a disease, which could lead to clinical symptoms in combination with other genetic and/or environmental factors. The cases described here are compatible with this concept: in case of CMAMMA, certain infections may be important triggers, which provoke metabolic dysregulation. Understanding of this rare condition, e.g., by identifying factors involved in triggering the development of symptoms, will improve as more patients are identified.

In conclusion, the clinical spectrum of CMAMMA may include childhood psychiatric features. CMAMMA due to mutation in ACSF3 gene could be misdiagnosed as a classic MMAemia when urine is used as the sole matrix. Plasma MA/MMA ratio can serve as fast diagnostic tool for detection of CMAMMA. With early diagnosis of CMAMMA, additional investigation or unnecessary treatment (vitamin B12) can be avoided.

Acknowledgments We like to thank Martina de Barse and Karen van Baal.

Take-Home Message

Childhood psychiatric presentation can be added to the clinical spectrum of CMAMMA, a disorder which can easily be diagnosed by calculation the MA/MMA ratio in plasma.

Compliance with Ethics Guidelines

Conflict of Interest

Monique G.M. de Sain-van der Velden, Maria van der Ham, Judith J. Jans, Gepke Visser, Hubertus C.M.T. Prinsen, Nanda M. Verhoeven-Duif, Koen L. I. van Gassen, and Peter M. van Hasselt declare that they have no conflict of interest.

Informed Consent

All procedures followed were in accordance with the ethical standards of the responsible committee on human experimentation (institutional and national) and with the Helsinki Declaration of 1975, as revised in 2000 (5). Informed consent was obtained from all patients for being included in the study.

Animal Rights

This article does not contain any studies with animal subjects.

Details of the Contributions of Individual Authors

Monique G.M. de Sain-van der Velden and Peter M. van Hasselt were involved in conception and design, analysis and interpretation of data, and drafting the article.

Maria van der Ham was involved in conception and design, analysis and interpretation of data, and revising it critically for important intellectual content.

Koen L. I. van Gassen was involved in analysis and interpretation of data and revising it critically for important intellectual content.

Judith J. Jans, Gepke Visser, Hubertus C.M.T. Prinsen, and Nanda M. Verhoeven-Duif were involved in interpretation of data and revising it critically for important intellectual content.

References

Alfares A, Nunez LD, Al-Thihli K et al (2011) Combined malonic and methylmalonic aciduria: exome sequencing reveals mutations in the ACSF3 gene in patients with a non-classic phenotype. J Med Genet 48:602–605

de Sain-van der Velden MG, van der Ham M, Jans JJ et al (2015) Suitability of methylmalonic acid and total homocysteine analysis in dried bloodspots. Anal Chim Acta 853:435–441

de Wit MC, de Coo IF, Verbeek E et al (2006) Brain abnormalities in a case of malonyl-CoA decarboxylase deficiency. Mol Genet Metab 87:102–106

Honour JW (2011) Development and validation of a quantitative assay based on tandem mass spectrometry. Ann Clin Biochem 48:97–111

Lam C, Carter JM, Cederbaum SD et al (2013) Analysis of cases of 3-methylcrotonyl CoA carboxylase deficiency (3-MCCD) in the California newborn screening program reported in the state database. Mol Genet Metab 110:477–483

Levtova A, WatersP J, Buhas D et al (2015) Combined malonic and methylmalonic aciduria due to ACSF3 deficiency (CMAMMA) is probably a benign condition. J Inherit Metab Dis 38(Suppl 1):S2

McHugh D, Cameron CA, Abdenur JE et al (2011) Clinical validation of cutoff target ranges in newborn screening of metabolic disorders by tandem mass spectrometry: a worldwide collaborative project. Genet Med 13:230–254

Pedersen CB, Kolvraa S, Kolvraa A et al (2008) The ACADS gene variation spectrum in 114 patients with short-chain acyl-CoA dehydrogenase (SCAD) deficiency is dominated by missense variations leading to protein misfolding at the cellular level. Hum Genet 124:43–56

Sloan JL, Johnston JJ, Manoli I et al (2011) Exome sequencing identifies ACSF3 as a cause of combined malonic and methylmalonic aciduria. Nat Genet 43:883–886

JIMD Reports
DOI 10.1007/8904_2016_533

RESEARCH REPORT

Pilot Experience with an External Quality Assurance Scheme for Acylcarnitines in Plasma/Serum

P. Ruiz Sala • G. Ruijter • C. Acquaviva • A. Chabli • M.G.M. de Sain-van der Velden • J. Garcia-Villoria • M.R. Heiner-Fokkema • E. Jeannesson-Thivisol • K. Leckstrom • L. Franzson • G. Lynes • J. Olesen • W. Onkenhout • P. Petrou • A. Drousiotou • A. Ribes • C. Vianey-Saban • B. Merinero

Received: 15 September 2015 / Revised: 17 December 2015 / Accepted: 18 December 2015 / Published online: 23 February 2016

Abstract The analysis of acylcarnitines (AC) in plasma/serum is established as a useful test for the biochemical diagnosis and the monitoring of treatment of organic acidurias and fatty acid oxidation defects. External quality assurance (EQA) for qualitative and quantitative AC is offered by ERNDIM and CDC in dried blood spots but not in plasma/serum samples. A pilot interlaboratory comparison between 14 European laboratories was performed over 3 years using serum/plasma samples from patients with an established diagnosis of an organic aciduria or fatty acid oxidation defect. Twenty-three different samples with a short clinical description were circulated. Participants were asked to specify the method used to analyze diagnostic AC, to give quantitative data for diagnostic AC with the corresponding reference values, possible diagnosis, and advice for further investigations.

Although the reference and pathological concentrations of AC varied among laboratories, elevated marker AC for propionic acidemia, isovaleric acidemia, medium-chain acyl-CoA dehydrogenase, very long-chain acyl-CoA dehydrogenase, and multiple acyl-CoA dehydrogenase defi-

Communicated by: Brian Fowler, PhD

Competing interests: None declared

P.R. Sala · B. Merinero (✉)
Centro de Diagnóstico de Enfermedades Moleculares, Universidad Autónoma de Madrid, IDIPAZ, CIBER de Enfermedades Raras, 28049 Madrid, Spain
e-mail: bmerinero@cbm.csic.es

G. Ruijter
Department of Clinical Genetics, Erasmus Medical Centre, Rotterdam, The Netherlands

C. Acquaviva · C. Vianey-Saban
Service Maladies Héréditaires du Métabolisme, Centre de Biologie et Pathologie Est, Lyon, France

A. Chabli
Biochimie métabolomique et protéomique, Hopital Necker Enfants Malades, Paris, France

M.G.M. de Sain-van der Velden
Department of Medical Genetics, University Medical Centre Utrecht, Utrecht, The Netherlands

J. Garcia-Villoria · A. Ribes
Department of Biochemistry and Molecular Genetics, Div Inborn Errors Metab, Hospital Clinic, IDIBAPS, CIBERER, Barcelona, Spain

M.R. Heiner-Fokkema
Department of Laboratory Medicine, University Medical Centre Groningen, Groningen, The Netherlands

E. Jeannesson-Thivisol
Service de Biochimie et Biologie Moléculaire, CHU de Nancy, Vandoeuvre-Nancy, France

K. Leckstrom
Department Clinical Chemistry, Sahlgrenska University Hospital, Gothenburg, Sweden

L. Franzson
Department of Genetics and Molecular Medicine, Landspitali, Reykjavik, Iceland

G. Lynes
Neurometabolic Unit, National Hospital for Neurology and Neurosurgery, London, UK

J. Olesen
Department of Clinical Genetics, Copenhagen University Hospital, Copenhagen, Denmark

W. Onkenhout
Department of Clinical Chemistry and Laboratory Medicine, Leiden University Medical Centre, Leiden, The Netherlands

P. Petrou · A. Drousiotou
Department of Biochemical Genetics, The Cyprus Institute of Neurology and Genetics, Nicosia, Cyprus

ciencies were correctly identified by all participants allowing the diagnosis of these diseases. Conversely, the increased concentrations of dicarboxylic AC were not always identified, and therefore the correct diagnosis was not reach by some participants, as exemplified in cases of malonic aciduria and 3-hydroxy-3-methylglutaryl-CoA lyase deficiency. Misinterpretation occurred in those laboratories that used multiple-reaction monitoring acquisition mode, did not derivatize, or did not separate isomers. However, some of these laboratories suggested further analyses to clarify the diagnosis.

This pilot experience highlights the importance of an EQA scheme for AC in plasma.

Introduction

Acylcarnitines (AC) are esters formed by conjugation of acyl-CoAs and free carnitine by means of carnitine acyl transferases with different substrate specificities, either involved in the mitochondrial β-oxidation of fatty acids or in branched-chain amino acids catabolism. When acyl-CoAs accumulate in the mitochondrial matrix due to a specific metabolic disease, AC formation is favored, and then accumulation of AC in all physiological fluids reflects the mitochondrial acyl-CoA status. Consequently, the analysis of AC provides indirect evidence of mitochondrial metabolism (Bohles et al. 1994; Sewell and Bohles 1995).

The development of tandem mass spectrometry (MS/MS) facilitated the analysis of these compounds in the 1990s (Millington et al. 1990; Vreken et al. 1999). The recognition of disease-specific AC profiles in plasma and urine has proven very useful for the biochemical diagnosis and/or treatment monitoring of organic acidurias and fatty acid oxidation (FAO) defects, and therefore AC have become an important part of the investigation of inherited metabolic diseases in the biochemical genetic laboratories. Analysis of AC by MS/MS is also used in the expanded neonatal screening programs of many countries using dried blood spots (DBS) (McHugh et al. 2011).

More recently, there has been an increasing demand for satisfactory quality assurance in the biochemical genetic laboratories including external quality control to guarantee comparability of results between different centers (Fowler et al. 2008). Both institutions European Research Network for evaluation and improvement of screening, Diagnosis and treatment of Inborn Errors of Metabolism (ERNDIM, www.erndim.org) and Centers for Disease Control and Prevention (CDC, www.cdc.gov) offer excellent external quality assurance (EQA) schemes for qualitative and quantitative analysis of AC in DBS, respectively. The ERNDIM EQA scheme is probably more suitable for biochemical genetic laboratories, while the program of CDC is more useful for neonatal screening programs, where measurement of diagnostic AC is crucial for the identification of the diseases in asymptomatic neonates. However, AC are often determined in plasma or serum samples in biochemical genetic centers. Although quantitative analysis of a limited number of commercially available AC in serum has been introduced recently (ERNDIM Special Assays Serum scheme), so far no qualitative/interpretative EQA scheme exists for a comprehensive range of AC in plasma/serum samples. This study considers a pilot interlaboratory comparison between 14 European centers carried out between 2012 and 2014, by circulating plasma/serum samples from a range of well-defined FAO defects and organic acidurias in order to evaluate the analytical performance and interpretation of AC.

Samples and Methods

Samples

Twenty-three authentic serum or plasma samples from patients with one of the following eighteen different defects were used: five FAO defects [carnitine acylcarnitine translocase (CACT), long-chain 3-hydroxyacyl-CoA dehydrogenase (LCHAD), multiple acyl-CoA dehydrogenase (MAD), medium-chain acyl-CoA dehydrogenase (MCAD), very long-chain acyl-CoA dehydrogenase (VLCAD)], 12 organic acidurias [ethylmalonic encephalopathy (ETHE1), glutaric aciduria type I (GAI), holocarboxylase synthetase deficiency (HCS), 3-hydroxy-3-methylglutaryl-CoA lyase deficiency (HMGL), isobutyryl-CoA dehydrogenase deficiency (IBDH), isovaleric acidemia (IVA), β-ketothiolase deficiency (β-KT), malonic aciduria (MA), methylcrotonyl-CoA carboxylase deficiency (MCC), methylmalonic aciduria (MMA), combined methylmalonic aciduria and homocystinuria (MMA + Hcys), propionic acidemia (PA)], and one plasma sample from a patient affected with a combined defect of short-chain acyl-CoA dehydrogenase (SCAD) and IVA (SCAD + IVA). Diagnoses were confirmed biochemically, by enzyme testing and/or mutation analysis. Most cases were receiving L-carnitine supplementation at the time of sampling. Some defects were circulated twice to evaluate reproducibility of performance.

De-identified plasma samples, stored at −20°C over several years, were pooled together from samples remaining after analysis for diagnosis or treatment monitoring. Aliquots (60 μL), each with a short clinical description, were circulated twice a year at room temperature by regular mail from Madrid or Copenhagen to the different participants between 2012 and 2014. Samples were received by the participants within 2–7 days. Instructions were given that samples should be assayed within 5 days or should be frozen at −20°C until assay. Two aliquots from the samples

Table 1 List of acylcarnitine (AC) isomers without or with derivatization involved in this scheme

Underivatized			Derivatized		
m/z	Notation	AC	*m/z*	Notation	AC
232	C4	Butyryl Isobutyryl	288	C4	Butyryl Isobutyryl
244	C5:1	Tiglyl 3-Methylcrotonyl	300	C5:1	Tiglyl 3-Methylcrotonyl
246	C5:0	Isovaleryl 2-Methylbutyryl-(D+L) Pivaloyl	302	C5:0	Isovaleryl 2-Methylbutyryl-(D+L) Pivaloyl
248	C3DC C4OH	Malonyl 3-Hydroxybutyryl	360 304	C3DC C4OH	Malonyl 3-Hydroxybutyryl
262	C4DC	Methylmalonyl-(D + L) Succinyl	374	C4DC	Methylmalonyl-(D+L) Succinyl
	C5OH	3-Hydroxyisovaleryl 2-Methyl-3-hydroxybutyryl	318	C5OH	3-Hydroxyisovaleryl 2-Methyl-3-hydroxybutyryl
276	C5DC C6OH	Glutaryl Hydroxyhexanoyl	388	C5DC C10OH	Glutaryl Hydroxydecanoyl
290	C6DC	Methylglutaryl Adipyl	402	C6DC	Methylglutaryl Adipyl

(VLCAD/2013 and GAI/2014) were lost during transport and could not be analyzed by two laboratories.

Fourteen centers participated in this study: four laboratories studied all 23 samples from the beginning; then more laboratories progressively joined our program; thus, four laboratories analyzed 20 samples; one lab analyzed 11 samples; three analyzed seven samples and two additional laboratories only three samples.

AC Analytical Methods

Participants were asked to specify the method used, to give quantitative results for the AC relevant to the diagnosis with their corresponding reference values, the probable diagnosis and advice for further investigations. As in other qualitative/interpretative ERNDIM schemes, results were required to be returned within 3 weeks of receipt of the samples. On completion of each survey, a report was sent to participants to enable them to evaluate their own results.

All laboratories analyzed acylcarnitines by tandem mass spectrometry (MS/MS): 6/14 used custom-made or commercial mixes of deuterated AC (Chromsystems, Cambridge Isotope Laboratories, or PerkinElmer) to quantify samples (one-point calibration), and only two of them included deuterated glutarylcarnitine (C5DC); 3/14 used external calibration with unlabeled AC and some deuterated AC as internal standards; one lab used a combined methodology, and the remainder did not inform about the standards or the quantification method used.

Eight of fourteen laboratories analyzed the AC as butylated derivatives, five of fourteen analyzed them underivatized, and one lab analyzed both forms, butylated and underivatized acylcarnitines. Table 1 shows the list of AC isomers and differences in their identification by both methods. Nine of the fourteen laboratories used full-scan precursor ion acquisition mode, and 5/14 laboratories used the multiple-reaction monitoring (MRM) mode.

One lab included the separation of the short-chain isomers in its routine method, and two other laboratories only performed it when they considered necessary.

The presence of the marker AC was checked immediately before sending the samples to the participants and after 7 days by leaving the samples at room temperature, mimicking the transport conditions.

Results

The concentration variations of the AC in some problematic samples before sending and after 7 days at room temperature are presented in Table 2. Considerable differences in AC concentrations between the two measurements were observed in some samples, but in most cases the decreases in the AC concentrations did not prevent diagnosis. Two exceptions were the samples LCHAD/2012 and MMA + Hcys/2014. In these samples some of the diagnostically relevant AC were within the control range after 7 days at room temperature.

Table 2 Marker acylcarnitines (AC) before sending the samples and after 7 days at room temperature in some problematic samples (data are from Madrid)

Disease/year	Main marker AC	Day 0 (μmol/L)	Day 7 at room temperatures (μmol/L)	Upper reference level (μmol/L)
ETHE1/2014	C4	1.14	0.88	0.48
	C5	0.59	0.45	0.20
GAI/2012	C5DC	2.40	1.0	0.33
GAI/2014	C5DC	0.77	0.66	0.33
HMGL/2012	C5OH	0.11	0.13	0.05
	C6DC	0.15	0.21	0.04
HMGL/2014	C5OH	0.29	0.23	0.05
	C6DC	0.11	0.11	0.04
LCHAD/2012	C14OH	0.09	0.03	0.02
	C16OH	0.45	0.10	0.03
	C18:1OH	0.20	0.03	0.11
	C18OH	0.39	0.07	0.01
MA/2013	C3DC	0.66	0.71	0.04
MA/2014	C3DC	0.59	0.54	0.04
MMA/2012	C3	17.64	8.04	0.89
	C4DC	0.38	0.44	0.05
MMA+Hcys/2014	C3	1.09	0.65	0.89
	C4DC	0.11	0.09	0.05

ETHE1 ethylmalonic encephalopathy, *GAI* glutaric aciduria type I, *HMGL* 3-hydroxy-3-methylglutaryl-CoA lyase deficiency, *LCHAD* long-chain 3-hydroxyacyl-CoA dehydrogenase deficiency, *MA* malonic aciduria, *MMA* methylmalonic aciduria, *MMA+Hcys* combined methylmalonic aciduria and homocystinuria

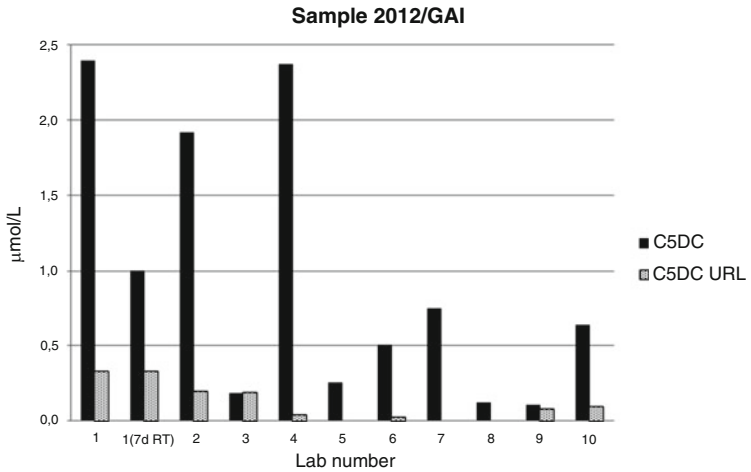

Fig. 1 Pathological and reference values for C5DC in sample GAI/2012 in the different participant laboratories. *URL* upper reference level, *RT* room temperature

Analytical Performance

Reference values and pathological concentrations of AC measured varied considerably among laboratories. Figure 1 shows pathological and reference values for C5DC, marker for GAI, as an example of the variation between participants.

The increases of the following species, C3 (PA); C5:0 (IVA); C5:1 and C5OH (β-KT); C8:0, C10:1 and C10:0 (MCAD); C14:1 (VLCAD); C5-C18 (MADD); C16OH and C18:1OH (LCHAD); C16:0 and C18:1 (CACT); and C4:0 and C5:0 (ETHE1 or SCAD + IVA), were correctly identified by all laboratories (Table 3). Only two laboratories separated the isomers of C5:0, confirming the

Table 3 External quality assurance pilot study of acylcarnitines (AC) in serum/plasma

Disease/year	Main marker AC	Concentrations of AC expressed as mean ± SD (range) (μmol/L)	Correct identification of the main marker AC/ total number of participants	Correct interpretation of the diagnosis/total number of participants	Diagnosis missed by labs using derivatized AC	Diagnosis missed by labs using underivatized AC
PA/2013	C3	39 ± 16 (24–67)	8/8	8/8	None	None
IVA/2012	C5:0	14.4 ± 1.1 (13.4–16)	4/4	4/4	None	None
β-KT/2013	C5:1	0.66 ± 0.24 (0.46–1.15)	7/8: C5:1 and C5OH	8/8	None	None
	C5OH	0.35 ± 0.15 (0.14–0.53)	1/8: C5:1			
β-KT/2014	C5:1	0.75 ± 0.74 (0.47–1.29)	12/12	12/12	None	None
	C5OH	0.39 ± 0.24 (0.23–1.13)				
MCAD/2012	C8:0	5.3 ± 2.4 (3.3–8.6)	4/4	4/4	None	None
	C10:1	1.75 ± 0.71 (1.3–2.8)				
VLCAD/2013	C14:1	0.82 ± 0.32 (0.52–1.49)	7/7	7/7	None	None
MAD/2013	C5:0	1.45 ± 0.46 (0.7–2.1)	8/8	8/8	None	None
	C8:0	1.69 ± 0.51 (1.02–2.04)				
	C10:0	2.8 ± 1.4 (1.3–4.9)				
LCHAD/2012	C16OH	0.27 ± 0.12 (0.07–0.45)	10/10	8/10: LCHAD/MTP	None	None
	C18:1OH	0.21 ± 0.16 (0.01–0.56)		2/10: LCHAD		
CACT/2013	C16:0	2.6 ± 0.5 (1.9–3.3)	8/8	6/8: CPTII/CACT	None	None
	C18:1	2.5 ± 0.4 (2.1–3.2)		2/8: CPTII		
ETHE1/2014	C4:0	1.5 ± 0.5 (0.98–2.8)	12/12	11/12	1[a]/9[a]	1[a]/5[a]
	C5:0	0.54 ± 0.15 (0.38–0.75)				
SCAD + IVA/ 2014	C4:0	6.8 ± 3.2 (4.2–12.5)	8/9: C4:0 and C5:0	4/9: SCAD and IVA	3/5	2/4
	C5:0	12.5 ± 3.5 (7.8–17.5)	1/9: C5:0			
IBDH/2014	isoC4 or C4	0.77 ± 0.26 (0.47–1.3)	6/9: C4 (only 2 as isoC4)	4/9: IBDH	3/5	2/4
HCS/2014	C3	1.2 ± 0.6 (0.83–2.1)	5/9: C3 + C5OH	3/9: HCS	5/5	1/4
	C5OH	0.39 ± 0.35 (0.25–1.17)	3/9: C5OH or C3			
MCC/2014	C5OH	5.5 ± 2.3 (1.2–7.8)	7/9: C5OH + C5:1	7/9: MCC	1/5	1/4
	C5:1	0.05; 0.031	2/9: C5OH/C4DC			
MA/2013	C3DC	0.85 ± 0.88 (0.02–1.32)	4/8	5/8	1/5	2/3
			1/8: C3DC/C4OH			
MA/2014	C3DC	1.00 ± 1.04 (0.53–1.51)	9/12	10/12	0/9[a]	2/5[a]
			1/12: C3DC/C4OH			
MMA/2012	C3	17.9 ± 3.3 (12.8–23.6)	8/10: C3 + C4DC	8/10	2/7	0/3
	C4DC	1.5 ± 2.1 (0.12–6.81)	2/10: C5OH/C4DC			
MMA/2014	C3	13.1 ± 2.9 (8–15.4)	10/12: C3 + C4DC	12/12	None	None
	C4DC	0.73 ± 0.48 (0.12–1.77)	2/12: C5OH/C4DC			
MMA+Hcys/ 2014	C3	1.2 ± 0.3 (0.78–1.6)	7/12: C3 + C4DC	7/12	3[a]/9[a]	3[a]/5[a]
	C4DC	0.33 ± 0.21 (0.11–0.62)	5/12: C3 or C4DC			

(continued)

Table 3 (continued)

Disease/year	Main marker AC	Concentrations of AC expressed as mean ± SD (range) (μmol/L)	Correct identification of the main marker AC/ total number of participants	Correct interpretation of the diagnosis/total number of participants	Diagnosis missed by labs using derivatized AC	Diagnosis missed by labs using underivatized AC
GAI/2012	C5DC	0.93 ± 0.93 (0.11–2.4)	9/10	10/10	None	None
GAI/2014	C5DC	0.41 ± 0.66 (0.11–0.77)	10/11	10/11	0/8[a]	1/5[a]
HMGL/2012	C5OH	0.25 ± 0.19 (0.11–0.53)	3/4: C5OH + C6DC	3/4	0/2	1/2
	C6DC	0.88 ± 0.84 (0.15–1.8)	1/4: C5OH			
HMGL/2014	C5OH	0.34 ± 0.09 (0.25–0.62)	9/12: C5OH + C6DC	9/12	0/9[a]	3/5[a]
	C6DC	0.29 ± 0.26 (0.8–0.92)	3/12: C5OH			

CACT carnitine acylcarnitine translocase deficiency, *CPTII* carnitine palmitoyl-CoA transferase type II deficiency, *ETHE1* ethylmalonic encephalopathy, *GAI* glutaric aciduria type I, *HCS* holocarboxylase synthetase deficiency, *HMGL* 3-hydroxy-3-methylglutaryl-CoA lyase deficiency, *IBDH* isobutyryl-CoA dehydrogenase deficiency, *IVA* isovaleric acidemia, β-*KT* β-ketothiolase deficiency, *LCHAD* long-chain 3-hydroxyacyl-CoA dehydrogenase deficiency, *MA* malonic aciduria, *MAD* multiple acyl-CoA dehydrogenase deficiency, *MCAD* medium-chain acyl-CoA dehydrogenase deficiency, *MCC* methylcrotonyl-CoA carboxylase deficiency, *MMA* methylmalonic aciduria, *MMA+Hcys* combined methylmalonic aciduria and homocystinuria, *MTP* mitochondrial trifunctional protein deficiency, *PA* propionic acidemia, *SCAD+IVA* combined defect of short-chain acyl-CoA dehydrogenase and IVA, *VLCAD* very long-chain acyl-CoA dehydrogenase deficiency

[a] One lab used combined methodology (butylated and underivatized AC)

elevation of isovalerylcarnitine in the samples instead of the other two C5:0 species 2-methylbutyrylcarnitine or pivaloylcarnitine.

Considering the quantitative results, it is interesting to note that the pathological levels of C5:0, C16 + C18:1, and those of C3 between 10 and 20 μmol/L (in MMA cases) were very similar in most laboratories. However, when C3 was lower than 5 μmol/L (as in the HCS case) or higher than 20 μmol/L (as in the PA case), the pathological levels varied from 0.83 to 2.1 μmol/L and from 24 to 67 μmol/L, respectively. These differences seem unrelated to the quantification methods used or to the derivatization of AC. The use of the same commercial mix of deuterated AC did not assure similar values.

On the other hand the isolated increase of C4 in the IBDH sample was not consistently identified, and only two laboratories identified isobutyrylcarnitine (isoC4) by separation of isomers (Fig. 2). Another difficult sample was that of HCS where the slightly elevated levels of C3 and C5OH were not detected by some laboratories.

The analytical performance of the dicarboxylic acylcarnitines (C3DC, C4DC, C5DC, and C6DC) was clearly unsatisfactory. One MA sample was circulated twice since some participants failed to correctly identify C3DC in the first round. In the second survey, we observed that two laboratories repeated the failure, because either C3DC was still not included in MRM acquisition or because C3DC and C4OH were isobaric in the underivatized method; consequently, relatively high reference values were in place (see Table 1).

Similarly one laboratory, which failed to identify C6DC in the first round because the MRM acquisition did not contain the transition for C6DC, did not modify the acquisition parameters between circulations. This resulted in a repeat failure with the second circulation of this sample.

Difficulty in the recognition of the abnormal profile (increases of C3 and C4DC) in three MMA samples (two mutase defects and one combined MMA and Hcys) was also observed. Only one laboratory routinely separates isomers of C4DC (D- and L-methylmalonyl carnitines and succinylcarnitine). The other two laboratories that were able to separate them did not use it in these samples. In the case of MMA + Hcys, both marker AC were only marginally elevated after 1 week at room temperature (Table 2), which could explain both the great dispersion in the quantitative results and the interpretation of this sample. In the other two MMA samples, the increases of C3 and C4DC were easily recognized by 8/10 and 10/12 laboratories, whereas 4/22 analyzing underivatized AC were unable to distinguish between C5OH and C4DC (Table 3).

The increase of C5DC in two GAI samples from low-excretor patients was detected by 86% of the participants. A wide range of reference and pathological C5DC levels was

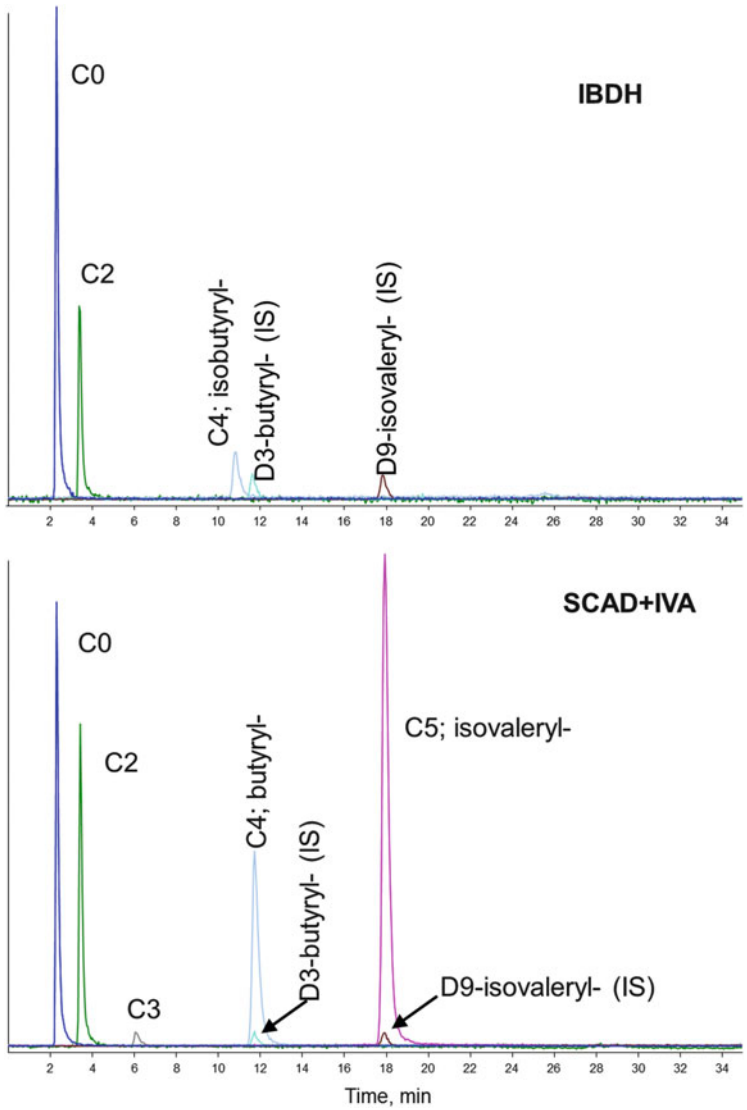

Fig. 2 Separation of isomers in IBDH deficiency and a combined defect of SCAD and IVA by HPLC/MS/MS as described by Ferrer et al. (2007). *IS* internal standard. Chromatograms from lab in Madrid

observed (Fig. 1) that seemed not to be related either to methodological aspects of the analysis, the use of deuterated C5DC as internal standard, or the inclusion of the derivatization step. C5DC was still not included in the list of AC acquired by MRM in one lab in the second round (sample GAI/2014), leading to a wrong diagnosis.

Interpretation

The diagnosis of PA, IVA, β-KT, MCAD, VLCAD, and MADD was reached by all participants (Table 3). Despite correct identification by all laboratories of [C16OH and C18:1OH] and [C16 and C18:1], markers for LCHAD/MTP defects and CPTII/CACT defects, respectively, some laboratories suggested only one of the two possible defects as possible diagnosis. Despite problems with the identification of C5DC, diagnosis of GAI was suggested by one participant based on the clinical information. Although most of the participants identified the marker AC of MMA (C3 and C4DC), two laboratories overlooked the increase of C4DC, and interpretation was correct in 20/22 cases.

Diagnostic proficiency was poor in cases of MA, HMGL, IBDH, combined SCAD + IVA defect, and a mild form of HCS. In the case of MA, a slight improvement in performance was observed in the second circulation. The interpretation was correct in 62.5% and 83% in the first and second round, respectively. In the case of HMGL, no improvement in performance was observed in samples that were circulated twice, with the same diagnostic proficiency

of 75% in both rounds. In these two diseases, two laboratories either did not include C3DC and C6DC in the list of AC acquired by MRM or did not review their reference values between the two circulations, making it difficult to reach a correct interpretation. In the case of IBDH, the increase of C4 was identified by six out of nine laboratories, but only four of them suggested the diagnosis of IBDH/SCAD, while the remaining two only suggested an SCAD defect. In the case of a combined defect SCAD + IVA, despite the correct identification of raised C4 and C5 AC by all but one laboratory (which overlooked the increase of C4), the correct diagnosis was only achieved by 4/9, the remaining suggested IVA or MADD. Due to the rarity of this combined defect and being unable to separate isomers, some laboratories suggested an SCAD defect combined with pivaloyl carnitine derived from treatment. In the HCS sample, the diagnostic significance of the slightly elevated levels of C3 and C5OH was not recognized by most laboratories resulting in an incorrect diagnosis.

Misinterpretation occurred mainly in those laboratories with analytical issues, namely, those that did not derivatize (due to isobaric AC species rather than sensitivity), did not separate isomers, failed to include some MRM pairs in the MRM acquisition list, or did not consider the concentrations of diagnostically significant AC to be raised against their reference values. However, some laboratories with good analytical performance failed in the interpretation, possibly because of inexperience with these rarer conditions, and they overlooked pointers in the clinical data, e.g., the combined defect of SCAD + IVA or the mild form of HCS. Generally laboratories correctly suggested further analyses such as organic acid analysis in urine to confirm a diagnosis.

Discussion

This pilot study demonstrates that the identification of the monocarboxylic AC is not a major problem in most laboratories despite the interlaboratory variation in quantitative results and reference values. Conversely, the identification of the dicarboxylic AC presented some difficulties, both in analytical performance and interpretation. In this pilot scheme, some causes of poor analytical performance have been identified; however, other pitfalls and problems in these methodologies have been reported previously and should also be considered, e.g., appropriate conditions of butylation, half-life of the butyl esters, or the hydrolysis of acylcarnitines to free carnitine (Johnson 1999). Therefore, it is essential to be aware of all the relevant AC markers, and where MRM acquisition mode is used, the specific transitions of these AC should be included in the experiment. Laboratories should also be aware that the number of isobaric AC of interest is greater without derivatization than with derivatization. Those laboratories that include a derivatization step should be careful with the reaction conditions and the elapsed time until the MS/MS analysis. For a comprehensive analysis, isomer separation by HPLC/MS/MS is necessary in cases where the specific isomer present defines the diagnosis but not always if the overall AC profile is sufficient to infer the biochemical diagnosis. Finally, single-point calibration methods are faster and less laborious, but accuracy and/or precision can be sacrificed where the concentration analyte is considerably different to that of the internal standard used for quantitation.

In order to improve the analytical performance of AC analysis, some commercially available AC (C8, C5DC, C16, C18) have been included in the ERNDIM quantitative Special Assays in Serum (SAS) scheme starting in 2014, but it is still too early to evaluate the results. Further AC (C3 and C5) are planned to be added to the 2016 SAS distributions.

The interpretation of the pathological profiles of the common disorders (PA, IVA, β-KT, MCAD, MADD, and VLCAD) is, in general, well performed by most laboratories. However, some defects that are more prevalent in the Mediterranean area (like HMGL) or in North Europe (like the mild variant of HCS) are less well identified. This fact emphasizes the need of circulation of samples from such rare disorders as they offer a unique training resource in order to not overlook some diagnostic AC and miss the diagnosis (Bonham 2014).

Recently, a harmonized scoring system has been adopted by the ERNDIM Scientific Advisory Board for all interpretative schemes (two points for analytical performance and two points for interpretative proficiency). Since 2014 the concept of critical error has been introduced for the performance assessment for analytical or interpretative errors that would be unacceptable for most laboratories and would have serious adverse effects on patient management. If we had applied this concept here, those laboratories that misdiagnosed HCS, HMGL, or MA would be classified as poor performers.

Although the number of participants in this pilot experience was limited (only 14 laboratories), the feasibility of this scheme has been demonstrated during 3 years regarding sample suitability, stability, and robustness of result presentation and reporting. This work highlights the necessity of an analytical and interpretative ERNDIM EQA scheme for AC in plasma samples, being that ERNDIM supports the development of new EQA schemes as part of its activity (Fowler et al. 2008).

Acknowledgments We thank Mrs. A Sánchez for technical assistance in preparing the samples. We are grateful to the Scientific Advisory Board of ERNDIM for support and helpful discussions.

Sentence Take-Home Message

The need of external quality assurance programs for analysis of acylcarnitines in plasma is ascertained.

Details of the Contributions of Individual Authors

Conception and design: PRS, JO, BM
Analysis and interpretation of data: PRS, BM
Drafting the article or revising critically: PRS, GR, CA, JGV, LF, GL, WO, PP, AR, CVS, BM
Agreement to submission: all authors

Compliance with Ethics Guidelines

Conflict of Interest

P Ruiz Sala, G Ruijter, C Acquaviva, A Chabli, MGM de Sain-van der Velden, J Garcia-Villoria, MR Heiner-Fokkema, E Jeannesson-Thivisol, K Leckstrom, L Franzson, G Lynes, J Olesen, W Onkenhout, P Petrou, A Drousiotou, A Ribes, C Vianey-Saban, and B Merinero declare that they have no conflict of interest.

Informed Consent

Ethical approval for the use of residual anonymized patient samples in this study was granted from the institutional Ethics Committee of the Universidad Autónoma de Madrid.

Details of Funding

The authors confirm independence from the sponsors; the content of the article has not been influenced by the sponsors.

References

Bohles H, Evangeliou A, Bervoets K, Eckert I, Sewell A (1994) Carnitine esters in metabolic disease. Eur J Pediatr 153: S57–S61

Bonham JR (2014) The organisation of training for laboratory scientists in inherited metabolic disease, newborn screening and paediatric clinical chemistry. Clin Biochem 47:763–764

Ferrer I, Ruiz-Sala P, Vicente Y, Merinero B, Perez-Cerda C, Ugarte M (2007) Separation and identification of plasma short-chain acylcarnitine isomers by HPLC/MS/MS for the differential diagnosis of fatty acid oxidation defects and organic acidemias. J Chromatogr B Analyt Technol Biomed Life Sci 860:121–126

Fowler B, Burlina A, Kozich V, Vianey-Saban C (2008) Quality of analytical performance in inherited metabolic disorders: the role of ERNDIM. J Inherit Metab Dis 31:680–689

Johnson DW (1999) Inaccurate measurement of free carnitine by the electrospray tandem mass spectrometry screening method for blood spots. J Inherit Metab Dis 22:201–202

McHugh D, Cameron CA, Abdenur JE, Abdulrahman M, Adair O, Al Nuaimi SA, Ahlman H, Allen JJ, Antonozzi I, Archer S, Au S, Auray-Blais C, Baker M, Bamforth F, Beckmann K, Pino GB, Berberich SL, Binard R, Boemer F, Bonham J, Breen NN, Bryant SC, Caggana M, Caldwell SG, Camilot M, Campbell C, Carducci C, Bryant SC, Caggana M, Caldwell SG, Camilot M, Campbell C, Carducci C, Cariappa R, Carlisle C, Caruso U, Cassanello M, Castilla AM, Ramos DE, Chakraborty P, Chandrasekar R, Ramos AC, Cheillan D, Chien YH, Childs TA, Chrastina P, Sica YC, de Juan JA, Colandre ME, Espinoza VC, Corso G, Currier R, Cyr D, Czuczy N, D'Apolito O, Davis T, de Sain-Van der Velden MG, Delgado Pecellin C, Di Gangi IM, Di Stefano CM, Dotsikas Y, Downing M, Downs SM, Dy B, Dymerski M, Rueda I, Elvers B, Eaton R, Eckerd BM, El Mougy F, Eroh S, Espada M, Evans C, Fawbush S, Fijolek KF, Fisher L, Franzson L, Frazier DM, Garcia LR, Bermejo MS, Gavrilov D, Gerace R, Giordano G, Irazabal YG, Greed LC, Grier R, Grycki E, Gu X, Gulamali-Majid F, Hagar AF, Han L, Hannon WH, Haslip C, Hassan FA, He M, Hietala A, Himstedt L, Hoffman GL, Hoffman W, Hoggatt P et al (2011) Clinical validation of cutoff target ranges in newborn screening of metabolic disorders by tandem mass spectrometry: a worldwide collaborative project. Genet Med 13:230–254

Millington DS, Kodo N, Norwood DL, Roe CR (1990) Tandem mass spectrometry: a new method for acylcarnitine profiling with potential for neonatal screening for inborn errors of metabolism. J Inherit Metab Dis 13:321–324

Sewell AC, Bohles HJ (1995) Acylcarnitines in intermediary metabolism. Eur J Pediatr 154:871–877

Vreken P, van Lint AE, Bootsma AH, Overmars H, Wanders RJ, van Gennip AH (1999) Quantitative plasma acylcarnitine analysis using electrospray tandem mass spectrometry for the diagnosis of organic acidaemias and fatty acid oxidation defects. J Inherit Metab Dis 22:302–306

JIMD Reports
DOI 10.1007/8904_2016_538

CASE REPORT

ECHS1 Deficiency as a Cause of Severe Neonatal Lactic Acidosis

Rebecca D. Ganetzky • Kaitlyn Bloom • Rebecca Ahrens-Nicklas • Andrew Edmondson • Matthew A. Deardorff • Michael J. Bennett • Can Ficicioglu

Received: 19 November 2015 / Revised: 11 January 2016 / Accepted: 13 January 2016 / Published online: 27 February 2016

Abstract Mitochondrial short-chain enoyl-CoA hydratase deficiency (ECHS1D) is caused by mutations in *ECHS1* (OMIM 602292) and is a recently identified inborn error of valine and fatty acid metabolism. This defect leads to secondary mitochondrial dysfunction. The majority of previously reported patients had the Leigh syndrome, with a median life expectancy of approximately 2 years. We report two siblings born 3 years apart with prenatal findings including facial dysmorphia, oligohydramnios, intrauterine growth restriction, and premature delivery. They had severe lactic acidosis with onset within the first hours of life, had congenital dilated cardiomyopathy, and died at 16 h of life and 2 days of life, respectively.

Biochemical evaluation of these patients showed elevated butyryl-carnitine in the blood and elevated methylmalonyl/succinyl-CoA and decreased hydroxybutyryl-CoA in frozen liver of patient 2, confirming abnormal short-chain fatty acid metabolism. Elevated butyryl-carnitine has been reported only in a single previous case of ECHS1 deficiency, which also had neonatal onset. Pyruvate and lactate levels were both elevated with a normal pyruvate-lactate ratio. This supports the previous hypothesis that lactic acidosis in these patients results from secondary inhibition of the pyruvate dehydrogenase complex. The biomarker 2,3-dihydroxy-2-methylbutyric acid was detected in patient 2, but at lower levels than in previously reported cases.

These cases extend our understanding of the severe end of the phenotypic spectrum of ECHS1 deficiency, clarify the range of biochemical abnormalities associated with this new disorder, and highlight the need to suspect this disease in patients presenting with comparable metabolic derangements and dysmorphic features.

Communicated by: Jörn Oliver Sass

Competing interests: None declared

R.D. Ganetzky · R. Ahrens-Nicklas · A. Edmondson · M.A. Deardorff · C. Ficicioglu (✉)
Department of Pediatrics, Division of Human Genetics, The Children's Hospital of Philadelphia, Perelman School of Medicine at the University of Pennsylvania, 3501 Civic Center Blvd, Philadelphia, PA 19104, USA
e-mail: ficicioglu@email.chop.edu

K. Bloom · M.J. Bennett
Department of Pathology and Laboratory Medicine, Michael Palmieri Metabolic Disease Laboratory, The Children's Hospital of Philadelphia, Perelman School of Medicine at the University of Pennsylvania, Philadelphia, PA 19104, USA

Introduction

Mutations in *ECHS1* causing deficiency of the short-chain enoyl-CoA hydratase have been recently reported to cause an inborn error of valine and fatty acid metabolism resulting in the Leigh syndrome (Peters et al. 2014). In particular, the formation of the highly reactive metabolites methyacrylyl-CoA and acryloyl-CoA is suspected to be the primary cause of toxicity through secondary disruption of the pyruvate dehydrogenase complex and electron transport chain (Peters et al. 2014; Haack et al. 2015).

Nineteen families (21 patients) affected with ECHS1 deficiency have been reported to date (Peters et al. 2014; Ferdinandusse et al. 2015; Sakai et al. 2015; Haack et al. 2015; Tetreault et al. 2015; Yamada et al. 2015). Previously affected patients have had predominant features of lactic acidosis, epilepsy, and death at a young age. The age of onset has varied; however, most cases have presented in early infancy. The median age of reported cases at either

death or at time of report is 36 months (mean 69 months). Only two previously reported patients (who were siblings) died in the neonatal period (Ferdinandusse et al. 2015).

Here we report two children from a single family affected by severe ECHS1D with evidence of prenatal onset, preterm delivery, severe and rapid onset of metabolic acidosis, and death within the first 2 days of life. Given the rarity and relatively new discovery of ECHS1D as a cause of disease, the full spectrum of disease is still not well understood. The purpose of this report is to extend understanding of the severe end of the spectrum of ECHS1D.

Clinical Case Report

Patient 1

Patient 1 was born to non-consanguineous Caucasian parents via an urgent Cesarean section at 34 weeks of gestation following a pregnancy complicated by intrauterine growth restriction (IUGR) and severe oligohydramnios. Complete agenesis of the corpus callosum was detected in the prenatal period.

Kussmaul respiration developed around 1 h after birth and an arterial blood gas showed severe metabolic acidosis (pH 6.85, lactate 20.8 mmol/L.) Acidosis was refractory to multiple administrations of intravenous bicarbonate.

On exam, the infant was dysmorphic with epicanthus, low-set ears, long philtrum, and flat midface. He did not have the facial features of Potter's sequence. He was severely hypotensive. He had hypospadias, large joint contractures, and absence of flexion creases. Echocardiogram showed severe dilated cardiomyopathy.

Despite intravenous glucose, bicarbonate, multiple pressor support, nitrous oxide, and high flow oscillator ventilation, the infant persisted with severe hypotonia, then developed wide-complex bradycardia, and passed away at 16 h of life.

Acylcarnitine profile was remarkable for mildly elevated butyryl-carnitine (1.42 μmol/L; normal <1.00). A simultaneous draw of lactate and pyruvate showed an essentially preserved ratio (lactate 18.11 mM, normal <1.6; pyruvate 0.84 mM, normal <0.14; ratio 22, normal 10–20). Plasma amino acids showed a striking elevation of alanine (1,425 μmol/L; normal <571). Urine organic acids were unable to be obtained as the patient had lifelong anuria.

Whole mitochondrial sequencing and sequencing of 101 nuclear genes associated with mitochondrial disease were negative. Clinical whole-exome sequencing identified two variants in *ECHS1*: p. A3D (c.8C>A; predicted possibly damaging by PolyPhen-2 (Adzhubei et al. 2010) and predicted damaging by SIFT (Kumar et al. 2009)) and p. V130D (c.389T>A; predicted probably damaging by PolyPhen-2 and predicted damaging by SIFT), which were in *trans*. These rare mutations were seen in 0/11072 and 4/120696 alleles in the Exome Aggregation Consortium, respectively (http://exac.broadinstitute.org, accessed November 2015). No mutations in other genes were reported by whole-exome sequencing.

Patient 2

Patient 2 is the younger sister of patient 1. She was born via vaginal delivery at 29 weeks of gestation following a pregnancy complicated by IUGR and oligohydramnios. She had milder lactic acidosis following delivery (6.4 mmol/L; normal <1.6); however, it worsened throughout the first day of life to a peak of 14 mmol/L. She additionally had complications of prematurity, including bilateral intraventricular hemorrhage.

Due to the severity of disease seen in her brother, and the poor neurologic outcome portended by her intraventricular hemorrhage, the family elected to withdraw care at 24 h of life.

Autopsy was performed and showed dilated cardiomyopathy, hepatosplenomegaly, a preauricular tag, incomplete separation of the right upper and middle lung lobes, and two splenules. Kidney morphology was normal.

Her biochemical testing was similar to that of her deceased sibling, patient 1. She had a very subtle elevation of butyryl-carnitine (1.05 μmol/L; normal <1.00) and elevated alanine (738 μmol/L, normal <571). Urine organic acids showed elevation of 2,3-dihydroxy-2-methylbutyric acid to 10 mmol/mol creatinine (normal is below the limit of detection, which is 1 mmol/mol creatinine.) Molecular testing for the known familial mutation was confirmed that she carried both of the *ECHS1* mutations identified in her brother.

Although not all features were shared between these patients, they were felt to have the same underlying condition because of the clinical similarity (oligohydramnios, IUGR, and dilated cardiomyopathy), the biochemical similarity (neonatal lactic acidosis and elevated butyryl-carnitine), and their shared mutations in *ECHS1*, with overlap in phenotype with previously reported patients with ECHS1D.

Additional family history is notable for uncomplicated pregnancies delivering normally sized term infants for two unaffected full siblings of patient 1 and patient 2, one delivered prior to patient 1 and one between patient 1 and patient 2.

Material and Methods

Tissue Extraction for Acyl-CoA Analysis

Human liver tissues from patient 2 and control samples were collected and immediately flash frozen in liquid nitrogen. Acyl-CoA profiling on tissue samples was performed and analyzed for acyl-CoA species as previously described (Palladino et al. 2012). The patient and control samples were done in triplicate. Acyl-CoA profiling identifies long, medium, short, and 3-hydroxyacyl-CoA species in tissues using flow-injection tandem mass spectrometry. The complete acyl-CoA profiles are identified using neutral loss of m/z 507 (Palladino et al. 2012). The student's *t*-test was used for statistical analysis.

Results

Acyl-CoA Analysis

The free acyl-CoA profile demonstrated a pattern consistent with fasting in the liver. There was elevated methylmalonyl/succinyl-CoA (C4-DC) (patient (measure in triplicate), 1208 ± 736 nmol/g; control (measure in triplicate), 776 ± 136 nmol/g; $p = 0.2884$), although these results did not reach statistical significance. 3-Hydroxybutyryl-CoA (C4-OH) was significantly decreased (patient (measure in triplicate), 1456 ± 512 nmol/g; control (measure in triplicate), 5306.3 ± 958.6 nmol/g; $p = 0.0016$) using student's *t*-test. Although this result was significant, it was not replicated in the previously published patient (Ferdinandusse et al. 2015).

Discussion

Here we report two siblings with prenatal onset of ECHS1D manifesting as severe oligohydramnios resulting in fetal akinesia sequence, intrauterine growth retardation, and dysmorphic facial features reminiscent of fetal alcohol syndrome, as well as multiple minor anomalies including hypospadias and splenule formation. Severe and ultimately fatal biochemical deterioration occurred within the first day of life in both cases.

These siblings are the first reported cases of prenatal onset of disease in ECHS1D; compared to previously reported cases, their presentation and death occurred rapidly after birth (Table 1.) Despite previously reported intrafamilial variability, both of these patients had similar and severe manifestations. In their severity, these two cases extend the range of the previously reported phenotype associated with ECHS1D. The underlying genotype-phenotype correlation remains unclear. Both mutations in this case are missense mutations and do not alter import into the mitochondria, so the cause of their severity is not readily apparent (Claros and Vincens 1996). More cases will help clarify mutations associated with severe disease.

Striking components of the phenotype included dysmorphic features and multiple minor congenital anomalies. This underscores the importance of considering inborn errors of mitochondrial metabolism in children with structural anomalies. ECHS1D should be considered in children with dysmorphia or congenital anomalies and lactic acidosis.

Acyl-CoA profiling is a very sensitive assay used for identifying subtle changes in specific biomarkers linked to disease. The analysis of the CoA data for patient 2 indicated accumulation of the abnormal short-chain CoA species C4-DC and decreased C4-OH. One previously reported patient with ECHS1D on whom CoA analysis has been performed had similar results. The meaning of these findings is limited because of small number of patients, but over time collection of these data from additional patients will allow for identification of consistent variations that will contribute to our understanding of the pathobiochemistry of this disease.

Diagnosis in patient 1 was made by whole-exome sequencing; however, the biochemical diagnosis was strongly suspected in the second sibling due to elevations in butyryl-carnitine on the acylcarnitine profile and 2,3-dihydroxy-2-methylbutyric acid on urine organic acids. Elevated lactate and pyruvate with a preserved ratio in this case support the previously hypothesized mechanism of the disease: the inhibition of the pyruvate dehydrogenase enzyme (Peters et al. 2014). Elevated butyryl-carnitine was noted in the previously reported family with neonatal onset (Ferdinandusse et al. 2015), suggesting that this marker is more sensitive in the severe cohort. Taken together, these biochemical features suggest that this condition is diagnosable on standard biochemical testing,

Table 1 Clinical features of previously reported patients with ECHS1 deficiency

Reference	Current Pt 1	Current Pt 2	1 Peters et al. (2014)	2	3 Sakai et al. (2015)	4 Ferdinandusse et al. (2015)	5	6	7	8 Haack et al. (2015)	9	10	11	12	13
Onset	Prenatal	Prenatal	Birth	Birth	2 months	1 day	1 day	Early infancy	1 year	Birth	Birth	Birth	Birth	5 days	Birth
Dysmorphia	+	+/−	−	−	−	−	−	−	−	−	−	−	−	−	−
IUGR	++	+	−	−	−	−	−	−	−	−	−	−	−	−	−
Oligohydramnios	++	+	−	−	−	−	−	−	−	−	−	−	−	−	−
Premature delivery	(Emergent c-section)	+	−	−	−	−	−	−	−	−	−	−	−	−	−
Hypoplastic corpus callosum	++	−	+	−	−	−	−	+	−	−	−	−	+	+	−
Structural anomalies	Hypospadias	Splenules	−	VSD	−	−	Periventricular cysts	−	−	−	−	−	−	−	−
Neonatal lactic acidosis	+++	++	+	−	−	+	+	−	−	+++	+	+	−	++	−
Cardiomyopathy	DCM	DCM	−	HCM	−	Poor contractility	−	−	−	HCM	HCM	N/A	N/A	HCM	DCM
Acylcarnitine profile	Elevated C4	Elevated C4	Normal	Normal	Normal	Mild elevated C3, C4, C5	Elevated C3, C4	N/A	Elevated C4OH	Normal	Normal	Normal	N/A	Normal	Normal
Lactate	High	High	High	High	High	High	High	High	Intermittently high	High	High	High	N/A	High	High
Pyruvate	High	High	High	High	Nl	High	N/A	N/A	N/A	N/A	N/A	N/A	N/A	N/A	N/A
Lactate/pyruvate ratio	Nl	Nl	Nl	Nl	High	Nl									
Urinary 2-methyl, 2,3-dihydroxybutyrate	N/A	Small peak	1,560–2,500 µmol/mmol creatine	782–972 µmol/mmol creatine	−	N/A	Large peak	+, not quantified	+, not quanitied	Normal	229-fold ULN	N/A	N/A	39-fold ULN	Nl
Death	16 h	2 days	4 months	8 months	Alive at 4 years	24 h	2 days	Alive at 7 years	Alive at 1 year	4 months	11 months	2.3 years	7.5 years	Alive at 2 years	Alive at 3 years
Genetic mutation	c.8C>A/c.389T>A	c.8C>A/c.389T>A	c.414+3G>C/c.473T>C	c.414+3G>C/c.473T>C	c.2T>G/c.5C>T	c.817G>A/c.817G>A	c.817G>A/c.817G>A	c.433C>T/c.476A>G	c.673T>C c.674G>C	c.176A>G/c.476A>G	c.197T>C/c.449A>G	c.476A>G/c.476A>G	c.161G>A/c.817A>G	c.673T>C/c.673T>C	c.98T>C/c.176A>G
Protein effect	A3D/V130D	A3D/V130D	A158D/splicing	A158D/splicing	M1R/A2V	K273E/K273E	K273E/K273E	L145F/Q159R	C225R/C225S	N59S/Q159R	I66T/D150G	Q159R/Q159R	R54H/K273E	C225/C225R	F33S/N59S

Reference	14 Haack et al. (2015)	15	16	17	18 Yamada et al. (2015)	19	20 Tetreault et al. (2015)	21	22	23
Onset	2 years	1 year	18 months	11 months	10 months	7 months	2.5 months	2.9 years	10 months	6 months
Dysmorphia	−	+	−	−	−	−	−	−	−	−
IUGR	−	−	−	−	−	−	−	−	−	−
Oligohydramnios	−	−	−	−	−	−	−	−	−	−
Premature delivery	−	−	−	−	−	−	−	−	−	−
Hypoplastic corpus callosum	−	−	−	−	−	−	−	−	−	−
Structural anomalies	−	Gastroschisis	−	−	−	−	−	−	−	−
Neonatal lactic acidosis	−	−	−	−	−	−	−	−	−	−
Cardiomyopathy	N/A	N/A	−	−	N/A	N/A	N/A	N/A	N/A	N/A
Acylcarnitine profile	N/A	N/A	N/A	N/A	N/A	N/A	Normal	Normal	Normal	Normal
Lactate	N/A	High	High	High	Normal	High in urine	High	Intermittently high	Intermittently high	Normal
Pyruvate	N/A	N/A	N/A	N/A	Normal	N/A	N/A	N/A	N/A	N/A
Lactate/pyruvate ratio					Normal	N/A	N/A	N/A	N/A	N/A
Urinary 2-methyl, 2,3-dihydroxybutyrate	Sixfold ULN	N/A	N/A	Normal	Upper limit of normal	Slightly elevated	Normal	Normal	Normal	Normal
Death	Alive at 5 years	Alive at 8 years	Alive at 16 years	Alive at 31 years	Alive at 7 years	5 years	10 months	Alive at 18 years	Alive at 13 years	Alive at 12 years
Genetic mutation	c.268G>A/c.583G>A	c.161G>A/c.394G>A	c.161G>A/c.431dup	c.229G>C/c.476A>G	c.176A>G/c.413C>T	c.176A>G/c.413C>T	c.538A>G/c.583G>A	c.538A>G/c.713C>T	c.538A>G/c.713C>T	c.473C>T/c.414+3G>C
Protein effect	G90R/G195S	R54H/A132T	R54H/L154Afs*6	E77Q/Q159R	N59S/A138V	N59S/A138V	T180A/G195S	T180A/A238V	T180A/A238V	p.A581I/splicing

which has the possibility for providing families with a more rapid diagnosis than molecular testing.

Acknowledgments The authors thank the family for their participation in this work. The authors also thank the National Phenylketonuria Alliance, which provided salary support for RDG through the Koch Memorial Fellowship.

Synopsis

We present two siblings with the most severe form of short-chain enoyl-CoA hydratase deficiency, including oligohydramnios, preterm delivery, dysmorphic features, agenesis of the corpus callosum, neonatal cardiomyopathy, and primary lactic acidosis with biochemical features including elevated C4, elevated pyruvate and lactate, and mild elevation of 2,3-dihydroxy-2-methylbutyric acid.

Compliance with Ethics Guidelines

Conflict of Interest

Rebecca D. Ganetzky, Kaitlyn Bloom, Rebecca Ahrens-Nicklas, Andrew Edmondson, Matthew A. Deardorff, Michael J. Bennett, and Can Ficicioglu declare that they have no conflicts of interest.

Informed Consent/Animal Rights

This article does not contain any studies with human or animal subjects performed by any of the authors.

Details of the Contributions of Individual Authors

RDG performed clinical and biochemical evaluation for patient 1, analyzed the molecular data, and conceived and wrote the manuscript and collated data for Table 1. KB performed CoA analysis and wrote the method and discussion sections related to CoA data. RAN, AE, and MAD performed clinical evaluation and designed biochemical testing strategy for patient 2. MJB designed CoA analysis and edited the manuscript. CF conceived and edited the manuscript, provided oversight, and serves as the guarantor for the article.

All authors approved the final manuscript as submitted and agree to be accountable for all aspects of the work.

Details of Funding

RDG received salary support from the National Phenylketonuria Alliance through the Koch Memorial Fellowship. MB and KB were supported in their work by the Evelyn Willing Bromley Endowed Chair in Clinical Laboratories and Pathology.

References

Adzhubei IA, Schmidt S, Peshkin L et al (2010) A method and server for predicting damaging missense mutations. Nat Methods 7:248–249. doi:10.1038/nmeth0410-248

Claros MG, Vincens P (1996) Computational method to predict mitochondrially imported proteins and their targeting sequences. Eur J Biochem 241:779–786

Ferdinandusse S, Friederich MW, Burlina A et al (2015) Clinical and biochemical characterization of four patients with mutations in ECHS1. Orphanet J Rare Dis 10:79. doi:10.1186/s13023-015-0290-1

Haack TB, Jackson CB, Murayama K et al (2015) Deficiency of ECHS1 causes mitochondrial encephalopathy with cardiac involvement. Ann Clin Transl Neurol 2:492–509. doi:10.1002/acn3.189

Kumar P, Henikoff S, Ng PC (2009) Predicting the effects of coding non-synonymous variants on protein function using the SIFT algorithm. Nat Protoc 4:1073–1081. doi:10.1038/nprot.2009.86

Palladino A, Chen J, Kallish S et al (2012) Measurement of tissue acyl-CoAs using flow-injection tandem mass spectrometry: acyl-CoA profiles in short-chain fatty acid oxidation defects. Mol Genet Metab 107:679–683. doi:10.1016/j.ymgme.2012.10.007

Peters H, Buck N, Wanders R et al (2014) ECHS1 mutations in Leigh disease: a new inborn error of metabolism affecting valine metabolism. Brain 137:2903–2908. doi:10.1093/brain/awu216

Sakai C, Yamaguchi S, Sasaki M et al (2015) ECHS1 mutations cause combined respiratory chain deficiency resulting in Leigh syndrome. Hum Mutat 36:232–239. doi:10.1002/humu.22730

Tetreault M, Fahiminiya S, Antonicka H et al (2015) Whole-exome sequencing identifies novel ECHS1 mutations in Leigh syndrome. Hum Genet 134:981–991. doi:10.1007/s00439-015-1577-y

Yamada K, Aiba K, Kitaura Y et al (2015) Clinical, biochemical and metabolic characterisation of a mild form of human short-chain enoyl-CoA hydratase deficiency: significance of increased N-acetyl-S-(2-carboxypropyl)cysteine excretion. J Med Genet 52:691–698. doi:10.1136/jmedgenet-2015-103231

JIMD Reports
DOI 10.1007/8904_2016_539

RESEARCH REPORT

Chronic Oral L-Carnitine Supplementation Drives Marked Plasma TMAO Elevations in Patients with Organic Acidemias Despite Dietary Meat Restrictions

Marcus J. Miller • Bret L. Bostwick • Adam D. Kennedy • Taraka R. Donti • Qin Sun • V. Reid Sutton • Sarah H. Elsea

Received: 04 November 2015 / Revised: 20 January 2016 / Accepted: 21 January 2016 / Published online: 03 March 2016

Abstract Recent studies have implicated trimethylamine *N*-oxide (TMAO) in atherosclerosis, raising concern about L-carnitine, a common supplement for patients with inborn errors of metabolism (IEMs) and a TMAO precursor metabolized, in part, by intestinal microbes. Dietary meat restriction attenuates carnitine-to-TMAO conversion, suggesting that TMAO production may not occur in meat-restricted individuals taking supplemental L-carnitine, but this has not been tested. Here, we mine a metabolomic dataset to assess TMAO levels in patients with diverse IEMs, including organic acidemias. These data were correlated with clinical information and confirmed using a quantitative TMAO assay. Marked plasma TMAO elevations were detected in patients treated with supplemental L-carnitine, including those on a meat-free diet. On average, patients with an organic acidemia had ~45-fold elevated [TMAO], as compared to the reference population. This effect was mitigated by metronidazole therapy lasting 7 days each month. Collectively, our data show that TMAO production occurs at high levels in patients with IEMs receiving oral L-carnitine. Further studies are needed to determine the long-term safety and efficacy of chronic oral L-carnitine supplementation and whether suppression or circumvention of intestinal bacteria may improve L-carnitine therapy.

Communicated by: Anita MacDonald, PhD, BSc

M.J. Miller · B.L. Bostwick · T.R. Donti · Q. Sun · V.R. Sutton · S.H. Elsea (✉)
Department of Molecular and Human Genetics, Medical Genetics Laboratory, Baylor College of Medicine, Houston, TX 77030, USA
e-mail: elsea@bcm.edu

A.D. Kennedy
Metabolon Inc., Durham, NC 27713, USA

Introduction

Supplemental L-carnitine is widely used in the treatment of inborn errors of metabolism (IEMs). Daily oral doses of high levels (~100 mg L-carnitine/kg body weight) of this compound are routinely employed in the treatment of organic acidemias and primary carnitine uptake deficiency (OMIM212140) and less frequently in the treatment of multiple other IEMs including, but not limited to, urea cycle defects, fatty acid oxidation disorders, mitochondrial disease, maple syrup urine disease (OMIM248600), and lysinuric protein intolerance (OMIM222700) (Mori et al. 1990; Davies et al. 1991; Kolker et al. 2011; Sebastio et al. 2011; Magoulas and El-Hattab 2012; Mescka et al. 2015; Tischner and Wenz 2015). Carnitine plays an essential role in mitochondrial shuttling; supplementation is therefore aimed at replenishing depleted carnitine stores and conjugating and removing the toxic buildup of organic acids. No long-term placebo-controlled studies have been completed to test the safety and efficacy of this therapy, but for many IEMs there are strong theoretical and observational data advocating for the use of L-carnitine supplementation (Walter 2003; Winter 2003; Nasser et al. 2012). In individuals without an IEM, carnitine is naturally supplied primarily through consumption of meat, with the remainder produced by an endogenous synthesis pathway (Rebouche 2004).

When orally consumed, L-carnitine can be metabolized by intestinal bacteria to form trimethylamine (TMA), a volatile compound associated with a pungent fishy odor (Zhang et al. 1999). TMA is readily absorbed in the gastrointestinal tract and further processed by the hepatic enzyme flavin monooxygenase 3 (FMO3) to produce trimethylamine *N*-oxide (TMAO) (Lang et al. 1998) (Fig. 1a). Carnitine to TMAO conversion varies widely

between individuals with reports that, for some, as much as ~50% of ingested carnitine is eventually excreted in the urine as TMAO (Rebouche 1991). Interindividual differences in the intestinal microbiome may explain some of the variation in conversion rates. Individuals treated with antibiotics targeting intestinal bacteria or those that adhere to a vegan or vegetarian diet have significantly lower baseline levels of plasma TMAO and do not produce appreciable levels of this compound when given oral L-carnitine for short periods of time (Koeth et al. 2013).

Recent studies have identified plasma TMAO as a dose-dependent risk factor for cardiovascular disease that may advance atherosclerosis through the promotion of cholesterol storage in macrophages (Wang et al. 2011; Koeth et al. 2013; Tang et al. 2013). These findings hold obvious implications about the long-term consequences of chronic oral L-carnitine supplementation in healthy individuals on a standard western diet. However, in patients with IEMs, carnitine-TMAO conversion is not established, and it has been postulated that dietary protein restriction may mitigate gut microbial breakdown of supplemental L-carnitine, similar to what is seen in vegan/vegetarian individuals. Additionally, for the organic acidemias, methylmalonic and propionic acidemia (OMIM 251000 and 606054, respectively), monthly prophylactic treatment with the antibiotic metronidazole is also commonly used to reduce intestinal bacteria and the affiliated production of propionate, and this may confer the unexpected benefit of reducing TMAO production as well (Thompson et al. 1990). Taken together, the outcome of carnitine supplementation is not obvious for many IEMs, especially the organic acidemias, and to date, no studies have assessed the levels of TMAO in this population.

To test the hypothesis that chronic oral supplemental L-carnitine could lead to TMAO production in patients undergoing standard treatment for an organic acidemia, we mined a metabolomic dataset previously generated by our lab, which contains metabolic information on patients with a wide variety of IEMs (Miller et al. 2015). Findings from this analysis were correlated with clinical data and confirmed using a targeted tandem mass spectrometry (MS/MS) assay that allowed absolute quantification of TMAO.

Methods

The methods and a general overview of findings from the metabolomic analyses in this report have been previously described (Miller et al. 2015). Briefly, an untargeted MS/MS-based metabolomic platform was used to semiquantitatively analyze ~900 unique small molecule plasma analytes in each of 190 patient specimens including 69 patients without a diagnosed genetic disorder. This latter patient group is likely comprised of individuals on a standard omnivorous western diet and not on supplemental carnitine; we refer to this as the "reference population" for the remainder of the manuscript. Raw spectral intensity values were normalized to allow comparison across independent MS/MS batches, and these normalized values were then used to scale all analyte values to the median of the reference population ($n = 69$). The median age of the reference population was 5 years (inner quartile range (IQR) = 2.4–13.1). A two-tailed heteroscedastic student's *t*-test was used to compare $\log_2$-transformed data. Linear regression analysis was completed using the freely available statistical package R.

For quantitative TMAO analysis, plasma specimens were diluted 1:10 in acetonitrile containing a spiked isotopic standard, TMAO-D9 (Cambridge isotope DLM-4779-1). Specimens were clarified by centrifugation and supernatants were subjected to liquid chromatography tandem mass spectrometry (LC-MS). Chromatographic separation was achieved using an Aquity UPLC (Waters) equipped with an Atlantis HILIC Silica 5 μm 1 × 100 mm column (Waters) and an isocratic mobile phase—80% acetonitrile 0.1% formate and 20% 50 mM ammonium acetate pH 4.8. MS analysis was completed in positive ion mode using an Aquity TQ tandem MS (Waters) with the following transitions: TMAO 76.1 > 58.1 *m/z* and TMAO-D9 85.3 > 66.2 *m/z*. Quantitative values were calculated by fitting a sample's TMAO/TMAO-D9 response factor to a linear model generated via the analysis of six standards ranging in concentration from 0.2 to 625 μM TMAO.

Results

In a prior study, we explored the clinical utility of an untargeted metabolomic platform in the retrospective analysis of plasma specimens collected from patients with a wide range of IEMs, as well as individuals without a biochemical diagnosis (Miller et al. 2015). This sample set included specimens from multiple unrelated patients receiving treatment for organic acidemias, including glutaric acidemia type 1 (OMIM#231670), methylmalonic acidemia, and propionic acidemia. This group represents the cohort of individuals in our sample set most likely to be on L-carnitine supplementation while also adhering to a meat-restricted diet. Clinical information was available for the majority of the subjects, and for these cases we confirmed daily oral L-carnitine supplementation and restrictions of dietary meat consumption (Table 1).

Dietary compliance was independently audited by further mining of the metabolomic data. 3-methylhistidine (3-MH) is a muscle breakdown product that is significantly elevated following meat consumption (Cross et al. 2011).

Table 1 Clinical information for patients in the organic acidemia cohort

ID	Disorder[a]	Age at sampling (years)	Daily L-carnitine dosage (mg/kg body weight)[b]	Recent antibiotics exposure[c]	TMAO[d]	3-MH[d]
PAT1	GA 1	9.8	Unknown	Unknown	18.14	No ID
PAT2	GA 1	3.6	88	No	31.14	No ID
PAT3	GA 1	4.8	91	No	73.48	No ID
PAT4	GA 1	6.3	75	No	182.96	No ID
PAT5	GA1	3.6	Unknown	Unknown	142.01	No ID
PAT6	MMA	10.6	83 IV	Vanc./Zosyn	2.17	0.97
PAT7a	MMA	4.9	100	No	117.30	No ID
PAT7b	MMA	5.0	100	No	32.83	No ID
PAT8	MMA	2.1	103	No	0.64	No ID
PAT9	MMA	6.1	Unknown	Unknown	78.09	No ID
PAT10a	MMA	36.3	19	No	312.83	3.22
PAT10b	MMA	36.7	19	No	164.24	19.13
PAT11	MMA	8.7	97	No	50.35	0.96
PAT12	PA	0.9	109	Metron. (7 days/month)	0.25	0.19
PAT13	PA	2.1	51	Metron. (7 days/month)	0.62	No ID
PAT14	PA	3.9	145	Metron. (7 days/month)	0.28	No ID
PAT15	PA	2.0	96	Augmen.	50.13	0.66
PAT16a	PA	4.5	Unknown	Unknown	113.43	No ID
PAT16b	PA	4.9	Unknown	Unknown	127.24	0.27
PAT17	PA	0.4	80	Metron. (5 days/month)	73.26	0.19
PAT18	PA	3.4	75	Metron. (5 days/month)	85.45	No ID
PAT19	PA	7.4	84	No	15.25	0.78

[a] *GA1* glutaric acidemia type 1, *MMA* methylmalonic acidemia, *PA* propionic acidemia

[b] IV indicates a patient whom was taken off oral carnitine (prior chronic PO dose is listed) and instead was on intravenous carnitine replacement for 10 days prior to sampling as a result of illness and inpatient hospitalization

[c] Antibiotic treatments within 30 days of sampling are listed. Metron. = oral metronidazole; Vanc./Zosyn = intravenous Vancomycin and Zosyn.; Augmen. = Augmentin, 10-day course. Treatment regimens are listed in parenthesis, so "7 days/month" = antibiotic is given for 7 days out of the month

[d] Values are reported as multiples of the median value of the analyte determined in the reference population. Compounds below the level of detection = "No ID"; 3-MH = 3-methylhistidine

This compound was positively identified in the plasma of 77% of the patients in our reference population, whereas for most organic acidemia patients, 3-MH was undetectable (73% of patients) or well below the median value for the reference population, thus suggesting compliance with a meat-restricted diet for the majority of subjects (Table 1).

Despite the apparent compliance with meat restriction, metabolomic analysis identified marked elevations of TMAO in the majority of patients with an organic acidemia (Fig. 1b). For 14 of 19 patients with an organic acidemia, TMAO levels were greater than 15 times the median level of the reference population (multiples of the median, MoM) with an overall average TMAO level in the organic acidemia cohort of 65 MoM (p-value $= 2.19 \times 10^{-8}$). Metabolomic findings were confirmed by reanalysis of a subset of specimens using a targeted MS/MS assay that provided absolute quantification and lower limits of detection (Fig. 1c). Importantly, quantitative values generated by this method correlated with metabolomic data ($R^2 = 0.68$) and confirmed the significant elevations of TMAO in many organic acidemia patients. Patients with an organic acidemia had an average plasma TMAO concentration of 120 μM (IQR = 24.3–194.6 μM) as compared to 2.75 μM (IQR = 1.1–4.5 μM) in the reference population. The average TMAO concentration detected in our reference population was similar to previous reports of baseline TMAO levels in healthy individuals on an omnivorous diet and not taking an L-carnitine supplement (TMAO = ~3–4 μM) (Koeth et al. 2013).

More sporadic patterns of extreme TMAO elevations were noted in additional IEM patient groups, with the pattern likely reflecting the sporadic use of L-carnitine

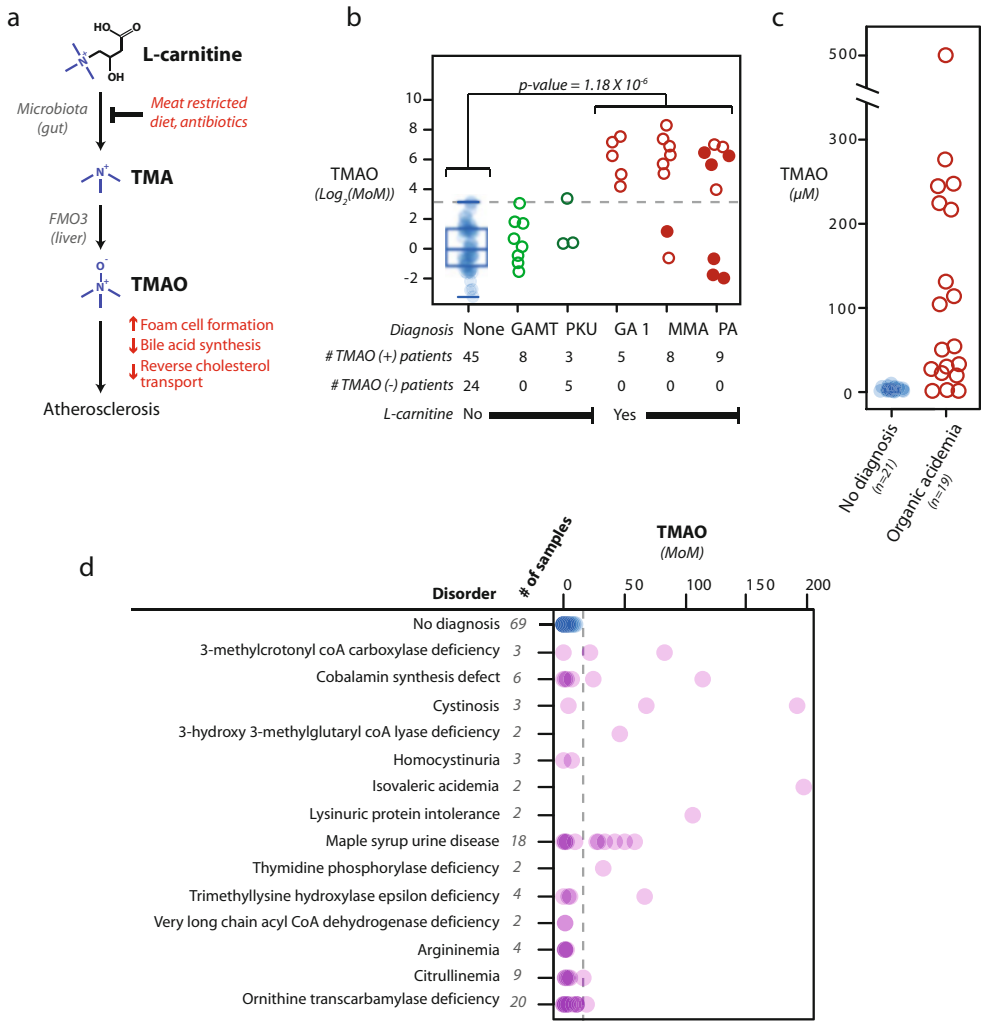

Fig. 1 High levels of TMAO detected in the plasma of patients with IEMs requiring L-carnitine supplementation. (**a**) The diagram illustrates the current model for L-carnitine microbial metabolism and its association with atherosclerosis (Modified from (Backhed 2013)). (**b**) Plasma TMAO levels discovered via metabolomic analysis are plotted in terms of $\log_2$-transformed multiples of the median (MoM) of the reference population. Samples from patients without a diagnosis are plotted with *blue dots* ($n = 69$), and *the gray dashed line* indicates the highest TMAO value from this group. *Filled circles* indicate the organic acidemia patients treated with antibiotics within the 30 days prior to sampling. *GAMT* guanidinoacetate methyltransferase deficiency, *PKU* phenylketonuria, *GA 1* glutaric acidemia type 1, *MMA* methylmalonic acidemia, *PA* propionic acidemia. Below the plot is listed the number of patients for which TMAO was confidently identified (TMAO(+)) or below the level of detection (TMAO(−)) for the metabolomic platform. (**c**) A subset of specimens was reanalyzed using a quantitative TMAO analysis. Organic acidemia includes MMA, PA, and GA 1 patients. (**d**) The TMAO values from metabolomic analyses of plasma samples from additional IEM patients are shown. The *gray dashed line* indicates the highest TMAO level seen in the reference population ("no diagnosis")

supplementation in the treatment of these diseases. Examples of patients with extreme plasma TMAO levels include those with cobalamin synthesis disorders, cystinosis (OMIM219800), isovaleric acidemia (OMIM243500), and maple syrup urine disease (OMIM248600) (Fig. 1d). It is notable that multiple patients in our dataset were not on supplemental L-carnitine and consequently had very low levels of plasma TMAO; these include the patients in the reference population who did not have a diagnosis ($n = 69$) or patients with IEMs that are not typically treated with L-carnitine supplementation (e.g., guanidinoacetate methyltransferase deficiency (OMIM612736; $n = 8$) and phenylketonuria (OMIM261600; $n = 8$)). For nearly all patients within this group, TMAO was either below the level of detection or detected at a low-to-moderate level (Fig. 1b).

Given the established relationship between TMAO production and intestinal microbiota, we were interested in the effects of antibiotics in our organic acidemia cohort. Overall, seven patients were prescribed antibiotics, typically metronidazole, at the time of sampling or within the

30 days prior to sampling (filled dots in Fig. 1b and Table 1). Challenging this analysis was our inability to confirm compliance or timing of metronidazole treatments relative to sampling. However, it is noteworthy that within the organic acidemia cohort, five patients had biochemical evidence of attenuated microbial carnitine-TMAO conversion, e.g., low-to-normal plasma TMAO levels. Of these five, four were on antibiotic treatments immediately preceding or during sampling (PAT12-14 and PAT6; Table 1). Patients on 7 days per month metronidazole therapy had normalized TMAO levels (PAT12-14), whereas two patients on 5 days per month metronidazole therapy had extreme TMAO elevations (PAT 17-18) suggesting that the duration of antibiotic therapy may impact microbial L-carnitine degradation (Table 1).

Discussion

The identification of high levels of TMAO in patients with an organic acidemia is clinically important for two reasons. First, it disproves the hypothesis that dietary protein/meat restriction may protect these patients from intestinal microbial conversion of carnitine to TMAO. The TMAO levels in most patients with an organic acidemia were well above the levels observed in even the most extreme examples in our reference population. Given that improved therapies have increased the survival of individuals with organic acidemias, these data indicate that long-term studies of oral carnitine supplementation in this population are needed to understand the risk of atherosclerosis. Second, our findings also have important implications regarding the efficacy of carnitine therapy in patients with IEMs. The bioavailability of supplemental L-carnitine has been previously noted to be <25%, and trials replacing oral L-carnitine with venous boluses of L-carnitine have shown promising preliminary results (Winter 2003; Rebouche 2004). Taken together with our findings, gut microbial carnitine-TMAO conversion may be an underappreciated detriment to carnitine therapy. Future improvements may be achieved by cyclic oral antibiotics that limit the microbial conversion of carnitine to TMAO or through the use of parenteral supplementation that would bypass the intestinal microbiome.

In conclusion, these findings demonstrate that oral L-carnitine could be conferring an increased risk to develop atherosclerosis over years of therapy due to chronic and extreme elevations in TMAO. Further investigation of the intestinal microbiome metabolism of orally supplemented L-carnitine in patients with IEMs is needed to answer the following questions raised by this study: (1) Does chronic oral L-carnitine supplementation increase the risk of atherosclerosis in individuals with organic acidemias? (2) Can cyclic administration of an oral antibiotic, such as metronidazole 7 days per month, reduce TMAO levels while increasing plasma carnitine levels in individuals with organic acidemias on chronic oral L-carnitine supplementation? (3) Can periodic parenteral L-carnitine supplementation improve plasma carnitine levels and outcome measures while leading to normal TMAO levels? Due to the pervasive use of oral L-carnitine supplementation in the field of inherited metabolic disease, it is critical that these questions are answered to improve outcomes and minimize the risks of long-term problems in individuals with IEMs.

Acknowledgments We would like to thank the Rimoin family and the American College of Medical Genetics (ACMG) Foundation for recognizing this work with the inaugural Dr. David L. Rimoin Inspiring Excellence Award at the ACMG 2015 annual meeting. Thanks also to Drs. Mahim Jain and Robert Collins for technical assistance and to Dr. Brenden Lee for reviewing the manuscript. This work was funded, in part, by the T32 GM07526-37 Medical Genetics Research Fellowship Program (MJM).

One-Sentence Take-Home Message

L-carnitine supplementation leads to marked plasma accumulation of trimethylamine *N*-oxide in many patients with IEMs, highlighting the need for additional studies on the safety and efficacy of this treatment.

Compliance with Ethics Guidelines

Human Subjects

All procedures followed were in accordance with the ethical standards of the US Department of Health and Human Services and were approved by the Baylor College of Medicine Institutional Review Board in accordance with the Helsinki Declaration of 1975, as revised in 2000. This study was approved with a waiver of informed consent.

Conflict of Interest Statement

Marcus J. Miller, Bret L. Bostwick, Donti Taraka, Qin Sun, V. Reid Sutton, and Sarah H. Elsea are members of the Department of Molecular and Human Genetics at Baylor College of Medicine, and this department, alone or as part of a joint venture with Miraca Holdings, offers a number of clinical tests on a fee-for-service basis, but these in no way conflict with the research reported here. Adam D. Kennedy is an employee of Metabolon, Inc. and, as such, has affiliations with or financial involvement with Metabolon, Inc. The authors have no other relevant affiliations or financial involvement with any organization or entity with a financial interest in or financial conflict with the subject matter or materials discussed in the manuscript apart from those disclosed.

References

Backhed F (2013) Meat-metabolizing bacteria in atherosclerosis. Nat Med 19(5):533–534

Cross AJ, Major JM, Sinha R (2011) Urinary biomarkers of meat consumption. Cancer Epidemiol Biomarkers Prev 20 (6):1107–1111

Davies SE, Iles RA, Stacey TE, de Sousa C, Chalmers RA (1991) Carnitine therapy and metabolism in the disorders of propionyl-CoA metabolism studied using 1H-NMR spectroscopy. Clin Chim Acta 204(1–3):263–277

Koeth RA, Wang Z, Levison BS et al (2013) Intestinal microbiota metabolism of L-carnitine, a nutrient in red meat, promotes atherosclerosis. Nat Med 19(5):576–585

Kolker S, Christensen E, Leonard JV et al (2011) Diagnosis and management of glutaric aciduria type I–revised recommendations. J Inherit Metab Dis 34(3):677–694

Lang DH, Yeung CK, Peter RM et al (1998) Isoform specificity of trimethylamine N-oxygenation by human flavin-containing monooxygenase (FMO) and P450 enzymes: selective catalysis by FMO3. Biochem Pharmacol 56(8):1005–1012

Magoulas PL, El-Hattab AW (2012) Systemic primary carnitine deficiency: an overview of clinical manifestations, diagnosis, and management. Orphanet J Rare Dis 7:68

Mescka CP, Guerreiro G, Hammerschmidt T et al (2015) L-Carnitine supplementation decreases DNA damage in treated MSUD patients. Mutat Res 775:43–47

Miller MJ, Kennedy AD, Eckhart AD et al (2015) Untargeted metabolomic analysis for the clinical screening of inborn errors of metabolism. J Inherit Metab Dis 38(6):1029–1039

Mori T, Tsuchiyama A, Nagai K, Nagao M, Oyanagi K, Tsugawa S (1990) A case of carbamylphosphate synthetase-I deficiency associated with secondary carnitine deficiency–L-carnitine treatment of CPS-I deficiency. Eur J Pediatr 149(4):272–274

Nasser M, Javaheri H, Fedorowicz Z, Noorani Z (2012) Carnitine supplementation for inborn errors of metabolism. Cochrane Database Syst Rev 2:CD006659

Rebouche CJ (1991) Quantitative estimation of absorption and degradation of a carnitine supplement by human adults. Metabolism 40(12):1305–1310

Rebouche CJ (2004) Kinetics, pharmacokinetics, and regulation of L-carnitine and acetyl-L-carnitine metabolism. Ann N Y Acad Sci 1033:30–41

Sebastio G, Sperandeo MP, Andria G (2011) Lysinuric protein intolerance: reviewing concepts on a multisystem disease. Am J Med Genet C Semin Med Genet 157C(1):54–62

Tang WH, Wang Z, Levison BS et al (2013) Intestinal microbial metabolism of phosphatidylcholine and cardiovascular risk. N Engl J Med 368(17):1575–1584

Thompson GN, Chalmers RA, Walter JH et al (1990) The use of metronidazole in management of methylmalonic and propionic acidaemias. Eur J Pediatr 149(11):792–796

Tischner C, Wenz T (2015) Keep the fire burning: current avenues in the quest of treating mitochondrial disorders. Mitochondrion 24:32–49

Walter JH (2003) L-carnitine in inborn errors of metabolism: what is the evidence? J Inherit Metab Dis 26(2–3):181–188

Wang Z, Klipfell E, Bennett BJ et al (2011) Gut flora metabolism of phosphatidylcholine promotes cardiovascular disease. Nature 472 (7341):57–63

Winter SC (2003) Treatment of carnitine deficiency. J Inherit Metab Dis 26(2–3):171–180

Zhang AQ, Mitchell SC, Smith RL (1999) Dietary precursors of trimethylamine in man: a pilot study. Food Chem Toxicol 37 (5):515–520

JIMD Reports
DOI 10.1007/8904_2016_534

RESEARCH REPORT

A Founder Effect for the *HGD* G360R Mutation in Italy: Implications for a Regional Screening of Alkaptonuria

Berardino Porfirio • Roberta Sestini • Greta Gorelli • Miriam Cordovana • Alessandro Mannoni • Jeanette L. Usher • Wendy J. Introne • William A. Gahl • Thierry Vilboux

Received: 16 October 2015 / Revised: 28 December 2015 / Accepted: 31 December 2015 / Published online: 10 March 2016

Abstract We sought to establish rapid and specific genotyping methods for G360R mutation and for seven tightly linked markers in the homogentisate dioxygenase gene to address the question of whether G360R is a mutational hot spot or the result of a founder effect, as it has been repeatedly found in alkaptonuric patients from a geographic isolate in Italy.

For G360R and single nucleotide polymorphism genotyping, high-resolution melting analysis was performed. Microsatellites were analysed by multiplex PCR and capillary electrophoresis. To investigate the natural history of the G360R mutation, we genotyped markers in 52 controls and in 8 unrelated patients from the UK and USA, who also segregated the G360R mutation, and calculated its age using DMLE+2.3 software.

A distinct G360R-bearing haplotype was identified in all patients of Caucasian descent. Estimated mutation age was 545 generations (95% credible set, 402–854), suggesting that G360R arose in an ancestor who lived 8,000–10,000 years BC. Archaeological, historical and demographic data support that a G360R carrier has settled the remote valley where present-day population might have a heterozygote frequency of at least 6%.

Given the late health-threatening complications of alkaptonuria and a cure within reach, inhabitants of this isolate would benefit from screening and genetic counselling.

Communicated by: Verena Peters

Competing interests: None declared

This paper is dedicated to the memory of Dr. Claudio Castellan

Electronic supplementary material: The online version of this chapter (doi:10.1007/8904_2016_534) contains supplementary material, which is available to authorized users.

B. Porfirio (✉) · R. Sestini · G. Gorelli · M. Cordovana
Department of Clinical and Experimental Biomedical Sciences "Mario Serio", Clinical Physiopathology Unit, University of Florence, Viale Gaetano Pieraccini 6, 50139 Florence, Italy
e-mail: nporfirio@unifi.it

A. Mannoni
Internal Medicine Division, Rheumatology Unit, Ospedali S. Maria Nuova e Palagi, ASL 10 Firenze, Florence, Italy

J.L. Usher
Department of Clinical Biochemistry and Metabolic Medicine, Royal Liverpool and Broadgreen University Hospital Trust, Liverpool, UK

W.J. Introne · W.A. Gahl · T. Vilboux
Medical Genetics Branch, National Human Genome Research Institute, National Institutes of Health, Bethesda, MD 20892, USA

W.J. Introne · W.A. Gahl
Office of the Clinical Director, National Human Genome Research Institute, National Institutes of Health, Bethesda, MD 20892, USA

W.A. Gahl
NIH Undiagnosed Diseases Program, Common Fund, Office of the Director, National Institutes of Health, Bethesda, MD 20892, USA

T. Vilboux
Division of Medical Genomics, Inova Translational Medicine Institute, Falls Church, VA 22042, USA

Introduction

Alkaptonuria (AKU, OMIM 203500) is an autosomal recessive disease caused by mutations of the *HGD* gene encoding homogentisate 1,2-dioxygenase (HGD; EC 1.13.11.5), an enzyme involved in the catabolism of tyrosine (Fernández-Cañón et al. 1996). *HGD* is located on chromosome 3q13.33 (genomic coordinates [GRCh37]: 3:120,347,014–120,401,417) and consists of 14 exons encompassing 2,012 bp (OMIM 607474, coding sequence:

NM_000187.3). Over the past years, the *HGD* mutation spectrum has been described in series of AKU patients from different countries (http://hgddatabase.cvtisr.sk/). At this writing, 174 unique *HGD* sequence variants found in 398 individuals carrying a total of 751 variants are reported in the database. In particular, the missense mutation c.1078G>C; p.Gly360Arg (henceforth, G360R) in exon 13 has been detected 13 times in patients from Italy, Australia, the UK, France and the USA (Zatkova et al. 2012). G360R was originally described by Porfirio et al. (2000) who found two independent G360R-bearing AKU chromosomes in two patients from different ends of the Italian peninsula; one patient was a compound heterozygote from Calabria, Southern Italy, whereas the other was the affected son of a consanguineous marriage from South Tyrol, a German-speaking region on the Austrian border. The G360R mutation disrupts a BstNI restriction site, making PCR-RFLP useful in genotyping family members and scanning the general population to rule out this mutation as a coincidental polymorphism segregating in those AKU families (Porfirio et al. 2000). Seven intragenic markers were used to trace the haplotype background of these G360R mutations. Familial segregation provided unequivocal derivation of the haplotypes present on the AKU chromosomes and clearly showed that a single haplotype, closely related to the common A haplogroup (Beltrán-Valero de Bernabé et al. 1998), was harbouring the G360R mutation (Porfirio et al. 2000). Subsequently, another ten compound heterozygous patients were reported to carry G360R (Grasko et al. 2009; Vilboux et al. 2009; Usher et al. 2015). Since G360R takes place in a G run, a sequence motif known as a mutational hot spot in *HGD* (Beltrán-Valero de Bernabé et al. 1999), referral of two large, apparently unrelated, South Tyrolean AKU families, has recently renewed our interest in the origin and spread of G360R mutation among populations of European ancestry.

High-resolution melting analysis (HRMA) has significantly hastened mutation scanning processes (Wittwer 2009). The method involves precise monitoring of the change in fluorescence caused by the release of an intercalating DNA dye from a DNA duplex as it is denatured by increasing temperature. Therefore, in the present study, we sought to establish rapid and specific genotyping methods for G360R and seven *HGD* intragenic markers to address the question of whether G360R is a mutational hot spot or the result of a founder effect by analysing two new large AKU families from Italy and eight singleton AKU patients from the UK and USA.

Materials and Methods

Patients and Controls

The Italian subjects involved gave written informed consent in accordance to the Helsinki Declaration, and the study was approved by our institutional review board. The US and UK DNA samples were provided upon material transfer agreements between the respective Institutions.

A total of 40 genomic DNA samples, derived from two German-speaking South Tyrolean families with G360R, were genotyped at seven tightly linked markers spanning a region of 44.2 Kb (see below). All haplotype sets were generated by inheritance from the observed genotypes in the family members. In another eight UK and US families in whom G360R was detected, only the index case was available for genotyping. Haplotypes were manually constructed by assigning the phase of heterozygous positions, whenever possible, with the guidance of known *HGD* haplotypes associated to individual AKU mutations (http://hgddatabase.cvtisr.sk/). One hundred and four control chromosomes were also studied. Controls included 17 subjects who were spouses of family members, as well as 35 unrelated individuals from the same geographic area. Haplotype frequencies in the general population were derived using a Bayesian method implemented in PHASE v.2.1 software (Stephens and Scheet 2005).

Markers

Three short tandem repeat (STR) markers, a (CA)n in intron 4 (HGO-3, D3S4556), a (CT)n in intron 4 (HGO-1, D3S4496) and a (CA)n in intron 13 (HGO-2, D3S4497), have been described previously (Granadino et al. 1997; Beltrán-Valero de Bernabé et al. 1998) and were analysed by multiplex PCR with modifications to comply with dye-primer detection. PCR products were subjected to electrophoresis on an ABI PRISM 310 Genetic Analyzer (Applied Biosystems, Foster City, CA, USA). Size calling was performed using the GeneMapper software (Applied Biosystems, Monza, Italy). Four single nucleotide polymorphisms (SNPs), IVS2+35T/A (rs2733825), c.240T/A H80Q (rs2255543, exon 4), IVS5+25T/C (rs2551607) and IVS6 +46C/A (rs3817627), have also been described (Beltrán-Valero de Bernabé et al. 1998) and were studied by HRMA following primer redesign (sequences and conditions available on request). Genotype assignment was made possible by comparison with known sequenced samples.

Differences in haplotype frequencies between patients and normal subjects were analysed using the χ^2 test. The statistical threshold was set at 0.05.

G360R HRMA

Primers flanking the c.1078G>C substitution were designed using Primer3web v. 4.0.0 software (http://bioinfo.ut.ee/primer3/), and their sequences are available upon request. The fluorescent high-resolution DNA melting curves of the resulting 116-bp PCR product were predicted using uMelt software (https://www.dna.utah.edu/umelt/umelt.html). Genomic DNA (20 ng) was amplified in a final volume of 20 μL containing 1.25 μL of PCR Buffer (Applied Biosystems, Monza, Italy), 1.5 mmol/L of magnesium chloride (Applied Biosystems, Monza, Italy), 300 nmol/L of each primer, 1.5 μmol/L of SYTO9 Dye (Invitrogen, Basel, Switzerland) and 1.25 U of AmpliTaq Gold Polymerase (Applied Biosystems, Monza, Italy). One-tube PCR and HRMA were performed on Rotor Gene 6000 (Corbett Research, Sydney, Australia). Thermal cycler was set at 95°C for 10 min to allow initial genomic DNA denaturation followed by 35 cycles of 1 min at 95°C, 1 min at 60°C and 1 min at 72°C and by a final extension at 72°C for 15 min. The resulting PCR products underwent HRMA as follows: samples were denaturated at 95°C for 1 min and then rapidly cooled to 40°C for 1 min in order to facilitate heteroduplex formation. Melting curve data were acquired in a wide temperature range (78–88°C) at a ramping rate of 0.1°C/s. Results were analysed as both normalised fluorescence and the derivative function of fluorescence raw data versus temperature (supplementary Figs. 1 and 2, respectively). Since the mutant allele 1078C homozygotes may not be easily distinguishable from wild-type 1078G homozygotes by traditional HRMA methods, a spike-in control DNA approach was used (Liew et al. 2004). Briefly, PCR was performed on both the native samples and 1:1 mixtures of the test samples with a reference 1078G homozygous sample. Homozygous 1078C test samples were converted to heterozygosity, a condition associated with an abnormal melting curve owing to heteroduplex formation.

Sanger Sequencing

Amplicons were purified using the QIAquick PCR Purification Kit (Qiagen, Crawley, UK). Direct DNA sequencing of purified PCR products was performed using dideoxynucleotide termination chemistry. Sequencing reactions were purified using the Dye Ex 2.0 Spin Kit (Qiagen, Crawley, UK), and samples were run on the ABI PRISM 310 Genetic Analyzer (Applied Biosystems, Foster City, CA, USA).

Dating the G360R Mutation

An attempt was made to estimate G360R mutation age by DMLE+2.3 software (Reeve and Rannala 2002). Parameter settings were as follows. The required map distances between markers and mutation site were taken from NG_011957.1 genomic reference sequence. The proportion of mutation-carrying chromosomes sampled was estimated based on the assumptions that (1) AKU has a worldwide prevalence of 1–4 in one million and hence the overall frequency of disease-causing alleles at the *HGD* locus is 0.001–0.002 (the geometric mean 0.0014 was used for computation); (2) G360R was found 13 times among 751 entries and hence represents 1.7% of all, Western- and publication-biased, AKU variants (http://hgddatabase.cvtisr.sk/); and (3) the European and US populations currently embrace 507 million (http://ec.europa.eu/eurostat/) and 319 million (http://census.gov) residents, respectively. This leads to 19,659 (0.0014 × 0.017 × 826,000,000) G360R mutation-carrying chromosomes in the reference population. We have analysed ten independent G360R chromosomes, so the desired proportion is 0.0005087 (10/19,659). The growth rate per generation (^{gen}r) was set at 0.0093 and was calculated according to the formula $^{gen}r = \ln(P_t/P_0)/g$, where P_t is the present-day reference population size (Europe and the USA), P_0 is the estimate of the human population size 10,000 years BC (1–10 millions according to several sources (e.g. Livi-Bacci 2012); the geometric mean 3,162,304 was used for computation) and g is the number of generations between these two time points, assuming 20 years per generation. Other DMLE parameter settings remained at their default values.

Results

Haplotype associations between alleles at all seven polymorphic sites within the *HGD* gene were tentatively considered in the 104 control chromosomes. However, as it could be expected, the haplotypes generated by PHASE were most often uncertain due to both the small sample size and the high level of variation at D3S4497 and D3S4556. Thus, we restricted the analysis of the control chromosomes to the haplotype associations at the four SNPs and the dimorphic D3S4496. Figure 1 shows the maximum parsimony relationships among the seven 5-loci haplotypes (rs2733825, rs2255543, D3S4496, rs2551607, rs3817627) of which our population is composed.

HRMA and, for comparison, Sanger sequencing were used to detect G360R in the 40 members of the two new AKU pedigrees. Table 1 shows molecular confirmation of the homozygous status in 7 patients and that of obligate

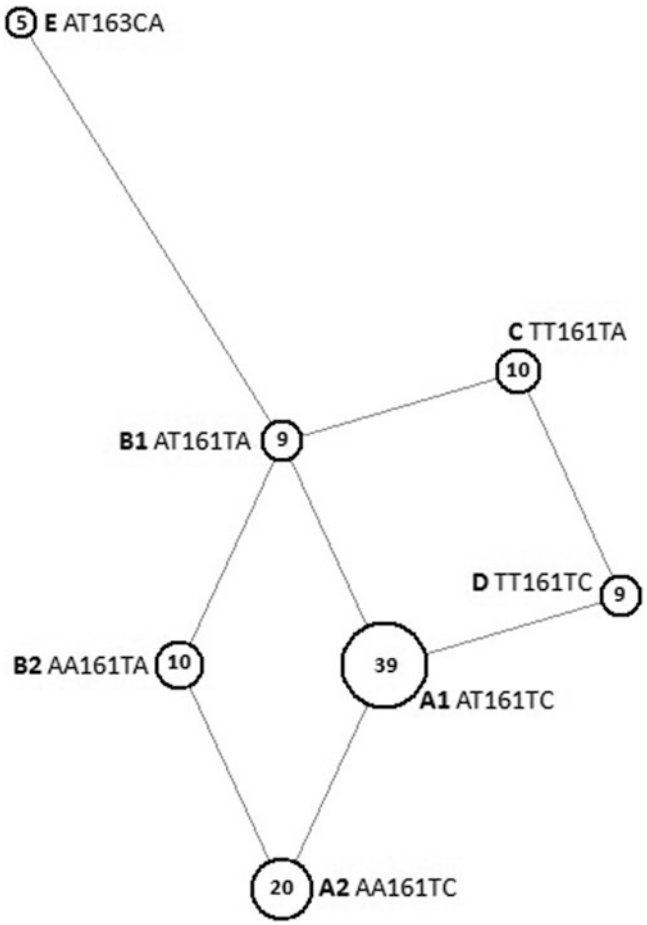

Fig. 1 Maximum parsimony network showing the seven 5-loci *HGD* haplotypes found in a sample of 52 normal South Tyrolean subjects. Nodes are proportional to the haplotype frequencies (estimated numbers within each node) and are labelled with an alphanumerical string formed by haplotype name and composition. All branches imply a single substitution (e.g. A1 and A2 differ at position 2 where A and T, respectively, are present), with the exception of B1-E which requires two events (161T as opposite to 163C at positions 3 and 4, respectively)

heterozygosity in 12 patients' sons as well as in the patients' parents of only one family, the other couple being unavailable. Among the eight unaffected patients' sibs, we found six G360R carriers. Moreover, among 11 sons of these carriers, another six carriers were identified. Notably, a G360R homozygote was also detected, pointing to the presence of another "independent" obligate carrier among the partners of family members.

The extended 7-loci haplotypes (rs2733825, rs2255543, D3S4556, D3S4496, rs2551607, rs3817627, D3S4497) were characterised in the 40 members of the two new AKU pedigrees. The G360R mutation in both families was on the same A2-extended *HGD* haplotype A-A-193-161-T-C-197 originally described (Porfirio et al. 2000). Table 2 shows that this haplotype is highly conserved (only HGO-2 changed) on six of eight independent G360R-bearing chromosomes from the UK and USA. Exceptions mainly come from the US patient of Indian origin, whose G360R-bearing haplotype was different at five of seven loci.

Finding that all but one patient in our cohort shared very similar if not identical allele sequence in the vicinity of the G360R mutation pointed to a common origin. To support this hypothesis, we considered the frequency of the G360R-bearing haplotype in the normal population. The frequency of the 5-loci A2 haplotype in the sample of normal controls proved to be statistically lower than that in the patients, i.e. 20/104 (19%) versus 10/20 (50%), $P<0.003$. This is consistent with the existence of a founding ancestor for the G360R mutation in the *HGD* gene.

Assuming the existence of a common ancestral mutation event, with the aid of DMLE software, an attempt was made to estimate when this *HGD* G360R mutation occurred. The results of the likelihood analysis of mutation age are very sensitive to the assumptions about the model, particularly the assumptions of a uniform relationship between recombination rate and physical distance and equal mutation rates (Rannala and Bertorelle 2001). To check for these potential flaws, we carried out two separate analyses for SNPs (and the dimorphic D3S4496) and for microsatellites, leading to G360R age estimates of 534 generations (95% credible set, 398–857) and 558 generations (95% credible set, 408–860), respectively (Fig. 2a). Another factor affecting mutation age estimate is the population growth rate (Slatkin and Rannala 2000). In the model, it is assumed that the population has been growing exponentially at the same rate in the past. To explore the effects of variable growth dynamics over time, we ran the programme with both a double (${}^{gen}r = 0.0186$) and a half (${}^{gen}r = 0.00465$) growth rate setting using the whole set of markers. The most credible *HGD* G360R age set spanned from 276 to 1,686 generations (about 5,500–33,700 years); the older the age, the lower the growth rate considered (Fig. 2b). Using the whole set of flanking markers and the intermediate population growth rate, G360R mutation age was estimated in 545 generations (95% credible set, 402–854), corresponding to 10,900 years.

Discussion

Finding a single mutation responsible for all our South Tyrolean cases prompted us to hypothesise a founder effect in our cohort of patients. A haplotype analysis was consequently performed to check whether our patients had a common G360R-bearing haplotype, since a founder effect is expected to result in a common allele sequence in the vicinity of the mutation due to the existence of a single progenitor. Furthermore, we extended our study to all available G360R-bearing AKU patients worldwide.

Table 1 Assessment by high-resolution melting analysis (HRMA) and by Sanger sequencing of the genotypes at *HGD* c.1078G>C of both the 40 available members and their 17 available spouses from two AKU pedigrees

HGD c.1078G>C		# of members by family	HRMA	Sanger	False positives	False negatives
Obligate CG carriers		12 + 2	14	14	0	0
CC affected		4 + 3	7	7	0	0
Unaffected patients' sibs	GG normals	1 + 1	2	2	0	0
	CG carriers	4 + 2	6	6	0	0
Carriers' sons	GG normals	4 + 0	4	4	0	0
	CG carriers	6 + 0	6	6	0	0
	CC affected	1 + 0	1	1	0	0
Spouses	GG normals	10 + 6	16	16	0	0
	CG carriers	1 + 0	1	1	0	0

Table 2 *HGD* G360R-harbouring haplotypes identified in ten independent AKU chromosomes

Chromosome identifier	Geographic origin	IVS2+35T/A	c.240T/A	HGO-3	HGO-1	IVS5+25T/C	IVS6+46C/A	HGO-2
AKU 030	South Tyrol	A	A	193	161	T	C	197
AKU 031	Calabria	A	A	193	161	T	C	197
AKU 019	UK, Caucasian	A	A	193	161	T	C	179
AKU 121	USA, Hispanic	A	A	193	161	T	C	179
AKU 185	USA, Caucasian	A	A	193	161	T	C	189
AKU 187	USA, Caucasian	A	A	193	161	T	C	179
AKU 188	USA, Caucasian	A	A	193	161	T	C	179
AKU 189	USA, Caucasian	A	A	193	161	T	C	183
AKU 003	USA, Caucasian	A	A	195	161	T	C	189
AKU 186	USA, Indian	T	T	197	161	T	A	179

The estimated age of 10,900 (5,500–33,700) years for G360R would mean that the mutation took place after human populations left Africa (around 100,000 years ago) to spread in the Middle East, South Asia and Europe around 40,000 years ago (Shriner et al. 2014). Although no data are available on sub-Saharan populations (http://hgddatabase.cvtisr.sk/), lack of G360R detection among African-American AKU patients would seem to confirm indirectly that this mutation is rare (if not absent) in Africa (Phornphutkul et al. 2002; Vilboux et al. 2009).

If the G360R mutation occurred before the migrant human populations separated to reach Europe or Asia, we could expect to find it in both continents. Although this might be suggested by the presence of G360R in a US patient of Indian ancestry, its occurrence in Asia has never been documented (http://hgddatabase.cvtisr.sk/). As mentioned above, G360R reportedly lies in a mutational hot spot. Therefore, its presence in the US-Indian patient may be well interpreted also by this mechanism, which parsimoniously accounts for the detection of a 5-loci C haplotype harbouring that G360R mutation instead of the 5-loci A2 haplotype found in all other patients.

Numerous archaeological findings (Dondio 1995) witness a diffused human presence in South Tyrol since the Mesolithic (10,000 years ago). The members of the South Tyrolean families reported here come from very small villages scattered along a remote high valley (supplementary Fig. 3). Present-day residents hardly count 9,000 units (http://demo.istat.it/). Moreover, the analysis of demographical records shows that the population is very stable and the absolute number of inhabitants has been almost the same across the years (http://www.istat.it/it/archivio/). The presence of Italian speakers in the villages has always been very limited as a result of negligible immigration and admixture (http://www.provinz.bz.it/astat/it/). The presence of a limited number of surnames also accounts for geographic and cultural isolation and suggests a high endogamy rate. Therefore, not surprisingly, we observed a *HGD* G360R homozygote born from an unaffected patient's sib and an "unrelated" carrier. We cautiously estimate that *HGD*

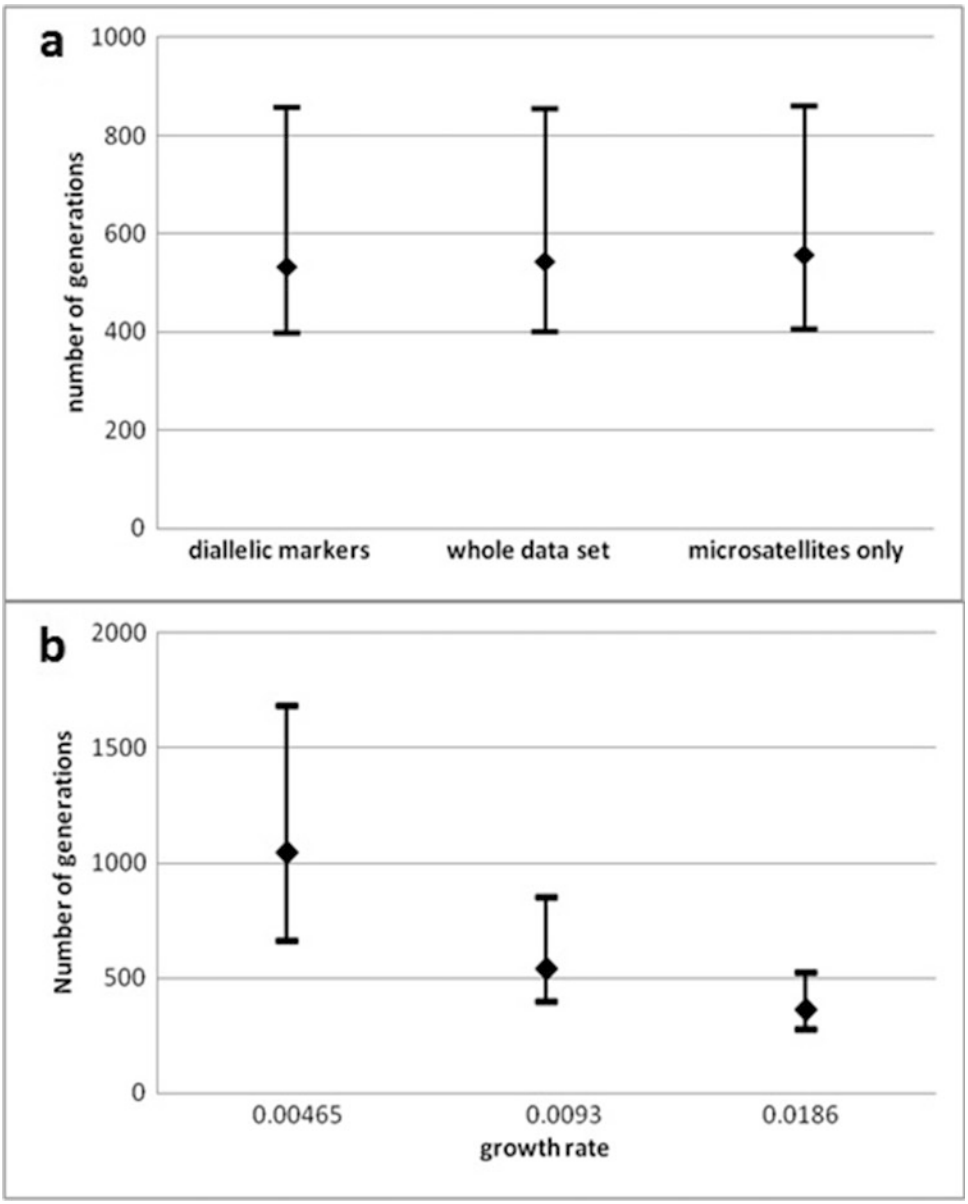

Fig. 2 Estimated age of G360R mutation using the DMLE software varying either the marker numbers and types with fixed 0.0093 growth rate (**a**) or the growth rates with the whole set of markers (**b**). *Error bars* represent the Bayesian 95% credible interval

G360R carriers might be 6%, meaning that the inhabitants of this valley would benefit from genetic counselling.

Loss-of-function homozygous or compound heterozygous *HGD* mutations cause the inability for AKU patients to metabolise homogentisic acid (HGA). Affected individuals excrete HGA in the urine, which assumes a characteristic dark colour when exposed to air. AKU is a slowly progressive disease with obvious manifestations (ochronosis) occurring after more than three decades. Ochronosis consists of a deposition of brown-black pigment in connective tissues, such as the cartilage, skin and sclerae. Musculoskeletal involvement is the most serious complication of this condition, leading to a severe and sometimes crippling form of arthropathy (Mannoni et al. 2004). It has been pointed out that if HGA levels are reduced before the onset of overt disease, this might prevent the debilitating progression of AKU (Suwannarat et al. 2005). In fact, the ability of nitisinone to reduce plasma HGA levels and urinary excretion holds promises for treatment (Ranganath et al. 2015).

It would thus seem that a local programme to identify asymptomatic persons having AKU deserves consideration since all fundamentals of screening are met (Bonita et al. 2006). From its nature, a screening must have the potential

for decreasing morbidity in high-prevalence groups through its capacity to detect a disease at a stage when cure or control is possible. Biochemical evaluation (exposure of urine to alkali) of at-risk population is reliable and feasible at very low cost (Valmikinathan and Verghese 1966). The test is reasonably sensitive and specific with high predictive values. Moreover, biochemical screening can easily be followed by genetic testing with the HRMA procedure described here.

The observation that a high proportion of families with *HGD* alterations from South Tyrol may harbour a founder mutation has significant impact in health community policies, since a role for heterozygous mutations of *HGD* as one of the liability genetic determinants in complex traits of rheumatologic interest has been envisaged (Mistry et al. 2013; Gallagher et al. 2015). Biochemical screening could be undertaken as a first step before direct molecular analysis for G360R, at least in individuals of ascertained South Tyrolean ancestry. The identification of a large set of families carrying an identical AKU mutation would also provide unique opportunities to study the effects of other genetic and environmental factors on penetrance and disease phenotype.

Acknowledgements The study was supported by a research grant (Ricerca d'Ateneo 2014) from the University of Florence, Italy, to BP.

Synopsis

Inhabitants of a geographic isolate, where a founder mutation of the homogentisate dioxygenase gene was characterised, would benefit from screening and genetic counselling for alkaptonuria.

Compliance with Ethics Guidelines

Conflict of Interest

All authors, Berardino Porfirio, Roberta Sestini, Greta Gorelli, Miriam Cordovana, Alessandro Mannoni, Jeanette L. Usher, Wendy J. Introne, William A Gahl and Thierry Vilboux, declare that they have no conflict of interest.

Informed Consent

The Italian subjects involved gave written informed consent in accordance to the Helsinki Declaration, and the study was approved by our institutional review board. Proof that informed consent was obtained will be available upon request. The US and UK DNA samples were provided upon material transfer agreements between the respective Institutions.

Animal Rights

This article does not contain any studies with animal subjects performed by the any of the authors.

Details of the Contributions of Individual Authors

BP planned, conducted and reported the work described in the article with the substantial contribution of RS, GG, MC, JLU and TV for data gathering, analysis and interpretation and of AM, WJI and WAG for revising the manuscript critically for important intellectual content.

BP serves as guarantor for the article, accepts full responsibility for the work and/or the conduct of the study, had access to the data and controlled the decision to publish.

Competing Interest

None.

Electronic-Database Information

Accession numbers and URLs for data in this article are as follows:

http://bioinfo.ut.ee/primer3/ (for guidance in the identification of PCR primers)

http://census.gov/ (for current US population census data)

http://demo.istat.it/ (for current population census of the present-study South Tyrolean valley)

http://ec.europa.eu/eurostat/ (for current European population census data)

http://enzyme.expasy.org/ (the enzyme nomenclature database for HGD [EC 1.13.11.5])

http://hgddatabase.cvtisr.sk/ (a Leiden Open Variation Database [LOVD] v.2.0 on *HGD* mutations and polymorphisms curated by A. Zatkova)

http://stephenslab.uchicago.edu/phase/download.html (to get PHASE v.2.1, a programme for reconstructing haplotypes from population data)

http://www.dmle.org/ (to get the DMLE+ v2.3 linkage disequilibrium mapping software)

http://www.istat.it/it/archivio/ (for historical population censuses of the present-study South Tyrolean valley)

http://www.ncbi.nlm.nih.gov/nuccore/ (for genomic sequences of *HGD* and its transcript, accession numbers NG_011957.1 and NM_000187.3, respectively)

http://www.provinz.bz.it/astat/it/ (for data on language usage, migration rates, marriages in the present-study South Tyrolean valley)

https://www.dna.utah.edu/umelt/umelt.html (for HRMA pattern prediction)

Online Mendelian Inheritance in Man (OMIM), http://www.ncbi.nlm.nih.gov/omim/ (for AKU [OMIM 203500] an *HGD* [OMIM 607474])

References

Beltrán-Valero de Bernabé D, Granadino B, Chiarelli I et al (1998) Mutation and polymorphism analysis of the human homogentisate 1, 2-dioxygenase gene in alkaptonuria patients. Am J Hum Genet 62:776–784

Beltrán-Valero de Bernabé D, Jimenez FJ, Aquaron R, Rodríguez de Córdoba S (1999) Analysis of alkaptonuria (AKU) mutations and polymorphisms reveals that the CCC sequence motif is a mutational hot spot in the homogentisate 1,2 dioxygenase gene (HGO). Am J Hum Genet 64:1316–1322

Bonita R, Beaglehole R, Kjellström T (2006) Basic epidemiology, 2nd edn. World Health Organization

Dondio W (1995) La regione atesina nella preistoria. Rætia

Fernández-Cañón JM, Granadino B, Beltrán-Valero de Bernabé D et al (1996) The molecular basis of alkaptonuria. Nat Genet 14:19–24

Gallagher JA, Ranganath LR, Boyde A (2015) Lessons from rare diseases of cartilage and bone. Curr Opin Pharmacol 22:107–114

Granadino B, Beltrán-Valero de Bernabé D, Fernández-Cañón JM, Peñalva MA, Rodríguez de Córdoba S (1997) The human homogentisate 1,2-dioxygenase (HGO) gene. Genomics 43:115–122

Grasko JM, Hooper AJ, Brown JW, McKnight CJ, Burnett JR (2009) A novel missense HGD gene mutation, K57N, in a patient with alkaptonuria. Clin Chim Acta 403:254–256

Liew M, Pryor R, Palais R et al (2004) Genotyping of single-nucleotide polymorphisms by high-resolution melting of small amplicons. Clin Chem 50:1156–1164

Livi-Bacci M (2012) A concise history of world population, 5th edn. Wiley-Blackwell

Mannoni A, Selvi E, Lorenzini S et al (2004) Alkaptonuria, ochronosis, and ochronotic arthropathy. Semin Arthritis Rheum 33:239–248

Mistry JB, Bukhari M, Taylor AM (2013) Alkaptonuria. Rare Dis 1:27475

Phornphutkul C, Introne WJ, Perry MB et al (2002) Natural history of alkaptonuria. N Engl J Med 347:2111–2121

Porfirio B, Chiarelli I, Graziano C et al (2000) Alkaptonuria in Italy: polymorphic haplotype background, mutational profile, and description of four novel mutations in the homogentisate 1,2-dioxygenase gene. J Med Genet 37:309–312

Ranganath LR, Timmis OG, Gallagher JA (2015) Progress in alkaptonuria –are we near to an effective therapy? J Inherit Metab Dis 38:787–789

Rannala B, Bertorelle G (2001) Using linked markers to infer the age of a mutation. Hum Mutat 18:87–100

Reeve JP, Rannala B (2002) DMLE+: Bayesian linkage disequilibrium gene mapping. Bioinformatics 18:894–895

Shriner D, Tekola-Ayele F, Adeyemo A, Rotimi CN (2014) Genome-wide genotype and sequence-based reconstruction of the 140,000 year history of modern human ancestry. Sci Rep 4:6055

Slatkin M, Rannala B (2000) Estimating allele age. Annu Rev Genomics Hum Genet 1:225–249

Stephens M, Scheet P (2005) Accounting for decay of linkage disequilibrium in haplotype inference and missing data imputation. Am J Hum Genet 76:449–462

Suwannarat P, O'Brien K, Perry MB et al (2005) Use of nitisinone in patients with alkaptonuria. Metabolism 54:719–728

Usher JL, Ascher DB, Pires DE, Milan AM, Blundell TL, Ranganath LR (2015) Analysis of HGD gene mutations in patients with alkaptonuria from the United Kingdom: identification of novel mutations. JIMD Rep 24:3–11

Valmikinathan K, Verghese N (1966) Simple colour reaction for alkaptonuria. J Clin Pathol 19:200

Vilboux T, Kayser M, Introne W et al (2009) Mutation spectrum of homogentisic acid oxidase (HGD) in alkaptonuria. Hum Mutat 30:1611–1619

Wittwer CT (2009) High-resolution DNA melting analysis: advancements and limitations. Hum Mutat 30:857–859

Zatkova A, Sedlackova T, Radvansky J et al (2012) Identification of eleven novel homogentisate 1,2 dioxygenase (HGD) variants in alkaptonuria (AKU) patients and establishment of a novel LOVD based HGD mutation database. JIMD Rep 4:55–65

JIMD Reports
DOI 10.1007/8904_2016_542

CASE REPORT

Rapid Desensitization for Immediate Hypersensitivity to Galsulfase Therapy in Patients with MPS VI

Zeynep Tamay · Gulden Gokcay · Fatih Dilek · Mehmet Cihan Balci · Deniz Ozceker · Mubeccel Demirkol · Nermin Guler

Received: 08 February 2014 / Revised: 27 March 2014 / Accepted: 07 April 2014 / Published online: 08 March 2016

Abstract Mucopolysaccharidosis type VI (MPS VI) is a progressive, chronic, and multisystem lysosomal storage disease. Enzyme replacement therapy (ERT) with the recombinant human arylsulfatase B enzyme (galsulfase [Naglazyme]) is recommended as first-line therapy. It is generally reported as safe and well tolerated. Frequently observed mild to moderate infusion-related reactions which can be easily handled by reducing or interrupting the infusion and/or administering additional antihistamines, antipyretics, and corticosteroids are mostly mediated by non-IgE mechanisms. Here we report two children with MPS VI who experienced IgE-mediated reactions with galsulfase at the second year of the therapy. One child had anaphylaxis and the other had urticarial eruptions. They could receive ERT after successful rapid desensitization. To our knowledge, this is the second report on galsulfase allergy with IgE-mediated reaction. It is important to recognize IgE-mediated reactions since they can be life-threatening and do not respond to the standard therapies. We recommend allergy skin tests in the evaluation of infusion-related reactions unresponsive to standard therapies, so that continuation of ERT will be feasible after successful desensitization.

Abbreviations

BWH	Brigham and Women's Hospital
ERT	Enzyme replacement therapy
GAG	Glycosaminoglycan
MPS VI	Mucopolysaccharidosis type VI
N-acetylgalactosamine -4-sulfatase	Arylsulfatase B

Introduction

Mucopolysaccharidosis type VI (MPS VI or Maroteaux-Lamy syndrome; OMIM 253200) is a lysosomal storage disorder caused by deficient activity of *N*-acetylgalactosamine-4-sulfatase (arylsulfatase B or ASB; EC 3.1.6.12), which catabolizes the glycosaminoglycan (GAG) dermatan sulfate. Accumulation of GAG in lysosomes in a wide range of tissues causes progressive multisystem involvement with physical and functional impairment and shortened lifespan (Valayannopoulos et al. 2010). ERT is recommended as first-line therapy for MPS VI with the approval of the recombinant human arylsulfatase B enzyme (galsulfase [Naglazyme]) by the US Food and Drug Administration and the European Medicines Agency. The recommended dose of Naglazyme is 1 mg/kg body weight administered once weekly as an intravenous infusion over a duration of 4 h (Harmatz et al. 2013). It is generally reported as safe and well tolerated. Infusion-related reactions

Communicated by: Olaf Bodamer, MD

Competing interests: None declared

Z. Tamay (✉) · D. Ozceker
Division of Pediatric Allergy and Clinical Immunology, Department of Pediatrics, Istanbul Medical Faculty, Istanbul, Turkey
e-mail: eztamay@yahoo.com

N. Guler
Department of Pediatrics, Faculty of Medicine, Istanbul Bilim University, Istanbul, Turkey

G. Gokcay · M.C. Balci · M. Demirkol
Division of Pediatric Nutrition and Metabolism, Department of Pediatrics, Istanbul Medical Faculty, Istanbul, Turkey

F. Dilek
Division of Pediatric Allergy and Clinical Immunology, Department of Pediatrics, Bezmialem Vakıf University, Istanbul, Turkey

were described in several studies and case reports, but probable IgE-mediated allergy has been reported only in one patient. Frequently observed reactions were mild to moderate infusion-related reactions, which were easily resolved by slowing or temporary interruption of the infusion and/or administration of additional antihistamines, antipyretics, and corticosteroids (Harmatz et al. 2006; Horovitz et al. 2013). Here we report two children with MPS VI who experienced IgE-mediated hypersensitivity reactions with galsulfase and could receive ERT after successful rapid desensitization.

Case 1

A 9-year-old male child had been diagnosed with MPS VI when he was 12 months old with facial coarsening, hepatosplenomegaly, chest deformity, and high urinary GAG levels. Diagnosis had been confirmed with enzyme studies [lymphocyte arylsulfatase B (ARSB) 3.8 μkat/kg protein (control range 27.4; 17–40.8 μkat/kg protein; Sahlgrenska University)] at the age of 2.5 years, and ERT (1 mg/kg galsulfase solution, intravenous and weekly) had been initiated at the age of 7 years. According to the standard institutional practice, galsulfase solution had been diluted with sterile 0.9% sodium chloride solution to 100 ml. After parenteral pheniramine maleate (1 mg/kg) premedication, approximately 3% of the total solution had been infused during the first hour and the remaining volume in 3 h. The patient had no adverse reactions during weekly galsulfase infusions for the first 2 years of ERT. In the following 6 months, he had some mild itching and urticarial eruptions during infusions, but these reactions were controlled by elongation of the duration of infusion therapy. He was referred to the Allergy Outpatient Clinic after an anaphylaxis with generalized urticaria, angioedema of the lips and the face, stridor, and wheezing during a galsulfase therapy.

Allergy skin tests were performed with galsulfase solution using standard methods. Skin prick tests with 1:1,000, 1:100, and 1:10 dilution and full concentration (1 mg/ml) and intradermal tests with 1:100 and 1:10 dilution were performed. Although the patient's skin prick tests were negative, intradermal test with 1:100 dilution showed positive reaction (Fig. 1). The allergy skin prick tests were performed in additional eight children with MPS VI who were already receiving galsulfase therapy, and all were negative.

A modified version of the standardized desensitization protocol of Brigham and Women's Hospital (BWH) Desensitization Program was used (Castells 2006a, b; Castells et al. 2012). The patient was premedicated with intravenous pheniramine maleate (1 mg/kg), ranitidine (1 mg/kg), and methylprednisolone (1 mg/kg) 20 min before the desensitization procedure. The 20-step standard

Fig. 1 Positive intradermal skin prick test of case 1

protocol with five solutions containing 1:10,000, 1:1,000, 1:100, 1:10, and full dose of galsulfase was administered sequentially. Each solution was administered gradually in four different steps with 15 min intervals (Table 1). Generalized urticarial rash, angioedema of the lips, stridor, and wheezing occurred at the beginning of third solution (1:100 dilution). The infusion was paused, and initially intravenous pheniramine maleate, ranitidine, and inhaled adrenaline were administered. Salbutamol was also administered because of refractory lower respiratory symptoms. On resolution of the reaction, the protocol was restarted from the same step. Urticarial rash reoccurred at the end of the last step of the final fifth solution. The infusion was paused again and 5 mg montelukast, a leukotriene receptor antagonist, was given orally. When the reaction resolved, the infusion was restarted and completed.

One day before the next desensitization procedure, a week later, the patient was premedicated with oral H1-antihistamine (cetirizine) and H2-antihistamine (ranitidine). The patient completed the desensitization procedure without further reactions. The following four desensitizations were uneventful; therefore, premedication with methylprednisolone and the first two dilutions were omitted. Twelve-step protocol with three solutions was applied uneventfully for 5 months (Table 2). ERT had to be stopped for 2 months because of drug unavailability. With the start of treatment, 20-step desensitization protocol was restarted with premedication. During the infusion, urticarial eruptions and mild wheezing occurred at the beginning of the last solution. The infusion was paused, symptomatic treatment with H1 antihistamine and inhaled salbutamol was given, and the infusion was restarted after the reaction had resolved. The infusion rate could not be increased due to urticarial eruptions and stopped at the 16th step. To resolve this problem, oral montelukast was added to the premedication given the night before the desensitization day. On the

Table 1 20-Step, five-bag desensitization protocol for case 1

Step	Solution	Rate (ml/h)	Time (min)	Volume infused per step (ml)	Dose administered (mg)	Cumulative dose (mg)
1	1	1	15	0.25	0.000005	0.000005
2	1	2	15	0.50	0.00001	0.000015
3	1	4	15	1.00	0.00002	0.000035
4	1	8	15	2.00	0.00004	0.000075
5	2	2	15	0.50	0.0001	0.000175
6	2	5	15	1.25	0.00025	0.000425
7	2	10	15	2.50	0.0005	0.000925
8	2	20	15	5.00	0.001	0.001925
9	3	1	15	0.25	0.0005	0.002425
10	3	2	15	0.50	0.001	0.003425
11	3	4	15	1.00	0.002	0.005425
12	3	8	15	2.00	0.004	0.009425
13	4	2	15	0.50	0.001	0.010425
14	4	5	15	1.25	0.025	0.035425
15	4	10	15	2.50	0.05	0.085425
16	4	20	15	5.00	0.10	0.185425
17	5	5	15	1.25	0.25	0.435425
18	5	10	15	2.50	0.5	0.935425
19	5	20	15	5.00	1.0	1.935425
20	5	39	100.4	65.25	18.064575	20.000000
Total time (min)=				385.4 = 6.4 h		

Solution 1 (1/10,000): 100 ml; 0.00002 mg/ml
Solution 2 (1/1,000):100 ml; 0.0002 mg/ml
Solution 3 (1/100): 100 ml; 0.002 mg/ml
Solution 4 (1/10): 50 ml; 0.02 mg/ml
Solution 5 (1/1): 100 ml; 0.2 mg/ml

Table 2 12-Step, three-bag desensitization protocol for case 1

Step	Solution	Rate (ml/h)	Time (min)	Volume infused per step (ml)	Dose administered (mg)	Cumulative dose (mg)
1	1	1	15	0.25	0.0005	0.0005
2	1	2	15	0.5	0.001	0.0015
3	1	4	15	1	0.002	0.0035
4	1	8	15	2	0.004	0.0075
5	2	2	15	0.5	0.01	0.0175
6	2	5	15	1.25	0.025	0.0425
7	2	10	15	2.5	0.05	0.0925
8	2	20	15	5	0.10	0.1925
9	3	5	15	1.25	0.25	0.4425
10	3	10	15	2.5	0.50	0.9425
11	3	20	15	5	1.00	1.9425
12	3	39	120.4	78.25	18.0575	20.0000
Total time (min)=			285.4 = 4.75 h			

Solution 1 (1/100): 100 ml; 0.002 mg/ml
Solution 2 (1/10): 50 ml; 0.02 mg/ml
Solution 3 (1/1): 100 ml; 0.2 mg/ml

desensitization day, premedication with H1 and H2 antihistamine was given before the 16th step. No more reactions occurred during therapy after four desensitizations. The desensitization protocol was shifted from 20-step to 12-step. The patient continues to receive galsulfase therapy uneventfully, on weekly basis since 10 months.

Case 2

A 4-year-old male child had been diagnosed as MPS VI with coarse facial appearance, macrocephaly, and pectus carinatum when he was 11 months old. The diagnosis had been confirmed with enzyme assays [leukocyte ARSB 0.00 μmol/g/h (control 12.6 μmol/g/h, Willink Laboratory, Genetic Medicine, St Mary's Hospital)], and ERT (1 mg/kg galsulfase solution, intravenous and weekly) was initiated. The therapy was well tolerated for 26 months until the patient started to have recurrent urticarial eruptions during the last three galsulfase therapies. He was referred to the Allergy Outpatient Clinic for further evaluation.

The history revealed that this child had been tested for allergic reaction to galsulfase as our first patient's control case. His skin prick and intradermal tests were negative 10 months before the beginning of the allergic reactions. The repeated allergy skin tests revealed positive reaction with intradermal skin test at a dilution of 1:100. The same premedication and the 20-step standard protocol were administered sequentially. The desensitization protocol was shifted from 20-step to 12-step after four uneventful desensitizations. The patient continues to receive galsulfase therapy on weekly basis, without any adverse reactions since 5 months.

Discussion

Rapid desensitization is the induction of temporary clinical tolerance to a drug, thereby allowing the patient to be treated with the medication, which had caused hypersensitivity reaction (Brennan et al. 2009; Castells 2006a, b; Castells et al. 2012; Liu et al. 2011). Rapid desensitization targets mast cells so that it can be used for IgE-mediated anaphylactic or (non-IgE-mediated) anaphylactoid immediate type reactions (Liu et al. 2011). Here, we report two MPS VI cases with IgE-mediated hypersensitivity to galsulfase solution confirmed by positive intradermal tests and successful rapid desensitizations.

We used a modified version of BWH Desensitization Program, a universal protocol for drug-induced immediate type of hypersensitivity reactions, developed by Castells (2006a, b) and Castells et al. (2012). This protocol is a 12- to 20-step standard protocol, in which tolerance was achieved by delivering double doses of antigen at fixed time intervals. We initially used the 20-step protocol in both cases and continued with the 12-step standard protocol.

Reported infusion-related reactions to ERT ranged from 3% to 36% (Harmatz et al. 2008; Miebach 2009). Miebach reported hypersensitivity reactions in 28 (36%) out of 77 patients with MPS type I, type II, and type VI, all of which were controlled by reducing the infusion rate and/or administering antihistamines, antipyretics, and low-dose corticosteroids (2009). Horovitz et al. reported infusion-related reactions in eight (24%) out of 34 patients with MPS VI, and none of them were severe reactions (2013). Intervention and/or premedication with antihistamines, steroids, and antipyretics and decreasing the rate of infusion were sufficient to overcome the reactions.

Kim et al. reported severe anaphylactoid reactions to galsulfase infusion in a 3.5-year-old patient with MPS VI during the fourth and fifth weeks of the therapy (2008). The patient could not receive all of the galsulfase infusion in spite of interruption of the infusion and intervention with antihistamines and steroids. They were able to prevent reactions with oral prednisolone the day before each infusion, intravenous methylprednisolone, and diphenhydramine 1 h before each infusion and decreasing the rate of infusion. The first case with probable IgE-mediated allergic reactions was reported by Begin et al. (2013). A 10-year-old girl with MPS VI had presented with urticarial eruptions, severe conjunctivitis, and lip angioedema during galsulfase therapy after an uneventful duration of ERT for 1 year. Intradermal skin test at a dilution of 1:10 (0.1 mg/ml) was positive, and they also successfully desensitized the patient with a different rapid desensitization protocol (Begin et al. 2013).

We confirmed that IgE-mediated reactions to galsulfase can occur in patients with MPS VI. Case 1 had presented with anaphylaxis and case 2 had presented only with urticarial eruptions. In both cases, there was an interval of 2 years with the beginning of the ERT and IgE-mediated reactions. The case with probable IgE-mediated allergy reported by Begin et al. also had one uneventful year before the onset of the first allergic reaction (2013). We suggest that frequently observed mild to moderate infusion-related reactions which can be easily handled by reducing or interrupting the infusion and/or administering additional antihistamines, antipyretics, and corticosteroids are mostly mediated by non-IgE mechanisms. However, it is important to recognize late-appearing IgE-mediated reactions since they can be life-threatening and do not respond to the standard therapies. IgE-mediated reactions occur after an

interval during which the host is sensitized with the offending allergen.

Non-IgE-mediated infusion-related reactions are mostly observed at the earlier phases of ERT, whereas IgE-mediated reactions are more common during the later stages since a time interval for sensitization is necessary. We recommend allergy skin tests in the evaluation of infusion-related reactions unresponsive to the standard therapies, so that continuation of ERT will be feasible after successful desensitization.

Take-Home Message

Allergy skin tests should be performed in the evaluation of infusion-related reactions unresponsive to standard therapies, so that continuation of ERT will be feasible after successful desensitization.

Compliance with Ethics Guidelines

Conflict of Interest

Zeynep Tamay, Gulden Gökçay, Fatih Dilek, Mehmet C Balci, Deniz Ozceker, Mubeccel Demirkol, and Nermin Guler declare that they have no conflict of interest.

Competing Interests

All procedures followed were in accordance with the ethical standards of the responsible committee on human experimentation (institutional and national) and with the Helsinki Declaration of 1975, as revised in 2000. Informed consent was obtained from all patients for being included in the study.

This article does not contain any animal subjects performed by the any of the authors.

Details of the Contributions of Individual Authors

Zeynep Tamay designed and reported the cases; Fatih Dilek, Mehmet C Balci, and Deniz Ozceker conducted the rapid desensitization procedures; Gulden Gokcay revised the language and also revised the intellectual content with Mubeccel Demirkol and Nermin Guler.

References

Begin P, Chapdelaine H, Lemyre E, Paradis L, Roches A (2013) Successful desensitization in a type VI mucopolysaccharidosis patient with probable IgE-mediated allergy to galsulfase [Naglazyme]. Ann Allergy Asthma Immunol 110:55–56

Brennan P, Bouza RT, Hsu FI, Sloane DE, Castells M (2009) Hypersensitivity reactions to mAbs: 105 desensitizations in 23 patients, from evaluation to treatment. J Allergy Clin Immunol 124:1259–1266

Castells M (2006a) Desensitization for drug allergy. Curr Opin Allergy Clin Immunol 6:476–481

Castells M (2006b) Rapid desensitization for hypersensitivity reactions to chemotherapy agents. Curr Opin Allergy Clin Immunol 6:271–277

Castells M, Sancho-Serra Mdel C, Simarro M (2012) Hypersensitivity to antineoplastic agents: mechanisms and treatment with rapid desensitization. Cancer Immunol Immunother 61:1575–1584

Harmatz P, Giugliani R, Schwartz I et al (2006) Enzyme replacement therapy for mucopolysaccharidosis VI: a phase 3, randomized, double-blind, placebo-controlled, multinational study of recombinant human N-acetylgalactosamine 4-sulfatase (recombinant human arylsulfatase B or rhASB) and follow-on, open-label extension study. J Pediatr 148:533–539

Harmatz P, Giugliani R, Schwartz IV et al (2008) Long-term follow-up of endurance and safety outcomes during enzyme replacement therapy for mucopolysaccharidosis VI: final results of three clinical studies of recombinant human N-acetylgalactosamine 4-sulfatase. Mol Genet Metab 94:469–475

Harmatz PR, Garcia P, Guffon N et al (2013) Galsulfase (Naglazyme^{R}) therapy in infants with mucopolysaccharidosis VI. J Inherit Metab Dis. doi:10.1007/s10545-013-9654-7 [Epub ahead of print]

Horovitz D, Magalhaes T, Acosta A et al (2013) Enzyme replacement therapy with galsulfase in 34 children younger than five years of age with MPS VI. Mol Genet Metab 109:62–69

Kim KH, Decker C, Burton BK (2008) Successful management of difficult infusion-associated reactions in a young patient with mucopolysaccharidosis type VI receiving recombinant human arylsulfatase B (galsulfase [Naglazyme]). Pediatrics 3:714–717

Liu A, Fanning L, Chong H et al (2011) Desensitization regimens for drug allergy: state of the art in the 21st century. Clin Exp Allergy 41:1679–1689

Miebach E (2009) Management of infusion-related reactions to enzyme replacement therapy in a cohort of patients with mucopolysaccharidosis disorders. Int J Clin Pharmacol Ther 47: S100–S106

Valayannopoulos V, Nicely H, Harmatz P, Turbeville S (2010) Mucopolysaccharidosis VI. Orphanet J Rare Dis 5:5

JIMD Reports
DOI 10.1007/8904_2016_532

CASE REPORT

Acute Metabolic Crises in Maple Syrup Urine Disease After Liver Transplantation from a Related Heterozygous Living Donor

Aisha Al-Shamsi · Alastair Baker · Anil Dhawan · Jozef Hertecant

Received: 9 October 2015 / Revised: 13 December 2015 / Accepted: 15 December 2015 / Published online: 28 April 2016

Abstract Maple syrup urine disease (MSUD) is an autosomal recessive disorder associated with impaired metabolism of branched-chain amino acids (BCAA) leucine, isoleucine, and valine. Children with MSUD suffer from bouts of metabolic decompensation, which may lead to neurological damage. Liver transplantation from unrelated deceased donors has been considered curative. The natural history of the disease following transplantation using a haploidentical (obligate heterozygous) living donor is still unclear, although previously described as favorable. We describe acute metabolic crises in a 20-month-old child with MSUD type II. The first well-documented one occurred 5 months after a successful liver transplantation from his mother. The patient developed encephalopathy with progressive lethargy and seizures after an episode of gastroenteritis with dehydration. Plasma levels of leucine, isoleucine, and valine were markedly elevated and alloisoleucine was detected. He promptly responded to dialysis and BCAA-free dietetic management and subsequently could resume a normal diet. Since then he has had another symptomatic metabolic crisis with seizures. This case strongly suggests that some recipients of liver transplantation from a haploidentical parent possess limited capacity to oxidize BCAA at the time of catabolic stress and dehydration and remain at risk of severe metabolic crises. Thus, careful metabolic monitoring and prompt treatment post liver transplantation are still required to avoid neurological sequelae of MSUD, particularly if the donor is heterozygous for MSUD.

Abbreviations

BCAA	Branched-chain amino acids
BCKDH	Branched-chain keto acid dehydrogenase complex
MSUD	Maple syrup urine disease

Introduction

MSUD was first described in 1954 by Menkes et al. in four siblings with progressive infantile cerebral dysfunction and urine odor resembling maple syrup (Menkes et al. 1954). Markedly increased blood levels of leucine, isoleucine, and valine as well as ketonuria were then reported by Westall et al. (1957).The disease results from a deficiency in one of the three subunits of the branched-chain keto acid dehydrogenase (BCKDH) complex. This mitochondrial enzyme catalyzes the oxidative decarboxylation of branched-chain keto acids (BCKA) that are derived from the transamination of valine, leucine, and isoleucine. The management involves life-long dietary leucine restriction through a protein-restricted diet and BCAA-free medical foods, isoleucine and valine supplementation as needed, as well as careful clinical and biochemical monitoring. Metabolic decompensations can be complicated by brain edema and irreparable neurologic injury. They require aggressive management that includes treating the precipitating stress, maximizing calorie intake, and continuing the standard

Communicated by: Francois Feillet, MD, PhD

Competing interests: None declared

A. Al-Shamsi · J. Hertecant (✉)
Department of Pediatrics, Tawam Hospital, Al-Ain, United Arab Emirates
e-mail: aishamsi@seha.ae; jhertecant@seha.ae

A. Baker · A. Dhawan
Pediatric Liver Department, King's College Hospital, London, UK
e-mail: alastair.baker@nhs.net; anil.dhawan@kcl.ac.uk

treatment of the disease. Dialysis is sometimes necessary to remove the excess BCAA (Westall et al. 1957).

Liver transplantation using deceased unrelated donors is considered potentially curative, offering complete protection from metabolic decompensations on a normal diet (Wendel et al. 1999; Bodner-Leidecker et al. 2000). Here, we report a child with MSUD type II who underwent a successful liver transplant from his mother but developed at least two episodes of severe symptomatic metabolic decompensation requiring intensive management. To the best of our knowledge, this is the first case of a well-documented occurrence of this complication.

Patient

The child of a consanguineous marriage presented with progressive irritability, lethargy, convulsions, and encephalopathy at 10 days of age and was diagnosed with MSUD type II (MIM 248610). Initial amino acid profile showed elevated leucine (1,950 μM, normal 75 to 163), isoleucine (316 μM, normal 40 to 88), valine (450 μM, normal 126 to 220), and alloisoleucine (detected). He was treated with dietary leucine restriction, BCAA-free medical foods, and isoleucine and valine supplementations. He recovered very well. *DBT* gene sequencing showed a homozygous splicing mutation c.1281+1G>T in exon 10. The parents were proven to be heterozygous for the same mutation. *BCKDHA* and *BCKDHB* genes were normal.

He had seven metabolic decompensations in the first 8 months of life with maximum leucine levels between 500 and 1,000 μM. He also had poor weight gain and mild hypotonia. His tolerated leucine level ranging between 48 and 272 μM (normal 75 to 163) whenever he was well prior to the liver transplantation.

At 15 months of age, liver transplantation was performed at King's College Hospital, London UK. His mother, 24 years old, was the donor; she was healthy and had no history of metabolic decompensation. During the immediate postoperative period, his branched-chain amino acid levels settled slowly. However, he made good clinical progress and was discharged 11 days after the procedure on an unrestricted diet and immunosuppression with tacrolimus, mycophenolate mofetil and prednisolone. Shortly thereafter, he developed biochemical hepatitis (elevated transaminases) associated with CMV viremia. During follow-up, he suffered a brief episode of lethargy and seizure attributed to tacrolimus toxicity. It was treated with intravenous fluid and recovered completely within 2 days; an amino acid profile was not requested. Afterwards, while consuming a normal protein containing diet, he remained clinically stable; his hypotonia improved considerably and his seizures did not recur.

At 20 months of age, 5 months after the transplant, he presented to our center with symptoms of gastroenteritis and dehydration. He was admitted for intravenous rehydration for 1 day and went home. Three days later, he developed lethargy, convulsions, and encephalopathy requiring intensive management with high calories, BCAA-free medical foods, supplementation of isoleucine and valine, insulin administration and peritoneal dialysis. The amino acid profile of the initial admission for gastroenteritis reached us after a few days and showed elevated leucine (991 μM, normal range 73–161), isoleucine (521 μM, normal 46–90), valine (1,162 μM, normal 149–277) and alloisoleucine (detected). The amino acid profile at the time of encephalopathy and convulsions showed leucine (2,001 μM, normal range 73–161), isoleucine (877 μM, normal 46–90) and valine (1,653 μM, normal 149–277). His ALT was 30 IU/L (normal range 11–39) and his AST was 35 IU/L (normal range 22–58); the other liver tests were also normal. His ammonia level was 46 μmol/L. Liver Doppler study was normal, including the hemodynamic status of both arterial and venous vasculature. He recovered within 48 h and resumed his normal diet, without any protein restriction. His amino acid profiles during the illness are shown in Fig. 1.

After that crisis, he remained well on a normal protein diet. His BCAA were done repeatedly and remained within the normal range.

At the age 26 months, 10 months after the transplantation, he presented again with an episode of seizures. This was his third one, after the one shortly after transplantation, which was attributed to tacrolimus toxicity, and the second one, 5 months after transplantation, while he was on unrestricted protein intake. This third episode was described as tonic movements of the right leg with uprolling of the eyes lasting for about 1 min. The amino acid profile on admission showed elevated leucine (990 μM, normal range 73–161), isoleucine (461 μM, normal 46–90), valine (892 μM, normal 149–277) and alloisoleucine (detected). Interestingly, a routine amino acid profile had been done 2 days prior to the admission. It was completely normal with leucine (66 μM, normal range 73–161), isoleucine (61 μM, normal 46–90) and valine (154 μM, normal 149–277). The patient recovered nearly completely within 24 h with IV fluids and his medical food. Since then, he again has been doing very well on normal diet. His last amino acid profile showed leucine, isoleucine, and valine values of 122, 53, and 145 μM, respectively; all are normal.

Discussion

The natural history of MSUD following liver transplant has been reported repeatedly. In all cases reported till now, the patients tolerated a normal diet and did not experience

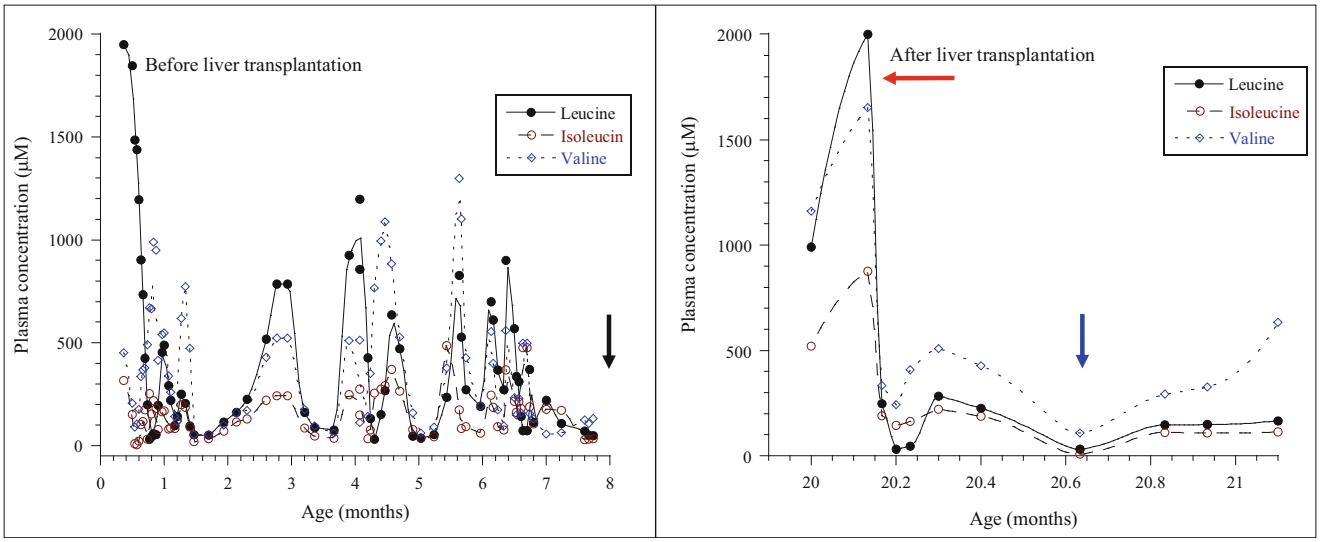

Fig. 1 Concentrations of branched-chain amino acids (BCAA) in plasma after liver transplantation in the index case. BCAA increased with acute dehydration evolving into encephalopathy (*horizontal arrow*) followed by normalization of BCAA on unrestricted diet after 48 h of intensive metabolic management (*vertical arrow*). The *Y*-axis indicates the BCAA plasma concentrations in µM/L and the *X*-axis days posttransplantation when patient presented with metabolic crisis

symptomatic metabolic crises after transplantation. These observations suggested that liver transplant sufficiently corrects BCAA metabolism in MSUD (Wendel et al. 1999).

Mazariegos et al. conducted a cohort study to assess the neurocognitive function of children with MSUD who had a liver transplant. Thirty-five patients (age, 9.9 ± 7.9 years) were followed between 2004 and 2009. They showed that liver transplant is an effective long-term treatment for MSUD and may arrest further brain damage (Mazariegos et al. 2012). However, they did report a child who developed hyperleucinosis during an episode of gastro-enteritis and dehydration; this episode occurred 55 months post transplant from a non-related donor. The plasma leucine level reached 2,170 µM, isoleucine 1,009 µM and valine 1,483 µM. Surprisingly, this patient did not develop obvious neurological symptoms during this episode. His BCAA levels normalized within a few days of intravenous hydration, without specific metabolic treatment (Mazariegos et al. 2012).

Our patient, who received a graft from an asymptomatic carrier parent, showed some delay in normalizing BCAA levels despite very good early graft function. A minor episode of lethargy and brief seizures occurred 2 months after transplant, which, retrospectively, was probably due to a metabolic crisis. Both 5 and 10 months after transplant, he had a characteristic metabolic crisis with encephalopathy and seizures; his branched amino acid levels were very high, and he required emergency metabolic treatment. However, the patient then was able to return to a normal diet with normal BCAA levels.

As far as we know, this is the first time acute well-documented metabolic crises with severe neurological symptoms have occurred in a transplanted MSUD patient.

Mazariegos et al. suggested that visceral ischemia, hepatic vascular compromise, dehydration or factors restricting hepatic blood flow can compromise BCAA clearance by the graft (Mazariegos et al. 2012). It is not likely that any of these played a major role in our patient's metabolic crises because both his liver echo-Doppler and liver function tests were normal at the time of the crisis at 5 months post transplant, which was the most serious one.

We hypothesized unknown factors in the metabolism of the transplant from the mother that would decrease its BCKDH branched-chain keto acid dehydrogenase complex activity more than would be expected in a heterozygote carrier. To gather evidence for this, we asked the mother to follow a high-protein diet for several days and then checked her branched amino acids. They remained in the low normal range (leucine 73 µM (normal range 97–161), isoleucine 38 µM (normal 46–90), and valine 145 µM (normal 178–284)). Thus, it appears that the mother has normal protein tolerance rather than an unusual dominant-negative mutation or any other factor leading to significant impairment of branched-chain amino acid metabolism, in spite of her heterozygous state.

Feier et al. reported a 2-year-old patient with MSUD who underwent liver transplant from his mother. The recipient's

leucine levels were normal by the second postoperative day without any dietary restriction and neither the donor nor the recipient experienced metabolic decompensations after the transplant, showing the utility of this management (Feier et al. 2014). However, the non-symptomatic metabolic crisis described by Mazariegos and the events described in our patient indicate that the capacity of a grafted liver to oxidize BCAA can be overwhelmed by catabolic stress and dehydration and that the protection afforded by the liver transplant may not be complete in some cases. The liver probably accounts for only 9 to 13% of the whole body BCKDH activity enzyme activity; the rest is found in other tissues, mainly in muscle (54–66%) (Mazariegos et al. 2012). It is reasonable to assume that heterozygous carriers of MSUD would provide less BCKDH activity in a live donated organ and therefore less protection during stress, leading to an increased risk for symptomatic metabolic crises post transplant. However, we do not know if the patient described by Mazariegos with an asymptomatic increase in leucine after transplant, received it from a heterozygous carrier or not. The case of our patient reinforces once more the importance of the following recommendations of Mazariegos et al.: (1) Clinicians should continue monitoring amino acids in post transplant patients, particularly those who develop serious catabolic illness or unexplained encephalopathy; (2) visceral ischemia, hepatic vascular compromise, dehydration, or factors restricting hepatic blood flow can compromise BCAA clearance by the graft (Mazariegos et al. 2012).

Acknowledgment We want to thank the family. We also want to thank George Mazariegos from Pittsburgh, who contributed many useful ideas and kindly reviewed the article, as well as Fatma Al Jasmi and Abdul-kader Souid for reviewing the manuscript and useful suggestions.

Compliance with Ethics Guidelines

Conflict of Interest

The authors have declared that no conflict of interest exists.

References

Bodner-Leidecker A, Wendel U, Saudubray JM, Schadewaldt P (2000) Branched-chain L-amino acid metabolism in classical maple syrup urine disease after orthotopic liver transplantation. J Inherit Metab Dis 23:805–818

Feier FH, Miura IK, Fonseca EA, Porta G, Pugliese R, Porta A, Schwartz IV, Margutti AV, Camelo JS Jr, Yamaguchi SN, Taveira AT, Candido H, Benavides M, Danesi V, Guimaraes T, Kondo M, Chapchap P, Neto JS (2014) Successful domino liver transplantation in maple syrup urine disease using a related living donor. Braz J Med Biol Res 47(6):522–526

Mazariegos GV, Morton DH, Sindhi R, Soltys K, Nayyar N, Bond G et al (2012) Liver transplantation for classical maple syrup urine disease: long-term follow-up in 37 patients and comparative United Network for Organ Sharing experience. J Pediatr 160: 116–121. doi:10.1016/j.jpeds.2011.06.033

Menkes J, Hurst P, Craig JM (1954) A new syndrome: progressive familial infantile cerebral dysfunction associated with an unusual urinary substance. Pediatrics 14:462–466

Wendel U, Saudubray JM, Bodner A, Schadewaldt P (1999) Liver transplantation in maple syrup urine disease. Eur J Pediatr 158(Suppl 2):S60–S64

Westall RG, Dancis J, Miller S (1957) Maple syrup urine disease. Am J Dis Child 94:571–572

JIMD Reports
DOI 10.1007/8904_2015_475

RESEARCH REPORT

Identification of Cryptic Novel α-Galactosidase A Gene Mutations: Abnormal mRNA Splicing and Large Deletions

Takashi Higuchi · Masahisa Kobayashi · Jin Ogata · Eiko Kaneshiro · Yohta Shimada · Hiroshi Kobayashi · Yoshikatsu Eto · Shiro Maeda · Akira Ohtake · Hiroyuki Ida · Toya Ohashi

Received: 11 March 2015 / Revised: 20 May 2015 / Accepted: 11 June 2015 / Published online: 03 June 2016

Abstract Anderson-Fabry (FD) disease is an inborn error of metabolism caused by a deficiency of α-galactosidase A (*GLA*), a lysosomal enzyme. Many male FD patients display a classic FD phenotype; however, some female patients have neither reduced leukocyte GLA enzyme activity level nor FD symptoms. Thus, *GLA* gene analysis is especially important for diagnosing suspected FD in female subjects. In this study, we revealed 4 novel *GLA* gene mutations in 5 independent families using *GLA* cDNA analysis and multiplex ligation-dependent probe amplification (MLPA) analysis. These distinct mutations included a large deletion mutation from intron 1 to exon 5 (c.195-471_c.691del5.5k, corresponding to g.8508_g.14069del5.5k), an insertion mutation of splicing enhancer sequence in intron 4 (c.639+329_c.639+330ins113, corresponding to g.12627_g.12628ins113), an insertion mutation of retrotransposon L1 in exon 4 (c.634_c.635, corresponding to g.12293_g.12294), and a non-SNP deep intronic point mutation in intron 3 (c.547+395G>C, corresponding to g.11727G>C). It is difficult to detect these mutations with direct sequencing of only the exonic element. When exonic mutations are not found in the *GLA* gene from suspected FD patients, *GLA* cDNA and MLPA analyses should be performed to detect large deletion/insertion and intronic mutations including transcription abnormalities.

Communicated by: Markus Ries, MD, PhD, MHSc, FCP

Competing interests: None declared

Electronic supplementary material: The online version of this chapter (doi:10.1007/8904_2015_475) contains supplementary material, which is available to authorized users.

T. Higuchi (✉) · Y. Shimada · H. Kobayashi · H. Ida · T. Ohashi
Division of Gene Therapy, Research Center for Medical Sciences, The Jikei University School of Medicine, Tokyo, Japan
e-mail: tahiguchi@jikei.ac.jp

M. Kobayashi · J. Ogata · E. Kaneshiro · H. Kobayashi · H. Ida · T. Ohashi (✉)
Department of Pediatrics, The Jikei University School of Medicine, Tokyo, Japan
e-mail: tohashi@jikei.ac.jp

Y. Eto
Front-Line Clinic Center, Kanagawa, Japan

S. Maeda
Department of Advanced Genomic and Laboratory Medicine, Faculty of Medicine, University of the Ryukyus, Okinawa, Japan

A. Ohtake
Department of Pediatrics, Saitama Medical University, Saitama, Japan

Introduction

Anderson-Fabry disease (FD [OMIM 301500 (http://www.omim.org/)]) an X-linked lysosomal storage disorder caused by mutation of the α-galactosidase A (*GLA*) gene (Reference Sequence accession number NM_000619.2 (http://www.ncbi.nlm.nih.gov/nuccore), MIM 300644) resulting in deficient activity of GLA (Desnick et al. 2001). This causes storage of various glycolipids such as globotriaosylceramide in many tissues, including vascular endothelium, renal glomeruli and tubules, dorsal root ganglia, cardiomyocytes, cornea, and skin. The main clinical symptoms of FD are neuropathic pain, hypohidrosis, and cerebrovascular, renal, and cardiac disease (Desnick et al. 2001). Although FD is inherited in an X-linked recessive manner, heterozygous female patients often develop clinical symptoms (Kobayashi et al. 2008). Recently, enzyme replacement therapy (ERT) using recombinant human GLA was developed and found to improve various clinical, pathologic,

Table 1 Patients' symptoms and GLA enzyme activities

Family		Sex/age	Pain	Hypohidrosis	LVH	Renal disease	Eye disease (corneal opacity)	WBC GLA enzyme activity (nmol/mg/h)	Healthy control's GLA enzyme activity range (nmol/mg/h)
Family A	I-2	F/75	+	+	+	–	+	68.7	56.3–190.6
	II-1	F/48	–	–	–	–	–	61.6	”
	II-2	M/45	–	–	–	–	–	123.4	”
	II-3	M/43	+	+	+	–	+	0.13	”
	II-4	F/40	–	–	–	–	–	124.9	”
	II-5	F/38	–	–	–	–	–	86.4	”
	II-6	F/36	+	–	–	–	+	32.9	”
Family B	I-2	F/71	+	–	+	–	–	231.0	157–259
	II-3	F/40	+	–	+	–	–	160.6	”
	III-1	M/11	+	–	–	–	–	9.6	152–281
Family C	II-2	F/52	+	–	+	–	–	29.4	121.6–152.8
	III-1	F/22	+	+	–	–	–	47.9	”
	III-2	F/19	+	–	–	–	–	21.6	160.7–345.6
Family D	II-2	M/12	+	+	–	–	+	2.04	152–169
Family E	I-2	F/59	+	–	+	–	–	120.3	169.5–212.7
	II-1	M/27	+	–	–	–	–	5.06	”
	II-2	F/26	+	–	–	+	+	101.6	”

LVH left ventricular hypertrophy, +/– positive or negative symptom

and biochemical characteristics of FD (Desnick et al. 2001). Thus, correct diagnosis of FD and early initiation of ERT are very important to improve prognosis. In male patients, enzyme analysis is usually sufficient for diagnosis. However, in female patients, especially those without a family history of the disease, detection of the pathologic *GLA* mutation is often necessary for definitive diagnosis.

More than 750 variants and mutations (missense/nonsense (68.8%), splicing (4.7%), regulatory (0.4%), small deletions (14.2%), small insertions (5.0%), small indels (1.4%), large deletions (4.2%), large insertions (0.5%), and complex (0.8%); no repeats detected) have been identified in the *GLA* gene from FD patients in the Human Gene Mutation Database (http://www.hgmd.cf.ac.uk/). In the present study, using multiplex ligation-dependent probe amplification (MLPA) methods, mRNA analysis, and intronic sequencing, we examined *GLA* genes from FD patients who did not carry mutations in exons or exon/intron boundaries. We found 4 novel cryptic mutations related to FD: a 5.5 kb deletion mutation, an insertion mutation of splicing enhancer (SE) sequence, an insertion mutation of exon-skipping element by long interspersed nuclear element-1 (L1) retrotransposon element, and a point mutation in a non-protein-coding region.

Materials and Methods

Patients

A total of 17 individuals from 5 families (Family A–Family E) in which at least one member had FD were analyzed for *GLA* variants (Table 1). Of note, all male patients had classic, not late-onset, FD. A total of three individuals without FD were also examined as controls.

Genomic DNA Analysis and Sequence

Genomic DNA analysis was performed as previously described (Kobayashi et al. 2012). Briefly, genomic DNA was extracted from white blood cells (WBCs) in the blood using a DNA Midi Kit (Qiagen). Exon and flanking intron elements of the *GLA* gene were amplified by polymerase chain reaction (PCR), using AmpliTaq Gold 360 Master Mix (Life Technologies), and sequenced using the BigDye Terminator Kit (ver. 3.1) (Life Technologies) and ABI PRISM 3100 Genetic Analyzer (Life Technologies). PCR temperature cycles of 94°C>55°C>72°C were used. PCR products were separated with 10% polyacrylamide gel containing Tris/borate/EDTA electrophoresis buffer. The PCR primers used for *GLA* genomic DNA analysis and the cDNA sequencing primers are shown in Table S1.

MLPA Assay

In order to find long deletions, the MLPA assay was carried out following the manufacturer's instructions using the SALSA MLPA P159-A2 *GLA* kit probe mix (FALCO bio systems). The PCR products were run on the ABI PRISM 3100 Genetic Analyzer with GeneMapper Software ver. 4.0 using GeneScan LIZ 500 size standards (Life Technologies). Data obtained were analyzed using Peak Scanner Software v1.0 (Life Technologies). MLPA raw data were normalized and analyzed with Coffalyser.NET software.

Total RNA Extraction, cDNA Synthesis, and RT-PCR of *GLA*

Whole blood was collected into EDTA-2Na tubes (TERUMO) or Tempus Blood RNA Tubes (Life Technologies). Total RNA was extracted from whole blood using TRIzol Reagent (Life Technologies), followed by phenol-chloroform. After ethanol precipitation, RNA was dissolved in water. For RT-PCR, first-strand cDNA was synthesized with PrimeScript II 1st strand cDNA Synthesis Kit (TAKARA BIO) according to the manufacturer's protocol. *GLA* cDNA was amplified with KOD FX Neo (TOYOBO). RT-PCR primers and the nested PCR primers used for *GLA* cDNA are shown in Table S1. These primer sequences were designed based on previously reported sequences (Shimotori et al. 2008).

cDNA Cloning and Transformation

All nested PCR products were re-amplified using Platinum Taq DNA polymerase (Life Technologies) to add a 3′ A overhang to PCR products for TA cloning. cDNA and genomic DNA cloning were performed with a TOPO TA cloning kit with pCR2.1 TOPO vector (Life Technologies), which was transformed into competent DH5α (TAKARA BIO) following the manufacturers' protocols.

GLA Enzyme Activity

WBCs were extracted from heparinized whole blood from the patient and from a healthy volunteer, and GLA enzyme activity in the WBCs was analyzed using a fluorogenic substrate, 4-methylumbelliferyl-α-d-galactopyranoside, as described previously (Kobayashi et al. 2012).

Single-Nucleotide Polymorphism Genotyping Assay

In samples from Family E, we additionally performed a single-nucleotide polymorphism (SNP) genotyping assay to detect whether the variant was SNP or non-SNP. This assay was a high-throughput SNP genotyping system that combined the Invader assay with multiplex PCRs (Ohnishi et al. 2001). We screened II-1 in Family E, and the genotype and/or allele frequencies were compared with those of a cohort of Japanese subjects (n = 1,492) selected from the general population.

Results

Patient Profiles and Results of DNA Analysis

Family A

The proband (II-3) had typical classic FD symptoms and his WBC GLA activity was profoundly decreased (Table 1 and Fig. 1a). Thus, the diagnosis of FD was confirmed. PCR showed that exon 2–5 elements were not amplified; therefore, a large deletion was suspected. II-2 had normal GLA activity; thus, FD was excluded. For the male family members (I-2, II-1, II-4, II-5, and II-6), enzyme activities were in the normal range or marginally decreased. I-2 and II-6 had clinical symptoms consistent with FD, whereas II-1, II-4, and II-5 did not have any clinical symptoms of FD. The variant in this family was considered to be a large deletion variant; therefore, we carried out MPLA analysis.

Signals of exon 2–5 elements could not be detected in II-3 (lane 5, Fig. 1b). In I-2, II-5, and II-6, signal peaks of exon 2–5 elements were almost half those of the female control (lanes 3, 7, and 8, Fig. 1b). In contrast, signal peaks of II-1 and II-4 showed the same peak signal level as the female control for all exons (lanes 4 and 6, Fig. 1b). The relative peak areas determined in each *GLA* exon region in female patients (I-2, II-1, II-4, II-5, and II-6) were consistent with this observation (Fig. S1a). To identify the exact deletion area, we performed direct sequence genomic DNA analysis from II-3. We identified a deletion from c.195-471 (g.8508) within intron 1 to c.691 (g.14069) within exon 5 (Fig. 1c and Fig. S1b). Using cDNA sequence analysis, we showed that exons 2–5 were deleted. As a result, this leads to a frameshift and premature insertion of a stop codon at codon 66.

Family B

The clinical symptoms and WBC GLA activities are summarized in Table 1, and the family pedigree is shown in Fig. 2a. III-1 was considered at risk for FD because of his family history of FD and he therefore visited our clinic. He has experienced pain from childhood and his GLA activity was very low (Table 1). Thus, diagnosis of FD was confirmed. For further confirmation of FD in this patient and for diagnosis of female family members at risk, DNA

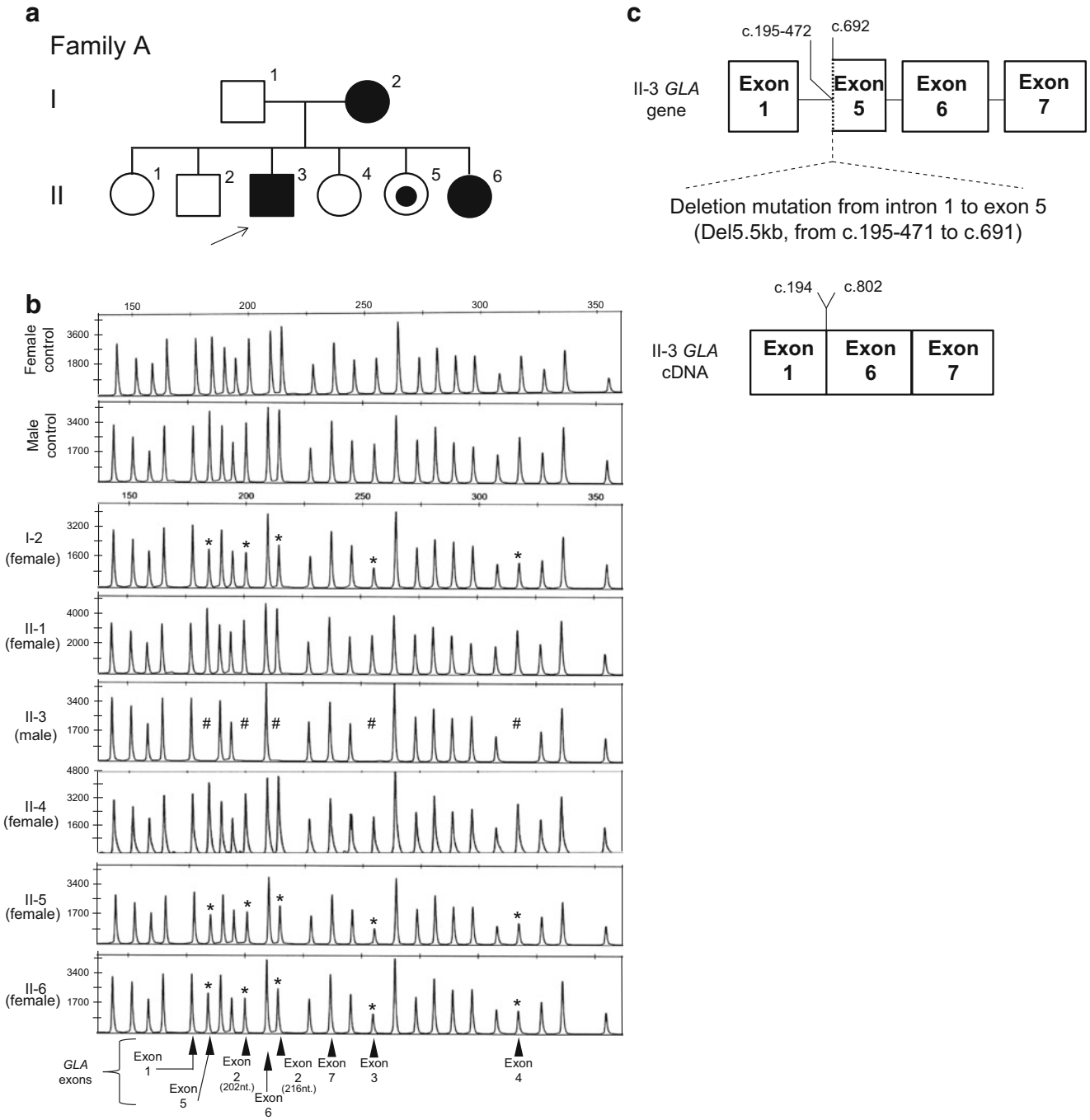

Fig. 1 Locate in *GLA* gene mutation in Family A. (**a**) Pedigree of Family A, *arrow*, proband; *filled symbol*, clinically and genetically affected patient; *small black dot*, asymptomatic mutation (*GLA*) carrier. (**b**) Detection of all *GLA* exon elements by MLPA analysis. Probe mix (P159-A2) contains 25 probes with 8 probes recognizing the *GLA* exons located in 7 different *GLA* exons. *Hash symbol*, not detected; *asterisk,* heterozygous peak; *x*-axis, nucleotide fragment size (nt.); *y*-axis, fluorescence intensity. (**c**) *GLA* genomic DNA structure (*upper panel*) and cDNA structure (*lower panel*) in II-3

analysis was carried out for III-1. However, all of the exons were successfully amplified, and there was no sequence change among exons and exon/intron boundaries in the *GLA* gene. Female family members I-2 and II-3 had left ventricular hypertrophy and low WBC GLA activities and were therefore considered to have FD. For further genetic analysis of this family, *GLA* cDNA was synthesized from III-1 and cloned into a cloning vector for sequencing.

A 304 bp insertion between exons 4 and 5 was identified by cDNA analysis. This insertion was from intron 4, c.639 +240_c.639+430 191bp (g.12538_g.12728) with a purine-rich additional 113 bp unknown sequence between c.639

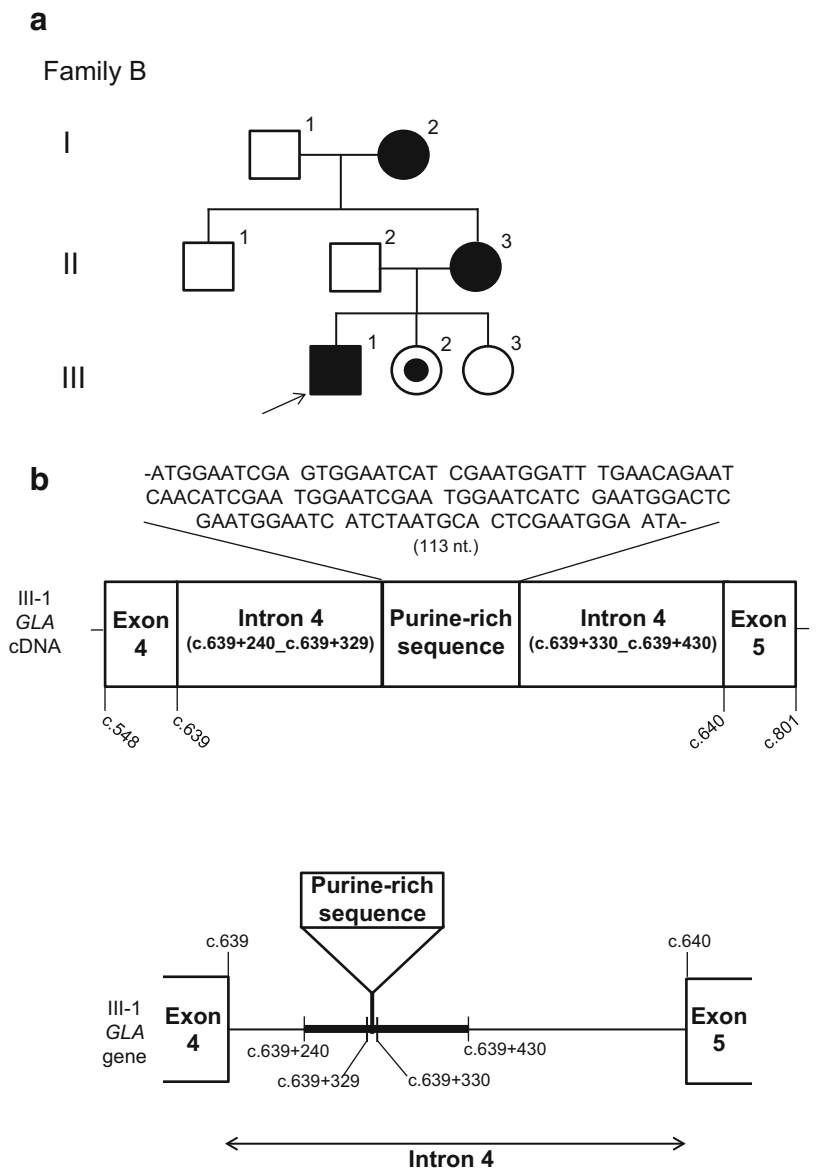

Fig. 2 Locate in *GLA* gene mutation in Family B. (**a**) Pedigree of Family B, *arrow*, proband; *filled symbol*, clinically and genetically affected patient; *small black dot,* asymptomatic mutation (*GLA*) carrier. (**b**) *GLA* cDNA structure between exon 4 and 5 (*upper panel*) and intron 4 genomic DNA structure (*lower panel*) in III-1. *Thick line*: alternative exon region involved in *GLA* cDNA in III-1

+329 (g.12627) and c.639+330 (g.12628) (Fig. 2b and Fig. S2). As a result, the *GLA* mRNA leads to frameshift and premature insertion of a stop codon at codon 220. We also analyzed genomic DNA and found a purine-rich 113 bp sequence between c.639+329 and c.639+330 (Fig. 2b and Fig. S2). Female members of this family I-2 and II-3 had the same variant heterozygously in *GLA* and were confirmed to have FD.

Family C

III-1 and III-2 were considered at risk of FD because their grandfather (I-1) was diagnosed with FD at another hospital (Fig. 3a). II-2 was an obligate heterozygote. Three female family members, II-2, III-1, and III-2, had experienced pain from childhood, and their WBC GLA activities were low (Table 1). No exonic mutations were found in their *GLA* gene. *GLA* cDNA from III-2 was sequenced, and a 304 bp insertion was found between exon 4 and 5 (data not shown). This insertion sequence was the same as for Family B. We amplified intron 4 in genomic DNA from II-2, III-1, and III-2. Two types of bands were seen in all family members (Fig. 3b). The smaller band was exactly the same size as for normal controls. By contrast, the larger band was the same size as that for III-1 in Family B. This fragment contained a

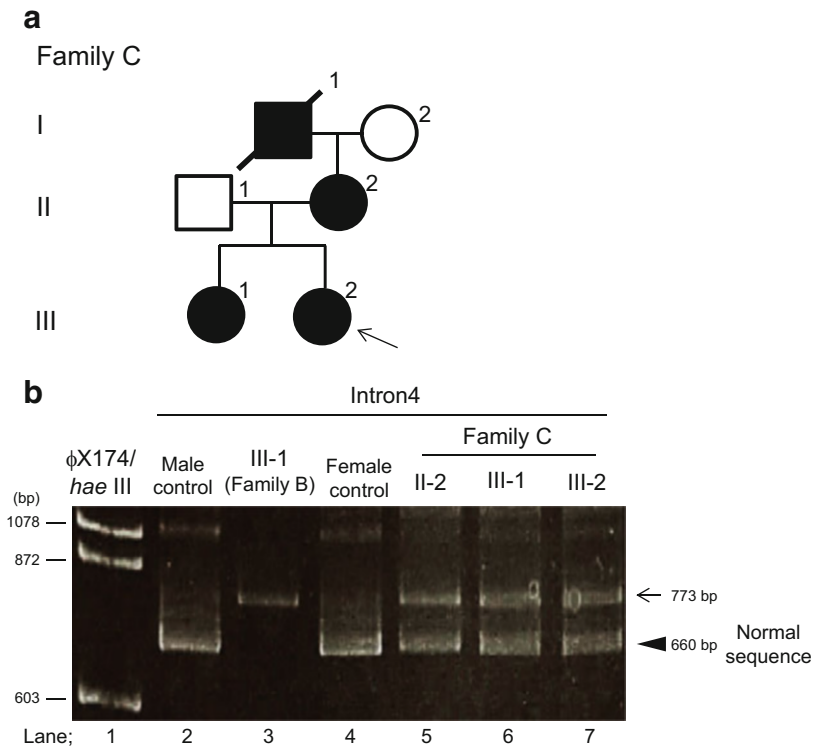

Fig. 3 Detection of *GLA* gene mutation in Family C. (**a**) Pedigree of Family C, arrow, proband; *filled symbol,* clinically and genetically affected patient. (**b**) Detection of inserted region with PCR analysis in Family C. Gel electroporation data show PCR-amplified product of intron 4 element. *Arrowhead*, normal sequence (660 bp); *arrow,* abnormal sequence (773 bp); lane 1, DNA size marker (φX174 DNA-HaeIII digest); lane 2, male control; lane 3, III-1 (Family B); lane 4, female control; lane 5, II-2; lane 6, III-1; lane 7, III-2

304 bp insertion. Thus, II-2, III-1, and III-2 had heterozygous FD.

Family D

The proband (II-2) had typical clinical signs of FD and his GLA activity was very low (Table 1 and Fig. 4a). We successfully amplified all exons and exon/intron boundaries (except exon 4) by PCR. The patient had no exonic mutations in any of the amplified DNA. Exon 4 element was completely skipped in *GLA* cDNA, as determined by cDNA sequence analysis (Fig. 4b and Fig. S3). His *GLA* mRNA leads to frameshift and premature insertion of a stop codon at codon 200. After TA cloning of genomic DNA of exon 4, each clone was sequenced. We found that poly (T) oligonucleotides and 139 base inverted long interspersed nuclear element-1 (LINE 1, L1) retrotransposon sequence were inserted after c.634 (g.12293). After the 139 bp insertion, a normal exon 4 beginning from c.620 (g.12279) followed. Thus, from c.620 to c.634 was duplicated.

Family E

The male family member, II-1, visited our clinic because he was at risk for FD (Fig. 5a). He had typical classic FD symptoms, and his WBC GLA enzyme activity was very low, indicating that he had FD (Table 1). No sequence change was found in the exons and exon/intron boundaries. Female family members, I-2 and II-2, had FD symptoms (Table 1). A 115 bp insertion sequence between exon 3 and 4 element was identified by cDNA sequence analysis. This insertion sequence was from intron 3, c.547+285_c.547+399 (g.11617_g.11731). This *GLA* mRNA leads to a frameshift and premature insertion of a stop codon at codon 223. We analyzed intron 3 and found one variant at the corresponding position c.547+395G>C (g.11727G>C) (Fig. 5b and Fig. S4). This variant was not found in the analysis of members from the general Japanese population by Multiplex-PCR Invasion Assay, indicating that this variant is pathogenic. I-2 and II-2 also had the same heterozygous sequence variation in *GLA*.

Discussion

Family A

It was difficult to diagnose FD due to large deletion of *GLA* in female subjects II-1, II-4, and II-5, as they did not show

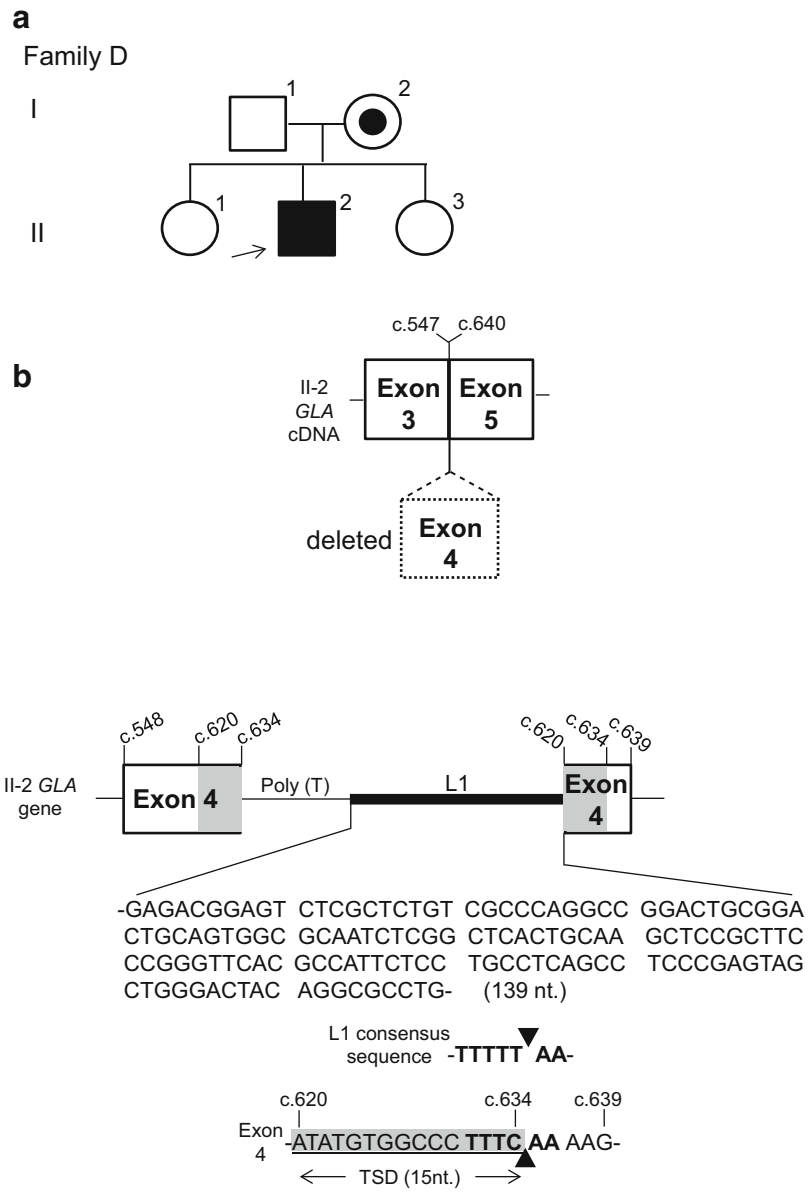

Fig. 4 Locate in *GLA* gene mutation in Family D. (**a**) Pedigree of Family D, arrow, proband; *filled symbol*, clinically and genetically affected patient; *small black dot*, asymptomatic mutation (*GLA*) carrier. (**b**) *GLA* cDNA structure between exon 3 and 5 (*upper panel*) and exon 4 structure (*lower panel*) in II-2. *Dashed line*, deletion exon 4 element; *thick line*, *L1* gene; *bold highlight*, L1 recognition sequence; *arrowhead*, L1 cutting site; *underlined and shaded region*, target site duplication (TSD) sequence

symptoms. MLPA analysis is a very effective tool to detect such large gene deletions.

Some previous studies have shown the effectiveness of MLPA analysis to detect large deletions of the *GLA* gene in female FD patients (Marziliano et al. 2012; Yoshimitsu et al. 2011; Schirinzi et al. 2008). We found deletion mutations with multiple exons from exon 2–5 elements using MLPA analysis in this family. Signals of exon 2–5 elements could not be detected in II-3 by MLPA analysis. As the exon 5 signal could not detect by MLPA analysis, we suspected that this subject had no exon 5 elements at all. However, he had more than half of *GLA* exon 5 element. This result might indicate a limitation of the probe's target in sequence-specific MLPA analysis. Some peaks in I-2 and II-6, and more in II-5, who had normal GLA activity and no FD symptoms, showed a pattern indicating heterozygous *GLA* mutation; conversely, II-1 and II-4 were genetically normal.

According to the genomic DNA sequence, II-3 had a 5.5 kb deletion mutation. There are a few reports about rare large deletions in *GLA* (Bernstein et al. 1989; Shabbeer et al. 2006; Rodríguez-Marí et al. 2003). In II-3, *GLA* had

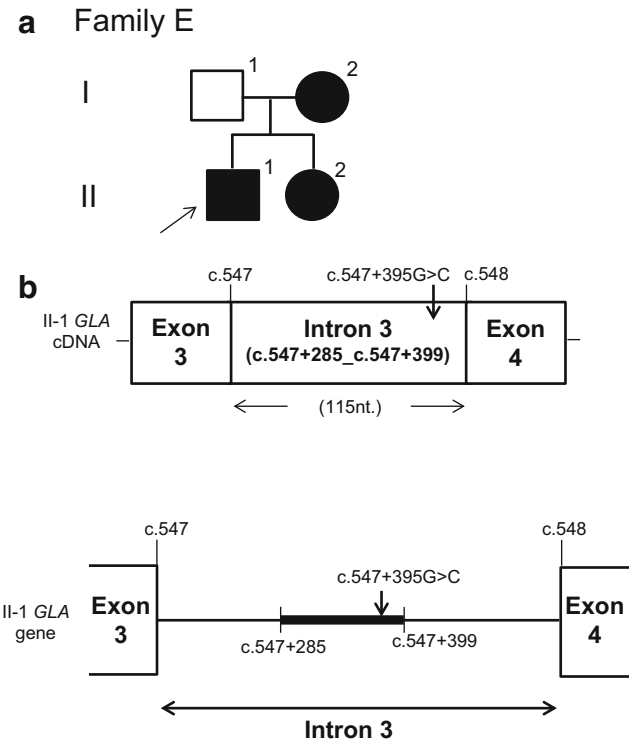

Fig. 5 Locate in *GLA* gene mutation in Family E. (**a**) Pedigree of Family E, *arrow,* proband; *filled symbol,* clinically and genetically affected patient. (**b**) *GLA* cDNA structure between exon 3 and 4 (*upper panel*) and intron 3 genomic DNA structure (*lower panel*) in II-1. *Arrow*, c.547+395G>C; *thick line,* alternative exon 3 element involved in *GLA* cDNA in II-1

8 nucleotide (-AGCAAAAT-) short inverted repeat sequences (IRs) at the 5′ and 3′ end of the deletion region. The IRs element is usually described as an important sequence for genomic instability and recognized as a hotspot that induces deletion and recombination in mammalian genomic DNA (Voineagu et al. 2008). In this family, 8 nucleotide IRs might involve a 5.5 kb deletion mutation of *GLA*.

II-3 *GLA* cDNA was constructed in exon 1, 6, and 7 elements. However, his *GLA* gene kept a fragment of exon 5. Therefore, we believe that the incomplete exon 5 is spliced out during mRNA mature processing.

In the present study, we revealed novel *GLA* mutations which have a large 5.5 kb deletion mutation. The MLPA method was very effective for use in women suspected of having FD due to a heterozygous large deletion mutation in *GLA*.

Families B and C

We found that an interesting novel long purine-rich insertion mutation involved SE within *GLA* intron 4 in two independent families (B and C). Most of the reported insertion mutations in FD are less than 20 bp and are located within the *GLA* exon element (Rosenberg et al 2000; Glass et al 2004). We identified a relatively long (113 bases) insertion within *GLA* intron 4. The 113 bases had a repeated sequence pattern (-gGAAT-). Such repeated 113 bp sequences are found throughout the human genome, such as in human satellite III-related DNA, SDS-stable vimentin-bound DNA fragments, and sequences of unknown function within chromosomes 16, 7, and 2. This 113 bp insertion element might come from satellite DNA. In addition, a purine-rich element could induce the enhancing pre-mRNA splicing system (Cooper and Mattox 1997; Hastings et al. 2001; Tanaka et al. 1994). We suspect that this 113 bp element within intron 4 plays a role in SE. Thus, 191 bp intronic sequences near the 113 bp element were recognized as new alternative exons in *GLA* cDNA.

Family D

We found an L1 retrotransposon sequence in the exon 4 of *GLA*. L1 is an abundant transposable element within the human genome. The *L1* gene is a retrotransposon capable of copying transposon genome into other parts of the genome, while leaving the transposable elements of the original genome (Kazazian 1998). L1 retrotransposon has a poly (A) tail at the 3′ end. This retrotransposon generally recognizes -TTTTTAA- consensus sequence. In this case, L1 recognized -TTTCAA- sequence located near the 3′ end of exon 4. L1 was sandwiched between 15 duplicate nucleotides sequence. This overlapped 15 nucleotide element is known as a target site duplication (TSD) sequence. An exonic/intronic L1 insertion mutation has also been found in some other genetic diseases (Awano et al. 2010; Kagawa et al. 2014), immunity disorders (Brouha et al. 2002), cancers (Wimmer et al. 2011), and neurologic diseases (Martínez-Garay et al. 2003). The L1 retrotransposon leads to splicing out of the exon 4 element in pre-mRNA maturation. Therefore, the *GLA* gene of this subject could not be transcribed into normal *GLA* mRNA.

Family E

We identified cDNA with a 115 bp sequence from intron 3 between exon 3 and 4. This 115 bp sequence was already known as cassette-type alternative exon 3 element (ENSE 00001812130 (http://www.ensembl.org/index.html)). The proband had a c.547+395G>C point mutation in *GLA* intron 3. This point mutation was not found in the general Japanese population, indicating that it is likely pathologic. In most intronic *GLA* gene mutations in subjects with FD, mutations are located in only the GT/AG exon/intron boundary or near the boundary; however, this mutation is located deep in the intron. There have been several other reports of deep intronic mutation in the *GLA* gene that might affect the mRNA splicing process (Ishii et al. 2002;

Filoni et al. 2008; Pisani et al. 2012). Especially those reports show that deep intronic point mutation could have a function of alternative splicing enhancer switch, because it recruits an alternative exon 4 and downregulates the normal *GLA* mRNA expression level (Ishii et al. 2002; Filoni et al. 2008). Thus, this c.547+395G>C mutation might be considered as an alternative splicing enhancer switch.

Conclusions

We revealed four novel *GLA* mutations in this study. One mutation was a large deletion and the others affected the mRNA splicing mechanism. *GLA* cDNA sequence analysis is an effective tool for finding not only exonic gene mutations but also functional intronic mutations related to the pre-mRNA splicing mechanism. MLPA analysis is a simple and powerful tool for analyzing large deletion mutations in genetic genealogy analysis.

Acknowledgment We thank our colleagues for their excellent technical assistance, Rie Ando (Oita Univ. Fac. of Med.), Miki Itohsa, Sayoko Iizuka, and Asako Morita (Div. of Gene Ther., The Jikei Univ.), and we thank Hidehito Kuroyanagi (Lab. of Gene Expres., Dep. of Func. Genomi., Med. Res. Inst., Tokyo Medical and Dental Univ.) for excellent discussions. We thank the primary medical doctors introducing the patients with FD to The Jikei Univ. hospital.

One-Sentence Take-Home Message

We found intronic novel *GLA* gene mutations related to FD with MLPA and cDNA analysis which are powerful molecular methods, although it is a classic procedure: a 5.5 kb deletion mutation, an insertion mutation of splicing enhancer sequence, an insertion mutation of L1 exon-skipping element, and a point mutation in a non-protein-coding region.

Details of the Contributions of Individual Authors

Conception and design of this study: TH, MK, and TO.

Acquisition of data: genetic analysis data; TH, JO, and EK, GLA enzyme activity analysis data; EK, SNPs analysis data; SM.

Interpretation of basic research data: TH, YS, HK, HI, and TO.

Care physician of patient: YE and TO (Family A), AO (Family B), TO (Family C, D, and E).

Drafting of the article: TH, MK, and TO.

Critical revision of the article for important intellectual content: MK, HI, and TO.

Final approval of the article: TH&TO.

Guarantor for the Article

Toya Ohashi, M.D., Ph.D.

Conflict of Interest

Higuchi T, Ogata J, Kaneshiro E, Shimada Y, and Maeda S declare that they have no conflict of interest.

Kobayashi M has received a speaker honorarium from Sumitomo Dainippon Pharma Co., Ltd., and Genzyme Japan Co., Ltd.

Kobayashi H has received a speaker honorarium from Sumitomo Dainippon Pharma Co., Ltd., and Genzyme Japan Co., Ltd.

Eto Y has received a speaker honorarium and active research support from Sumitomo Dainippon Pharma Co., Ltd., and Genzyme Japan Co., Ltd.

Akira Ohtake has received active research support from Sumitomo Dainippon Pharma Co., Ltd., and a speaker honorarium from Sumitomo Dainippon Pharma Co., Ltd., and Genzyme Japan Co., Ltd.

Ida H has received a speaker honorarium and active research support from Sumitomo Dainippon Pharma Co., Ltd., Genzyme Japan Co., Ltd., and Shire Japan Co., Ltd.

Ohashi T has received a speaker honorarium and active research support from Sumitomo Dainippon Pharma Co., Ltd., Genzyme Japan Co., Ltd., and Shire Japan Co., Ltd.

Our research activities have been fully disclosed and are managed under a Memorandum of Understanding with the Conflict of Interest Resolution Board of The Jikei University.

Details of Funding

This work was supported by grants from the Ministry of Health, Labour and Welfare (Grant No. H25-Zisedai-ipan-007, Dr. Onodera Research Group).

Details of Ethics Approval

This study was approved by the ethical committee of The Jikei University School of Medicine (Jikei Ethics Approval No. 19-040-4971).

Informed Consent

Informed consent was obtained from all patients for being included in the study.

Animal Rights

This article does not contain any studies with animal subjects performed by any of the authors.

References

Awano H, Malueka RG, Yagi M, Okizuka Y, Takeshima Y, Matsuo M (2010) Contemporary retrotransposition of a novel non-coding gene induces exon-skipping in dystrophin mRNA. J Hum Genet 55:785–790

Bernstein HS, Bishop DF, Astrin KH et al (1989) Fabry disease: six gene rearrangements and an exonic point mutation in the alpha-galactosidase gene. J Clin Invest 83:1390–1399

Brouha B, Meischl C, Ostertag E et al (2002) Evidence consistent with human L1 retrotransposition in maternal meiosis I. Am J Hum Genet 71:327–336

Cooper TA, Mattox W (1997) The regulation of splice-site selection, and its role in human disease. Am J Hum Genet 61:259–266

Desnick RJ, Ioannou YA, Eng CM (2001) Alpha-Galactosidase a deficiency: Fabry disease, 8th edn. In: The metabolic and molecular bases of inherited disease. McGraw-Hill, New York, pp 3733–3774

Filoni C, Caciotti A, Carraresi L et al (2008) Unbalanced *GLA* mRNAs ratio quantified by real-time PCR in Fabry patients' fibroblasts results in Fabry disease. Eur J Hum Genet 16: 1311–1317

Glass RB, Astrin KH, Norton KI et al (2004) Fabry disease: renal sonographic and magnetic resonance imaging findings in affected males and carrier females with the classic and cardiac variant phenotypes. J Comput Assist Tomogr 28: 158–168

Hastings ML, Wilson CM, Munroe SH (2001) A purine-rich intronic element enhances alternative splicing of thyroid hormone receptor mRNA. RNA 7:859–874

Ishii S, Nakao S, Minamikawa-Tachino R, Desnick RJ, Fan JQ (2002) Alternative splicing in the alpha-galactosidase A gene: increased exon inclusion results in the Fabry cardiac phenotype. Am J Hum Genet 70:994–1002

Kagawa T, Oka A, Kobayashi Y et al (2014) Recessive inheritance of population-specific intronic LINE-1 insertion causes a Rotor syndrome phenotype. Hum Mutant 36:327–332

Kazazian HH Jr (1998) Mobile elements and disease. Curr Opin Genet Dev 8:343–350

Kobayashi M, Ohashi T, Sakuma M, Ida H, Eto Y (2008) Clinical manifestations and natural history of Japanese heterozygous females with Fabry disease. J Inherit Metab Dis Supple 3: 483–487

Kobayashi M, Ohashi T, Fukuda T et al (2012) No accumulation of globotriaosylceramide in the heart of a patient with the E66Q mutation in the α-galactosidase A gene. Mol Genet Metab 107: 711–715

Martínez-Garay I, Ballesta MJ, Oltra S et al (2003) Intronic L1 insertion and F268S, novel mutations in RPS6KA3 (RSK2) causing Coffin-Lowry syndrome. Clin Genet 64:491–496

Marziliano N, Sapere N, Orsini F et al (2012) A quantitative-PCR protocol rapidly detects αGAL deletions/duplications in patients with Anderson-Fabry disease. Mol Genet Metab 105: 687–689

Ohnishi Y, Tanaka T, Ozaki K, Yamada R, Suzuki H, Nakamura Y (2001) A high-throughput SNP typing system for genomewide association studies. J Hum Genet 46:471–477

Pisani A, Imbriaco M, Zizzo C et al (2012) A classical phenotype of Anderson-Fabry disease in a female patient with intronic mutations of the *GLA* gene: a case report. BMC Cardiovasc Disord 12:39

Rodríguez-Marí A, Coll MJ, Chabás A (2003) Molecular analysis in Fabry disease in Spain: fifteen novel *GLA* mutations and identification of a homozygous female. Hum Mutat 22:258.17

Rosenberg KM, Schiffmann R, Kaneski C, Brady RO, Sorensen SA, Hasholt L (2000) Five novel mutations in fourteen patients with Fabry Disease. Hum Mutat 15:207–208

Schirinzi A, Centra M, Prattichizzo C et al (2008) Identification of *GLA* gene deletions in Fabry patients by Multiplex Ligation-dependent Probe Amplification (MLPA). Mol Genet Metab 94: 382–385

Shabbeer J, Yasuda M, Benson SD, Desnick RJ (2006) Fabry disease: identification of 50 novel alpha-galactosidase A mutations causing the classic phenotype and three-dimensional structural analysis of 29 missense mutations. Hum Genomics 2: 297–309

Shimotori M, Maruyama H, Nakamura G et al (2008) Novel mutations of the *GLA* gene in Japanese patients with Fabry disease and their functional characterization by active site specific chaperone. Hum Mutat 29:331

Tanaka K, Watakabe A, Shimura Y (1994) Polypurine sequences within a downstream exon function as a splicing enhancer. Mol Cell Biol 14:1347–1354

Voineagu I, Narayanan V, Lobachev KS, Mirkin SM (2008) Replication stalling at unstable inverted repeats: interplay between DNA hairpins and fork stabilizing proteins. Proc Natl Acad Sci U S A 105:9936–9941

Wimmer K, Callens T, Wernstedt A, Messiaen L (2011) The NF1 gene contains hotspots for L1 endonuclease-dependent de novo insertion. PLoS Genet 7, e1002371

Yoshimitsu M, Higuchi K, Miyata M et al (2011) Identification of novel mutations in the α-galactosidase A gene in patients with Fabry disease: pitfalls of mutation analyses in patients with low α-galactosidase A activity. J Cardiol 57:345–353

JIMD Reports
DOI 10.1007/8904_2016_536

RESEARCH REPORT

Severe Neonatal Presentation of Mitochondrial Citrate Carrier (SLC25A1) Deficiency

Amanda Smith • Skye McBride • Julien L. Marcadier • Jean Michaud • Osama Y. Al-Dirbashi • Jeremy Schwartzentruber • Chandree L. Beaulieu • Sherri L. Katz • FORGE Canada Consortium • Jacek Majewski • Dennis E. Bulman • Michael T. Geraghty • Mary-Ellen Harper • Pranesh Chakraborty • Matthew A. Lines

Received: 12 November 2015 / Revised: 07 January 2016 / Accepted: 12 January 2016 / Published online: 16 June 2016

Abstract Mutations of the mitochondrial citrate carrier (CIC) SLC25A1 cause combined D-2- and L-2-hydroxyglutaric aciduria (DL-2HGA; OMIM #615182), a neurometabolic disorder characterized by developmental delay, hypotonia, and seizures. Here, we describe the female child of consanguineous parents who presented neonatally with lactic acidosis, periventricular frontal lobe cysts, facial dysmorphism, recurrent apneic episodes, and deficient complex IV (cytochrome c oxidase) activity in skeletal muscle. Exome sequencing revealed a homozygous *SLC25A1* missense mutation [NM_005984.4: c.593G>A; p.(Arg198His)] of a ubiquitously conserved arginine residue putatively situated within the substrate-binding site I of CIC. Retrospective review of the patient's organic acids confirmed the D- and L-2-hydroxyglutaric aciduria typical of DL-2HGA to be present, although this was not appreciated on initial presentation. Cultured patient skin fibroblasts showed reduced survival in culture, diminished mitochondrial spare respiratory capacity, increased glycolytic flux, and normal mitochondrial bulk, inner membrane potential, and network morphology. Neither cell survival nor cellular respiratory parameters were improved by citrate supplementation, although oral citrate supplementation did coincide with amelioration of lactic acidosis and apneic attacks in the patient. This is the fifth clinical report of CIC deficiency to date. The clinical features in our patient suggest that this disorder, which can potentially be recognized either by molecular means or based on its characteristic organic aciduria, should be considered in the differential diagnosis of pyruvate dehydrogenase deficiency and respiratory chain disorders.

One-Sentence Summary A novel homozygous missense substitution in SLC25A1 was identified in a neonate presenting with lactic acidosis, intracerebral cysts, and an apparent mitochondrial complex IV defect in muscle.

Communicated by: Garry Brown

Competing interests: None declared

Electronic supplementary material: The online version of this chapter (doi:10.1007/8904_2016_536) contains supplementary material, which is available to authorized users.

A. Smith · S. McBride · S.L. Katz
Ottawa Hospital Research Institute, Ottawa, ON, Canada

A. Smith · C.L. Beaulieu · D.E. Bulman · M.T. Geraghty · P. Chakraborty · M.A. Lines
Children's Hospital of Eastern Ontario Research Institute, University of Ottawa, Ottawa, ON, Canada

J.L. Marcadier · O.Y. Al-Dirbashi · D.E. Bulman · M.T. Geraghty · P. Chakraborty · M.A. Lines (✉)
Division of Metabolics and Newborn Screening, Department of Pediatrics, Children's Hospital of Eastern Ontario, Ottawa, ON, Canada
e-mail: mlines@cheo.on.ca

J. Michaud
Department of Pathology and Laboratory Medicine, Children's Hospital of Eastern Ontario, University of Ottawa, Ottawa, ON, Canada

J. Schwartzentruber · J. Majewski
McGill University and Genome Quebec Innovation Centre, Montreal, QC, Canada

S.L. Katz
Division of Respirology, Department of Pediatrics, Children's Hospital of Eastern Ontario, Ottawa, ON, Canada

M.-E. Harper
Department of Biochemistry, Microbiology and Immunology, University of Ottawa, Ottawa, ON, Canada

Introduction

The mitochondrial citrate carrier (CIC) SLC25A1 is an inner membrane antiporter that mediates the exchange of a tricarboxylate dianion (e.g., citrate^{2-}, isocitrate^{2-}) for another tricarboxylate dianion, a dicarboxylate (e.g., malate^{2-}), or phosphoenolpyruvate (Palmieri 2004). The major described function of the CIC is to shuttle mitochondrially synthesized citrate to the cytoplasm, where it (1) furnishes (via citrate lyase) acetyl-coA to support fatty acid and sterol synthesis and (2) exerts feedback control over glycolysis by allosterically inhibiting phosphofructokinase. Recently, recessive mutations of *SLC25A1* in 20 persons with combined D,L-2-hydroxyglutaric aciduria (DL-2HGA; OMIM #615182), a disorder characterized clinically by severe developmental delay, hypotonia, and seizures, have been described (Edvardson et al. 2013; Nota et al. 2013). With subsequent reports, the clinical phenotype of DL-2HGA has since been expanded to include secondary microcephaly, hypoplasia or agenesis of the corpus callosum, optic nerve hypoplasia, dysmorphic features, lactic acidosis, and recurrent apneic crises (Chaouch et al. 2014; Mühlhausen et al. 2014; Prasun et al. 2015). Apart from a proposed defect of mitochondrial citrate efflux, little is known about the downstream pathophysiology of this condition, and the cellular bioenergetic implications of this basic transport defect remain poorly understood. Here, we report the clinical, biochemical, and molecular findings in a female neonate with a homozygous SLC25A1 mutation and a novel presentation with congenital lactic acidosis, leukoencephalopathy with cystic frontal lobe lesions, and dysmorphic features reminiscent of pyruvate dehydrogenase deficiency.

Materials and Methods

Patient DNA and Cellular Analyses

All procedures were in accord with the declaration of Helsinki. Informed consent was obtained from all study participants prior to enrollment. The research was approved by the Children's Hospital Research Ethics Board. DNA extraction, sequencing, and exome analysis were performed as previously described (McDonell et al. 2013). Primary patient fibroblast cultures were established based on a 2 mm sterile skin biopsy according to standard clinical protocols. All other experiments conducted in control and patient fibroblasts were performed as previously described by our group (Antoun et al. 2015).

Results

Clinical Description

The patient, a female, was the first child to first cousins of mixed Caucasian background. Routine antenatal ultrasound imaging was normal. The pregnancy was complicated by gestational diabetes and preeclampsia, for which labor was induced; delivery was by emergency Caesarian section at 35 weeks, 6 days, due to fetal distress. Birth weight was 2.16 kg (third–tenth centile). The baby briefly required bag-mask ventilation, followed by a further 15 min of continuous positive pressure, following which breathing was satisfactory and the patient was maintained in room air. Dysmorphic features were noted, including midface hypoplasia, a thin, smooth philtrum, micrognathia, and numerous small raised capillary hemangiomata in a general distribution. At 20 h of age, the patient developed apneic spells and stridor, in conjunction with abnormal jerking movements; a lactic acidosis was noted (lactate = 8.6 mmol/L; pH 7.36; bicarbonate = 17 mmol/L). With aggressive fluid and respiratory support, over the following 24 h, her serum lactate decreased to 2.7 mmol/L, but failed to normalize entirely, and has remained persistently elevated since birth (range, 2.5–8.6 mmol/L; typical resting values, 5–6 mmol/L). Echocardiography was normal. Cranial imaging, initially by ultrasound and subsequently by MRI, revealed diffuse white matter deficiency with cerebral volume loss, bilateral periventricular frontal lobe cysts, and severe hypoplasia of the corpus callosum (Fig. 1). Funduscopy revealed bilateral optic nerve hypoplasia; visual evoked potentials were absent. Her early clinical course was characterized by hypotonia, poor feeding, temperature instability, and progressively frequent episodes of central apnea. Tracheostomy was performed at age 3 months. Repeat MRI at that time showed progressive volume loss, hypomyelination, and presence of a lactate doublet on spectroscopy (Fig. 1). At 3 years of age, the patient remained ventilator dependent, with little psychomotor development, a paucity of spontaneous movement, frequent apneic crises, and periods of generalized extensor posturing.

Selected biochemical investigations in this patient included the following: plasma amino acids and acylcarnitine profile were normal. CSF lactate was 3.9 mmol/L (vs. 3.1 mmol/L in serum). CSF amino acids were within normal limits. Urine organic acids showed increased excretion of 2-ketoglutaric, fumaric, glutaric, 2-hydroxyglutaric, and (inconsistently) lactic and succinic acids. Muscle biopsy (age, 4 months) showed subtle nonspecific fiber size variation, normal Gomori trichrome staining, and

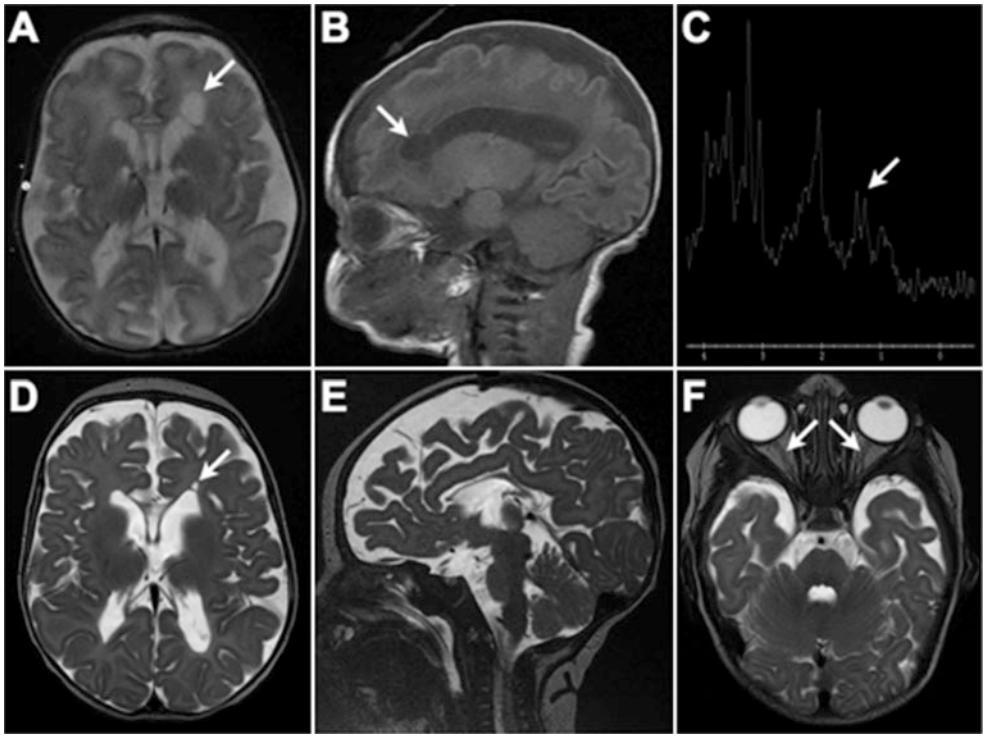

Fig. 1 *Cranial MRI appearance* at 5 days (**a**, **b**) and 3 months of age (**c**–**f**). (**a**) and (**b**) Diffuse deficiency of cerebral white matter with enlarged fluid spaces and marked hypoplasia of the corpus callosum. *Arrow* indicates connatal (frontal lobe) cyst; a similar (smaller) right-sided cyst was present but is not well shown on this axial slice. (**c**) Lactate doublet is present on MR spectroscopy. (**d**) Evolution of changes in panels **a** and **b**. Myelination is markedly reduced for age. Basal ganglia, brainstem, and cerebellum have a relatively normal appearance. (**f**) Small optic nerves and optic chiasm (not shown)

normal NADH, SDH, and cytochrome oxidase histochemical stains. The semi-thin toluidine blue staining revealed subsarcolemmal clearing, with accumulation of non-membrane-bound glycogen; this was confirmed at the ultrastructural level. Note was also made of occasional small aggregates of mitochondria with nonspecific pleomorphism (Supplemental Fig. 1). Respiratory chain testing revealed an isolated, marked decrease in complex IV in skeletal muscle activity, but not in cultured skin fibroblasts (Table 1).

Molecular Diagnosis

In order to identify the causative genetic lesion in this patient, we performed whole-exome sequencing of the proband. Among the resulting list of rare (allele frequency <1%) homozygous coding variants in our proband was a novel missense substitution in *SLC25A1* (NM_005984.3: c.593G>A; p.Arg198His; confirmed by Sanger sequencing) (Supplemental Fig. 2). This substitution is predicted to be damaging by multiple algorithms (Adzhubei et al. 2010; Kumar et al. 2009; Schwarz et al. 2014) and has not been observed in any of the 3513 exomes previously sequenced at our facility. It is not represented in the Exome Aggregation Consortium (ExAC) database (http://exac.broadinstitute.org/), although a different substitution of this same position, p.Arg198Cys, is represented at extremely low frequency (2/121148 alleles, 0.002%). With arginine 198 having previously been established to be essential for CIC's transporter function (see "Discussion"), DL-2HGA was suspected as the most likely diagnosis. Enantiomeric separation of 2-hydroxyglutaric acids in the patient's urine (VUmc Amsterdam; patient age 4 years, 2 months) showed hitherto unappreciated increases in the excretion of both D-2-hydroxyglutaric acid (248.6 mmol/mol creatinine, reference 2.8–17.0 mmol/mol creatinine) and L-2-hydroxyglutaric acid (50.0 mmol/mol creatinine, reference 1.3–18.9 mmol/mol creatinine), confirming the diagnosis. On retrospective review of the patient's previous (semi-quantitative) urine organic acids analyses, citrate was detected repeatedly, albeit in relatively small amounts.

The lactic acidosis, connatal white matter cysts, and reduced muscle complex IV activity in our patient were collectively indicative of a defect of mitochondrial energy metabolism. To produce a more detailed assessment of the patient's mitochondrial dysfunction, we assessed several parameters (basal and maximal respiration, mitochondrial bulk, inner membrane potential, and mitochondrial network structure) in primary patient fibroblasts (Fig. 2). Cells were exceedingly fragile in culture on standard media, displaying exaggerated senescence when passaged below ~60 % confluence. Micro-oximetry of the fibroblasts showed a dramatic decrease in spare respiratory capacity (Fig. 2a, b); this was

Table 1 Selected activities in skeletal muscle and cultured fibroblasts

Frozen skeletal muscle		
Enzyme	Patient muscle activity (μmol/min/g wet weight)	Reference interval (μmol/min/g wet weight)
I+III (NADH-cytochrome C reductase)	0.71	0.53–2.72
II+III (succinate-cytochrome C reductase)	1.24	0.55–3.46
IV (cytochrome oxidase)	0.09 (↓)	0.8–6.03
Citrate synthase	4.81	3.48–8.03
Cultured skin fibroblasts		
Enzyme	Patient fibroblasts (nmol/min/mg protein)	Reference interval (nmol/min/mg protein)
Pyruvate dehydrogenase (native)	0.67 ± 0.05 ($n = 3$)	0.7–2.5
Pyruvate dehydrogenase (dichloroacetate stimulated)	0.89 ± 0.05 ($n = 3$)	0.9–2.5
II+III (succinate-cytochrome C reductase)	5.85 ± 0.40 ($n = 8$)	4–12
IV (cytochrome c oxidase)	4.11 ± 0.57 ($n = 8$)	4–12
Lactate: pyruvate ratio	25.79 ± −4.38[a]($n = 4$)	10–25[a]

[a] nmol/h/mg protein

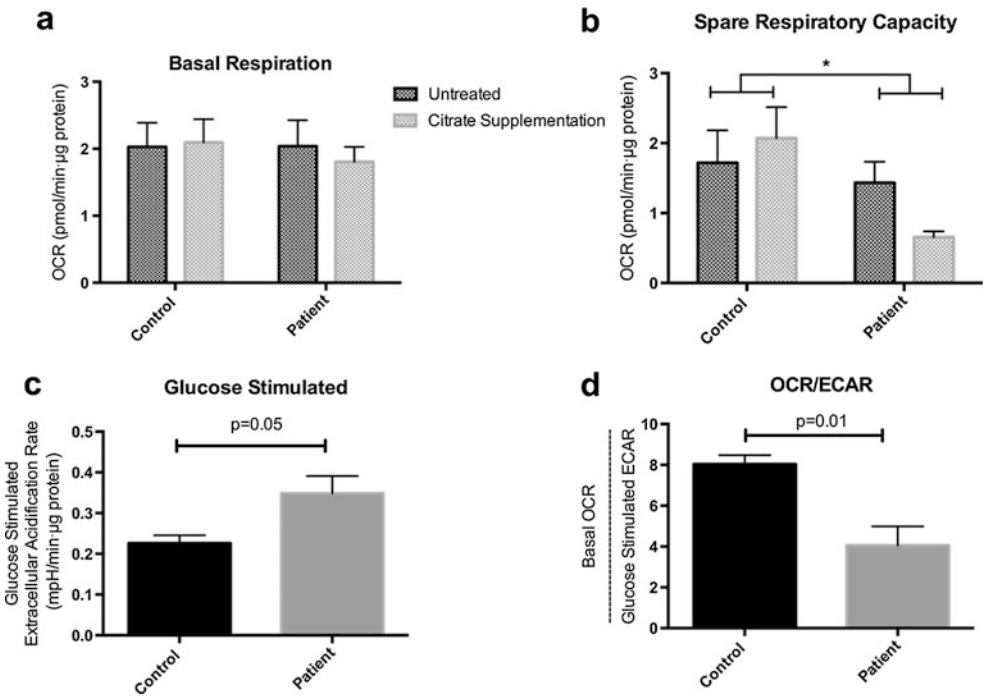

Fig. 2 *SLC25A1-deficient patient cells exhibit lessened spare respiratory capacity and increased glycolytic flux*. Micro-oximetry was performed, as per Antoun et al. (2015), on cells grown in standard medium and on cells grown in medium supplemented with 4 mM citrate. Oxygen consumption rate (OCR) was corrected for non-mitochondrial oxygen consumption and normalized to protein content. (**a**) Basal OCR of patient fibroblasts does not differ significantly from that of control fibroblasts. (**b**) Spare respiratory capacity is reduced in the patient fibroblasts; this was not ameliorated by citrate supplementation. (**c**) Glucose-stimulated extracellular acidification rate (ECAR), reflecting glycolytic flux, is markedly increased in the patient cells ($n = 3$). (**d**) OCR/ECAR ratio (basal OCR divided by glucose-driven ECAR) is markedly reduced in the patient, i.e., the patient cells are relatively reliant on glycolysis ($n = 3$). Values are presented as mean ± SEM, analyzed by unpaired, two-tailed student's *t*-test

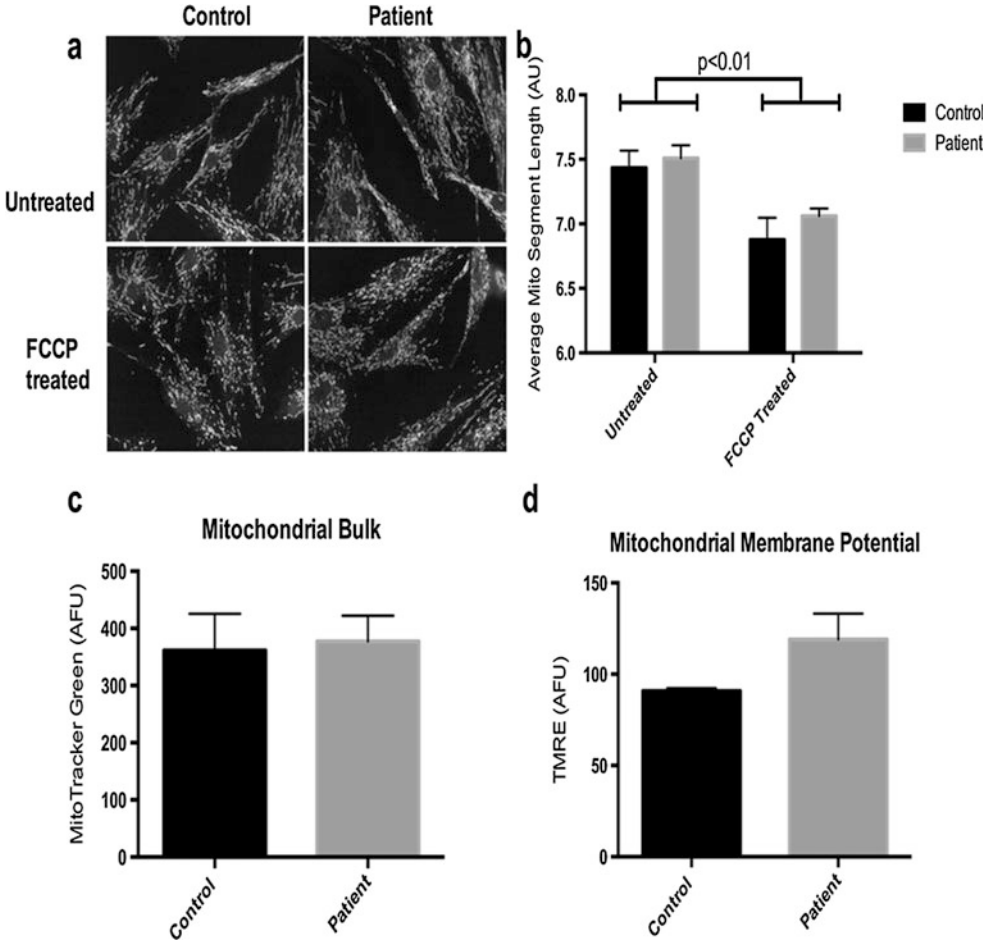

Fig. 3 *Normal patient mitochondrial networking, drug-induced fragmentation, total mitochondrial bulk, and inner membrane charge in skin-derived fibroblasts*. (**a**, **b**) High-throughput confocal imaging of fixed control (*left*) and patient (*right*) fibroblasts ± acute 60 μM FCCP treatment; immunostained for the outer membrane transporter TOMM-20 ($n = 4$). (**c**) Mitochondrial content (MitoTracker Green) ($n = 3$) and (**d**) inner membrane potential (TMRE) ($n = 3$) measured by flow cytometry. Values are presented as mean ± SEM; analyzed by (**b**) two-way ANOVA or (**c**) nonparametric Mann-Whitney test for unequal variance and (**d**) unpaired, two-tailed student's *t*-test

accompanied by an increase in glucose-supported extracellular acidification (Fig. 2c), a proxy measure of overall glycolytic flux. The oxygen consumption rate (OCR) to extracellular acidification rate (ECAR) ratio, a comparison of the cell's reliance on oxidative phosphorylation versus glycolysis, was dramatically lower in patient cells than in controls (Fig. 2d). High-throughput confocal microscopy of fixed cells stained for the outer membrane transporter TOMM-20 (Fig. 3a, b) revealed a normal-appearing mitochondrial network. Lastly, flow cytometric assays for (1) average cellular mitochondrial bulk and (2) mitochondrial inner membrane potential showed no statistical difference in either of these parameters versus controls (Fig. 3c, d).

The patient was prescribed an oral citrate supplement (3 mg/kg/day) at 33 months of age, and this coincided with an improvement in the frequency of her apneic attacks, increased spontaneous respiratory drive (i.e., lessened reliance on her mandatory "backup" ventilator rate and an increase in patient-triggered breaths). Blood lactate concentration decreased significantly (8.9 mmol/L to 3.8 mmol/L) during the first week of therapy, although lactate remained persistently elevated thereafter (last measurement, 5.2 mmol/L), and urinary 2-hydroxyglutarate excretion has also remained markedly increased. The patient's clinic performance status remains poor.

Discussion

This is the fifth report of DL-2HGA, our proband being the twentieth affected individual reported to date (Nota et al. 2013; Chaouch et al. 2014; Prasun et al. 2015; Edvardson et al. 2013). As far as we are aware, no other patient with DL-2HGA has been described to have a specific respiratory chain defect (complex IV deficiency) on muscle biopsy. In general terms, the findings in the patient suggest impaired oxidative phosphorylation, increased reliance on glycolysis, and preservation of mitochondrial bulk, inner membrane charge, and overall network structure. Contributing factors in the patient's lactic acidosis could include (1) NADH

accumulation due to respiratory chain dysfunction and/or (2) increased glycolytic flux, by allosteric disinhibition of phosphofructokinase (Newsholme et al. 1977).

The arginine residue (Arg198) altered by our proband's substitution is likely to be particularly crucial for CIC's carrier function. In the orthologous *S. cerevisiae* citrate transport protein CTP, the equivalent position (Arg189) is proposed to form direct physical contacts with citrate at one of the protein's two putative citrate-binding sites (Ma et al. 2007). Substitution of Arg189 with a cysteine drastically compromises both the kinetics and the selectivity of CTP, with a >300-fold increase in K_m, ~1,000-fold decrease in V_{max}, and a greatly increased affinity for dicarboxylic acids (e.g., malate) rather than citrate (Ma et al. 2007; Aluvila et al. 2010). An in silico structural model based on the homologous mitochondrial carrier ANT1 (PDB: 10KC) (Pebay-Peyroula et al. 2003) situates the side chain of Arg198 within CIC's positively charged site 1 pocket (Supplemental Fig. 3), and substitution of this residue with a significantly less basic histidine residue is likely to change the steric and electrostatic configuration of site 1.

Our patient's clinical presentation was initially considered to be suggestive of pyruvate dehydrogenase deficiency. As proved to be the case here, PDH-like facial dysmorphism, periventricular frontal lobe cysts, and hyperlactatemia are nonspecific signs that can be seen in many disorders of cellular energy metabolism. Because DL-2HGA is rare and its characteristic organic aciduria may be overlooked, panel- or exome-based molecular testing may be the most practical route to a diagnosis in some cases. The apparent clinical improvement in apneic episodes on oral citrate supplementation has been described in one other reported individual, although in both instances, treatment was started well into the disease course (Mühlhausen et al. 2014). The effect, if any, of earlier initiation of therapy on the remainder of the DL-2HGA phenotype (developmental delay, microcephaly, structural brain malformations, seizures, etc.) remains to be assessed prospectively in suitable cases.

Acknowledgments The authors gratefully acknowledge the contribution of the proband and her family, without whose participation this work could not be undertaken.

Compliance with Ethics Guidelines

Authors' Contributions

All authors contributed to the conception and design of the study. JLM, JeM, OA, PC, and ML acquired the clinical, biochemical, and pathological data. SM produced primary experimental data. Data were analyzed and interpreted by AS, SM, JeM, OA, JS, JaM, DB, and ML. The manuscript was drafted by AS, SM, and ML. Critical revisions were performed by all authors.

Guarantor

Dr. Matthew A. Lines

Competing Interest Statement

Amanda Smith declares she has no conflict of interest.

Skye McBride declares she has no conflict of interest.

Julien Marcadier declares he has no conflict of interest.

Jean Michaud declares he has no conflict of interest.

Osama Y. Al-Dirbashi declares he has no conflict of interest.

Jeremy Schwartzentruber declares he has no conflict of interest.

Chandree Beaulieu declares she has no conflict of interest.

Sherri L. Katz declares she has no conflict of interest.

Jacek Majewski declares he has no conflict of interest.

Dennis E. Bulman declares he has no conflict of interest.

Michael T. Geraghty declares he has no conflict of interest.

Mary-Ellen Harper declares she has no conflict of interest.

Pranesh Chakraborty declares he has no conflict of interest.

Matthew A. Lines declares he has no conflict of interest.

Funding

This work was supported by Genome Canada, the Canadian Institutes of Health Research (CIHR), and the Ontario Genomics Institute (OGI-049), with additional funding from Genome Québec and Genome British Columbia. SM and ML are supported by MitoCanada Foundation

Ethics Approval and Informed Consent

All procedures followed were in accordance with the Tri-Council Policy Statement: Ethical Conduct for Research Involving Humans (2010) and with the Helsinki Declaration of 1975, as revised in 2000. Informed consent was obtained from all patients participating in the study. The research protocol was approved by the Children's Hospital of Eastern Ontario Research Ethics Board.

References

Adzhubei IA, Schmidt S, Peshkin L et al (2010) A method and server for predicting damaging missense mutations. Nat Methods 4:248–249

Aluvila S, Kotaria R, Sun J et al (2010) The yeast mitochondrial citrate transport protein: molecular determinants of its substrate specificity. J Biol Chem 285:27314–27326

Antoun G, McBride S, Vanstone JR et al (2015) Detailed biochemical and bioenergetic characterization of *FBXL4*-related encephalomyopathic mitochondrial DNA depletion. JIMD Rep (epub ahead of print)

Chaouch A, Porcelli V, Cox D et al (2014) Mutations in the mitochondrial citrate carrier SLC25A1 are associated with impaired neuromuscular transmission. J Neuromusclular Disord 1:75–90

Edvardson S, Porcelli V, Jalas C et al (2013) Agenesis of corpus callosum and optic nerve hypoplasia due to mutations in SLC25A1 encoding the mitochondrial citrate transporter. J Med Genet 50:240–245

Kumar P, Henikoff S, Ng PC (2009) Predicting the effects of coding non-synonymous variants on protein function using the SIFT algorithm. Nat Protoc 7:1073–1081

Ma C, Remani S, Sun J et al (2007) Identification of the substrate binding sites within the yeast mitochondrial citrate transport protein. J Biol Chem 282:17210–17220

McDonell LM, Mirzaa GM, Alcantara D et al (2013) Mutations in STAMBP, encoding a deubiquitinating enzyme, cause microcephaly-capillary malformation syndrome. Nat Genet 45:556–562

Mühlhausen C, Salomons GS, Lukacs Z et al (2014) Combined D2-/L2-hydroxyglutaric aciduria (SLC25A1 deficiency): clinical course and effects of citrate treatment. J Inherit Metab Dis 37:775–781

Newsholme EA, Sugden PH, Williams T (1977) Effect of citrate on the activities of 6-phosphofructokinase from nervous and muscle tissues from different animals and its relationship to the regulation of glycolysis. Biochem J 166:123–129

Nota B, Struys EA, Pop A (2013) Deficiency in SLC25A1, encoding the mitochondrial citrate carrier, causes combined D-2- and L-2-hydroxyglutaric aciduria. Am J Hum Genet 92:627–631

Palmieri F (2004) The mitochondrial transporter family (SLC25): physiological and pathological implications. Pflugers Arch 447:689–709

Pebay-Peyroula E, Dahout-Gonzalez C, Kahn R et al (2003) Structure of mitochondrial ADP/ATP carrier in complex with carboxyatractyloside. Nature 426:39–44

Prasun P, Young S, Salomons G et al (2015) Expanding the clinical spectrum of mitochondrial citrate carrier (SLC25A1) deficiency: facial dysmorphism in siblings with epileptic encephalopathy and combined D, L-2-hydroxyglutaric aciduria. JIMD Rep 19:111–115

Sali A, Blundell TL (1993) Comparative protein modeling by satisfaction of spatial restraints. J Mol Biol 234:779–815

Schwarz JM, Cooper DN, Schuelke M et al (2014) MutationTaster2: mutation prediction for the deep-sequencing age. Nat Methods 11:361–362

JIMD Reports
DOI 10.1007/8904_2015_524

RESEARCH REPORT

Biomarkers in a Taurine Trial for Succinic Semialdehyde Dehydrogenase Deficiency

John M. Schreiber · Phillip L. Pearl · Irene Dustin · Edythe Wiggs · Emily Barrios · Eric M. Wassermann · K. Michael Gibson · William H. Theodore

Received: 14 August 2015 / Revised: 10 November 2015 / Accepted: 26 November 2015 / Published online: 24 June 2016

Abstract *Aim*: We tested the hypothesis that patients with succinic semialdehyde dehydrogenase (SSADH) deficiency on taurine would have decreased cortical excitability as measured by transcranial magnetic stimulation (TMS) and improved cognition, due to taurine's partial GABA(A and B) receptor agonist effects and rescue in the null mouse model from status epilepticus and premature lethality.

Method: Biomarkers including neuropsychological testing, TMS, and CSF metabolites were studied in a cohort of patients on and off three months' taurine treatment.

Results: Seven patients (5M/2F; age range 12–33 years) were enrolled in this open-label crossover study. Baseline average full-scale IQ (FSIQ) was 44.1 (range 34–55). Of six who returned at 6-month follow-up, five completed cognitive testing (3M/2F) on therapy; average FSIQ = 43.4 (range 33–51). CSF biomarkers ($n = 4$ subjects) revealed elevation in taurine levels but no change in free or total GABA. Baseline cortical excitability measured with TMS agreed with previous findings in this population, with a short cortical silent period and lack of long-interval intracortical inhibition. Patients on taurine showed a decrease in cortical silent period and short-interval intracortical inhibition compared to their off taurine study.

Interpretation: TMS demonstrated decreased inhibition in patients on taurine, in contrast to the study hypothesis, but consistent with its failure to produce clinical or cognitive improvement. TMS may be a useful biomarker for therapy in pediatric neurotransmitter disorders.

Succinic semialdehyde dehydrogenase (SSADH) deficiency is a rare autosomal recessive defect in the catabolic pathway of GABA (gamma-aminobutyric acid), leading to elevated levels of GABA and gamma-hydroxybutyric acid (GHB) in body fluids and brain parenchyma (Pearl et al. 2003a, b). The typical clinical phenotype has been described as a slowly progressive or static encephalopathy. Most patients present with developmental delay noted in the first 2 years of life, as well as hypotonia, hyporeflexia, ataxia, speech disturbance, and intellectual disability, and at least half have seizures.

Several lines of evidence indicate that SSADH deficiency results in chronic, overuse-dependent down-regulation of GABA(A) and GABA(B) receptors. In the mouse model, decreased binding of the selective GABA(A) receptor antagonist *tert*-butylbicyclophosphorothionate ([35S]TBPS) was observed in the cerebral cortex, hippocampus, and thalamus of the mutant strain compared to wild type, and reduced GABA(A)-mediated inhibitory postsynaptic potentials and enhanced postsynaptic population spikes were recorded from hippocampal slices of the mutant strain (Wu et al. 2006). There was also significantly decreased binding of a specific GABA(B) receptor antagonist in the mutant strain and attenuated GABA(B)-mediated synaptic potentials (Buzzi et al. 2006). We demonstrated

Communicated by: Verena Peters

J.M. Schreiber (✉) · I. Dustin · E. Wiggs · W.H. Theodore
Clinical Epilepsy Section, Bethesda, MD, USA
e-mail: jschreib@childrensnational.org

P.L. Pearl · E. Barrios
Department of Child Neurology, Children's National Medical Center (CNMC), Washington, DC, USA

E.M. Wassermann
Cognitive Neuroscience Section, NINDS, NIH, Bethesda, MD, USA

K.M. Gibson
Experimental and Systems Pharmacology, Washington State University (WSU), Spokane, WA, USA

decreased binding of flumazenil, a GABA(A) receptor agonist, in multiple regions of interest studied using cerebral PET (Pearl et al. 2009). In addition, transcranial magnetic stimulation (TMS) studies showed shortening of the cortical silent period and loss of long-interval intracortical inhibition using single and paired pulse stimulation, consistent with impaired GABA(B) receptor function (Reis et al. 2012).

The homozygous deficient mouse model is characterized by onset of absence seizures, typically at day P17, with evolution to ultimately fatal convulsive status epilepticus by three weeks of age. This process occurs coincident with weaning of suckling mice, and the observation that taurine is the major constituent of murine breast milk led to an experimental trial and survival benefit (Gupta et al. 2002). Taurine (2-aminoethanesulfonic acid) is an abundant free amino acid in various tissues and has important roles in neuromodulation and osmoregulation (Bidri and Choay 2003). Taurine may be an important modulator of GABA transmission. Taurine increases GABA function by acting as a low-affinity agonist for GABA(A) receptors (Junyent et al. 2009) and also activates metabotropic GABA(B) receptors to a lesser extent (Belluzzi et al. 2004). The rationale for our hypothesis that taurine may be effective for this condition was thus based on the aforementioned evidence for overuse-dependent downregulation of GABA (A) and GABA(B) receptor activity and perhaps interference with the neuronal hyperexcitability of the syndrome manifested by the transition from absence to convulsive seizures in the murine model.

Early reports of uncontrolled trials suggested a potential benefit of taurine intervention in patients (Saronwala et al. 2008), although we were unable to document significant changes using an adaptive behavior scale in an open-label study (Pearl et al. 2014). Here, we report the effects of taurine on TMS measures of cortical excitability and inhibition, CSF biomarkers, and cognitive testing in a group of these patients participating in the open-label taurine trial. We hypothesized that orally administered taurine would result in increased cortical inhibition, improvement in cognition, and an elevation in CSF taurine.

Method

Participants over age 12 years, with SSADH deficiency, who were already enrolled in the open-label taurine trial, were offered enrollment in this biomarker study. All studies were performed at the National Institutes of Health from June 2012 through March 2013. Subjects were eligible based on a diagnosis of SSADH deficiency by 4-OH-butyric aciduria and enzymatic or genotypic identification. Participants used GNC™ brand taurine supplements in tablet form and were titrated weekly from 50 mg/kg/day to a target dose of 200 mg/kg/day oral maximum of 10 g/day. Subjects were studied on and off taurine, with cognitive testing, CSF taurine and GABA measurements, and transcranial magnetic stimulation (TMS). The protocol provided for a 3-month treatment period and 3-month washout before repeat testing.

Cognitive Testing

Neuropsychological tests included the Wechsler Nonverbal Scale of Ability or the Wechsler Adult Intelligence Scale-III selected subtests and the *Neuropsychological Assessment Battery: Language Module*. Areas assessed with the Wechsler scales included nonverbal reasoning using pattern completion, a digit-symbol substitution for processing speed, and spatial span administered as a nonverbal test of attention, similar to digit repetition. Both forward and backward spans were assessed. A test of sequential reasoning was also included; using "story pictures" the subject was asked to arrange the pictures in logical order. Verbal abilities were further assessed with parts of the *Neuropsychological Assessment Battery: Language Module* through confrontation naming using large photographs.

CSF

Lumbar puncture was attempted during both visits for measurement of routine studies (cell count and differential, protein, glucose) in addition to taurine and GABA levels. Lumbar puncture was performed with local anesthetic only. The fluid designated for special metabolites was placed immediately in dry ice and then stored in a freezer. Samples were deep-frozen at minus 80 centigrade until analysis. GABA was then quantified by the method of Kok et al. (1993) using electron-capture negative-ion mass fragmentography and isotopically labeled GABA (13C/N15).

TMS

TMS was delivered through a round coil (90 mm diameter) connected to two Magstim 200^2 magnetic stimulators via a Bistim module (Magstim, Dyfed, UK). The coil was placed over the contralateral motor cortex at the site, and in the orientation, that consistently produced the maximum motor-evoked potential (MEP) amplitude from the right first dorsal interosseous (FDI) muscle.

Subjects were seated in a comfortable chair with their hands resting on a pillow. Electrodes were applied to the skin over the right FDI in a belly-tendon montage with the reference electrode placed at least 4 cm distal to the active electrode and a ground electrode positioned over the dorsum of the hand. The electromyogram (EMG) signal

was amplified (Coulbourn Isolated Bioamplifier, model V75-04), band-pass filtered (90 Hz to 1 kHz), digitized (analog/digital rate 40 kHz), and recorded (Signal version 4.05, Cambridge Electronics, UK) for offline analysis. The EMG was monitored continuously for relaxation by visual inspection. The resting motor threshold (MT) was determined by increasing stimulus intensity in increments of 5 % of maximum output until a MEP was recorded and then adjusting by 1% increments to the lowest stimulator output required to produce MEPs of at least 50 μV on five out of ten consecutive trials.

MEP recruitment curve (RC), cortical silent period (CSP), short- and long-interval intracortical inhibition (SICI and LICI), and intracortical facilitation (ICF) were measured. Subjects were instructed to rest during the RC and paired pulse paradigms and to sustain a contraction of the FDI by pinching the thumb and first finger during CSP determination. Individual trials were repeated or later excluded if muscle activity was apparent in the 100 ms before stimulation in the RC and paired pulse paradigms or if EMG amplitude dropped below baseline, determined visually, in the 100 ms prior to stimulation for CSP. For RC determination, five MEPs were recorded at each of eight percentages of the MT in the following order: 90, 130, 100, 140, 110, 150, 120, and 160%. The CSP was measured visually from the end of stimulus artifact to the first return of sustained EMG activity for ten trials at 110, 120, 130, and 140 % MT. For SICI and ICF measurements, we set the conditioning stimulus at 70 % and the test stimulus at 120 %, of MT. Interstimulus intervals were 2 and 10 ms. For LICI, we used 120 % of MT for both stimuli with an interstimulus interval of 100 ms. We used the mean MEP to the conditioning stimulus in the LICI experiment as the control MEP. ICI and ICF were determined by the ratio of the mean conditioned MEP to this control. We delivered and averaged ten trials for each measurement.

Statistical analysis was performed with SPSS 22 (IBM), using paired *t*-tests or repeated measures ANOVA for normally distributed continuous variables or nonparametric tests (related samples Wilcoxon signed-rank test or Spearman's correlation). A p value of <0.05 was considered significant.

Both the NINDS and CNMC institutional review boards approved this protocol. Written informed consent was obtained from all parents or guardians of subjects participating in the study.

Results

Results: Seven subjects were consented and enrolled in the NIH. Mean age was 20 years at enrollment (range 12–33) and 2/7 (29 %) were female. One subject was already taking taurine and completed the "on" assessment first. All subjects were titrated to 10 g daily, the maximum dose based on hypersomnolence noted on higher doses as reported in the open-label trial (Pearl et al. 2014). No adverse events were reported during TMS. One study patient had a new-onset seizure associated with stress, sleep deprivation, and diphenhydramine administration. Six subjects successfully completed TMS. One patient had been treated chronically with carbamazepine for epilepsy but had no seizures for several years prior to enrollment. We excluded one subject from the TMS analysis because we were unable to produce MEPs at the baseline assessment.

The TMS results are shown in Table 1. Treatment-related decreases in the CSP at 140 % MT and SICI both reached significance ($p < 0.05$) (Figs. 1 and 2). Baseline EMG activity was no different on or off taurine for each of the paired pulse stimuli ($p = 0.249$, 0.211, and 0.469 for SICI, ICF, and LICI, respectively). There was no significant main effect of taurine on RC, $F\ (1,\ 4) = 3.34$, $p = 0.142$, or CSP, $F\ (1,\ 5) = 1.361$, $p = 0.296$.

Baseline mean full-scale IQ, on the appropriate Wechsler scale for age, was 44.1 (range 34–55) and 3.6 SD below the population mean. There was no significant relationship between baseline IQ and MT, SICI, ICF, LICI, RC slope, or CSP at 140% MT. Of six individuals who returned at

Table 1 TMS results on and off taurine with corresponding p values

	"Off" mean ± SD	"On" mean ± SD	*P* value
RC slope	0.028 ± 0.015	0.022 ± 0.006	0.40
SICI	69 % ± 26	159 % ± 93	< 0.05
ICF	129 % ± 27	141 % ± 72 %	0.917
LICI	96 % ± 107	93 % ± 98	0.753
CSP at 140 % MT (ms)	128 ± 50	96 ± 48	< 0.05
MT (motor threshold)	53.67 % ± 11	55.17 % ± 12	0.586

SICI, ICF, and LICI values are expressed as a percent of the baseline conditioning MEP determined at the same stimulus intensity, 120% MT

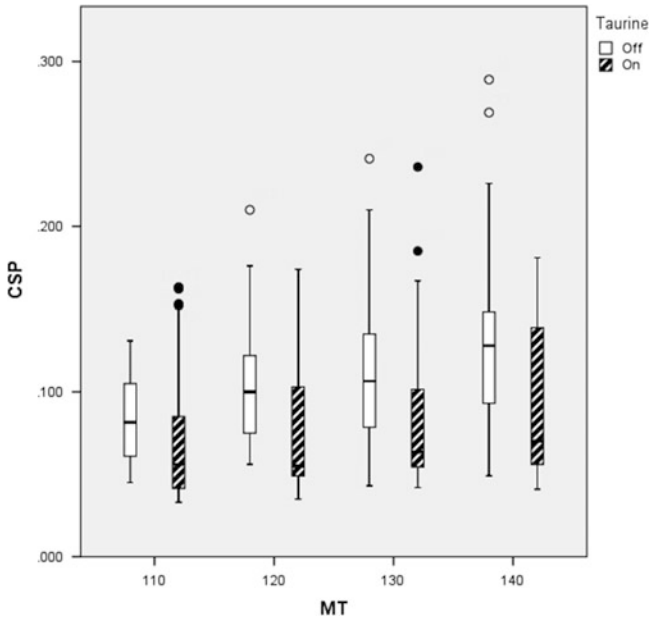

Fig. 1 Box plot (with 25–75 % quartiles, range, and outliers) of individual cortical silent period (CSP) measures (expressed in seconds) at different stimulus intensities off and on taurine; data combined from all subjects. Taurine treatment was associated with decreased cortical silent period values at the 140% MT ($p < 0.05$)

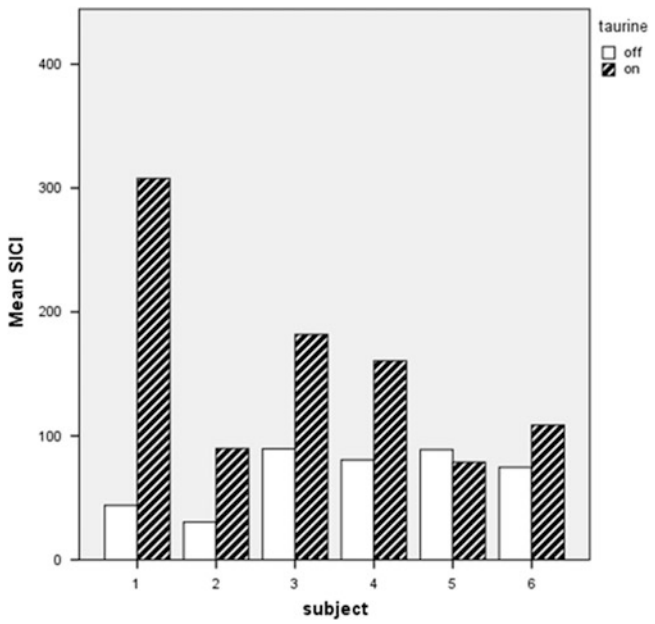

Fig. 2 Mean SICI (short-interval intracortical inhibition), expressed as percent of baseline MEP (motor-evoked potential), off and on taurine for each subject, showing a treatment-related decrease in inhibition ($p < 0.05$)

6-month follow-up, five completed testing (3M/2F) on therapy; average FSIQ = 43.4 (range 33–51; nonsignificant). Similarly, there was no change in confrontation naming, which was completed in four subjects; the average confrontation naming score off taurine was 22 (range 19–32) and on taurine was 20 (range 19–24). Results of CSF biomarkers ($n = 4$ subjects) are displayed in Table 2, demonstrating no change in CSF free or total GABA levels but a significant increase in CSF taurine, indicating that it does cross the blood–brain barrier.

Table 2 CSF taurine, free GABA, and total GABA levels on and off taurine, with corresponding *p* values

Measure (and ref range)	"Off" mean ± SEM	"On" mean ± SEM	*P* value (on vs. off)
Taurine (not established)	9 ± 1 μM	26 ± 6 μM	<0.05
Free GABA (32–170 nM)	394 ± 88 nM	403 ± 62	NS
Total GABA (3.3–12.1 mM)	14.3 ± 1 mM	14.9 ± 2.4	NS

Discussion

This study reports results of a clinical trial of taurine supplementation in SSADH deficiency along with biomarker data utilizing transcranial magnetic stimulation, CSF metabolites, and neuropsychological data. This is the first published report of formal IQ testing in this disorder. Our baseline (off taurine) measures agree with prior data in patients with SSADH deficiency (Reis et al. 2012), demonstrating a low recruitment curve slope, shortened cortical silent period, and markedly reduced long-interval intracortical inhibition with relatively preserved short-interval intracortical inhibition and intracortical facilitation. Furthermore, we found a shift from inhibition to facilitation in the short-interval paired pulse paradigm and a reduction in the CSP with taurine, implying a shift in the balance of cortical regulation toward greater excitability. Taurine was tolerated at high doses (10 g/day). Oral administration results in significant elevations in CSF taurine without significant changes in free or total GABA concentrations.

Taurine is an aminosulfonic acid, sold as a dietary supplement, and has neuromodulatory, osmoregulatory, and tropic roles. It may also serve a neuroprotective function, preventing glutamate-induced neuronal excitotoxicity (Chen et al. 2001). Taurine has shown benefit in the SSADH-deficient mouse model (Gupta et al. 2002).

Taurine induces chloride influx through GABA(A) receptors (Belluzzi et al. 2004), specific taurine receptors (Okamoto et al. 1983), and glycine receptors (Han et al. 2001) and may also activate metabotropic GABA(B) receptors to a lesser extent (Belluzzi et al. 2004). Furthermore, it directly attenuates NMDA receptors through multiple mechanisms, specifically by reducing affinity for glycine and reducing peak current without changing steady-state current through the NDMA receptor (Chan et al. 2014). SICI is thought to be mediated by GABA(A) receptors (Ilic et al. 2002), while GABA(B) receptor activity produces LICI (McDonnell et al. 2006). Therefore, we hypothesized that taurine would increase both short- and long-interval intracortical inhibitions. Our results indicate that taurine may have opposite effects on these phenomena.

The unexpected loss of SICI may be partially understood through taurine's action as a weak agonist at GABA(A) receptors. Taurine, at high doses, would interfere with synaptically released GABA, resulting in disinhibition of GABAergic transmission. Alternatively, chronic administration of taurine may further downregulate GABA receptors, as shown previously. In addition to reflecting reduced inhibition, the shift to facilitation exhibited by most of our subjects could also result from potentiation of excitatory mechanisms. Facilitation may occur at short interstimulus intervals when the intensity of the conditioning stimulus is increased (Ilic et al. 2002), and SICI probably represents the net effect of facilitatory and inhibitory influences. In general, while TMS is a noninvasive means of providing information about neurotransmission, there is surely some overlap in what networks and neurotransmitters contribute to a given measure.

Taurine administration was associated with a reduction in the CSP at only the highest stimulus intensity tested (140% MT), possibly indicating disproportionate antagonism of GABA(B) (relative to GABA(A)) receptors by taurine. CSP duration increases with intensity (Inghilleri et al. 1993), and while it is believed to reflect largely GABA(B) receptor function, GABA(A) receptor activation may contribute at lower stimulus intensities. Evidence from invasive experiments in animals (Mody et al. 1994) shows that GABA(A)-mediated inhibition can be evoked at lower stimulation thresholds than that produced by GABA(B) receptor activation. Moreover, lorazepam, which enhances the activity of GABA(A) receptors, has varying effects on the CSP at different stimulus intensities. It is therefore important to test a range of stimulus intensities when evaluating an intervention's effects on the CSP. Lorazepam, which potentiates GABA(A) receptor function, actually decreases CSP at higher stimulus intensities, perhaps due to selective inhibition of inhibitory interneurons in the motor cortex (Kimiskidis et al. 2006).

Other TMS measures did not reveal any significant changes with taurine administration. However, low patient recruitment rendered this study insufficiently powered to detect a significant change. MT, RC, and ICF are measures of excitability, reflecting chiefly the excitability of cortical interneurons, which is, in turn, a function of their excitatory input. LICI, like CSP, is thought to be determined mainly by GABA(B) receptor function (McDonnell et al. 2006). The lack of change in LICI would appear to contradict a decrease in CSP at the highest stimulus intensity, given that

both indicate GABA(B) receptor function. However, taurine's effects on the CSP were only seen at the highest stimulus intensity, 20% higher than the conditioning stimulus delivered during LICI.

We previously reported a lack of significant change in adaptive behavior in a group of 25 patients with SSADH deficiency using taurine in an open-label trial. The current study recruited a subset of the original cohort to study biomarkers selected to provide information about effects of GABAergic activity related to taurine intervention and is also the first systematic analysis of this patient population with neuropsychological testing. The mean score on the Wechsler scales is 100 +/15; our average nonverbal IQ score of 43.5 (range 33–55) is in the extremely low range and indicative of moderate intellectual impairment. Verbal tests yielded similar findings. Confrontation naming is a normed test with a mean of 50 ± 10. Our average naming score of 22 is in the impaired range and is indicative of limited recognition naming capacity. Following directions was also assessed by asking subjects to identify colors and simple shapes and then follow one-, two-, and three-step directions using those figures. All scores were below the first percentile. These results are consistent with the results of the Wechsler tests of ability and indicate that both nonverbal and verbal abilities are in the moderately impaired range. There was no significant change on or off taurine therapy.

Taurine appears effective in the mouse model of SSADH deficiency when administered from birth (Gupta et al. 2002). Early therapy may be the key – a "critical period" during which taurine or other interventions might be beneficial. The brain changes rapidly during early development; GABA receptor function shifts from depolarizing to hyperpolarizing shortly after birth (Cherubini et al. 1991). Affinity of taurine for glycine receptors drops after the neonatal period in the rat (Tang et al. 2008). The use-dependent downregulation of GABA(A) and GABA(B) receptors occurs in the first few weeks of life in the SSADH-deficient mouse (Buzzi et al. 2006; Wu et al. 2006), and metabolites are already elevated in newborn mice (Jansen et al. 2008). Perhaps earlier intervention would yield significant changes in cognition and behavior.

Oral taurine, administered chronically in patients with SSADH deficiency, produces decreased cortical inhibition as measured by TMS. This finding parallels the lack of apparent cognitive or clinical improvement.

Take-Home Message

Taurine therapy in succinic semialdehyde dehydrogenase deficiency, a disorder known to impair GABAergic neurotransmission, yields no improvement in cognitive outcomes and decreases cortical inhibition as measured by transcranial magnetic stimulation.

Compliance with Ethics Guidelines

The trial was funded by The National Institute of Neurological Disorders and Stroke Division of Intramural Research and NIH R01 HD58553.

Dr. Schreiber, Wiggs, Wassermann, and Theodore and Mrs. Dustin performed this research as part of their employment with the National Institutes of Health.

Otherwise, John M. Schreiber, Phillip L. Pearl, Irene Dustin, Edythe Wiggs, Emily Barrios, Eric M. Wassermann, K. Michael Gibson, and William H. Theodore declare that they have no conflict of interest.

All procedures followed were in accordance with the ethical standards of the responsible committee on human experimentation (institutional and national) and with the Helsinki Declaration of 1975, as revised in 2000. Written informed consent was obtained from all parents or guardians of subjects participating in the study. Proof that informed consent was obtained is available upon request.

John Schreiber, M.D., contributed to study design, data collection, statistical analysis, and manuscript preparation.

Phillip L. Pearl, M.D., contributed to study design and manuscript preparation.

Irene Dustin contributed to study design and manuscript review.

Edythe Wiggs, Ph.D., contributed to study design, data collection, and manuscript review.

Emily Barrios contributed to statistical analysis and manuscript review.

Eric M. Wassermann, M.D., contributed to study design and manuscript review.

K. Michael Gibson, Ph.D., contributed to study design, CSF analysis, and manuscript review.

William H. Theodore, M.D., contributed to study design and manuscript review.

References

Belluzzi O, Puopolo M, Benedusi M, Kratskin I (2004) Selective neuroinhibitory effects of taurine in slices of rat main olfactory bulb. Neuroscience 124:929–944

Bidri M, Choay P (2003) Taurine: a particular aminoacid with multiple functions. Ann Pharm Fr 61:385–391

Buzzi A, Wu Y, Frantseva MV et al (2006) Succinic semialdehyde dehydrogenase deficiency: GABAB receptor-mediated function. Brain Res 1090:15–22

Chan CY, Sun HS, Shah SM, Agovic MS, Friedman E, Banerjee SP (2014) Modes of direct modulation by taurine of the glutamate NMDA receptor in rat cortex. Eur J Pharmacol 728:167–175

Chen WQ, Jin H, Nguyen M et al (2001) Role of taurine in regulation of intracellular calcium level and neuroprotective function in cultured neurons. J Neurosci Res 66:612–619

Cherubini E, Gaiarsa JL, Ben-Ari Y (1991) GABA: an excitatory transmitter in early postnatal life. Trends Neurosci 14:515–519

Gupta M, Greven R, Jansen EE et al (2002) Therapeutic intervention in mice deficient for succinate semialdehyde dehydrogenase (gamma-hydroxybutyric aciduria). J Pharmacol Exp Ther 302: 180–187

Han NL, Haddrill JL, Lynch JW (2001) Characterization of a glycine receptor domain that controls the binding and gating mechanisms of the beta-amino acid agonist, taurine. J Neurochem 79:636–647

Ilic TV, Meintzschel F, Cleff U, Ruge D, Kessler KR, Ziemann U (2002) Short-interval paired-pulse inhibition and facilitation of human motor cortex: the dimension of stimulus intensity. J Physiol 545:153–167

Inghilleri M, Berardelli A, Cruccu G, Manfredi M (1993) Silent period evoked by transcranial stimulation of the human cortex and cervicomedullary junction. J Physiol 466:521–534

Jansen EE, Struys E, Jakobs C, Hager E, Snead OC, Gibson KM (2008) Neurotransmitter alterations in embryonic succinate semialdehyde dehydrogenase (SSADH) deficiency suggest a heightened excitatory state during development. BMC Dev Biol 8:112

Junyent F, Utrera J, Romero R et al (2009) Prevention of epilepsy by taurine treatments in mice experimental model. J Neurosci Res 87:1500–1508

Kimiskidis VK, Papagiannopoulos S, Kazis DA et al (2006) Lorazepam-induced effects on silent period and corticomotor excitability. Exp Brain Res 173:603–611

Kok RM, Howells DW, van den Heuvel CC, Guerand WS, Thompson GN, Jakobs C (1993) Stable isotope dilution analysis of GABA in CSF using simple solvent extraction and electron-capture negative-ion mass fragmentography. J Inherit Metab Dis 16: 508–512

McDonnell MN, Orekhov Y, Ziemann U (2006) The role of GABA(B) receptors in intracortical inhibition in the human motor cortex. Exp Brain Res 173:86–93

Mody I, De Koninck Y, Otis TS, Soltesz I (1994) Bridging the cleft at GABA synapses in the brain. Trends Neurosci 17:517–525

Okamoto K, Kimura H, Sakai Y (1983) Evidence for taurine as an inhibitory neurotransmitter in cerebellar stellate interneurons: selective antagonism by TAG (6-aminomethyl-3-methyl-4H,1,2,4-benzothiadiazine-1,1-dioxide). Brain Res 265:163–168

Pearl PL, Gibson KM, Acosta MT et al (2003a) Clinical spectrum of succinic semialdehyde dehydrogenase deficiency. Neurology 60: 1413–1417

Pearl PL, Novotny EJ, Acosta MT, Jakobs C, Gibson KM (2003b) Succinic semialdehyde dehydrogenase deficiency in children and adults. Ann Neurol 54(Suppl 6):S73–S80

Pearl PL, Gibson KM, Quezado Z et al (2009) Decreased GABA-A binding on FMZ-PET in succinic semialdehyde dehydrogenase deficiency. Neurology 73:423–429

Pearl PL, Schreiber J, Theodore WH et al (2014) Taurine trial in succinic semialdehyde dehydrogenase deficiency and elevated CNS GABA. Neurology 82:940–944

Reis J, Cohen LG, Pearl PL et al (2012) GABAB-ergic motor cortex dysfunction in SSADH deficiency. Neurology 79:47–54

Saronwala A, Tournay A, Gargus J (2008) Taurine treatment of succinate semialdehyde dehydrogenase (SSADH) deficiency reverses MRI-documented globus lesions and clinical syndrome. Conference Taurine treatment of succinate semialdehyde dehydrogenase (SSADH) deficiency reverses MRI-documented globus lesions and clinical syndrome., Phoenix AZ, 2008, 103.

Tang ZQ, Lu YG, Chen L (2008) Developmental stability of taurine's activation on glycine receptors in cultured neurons of rat auditory cortex. Neurosci Lett 430:54–59

Wu Y, Buzzi A, Frantseva M et al (2006) Status epilepticus in mice deficient for succinate semialdehyde dehydrogenase: GABAA receptor-mediated mechanisms. Ann Neurol 59:42–52

JIMD Reports
DOI 10.1007/8904_2015_522

RESEARCH REPORT

A Modified Enzymatic Method for Measurement of Glycogen Content in Glycogen Storage Disease Type IV

Haiqing Yi · Quan Zhang · Chunyu Yang · Priya S. Kishnani · Baodong Sun

Received: 21 September 2015 / Revised: 11 November 2015 / Accepted: 16 November 2015 / Published online: 26 June 2016

Abstract Deficiency of glycogen branching enzyme in glycogen storage disease type IV (GSD IV) results in accumulation of less-branched and poorly soluble polysaccharides (polyglucosan bodies) in multiple tissues. Standard enzymatic method, when used to quantify glycogen content in GSD IV tissues, causes significant loss of the polysaccharides during preparation of tissue lysates. We report a modified method including an extra boiling step to dissolve the insoluble glycogen, ultimately preserving the glycogen content in tissue homogenates from GSD IV mice. Muscle tissues from wild-type, GSD II and GSD IV mice and GSD III dogs were homogenized in cold water, and homogenate of each tissue was divided into two parts. One part was immediately clarified by centrifugation at 4°C (STD-prep); the other part was boiled for 5 min then centrifuged (Boil-prep) at room temperature. When glycogen was quantified enzymatically in tissue lysates, no significant differences were found between the STD-prep and the Boil-prep for wild-type, GSD II and GSD III muscles. In contrast, glycogen content for GSD IV muscle in the STD-prep was only 11% of that in the Boil-prep, similar to wild-type values. Similar results were observed in other tissues of GSD IV mice and fibroblast cells from a GSD IV patient. This study provides important information for improving disease diagnosis, monitoring disease progression, and evaluating treatment outcomes in both clinical and preclinical clinical settings for GSD IV. This report should be used as an updated protocol in clinical diagnostic laboratories.

Communicated by: Avihu Boneh, MD, PhD, FRACP

H. Yi · Q. Zhang · C. Yang · P.S. Kishnani · B. Sun (✉)
Division of Medical Genetics, Department of Pediatrics, Duke University School of Medicine, Durham, NC 27710, USA
e-mail: baodong.sun@duke.edu

Q. Zhang
College of Veterinary Medicine, Yangzhou University, Yangzhou, Jiangsu 225009, China

Introduction

In animal cells, glycogen synthesis is primarily catalyzed by two enzymes, glycogen synthase (GS, EC 2.4.1.11), which adds glucose residues to a linear chain, and glycogen branching enzyme (GBE, EC 2.4.1.18), which adds branches to the growing glycogen molecule. Although the majority of glycogen is degraded in the cytoplasm by the combined action of glycogen phosphorylase and glycogen debranching enzyme (GDE, EC 2.4.1.25/EC 3.2.1.33), a small percentage of glycogen is transported to and hydrolyzed in lysosomes by acid α-glucosidase (GAA, EC 3.2.1.20) (Huijing 1975; Chen et al. 2009).

Glycogen storage diseases (GSDs) are a group of inherited disorders caused by deficiency of a certain enzyme involved in glycogen synthesis or degradation. While the accumulation of glycogen in liver and muscle tissues is the common consequence of these diseases, the molecular structure and property of glycogen varies between specific GSDs. For example, deficiency of GAA in GSD II causes accumulation of glycogen with normal structure in the lysosomes. In GSD III, loss of GDE enzyme activity hinders further breakdown of glycogen from branching points, resulting in the accumulation of abnormal glycogen with short outer chains (Chen et al. 2009). In GSD IV, deficiency of GBE leads to the production of less-branched and poorly soluble polysaccharides (polyglucosan bodies, PB) in all body tissues (Brown and Brown 1966; Fernandes and Huijing 1968; Mercier and Whelan 1970).

Biochemical quantification of glycogen content is critical for disease diagnosis, disease progression monitoring, and therapeutic outcomes evaluation in both clinical and preclinical settings. An enzymatic method based on homogenization of tissues in cold water followed by *Aspergillus niger* amyloglucosidase (EC 3.2.1.3) digestion has become widely used for measuring glycogen content in tissue (Huijing 1970; Van Hove et al. 1996; Kikuchi et al. 1998; Raben et al. 2003). In the past decade, our team has had success using this method to quantify glycogen in various tissues from experimental animals with GSD type I, II, or III (Sun et al. 2005, 2007; Koeberl et al. 2006; Yi et al. 2012, 2014). Recently, in our work with a mouse model of GSD IV, we found that the measured tissue glycogen contents were at extremely low levels, which contradicts with the observation that strongly PAS-positive PB were present in these tissues. Considering the low solubility of the PB in GSD IV, we speculated that the majority of glycogen was lost during the lysate preparation. Here we describe a modified enzymatic method for glycogen quantification in GSD IV.

Materials and Methods

Animal Tissues

Muscle tissues were obtained from 3-month-old GAA knockout (GSD II) mice (Raben et al. 1998) and from 4-month-old GSD IIIa dogs (Yi et al. 2012). GSD IV (*Gbe1*$^{ys/ys}$) mice (Akman et al. 2015) were euthanized at age of 3 months following overnight fasting for collection of tissues. Muscle tissues from 3-month-old wild-type (C57BL/6) mice were used as controls. Fresh tissues were fixed in 10% neutral buffered formalin for PAS staining or frozen in −80°C freezer until use (Yi et al. 2012). All animal experiments were approved by the Institutional Animal Care & Use Committee at Duke University and were in accordance with the National Institutes of Health guidelines.

Tissue Lysate Preparation

Frozen tissues (50–100 mg) were homogenized in ice-cold deionized water (20 ml water/g tissue) and sonicated three times for 15 s with 30-s intervals between pulses, using a Misonix XL2020 ultrasonicator (Yi et al. 2012). Homogenate of each tissue was divided into two parts and processed separately: one part was immediately clarified by centrifugation at 4°C (STD-prep); the other part was boiled for 5 min then centrifuged at room temperature (Boil-prep).

Cell Culture and Cell Lysates

Fibroblasts derived from skin biopsies of a patient with GSD II and one with GSD IV were harvested after 3 days in culture in 10-cm plates (Van Hove et al. 1996). The cell pellet from each plate was resuspended in 300 μl cold water and sonicated three times. The STD-prep and Boil-prep cell lysates were then prepared as described above. Protein concentration of the STD-prep was determined using BCA method.

Glycogen Content Measurement

Glycogen contents in the tissue and cell lysates (both the STD-prep and the Boil-prep) were assayed as described (Van Hove et al. 1996; Yi et al. 2012).

Statistical Analysis of Glycogen Content

The significance of differences between the STD-prep and Boil-prep of the same group of samples was assessed using two-tailed, paired student *T*-test. Mean ± standard deviation were shown.

Results

Glycogen Staining and Quantitation in Skeletal Muscles from Wild-Type and GSD Animals

PAS staining of glycogen revealed no visible PAS-positive materials in wild-type (Wt) mice. In GSD II mice, glycogen-filled lysosomes of various sizes were scattered throughout the tissue; in GSD III dogs, filamentous glycogen aggregates and large pools of glycogen were seen; in GSD IV mice, granular glycogen particles were observed in most myocytes (Fig. 1a).

When glycogen was quantified in tissue lysates, no significant differences were found between the STD-prep and the Boil-prep for wild-type (Wt), GSD II and GSD III muscles (Fig. 1b). In contrast, the GSD IV muscle showed a very low level of glycogen in the STD-prep lysates (3.17 ± 1.15 μmol glucose/g tissue), similar to that of wild-type muscle, while the Boil-prep showed a markedly higher level (34.5 ± 12.7), indicating significant loss of glycogen in the STD-prep lysates (Fig. 1b).

Glycogen Staining and Quantitation in Other Tissues from GSD IV Mice

PAS staining of glycogen was also performed on other tissues of GSD IV mice at age 3 months. As shown in

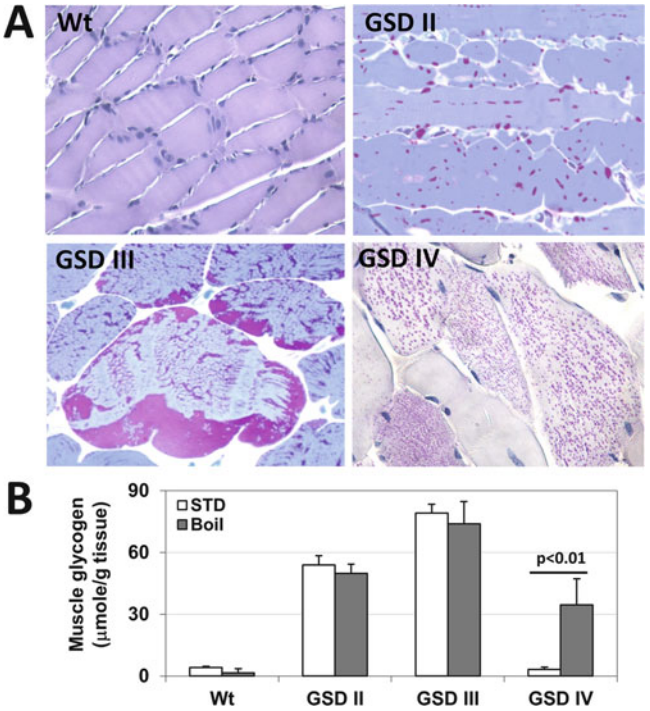

Fig. 1 Glycogen in skeletal muscles from wild-type (Wt) and GSD animals. (**a**) Representative PAS staining of muscle (gastrocnemius) sections form Wt mice, GSD II mice, GSD IIIa dogs, and GSD IV mice (magnification 400×). (**b**) Comparison of the STD-prep and the Boil-prep methods for quantitation of glycogen in muscles from animals in (**a**). n=5 for mice, n=4 for dogs

Fig. 2a, most hepatocytes were loaded with glycogen (fasted); the diaphragm has similar glycogen accumulation pattern as the gastrocnemius muscle; clusters of glycogen particles were occasionally found in the heart; PAS-positive granules were clearly present in the brain (cerebrum). Glycogen quantitation showed significantly lower glycogen contents in the STD-preps than in the Boil-preps for all the tissues (Fig. 2b). Glycogen content in the STD-prep was 28% of that in the Boil-prep for the liver (fasted) and was 21% for the heart and 8% for both the brain and diaphragm (Fig. 2b).

Glycogen Quantitation in Fibroblasts from Patients with GSD II and IV

In cultured human patient skin fibroblasts, the STD-prep of the GSD IV cells presented 50% less glycogen than the Boil-prep; the Boil-prep of GSD II cells presented 10% more glycogen than the STD-prep (Fig. 3).

Discussion

Mutations in the *Gbe1* gene cause a complete or partial loss of GBE activity in GSD IV, which leads to an increase in the ratio of GS to GBE, a critical determinant of PB formation during the process of glycogen synthesis (Raben et al. 2001; Pederson et al. 2003; Kakhlon et al. 2013). The Y329S is the most common mutation found in Jewish families of Ashkenazi ancestry with adult onset GSD IV, also referred to as adult polyglucosan body disease (Lossos et al. 1998; Mochel et al. 2012). Recently we obtained a new mouse model of GSD IV ($Gbe1^{ys/y}$ mice) carrying the knock-in Y329S mutation (Akman et al. 2015). The residual enzyme activity in the affected mice was approximately 10–19% of wild-type value in skeletal and cardiac muscles, 30% in the brain, and less than 1% in liver (data not shown). PAS staining showed significant PB accumulation in all these tissues.

In a standard enzymatic method for glycogen quantitation, tissue homogenization in cold water or buffer followed by an immediate centrifugation has been a widely used procedure for its simplicity, sensitivity, and ability to analyze other metabolites and enzyme activities in the same homogenate (Huijing 1970; Murat and Serfaty 1974; Van Hove et al. 1996). But this procedure is not suitable for GSD IV glycogen measurement due to the heavy loss of insoluble glycogen during sample preparation. In this study, we described a modified method that includes an extra boiling step prior to centrifugation of tissue homogenates to dissolve the insoluble glycogen in GSD IV (Mercier and Whelan 1970). To determine the length of boiling time needed for complete glycogen dissolution, we quantified glycogen after boiling the homogenates (150–300 μl) 3, 5,

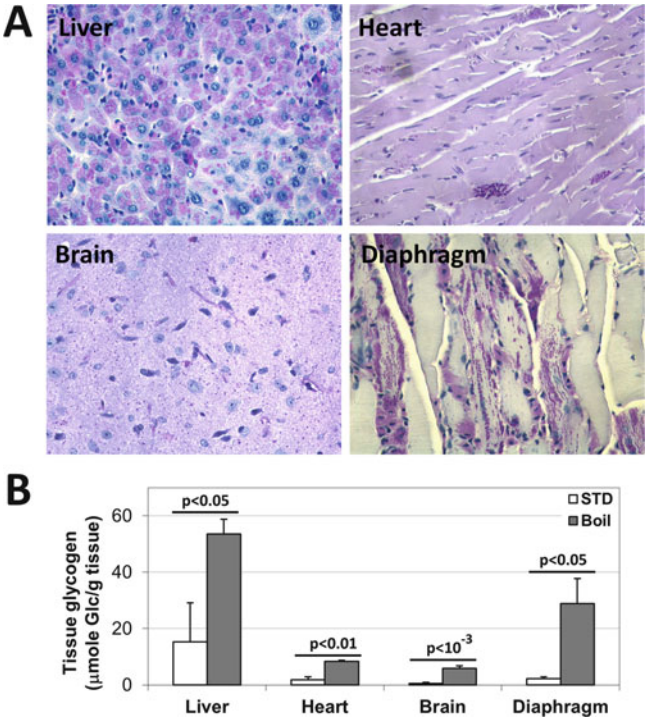

Fig. 2 Glycogen in other tissues from the GSD IV mice. (**a**) PAS staining shows glycogen deposits of various degrees in the liver, diaphragm, heart, and brain (cerebrum) of the GSD IV mice (magnification 400×). (**b**) Comparison of the STD-prep and the Boil-prep methods for quantitation of glycogen in these tissues. n=5 mice

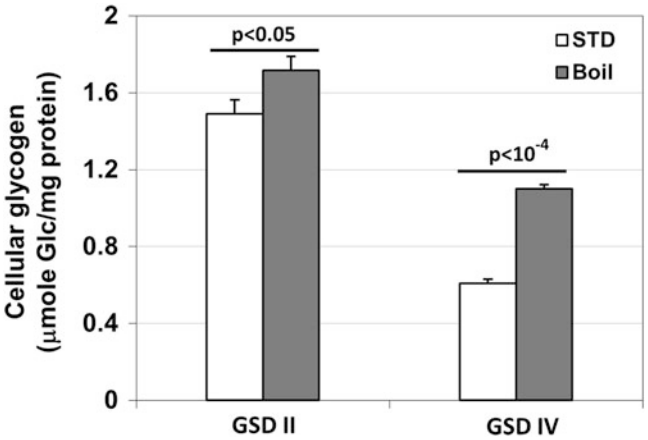

Fig. 3 Comparison of the STD-prep and the Boil-prep methods for quantitation of glycogen in cultured skin fibroblasts from a patient with GSD II and one with GSD IV. n=4 plates for each patient

10, and 15 min and saw no difference among all the time points (data not shown). This method is likely also applicable to Lafora disease, a related polyglucosan body disease caused by mutations in EPM2A or EPM2B (Minassian 2001), but this needs to be verified by experiments. Another more tedious and less sensitive method involving boiling tissue homogenate in KOH followed by ethanol precipitation of glycogen prior to the amyloglucosidase digestion is also suitable for determining glycogen content in GSD IV, but this procedure requires larger size of tissues, which limits its clinical application (Koeberl et al. 1990; Suzuki et al. 2001; Pederson et al. 2004).

This study provides an improved protocol for quantifying the insoluble glycogen in GSD IV without the need of glycogen isolation prior to the enzyme digestion. More importantly, the modified method allows determination of glycogen content in very small biopsy samples, which is extremely useful for clinical diagnostic laboratories. Vali-

dation with sufficient numbers of patient samples and normal controls will be necessary before applying this method to clinical diagnosis.

Acknowledgments We thank Dr. Craigen and Dr. Akman of Baylor College of Medicine for sharing their new mouse model of GSD IV (*Gbe1*$^{ys/ys}$ mice). We would also like to thank Cecelia Mizelle for helping edit the manuscript. This work was supported by the Alice and Y.T. Chen Research Center for Genetics and Genomics at Duke University.

Synopsis of the Article

An improved method for quantitation of insoluble glycogen in glycogen storage disease type IV is described.

Compliance with Ethics Guidelines

Conflict of Interest

Haiqing Yi, Quan Zhang, Chunyu Yang, Priya S. Kishnani, and Baodong Sun declare that they have no conflict of interest.

Informed Consent

This article does not contain any studies with human subjects performed by any of the authors. The research protocol with human GSD patients' cells in this study was approved and declared by Duke IRB as research not involving human subjects.

Animal Rights

All institutional and national guidelines for the care and use of laboratory animals were followed.

Details of the Contributions of Individual Authors

Haiqing Yi – conducted the majority of the experiments, reported the work, and prepared manuscript

Quan Zhang – conducted some of the experiments

Chunyu Yang – conducted some of the experiments

Priya S. Kishnani – reviewed and edited the manuscript

Baodong Sun – planned and supervised this study and wrote the manuscript

References

Akman HO, Emmanuele V, Kurt YG, Kurt B, Sheiko T, DiMauro S, Craigen WJ (2015) A novel mouse model that recapitulates adult onset glycogenosis type 4. Hum Mol Genet 24:6801–6810

Brown BI, Brown DH (1966) Lack of an alpha-1,4-glucan: alpha-1,4-glucan 6-glycosyl transferase in a case of type IV glycogenosis. Proc Natl Acad Sci U S A 56:725–729

Chen Y-T, Kishnani PS, Koeberl DD (2009) Glycogen storage diseases. In: Valle D, Beaudet A, Vogelstein B, Kinzler K, Antonarakis S, Ballabio A (eds) Scriver's online metabolic & molecular bases of inherited disease. McGraw-Hill, New York

Fernandes J, Huijing F (1968) Branching enzyme-deficiency glycogenosis: studies in therapy. Arch Dis Child 43:347–352

Huijing F (1970) A rapid enzymic method for glycogen estimation in very small tissue samples. Clin Chim Acta 30:567–572

Huijing F (1975) Glycogen metabolism and glycogen-storage diseases. Physiol Rev 55:609–658

Kakhlon O, Glickstein H, Feinstein N, Liu Y, Baba O, Terashima T, Akman HO, Dimauro S, Lossos A (2013) Polyglucosan neurotoxicity caused by glycogen branching enzyme deficiency can be reversed by inhibition of glycogen synthase. J Neurochem 127:101–113

Kikuchi T, Yang HW, Pennybacker M, Ichihara N, Mizutani M, Van Hove JL, Chen YT (1998) Clinical and metabolic correction of pompe disease by enzyme therapy in acid maltase-deficient quail. J Clin Invest 101:827–833

Koeberl DD, Bottema CD, Sommer SS (1990) Comparison of direct and indirect methods of carrier detection in an X-linked disease. Am J Med Genet 35:600–608

Koeberl DD, Sun BD, Damodaran TV, Brown T, Millington DS, Benjamin DK, Bird A, Schneider A, Hillman S, Jackson M et al (2006) Early, sustained efficacy of adeno-associated virus vector-mediated gene therapy in glycogen storage disease type Ia. Gene Ther 13:1281–1289

Lossos A, Meiner Z, Barash V, Soffer D, Schlesinger I, Abramsky O, Argov Z, Shpitzen S, Meiner V (1998) Adult polyglucosan body disease in Ashkenazi Jewish patients carrying the Tyr329Ser mutation in the glycogen-branching enzyme gene. Ann Neurol 44:867–872

Mercier C, Whelan WJ (1970) The fine structure of glycogen from type IV glycogen-storage disease. Eur J Biochem/FEBS 16:579–583

Minassian BA (2001) Lafora's disease: towards a clinical, pathologic, and molecular synthesis. Pediatr Neurol 25:21–29

Mochel F, Schiffmann R, Steenweg ME, Akman HO, Wallace M, Sedel F, Laforêt P, Levy R, Powers JM, Demeret S et al (2012) Adult polyglucosan body disease: natural history and key magnetic resonance imaging findings. Ann Neurol 72:433–441

Murat JC, Serfaty A (1974) Simple enzymatic determination of polysaccharide (glycogen) content of animal tissues. Clin Chem 20:1576–1577

Pederson BA, Csitkovits AG, Simon R, Schroeder JM, Wang W, Skurat AV, Roach PJ (2003) Overexpression of glycogen synthase in mouse muscle results in less branched glycogen. Biochem Biophys Res Commun 305:826–830

Pederson BA, Chen H, Schroeder JM, Shou W, DePaoli-Roach AA, Roach PJ (2004) Abnormal cardiac development in the absence of heart glycogen. Mol Cell Biol 24:7179–7187

Raben N, Nagaraju K, Lee E, Kessler P, Byrne B, Lee L, LaMarca M, King C, Ward J, Sauer B et al (1998) Targeted disruption of the acid alpha-glucosidase gene in mice causes an illness with critical features of both infantile and adult human glycogen storage disease type II. J Biol Chem 273:19086–19092

Raben N, Danon M, Lu N, Lee E, Shliselfeld L, Skurat AV, Roach PJ, Lawrence JC Jr, Musumeci O, Shanske S et al (2001) Surprises of genetic engineering: a possible model of polyglucosan body disease. Neurology 56:1739–1745

Raben N, Danon M, Gilbert AL, Dwivedi S, Collins B, Thurberg BL, Mattaliano RJ, Nagaraju K, Plotz PH (2003) Enzyme replacement therapy in the mouse model of Pompe disease. Mol Genet Metab 80:159–169

Sun B, Zhang H, Franco LM, Brown T, Bird A, Schneider A, Koeberl DD (2005) Correction of glycogen storage disease type II by an adeno-associated virus vector containing a muscle-specific promoter. Mol Ther J Am Soc Gene Ther 11:889–898

Sun B, Bird A, Young SP, Kishnani PS, Chen YT, Koeberl DD (2007) Enhanced response to enzyme replacement therapy in Pompe disease after the induction of immune tolerance. Am J Hum Genet 81:1042–1049

Suzuki Y, Lanner C, Kim JH, Vilardo PG, Zhang H, Yang J, Cooper LD, Steele M, Kennedy A, Bock CB et al (2001) Insulin control of glycogen metabolism in knockout mice lacking the muscle-specific protein phosphatase PP1G/RGL. Mol Cell Biol 21:2683–2694

Van Hove JL, Yang HW, Wu JY, Brady RO, Chen YT (1996) High-level production of recombinant human lysosomal acid alpha-glucosidase in Chinese hamster ovary cells which targets to heart muscle and corrects glycogen accumulation in fibroblasts from patients with Pompe disease. Proc Natl Acad Sci U S A 93:65–70

Yi H, Thurberg BL, Curtis S, Austin S, Fyfe J, Koeberl DD, Kishnani PS, Sun B (2012) Characterization of a canine model of glycogen storage disease type IIIa. Dis Model Mech 5:804–811

Yi H, Brooks ED, Thurberg BL, Fyfe JC, Kishnani PS, Sun B (2014) Correction of glycogen storage disease type III with rapamycin in a canine model. J Mol Med (Berl) 92:641–650

JIMD Reports
DOI 10.1007/8904_2015_523

RESEARCH REPORT

The Effect of Multiple Sulfatase Deficiency (MSD) on Dental Development: Can We Use the Teeth as an Early Diagnostic Tool?

Uri Zilberman · Haim Bibi

Received: 16 July 2015 / Revised: 17 November 2015 / Accepted: 18 November 2015 / Published online: 26 June 2016

Abstract *Background*: Multiple sulfatase deficiency (MSD) is a rare autosomal recessive inborn error of metabolism due to reduced catalytic activity of the different sulfatase. Affected individuals show neurologic deterioration with mental retardation, skeletal anomalies, organomegaly, and skin changes as in X-linked ichthyosis. The only organ that was not examined in MSD patients is the dentition.

Objectives: To evaluate the effect of the metabolic error on dental development in a patient with the intermediate severe late-infantile form of MSD (S155P).

Methods: Histological and chemical study were performed on three deciduous and five permanent teeth from MSD patient and pair-matched normal patients.

Results: Tooth germ size and enamel thickness were reduced in both deciduous and permanent MSD teeth, and the scalloping feature of the DEJ was missing in MSD teeth causing enamel to break off from the dentin. The mineral components in the enamel and dentin were different.

Conclusions: The metabolic error insults the teeth in the stage of organogenesis in both the deciduous and permanent dentition. The end result is teeth with very sharp cusp tips, thin hypomineralized enamel, and exposed dentin due to the break off of enamel. These findings are different from all other types of MPS syndromes.

Clinically the phenotype of intermediate severe late-infantile form of MSD appeared during the third year of life. In children of parents that are carriers, we can diagnose the disease as early as birth using X-ray radiograph of the anterior upper region or as early as 6–8 months when the first deciduous tooth erupt and consider very early treatment to ameliorate the symptoms.

Communicated by: Jutta Gaertner

U. Zilberman (✉)
Pediatric Dental Clinic, Barzilai Medical University Center, Ashkelon, Israel
e-mail: uri-z@smile.net.il

U. Zilberman · H. Bibi
Ben Gurion University of the Negev, Negev, Israel

H. Bibi
Pediatric Department, Barzilai Medical University Center, Ashkelon, Israel

Introduction

Multiple sulfatase deficiency (MSD, MIM 272200) is a rare autosomal recessive inborn error of metabolism. This error results in tissue accumulation of sulfatides, sulfated glycosaminoglycans, sphingolipids, and steroid sulfates (Hopwood and Ballabio 2001). The enzymatic defect affects the whole family of sulfatase enzymes. MSD is caused by mutations in the sulfatase-modifying factor 1 gene (SUMF1), located on 3p26.1 (Schlotawa et al. 2008), encoding the formylglycine-generating enzyme (FGE). The clinical presentation includes symptoms of the different sulfatase deficiencies. The abnormal activity leads to an accumulation of complex sulfatase esters and eventually to variable clinical phenotypes. Affected individuals show neurologic deterioration with mental retardation, skeletal anomalies, organomegaly, and skin changes as in X-linked ichthyosis. Different types of MSD can be distinguished according to the age of onset: neonatal, late infantile, and juvenile (Hopwood and Ballabio 2001). Neonatal is the most severe form with a broad range of mucopolysaccharidosis-like clinical symptoms and death within the first year of life. Late-infantile MSD, which includes the majority of cases, resembles late-infantile metachromatic leukodystrophy with progressive loss of mental and motor abilities, combined with other symptoms of single sulfatase defi-

ciencies like dysmorphism, skeletal changes, and ichthyosis. Attenuate form of late-infantile MSD with onset of symptoms in late childhood, beyond the second year of life, and slower progression was also documented (Schlotawa et al. 2008). Rare cases of juvenile-onset MSD have been reported with onset of symptoms in late childhood and slower progression (Blanco-Aguirre et al. 2001).

Clear genotype/phenotype correlation among patients with MSD was determined (Schlotawa et al. 2011). The patient with neonatal onset had marked impairments in both SUMF1 stability and almost undetectable enzyme activity. Patient with mild late-infantile onset were homozygous for a missense mutation (G263V; 607939.0018), which showed the highest residual enzymatic activity among the studied variants. Patients with the intermediate severe late-infantile form had mutations that compromised stability and caused low levels of residual enzyme activity (e.g., S155P; 607939.0010).

Despite thorough documented insult of various organs in MSD patients, there is lack of reports on the tooth as insulted organ. The teeth offer an excellent model with which to reconstruct the timing and progress of growth insults. Their development is a strictly ordered hierarchical process correlated with chronological age and begins in the 6th to 8th week in utero (Kraus and Jordan 1965; ten Cate 1998). Crown side is determined by two phases. The early stage is defined by the dentin-enamel junction (DEJ) that denotes the tooth germ. The final size is defined by the thickness of the enamel shell. Developmental insults leave a permanent imprint, mainly in enamel, whose onset and severity can be identified in fully formed teeth. Hereditary disorders were shown to affect both apposition and mineralization of enamel in deciduous and permanent teeth (Keinan et al. 2006, 2007).

The aim of this study is to examine deciduous and permanent tooth development in a girl diagnosed with intermediate severe late-infantile form of MSD.

Case Presentation

OM, a firstborn 3-year-old girl, showed progressive neurologic and motor deterioration that started 12 months earlier. Due to her symptoms, she was evaluated by extensive biochemical studies that showed low levels of the enzymes aryl sulfatase A as in metachromatic leukodystrophy, alpha-iduronate sulfate sulfatase as in Hunter disease, and heparin sulfaminidase as in Sanfilippo A syndrome. A high level of mucopolysaccharides and sulfatide were found in the urine. Based on these results, a diagnosis of MSD was established and genetic analyses were performed. The girl was homozygous to S155P mutation and her parents were found to be carriers. At the age of 9 years, she was referred to the pediatric dental clinic at Barzilai Medical University Center, Ashkelon, Israel, due to suspected pain from the teeth and self-mutilation of the inside of both cheeks. The girl was under medical surveillance and treated for grand mal epilepsy, tetraparesis, gastroesophageal reflux, chronic constipation, and mild ichthyosis. She was hospitalized several times due to aspiration pneumonia. The oral and dental examination revealed anterior open bite (Fig. 1a), deciduous and permanent teeth with very thin enamel on the buccal and lingual surfaces and missing enamel on the occlusal surface, and dark discoloration of dentin. The upper anterior X-ray showed upper incisors with large pulps and hypocalcified enamel in comparison with normal (Fig. 1b, c). The bite wing radiograph (Fig. 1d, e) showed very thin hypocalcified enamel on the occlusal surfaces of permanent molars and very high mesial pulp horns, in comparison with normal.

The dental treatment included extraction of 12 deciduous teeth (all canines, first and second molars) and four permanent first molars. During the following 4 years, additional 12 permanent teeth were extracted due to self-mutilation caused by the sharp edges of the exposed dentin cusps (premolars and molars) and malposition that interfered with occlusion and lip closure (upper lateral incisors and lower canines). Eventually the girl died at 13 years of age due to complicated aspiration pneumonia.

Materials and Methods

All procedures followed were in accordance with the ethical standards of the responsible committee on human experimentation of Barzilai Medical Center, Ashkelon, Israel, and with the Helsinki Declaration of 1975, as revised in 2000. Informed consent was obtained from the patient's parents for being included in the study.

Teeth Preparation

Three deciduous (upper canine, #53, and upper and lower second molars #65,85) and five permanent teeth (upper second incisor, #12; first premolar, #14; and molar, #26, and lower second premolar, #35, and molar #37) from MSD and pair-matched normal patients were embedded in epoxy (Epofix Kit, Struers) and sliced buccolingual along the long axis of the tooth. The anterior teeth were sliced through the middle of the crown, the premolars were sliced on a line connecting the buccal and lingual cusps, and the molars were sliced on a line connecting mesiobuccal and mesiolingual cusps using a wafer blade (Isomet 1000, Buehler).

Measurements Performed

a. The slice surfaces were polished and photographed using a light microscope at a 10× magnification. The

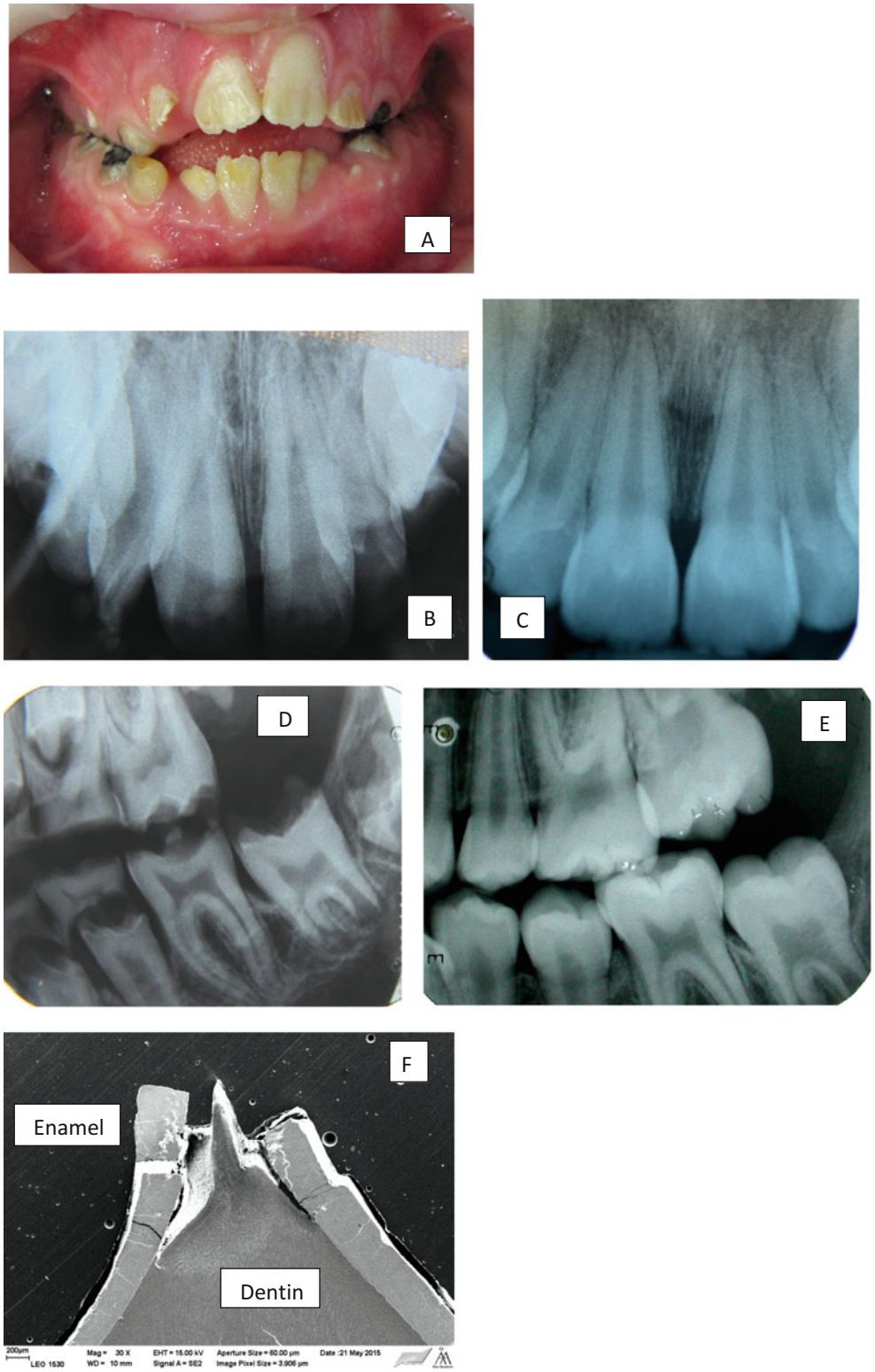

Fig. 1 Clinical and radiographic view of MSD dentition. *Note*: (**a**) Anterior view of MO. Note the yellowish color of teeth due to thin and hypomineralized enamel. (**b**) X-ray of MO upper anterior teeth. Note altered morphology and lack of enamel. (**c**) X-ray of normal upper anterior teeth. (**d**) Left bitewing of MO. Note very thin radiolucent enamel. (**e**) Left bitewing of normal teeth. Note thick radiolucent enamel. (**f**) SEM picture of MO premolar cusp. Note the break off of enamel from the dentin

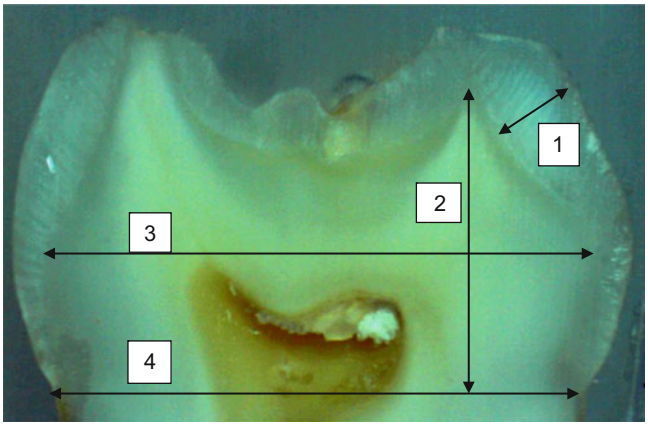

Fig. 2 The measurements performed on each tooth. *Note*: (*1*) Enamel width, (*2*) dentin cusp height, (*3*) maximal tooth germ width, (*4*) crown width at CEJ

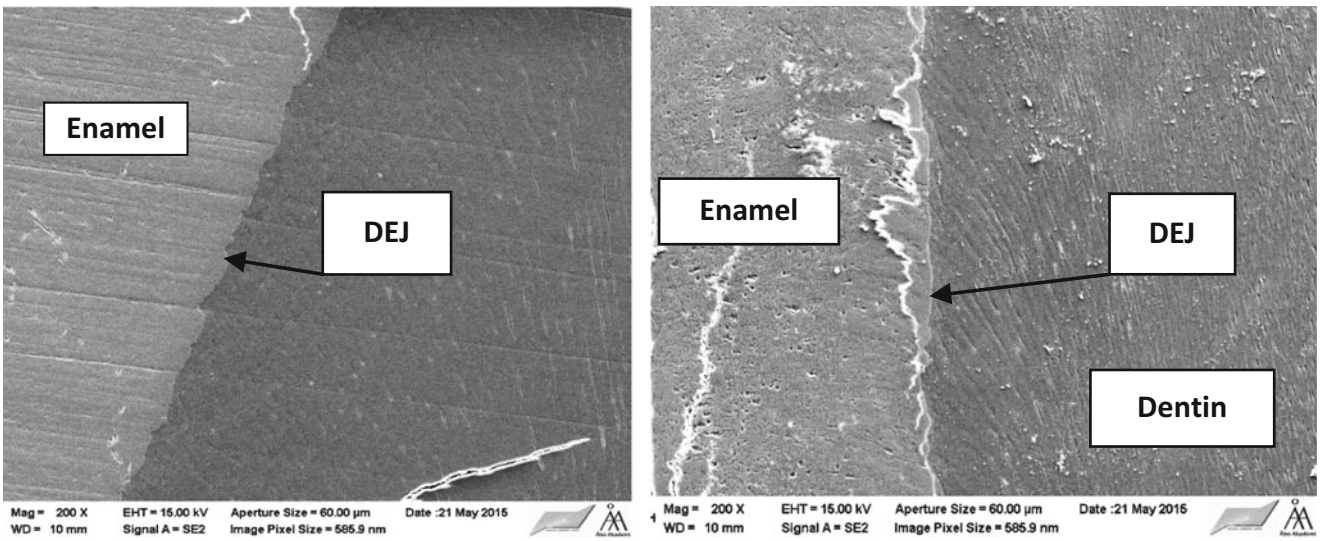

Fig. 3 DEJ structure. *Note*: MSD relatively straight junction (*right*) vs. scalloped normal DEJ (*left*)

enamel width, maximal dentin width, tooth width at the CEJ, enamel thickness, and crown dentin height were measured (Fig. 2), using a digital caliber.

b. The teeth surfaces were polished and analyzed using SEM under high vacuum mode and several observations were performed: the surface of the DEJ was observed at the enlargement of 200 in order to determine the degree of scalloping of the junction (Fig. 3), and the enamel and dentin chemical components were analyzed using the ESD program.

Results

The results of the measurements of tooth size are reported in Table 1. The buccolingual tooth germ size as determined by the DEJ was reduced in MSD teeth. Except tooth #14, the width at the CEJ in MSD teeth was reduced by 10–30%, less in anterior teeth and mainly in molars. The most striking finding was the width of the enamel. In MSD deciduous teeth, the enamel width was constant at 0.3 mm, and in permanent teeth it was constant at 0.4 mm on all surfaces. In normal deciduous teeth, the enamel width was around 0.9 mm in anterior tooth and 1.2 mm in molar, while in permanent teeth the enamel width was 1.2 mm in anterior tooth and 1.8–2.1 mm in posterior teeth.

The DEJ showed a smoother line in all MSD teeth compared to normal.

Table 2 shows the enamel and dentin chemical content of MSD teeth compared to normal. The main differences were found in the residual minerals. Except tooth #85, MSD teeth showed lower content of magnesium, silica was found only in MSD teeth, and chlorine content was

Table 1 Measurements of tooth components in mm

Tooth	Status	Width at DEJ	Max dentin width	Max dentin height	Enamel width
Upper deciduous canine #53	MSD	5.3	6.3		0.3
	Normal	6.5	6.7		0.9
Lower second deciduous molar #85	MSD	6.8	7.7	5.8	0.3
	Normal	9.2	10.0	5.7	1.2
Upper permanent second incisor #12	MSD	7.0	7.0	11.7	0.4
	Normal	7.5	7.3	11.8	1.1
Upper permanent first premolar #14	MSD	10.1	10.2	9.3	0.4
	Normal	10.1	10.4	10.2	1.8
Upper permanent first molar #26	MSD	11.5	12.1	6.8	0.4
	Normal	13.2	12.1	7.5	1.9
Lower permanent second premolar #35	MSD	8.6	9.0	7.0	0.4
	Normal	11.3	11.0	6.9	1.8
Lower permanent second molar #37	MSD	9.8	10.0	5.9	0.4
	Normal	11.4	11.5	6.2	2.1

Note: *MSD* multiple sulfatase deficiency, *DEJ* dentino-enamel junction

Table 2 Enamel and dentin components in mw%

		C	C	O	O	P	P	Ca	Ca	Ca/P	Mg	Mg	Si	Si	N
T		E	D	E	D	E	D	E	D	E	E	D	E	D	D
#53	MSD	7.84	13.12	39.73	39.25	16.51	11.56	33.99	23.32	2.06	0.13	0.25	0.65	0.25	11.41
	norm	7.00	12.72	39.94	36.66	17.55	12.51	35.96	25.08	2.04	0.24	0.57			11.93
#65	MSD	5.17	10.78	38.66	38.92	17.69	11.98	36.69	24.44	2.07	0.18	0.47	0.40	0.28	12.63
	norm	6.23	10.97	39.94	38.45	17.21	12.78	35.31	25.30	2.05	0.24	0.50			11.48
#85	MSD	6.34	12.42	41.14	39.36	16.90	11.63	36.93	22.72	2.18	0.28	0.39	0.46	0.50	12.51
	norm	6.40	12.53	37.58	36.25	17.69	12.45	37.15	25.84	2.10	0.25	0.61			11.72
#12	MSD	8.04	12.98	38.55	37.72	16.83	11.31	34.75	24.00	2.07		0.11	0.80	0.17	10.34
	norm	7.39	13.51	38.69	37.12	17.24	11.83	35.41	24.38	2.05	0.22	0.48			10.52
#14	MSD	7.19	11.58	38.35	37.16	16.91	12.48	35.43	25.56	2.09	0.16	0.47	0.87	0.10	12.15
	norm	7.30	14.47	37.72	35.32	17.75	13.03	36.00	27.03	2.03	0.28	0.65			08.77
#26	MSD	6.49	12.70	39.10	38.49	17.21	11.57	35.90	23.30	2.09	0.15	0.49	0.10		12.91
	norm	6.70	12.73	38.55	37.21	17.30	12.19	36.06	25.02	2.08	0.22	0.58			11.70
#35	MSD	8.98	14.95	34.20	34.05	17.74	12.51	37.52	25.54	2.11	0.14	0.36	0.26	0.23	11.83
	norm	5.93	11.95	40.65	37.77	17.12	12.19	35.18	24.62	2.05	0.24	0.57			12.33
#37	MSD	7.59	15.88	37.48	36.68	17.31	10.63	36.18	21.84	2.09	0.12	0.15	0.25		14.40
	norm	6.14	12.72	41.08	36.66	16.89	12.51	34.66	25.08	2.05	0.28	0.57			11.93

Note: *T* tooth no; see description in Table 1

C carbon, *O* oxygen, *P* phosphate, *Ca* calcium, *Ca/P* calcium/phosphate, *Mg* magnesium, *Si* silica, *N* nitrogen, *E* enamel, *D* dentin, *MSD* multiple sulfatase deficiency, *Norm* normal

higher in MSD teeth. The hydroxyapatite formula is $Ca_{10}(PO_4)_6(OH)_2$ with residual minerals and other calcium salts. The perfect ratio of Ca/P should be 1.67, but due to the additional calcium salts, the ratio is around 2 in normal teeth. The better the mineralization, the closer the ratio to the perfect ratio. The ratio of Ca/P was higher in the MSD enamel.

The chemical content in the dentin of MSD teeth was lower in phosphate, calcium, and magnesium, except tooth #35, and contained silica in six out of eight teeth.

Discussion

We present a girl that suffered from low levels of 3 sulfatase enzymes: aryl sulfatase A, alpha-iduronate sulfate sulfatase, and heparin sulfaminidase. Lack of aryl sulfatase A enzyme leads to the accumulation of galactosyl sulfatide in the white matter of the CNS and in the peripheral nervous system. Galactosyl sulfatide and lactosyl sulfatide also accumulate within the kidney, gallbladder, and other visceral organs. The problem with reduced activity of iduronate sulfate sulfatase concerns the breakdown of glycosaminoglycans (GAGs). As a result, GAGs build up in the cells throughout the body causing distinct facial features, large heads, and CNS involvement, leading to developmental delays and neurological problems. Low levels of heparin sulfaminidase affect the breakdown of glycosaminoglycan heparin sulfate which is found in the extracellular matrix and on cell surface glycoprotein. The primary stored substrate is heparin sulfate and the clinical features of the disease are mainly neurological (Hopwood and Ballabio 2001). The results of this study showed that both enamel and dentin are affected by MSD – the enamel in thickness and mineralization (higher Ca/P ratio in MSD teeth) and the dentin at the DEJ causing a straight junction and mineralization. During amelogenesis the percentage of protein by weight dropped from 30% during the secretory stage to 2% during the early maturation stage (Fukae and Shimizu 1974). The proteinase of the metalloproteinase class present early during the secretory stage is MMP20 (Begue-Kirn et al. 1998), and the proteinase expressed from the transitional through maturation stages is KLK4 (Hu et al. 2002). In a study on MMP20 null mouse (Caterina et al. 2002; Bartlett 2013), there was evidence of improper process of amelogenin. There was altered enamel protein and enamel rod pattern and hypoplastic enamel, which induced the enamel to break off from the dentin (Caterina et al. 2002; Bartlett 2013). This process is similar to our findings in MSD (Fig. 1f).

This is the first paper to discuss the effect of intermediate severe late-infantile form of MSD on dental tissues. There are very few papers that described the effect of various types of muccopolysaccharidosis on oral and dental tissues. The case presented showed reduced activity of three enzymes. The dental findings for each of the missing enzymes were previously described. Metachromatic leukodystrophy (lack of aryl sulfatase A enzyme) caused the accumulation of abnormal quantities of sulfatides within myelinated peripheral nerves in the oral region (Gardner and Zeman 1970) and of brown metachromatic granules (sulfatides) along the nerve fibers of the dental pulp (Gardner 1967). Hunter's syndrome (lack of alpha-iduronate sulfate sulfatase enzyme) caused localized lesions in the jaws that often resemble dentigerous cysts associated with unerupted first permanent molars. These lesions contain dense, fibrous connective tissues and large amounts of acid mucopolysaccharides. The gingival tissues are hyperplastic, hypertrophic, and enlarged while the tongue is macroglossic (Templeton-Downs et al. 1995). Enamel crystal organization is disturbed in Hunter's syndrome. The disruption affects the crystallography and nanostructure of enamel but has not yet been detected clinically (Al-Jawad et al. 2012). Sanfilippo syndrome (lack of heparin sulfaminidase enzyme) caused obliteration of pulp chambers and root canals in deciduous and permanent teeth (Mellara et al. 2012).

In other types of mucopolysaccharides accumulation, high palate, open bite, impacted teeth, changes in temporomandibular joint, taurodontism, long tooth roots, unerupted teeth, large dental follicles, and supernumerary teeth (Maroteaux–Lamy syndrome) were found (Kantaputra et al. 2014). In Morquio's disease the enamel layer was very thin but of normal radiodensity, and the radiographic appearance of the dentine, pulp chambers, and root canals was normal (Nelson and Kinirons 1988). Histological investigations have demonstrated that the enamel has increased porosity correlating to the striae of Retzius, and the hydroxyapatite crystals are smaller (Al-Jawad et al. 2012).

The observable clinical effect of the intermediate severe late-infantile form of MSD presented here started during the third year of life and was mainly in parallel to the progressive neurological and motor deterioration. The results from the dental analysis showed that the amelogenesis of the deciduous dentition was affected and showed very thin and hypomineralized enamel with a constant enamel thickness of 0.3 mm and opacity similar to dentin and reduced germ size as determined by the reduced measurements of height and width at the DEJ. In addition the scalloped feature of the DEJ was reduced and the enamel broke off from the dentin shortly after eruption, in both deciduous and permanent teeth. Each of the featured observed in MSD can be identified in other hereditary disorders of the dentition – the thin enamel can be found in hypoplastic amelogenesis imperfecta (e.g., MIM 104530 or MIM 204650), hypocalcified enamel can be found in hypocalcified amelogenesis imperfecta (e.g., MIM 130900 or MIM 104500), and enamel that breaks out of dentin with un-scalloped DEJ can be found in dentinogenesis imperfecta (e.g., MIM 125490). But all features together in both deciduous and permanent dentition are unique to this type of MSD. Since the stage of deciduous teeth amelogenesis begins at the fetus during the 6th–8th weeks in utero, these findings implicate that the effect of the disease starts during pregnancy, and one of the first organs to show deterioration is the dentition. In families of parents that are carriers for MSD, where there is a suspicion of MSD, we can diagnose

diseased children using an X-ray radiograph of the anterior region immediately after birth or at the age of 6–8 months when the first deciduous tooth erupt. The peculiar phenotype of the teeth is unique and can be easily diagnosed as MSD.

Compliance with Ethics Guidelines

Uri Zilberman and Haim Bibi declare that they have no conflict of interest.

All procedures followed were in accordance with the ethical standard of the responsible committee on human experimentation of Barzilai Medical University Center, Ashkelon, Israel, and with the Helsinki Declaration of 1975, as revised in 2000. Informed consent was obtained from the parents of the child included in this study. All details of the child included in this publication are anonymous.

Uri Zilberman performed the clinical treatment and the extractions of the teeth, the investment and the slicing of the teeth, and the SEM analysis. Uri Zilberman and Haim Bibi prepared the report and the answers to the reviewers' comments.

References

Al-Jawad M, Addison O, Khan MA, James A, Hendriksz C (2012) J Dent 40:1074–1080

Bartlett JB (2013) Dental enamel development: proteinases and their enamel matrix substrates. ISRN Dent. doi:10.1155/2013/684607

Begue-Kirn C, Krebsbach PH, Bartlett JD, Butler WT (1998) Dentin sialoprotein, dentin phosphoprotein, enamelysin and ameloblastin: tooth-specific molecules that are distinctively expressed during murine dental manifestation. Eur J Oral Sci 106:963–970

Blanco-Aguirre ME, Kofman-Alfaro SH, Rivera-Vega MR et al (2001) Unusual clinical presentation in two cases of multiple sulfatase deficiency. Pediatr Dermatol 18:388–392

Caterina JJ, Skobe Z, Shi J et al (2002) Enamelysin (MMP20) deficient mice display an amelogenesis imperfecta phenotype. J Biol Chem 51:49598–49604

Fukae M, Shimizu M (1974) Studies on the proteins of developing bovine enamel. Arch Oral Biol 19:381–386

Gardner DG (1967) Pulpectomy as a diagnostic procedure in metachromatic leukodystrophy. Oral Surg Oral Med Oral Pathol 23:379–384

Gardner DG, Zeman W (1970) Oral findings in metachromatic leukodystrophy. Oral Surg Oral Med Oral Pathol 29:431–436

Hopwood J, Ballabio A (2001) Multiple sulfatase deficiency and the nature of the sulfatase family. In: Scriver CR, Valle D, Sly WS (eds) The metabolic and molecular bases of inherited disease. McGraw-Hill, New York, pp 3725–3732

Hu JCC, Sun X, Zhang C, Liu S, Bartlett JD, Simmer JP (2002) Enamelysin and kallikrein-4 mRNA expression in developing mouse molars. Eur J Oral Sci 110:307–315

Kantaputra PN, Kayserili H, Güven Y, Kantaputra W, Balci MC, Tanpaiboon P, Uttarilli A, Dalal A (2014) Oral manifestations of 17 patients affected with mucopolysaccharidosis type VI. J Inherit Metab Dis 37:263–268

Keinan D, Smith P, Zilberman U (2006) Microstructure and chemical composition of primary teeth in children with Down syndrome and cerebral palsy. Arch Oral Biol 51:836–843

Keinan D, Smith P, Zilberman U (2007) Prenatal growth acceleration in maxilla deciduous canines of children with Down syndrome: histological and chemical composition study. Arch Oral Biol 52:961–966

Kraus BS, Jordan RE (1965) The human dentition before birth. Lea & Febiger, Philadelphia, pp 136–138

Mellara TS, Azevedo DT, Faria G et al (2012) Dental findings and management in a mucopolysaccharidosis type IIIB patient. J Dent Child (Chic) 79:176–180

Nelson J, Kinirons M (1988) Clinical findings in 12 patients with MPS IV A (Morquio's disease). Further evidence for heterogeneity. Part II: dental findings. Clin Genet 33:121–125

Schlotawa L, Steinfeld R, von Figura K, Dierks T, Gartner J (2008) Molecular analysis of SUMF1 mutation: stability and residual activity of mutant formylglycine-generating enzyme determine disease severity in multiple sulfatase deficiency. Hum Mutation 29:205–217

Schlotawa L, Ennemann EC, Radhakrishan K et al (2011) SUMF1 mutations affecting stability and activity of formylglycine generating enzyme predict clinical outcome in multiple sulfatase deficiency. Eur J Human Genet 19:253–261

Templeton-Downs A, Crisp T, Ferretti G (1995) Hunter's syndrome and oral manifestations: a review. Pediatr Dent 17:98–100

ten Cate AR (1998) Oral hystology. Development, structure and function. 5th edn. The CV Mosby Co., St. Louis, pp 73–102

JIMD Reports
DOI 10.1007/8904_2015_510

CASE REPORT

Novel Report of Phosphoserine Phosphatase Deficiency in an Adult with Myeloneuropathy and Limb Contractures

Heather M. Byers · Robin L. Bennett · Emily A. Malouf · Michael D. Weiss · Jie Feng · C. Ronald Scott · Suman Jayadev

Received: 07 August 2015 / Revised: 24 September 2015 / Accepted: 01 October 2015 / Published online: 21 November 2015

Abstract Serine is a nonessential amino acid that plays a vital role in proper development and functioning of the central nervous system (CNS). Serine deficiency leads to microcephaly, intellectual disability, seizures, and psychomotor retardation in children and severe axonal neuropathy in adults. Serine deficiency syndrome is due to a deficiency of one of three enzymes in the endogenous serine biosynthesis pathway: phosphoglycerate dehydrogenase, phosphoserine transaminase, or, most rarely, phosphoserine phosphatase. Of critical importance to clinical care, serine deficiency syndrome is treatable. Herein, we describe the novel presentation of phosphoserine phosphatase deficiency in an adult. The patient had intrauterine growth restriction, lifelong intellectual disability, childhood onset epilepsy, and borderline microcephaly. In adulthood, she developed progressively severe lower extremity hypertonia, axonal neuropathy, and hand contractures. Neuropathy was complicated by non-healing wounds. Fasting plasma amino acids showed low serine and glycine. Molecular analysis revealed compound heterozygous mutations in phosphoserine phosphatase (*PSPH*). Treatment with oral serine resulted in improvement of plasma serine levels, decreased neuropathic pain, and subjective improvement in energy level. Although the first case of phosphoserine phosphatase deficiency was described nearly 20 years ago, only eight cases have been reported, all in children. This is the first report of phosphoserine phosphatase deficiency in an adult.

Communicated by: Nicole Wolf, MD PhD

Competing interests: None declared

H.M. Byers · R.L. Bennett · E.A. Malouf · J. Feng · C.R. Scott · S. Jayadev (✉)
Division of Medical Genetics, University of Washington Medical Center, Seattle, WA, USA
e-mail: sumie@uw.edu

M.D. Weiss · S. Jayadev
Department of Neurology, University of Washington Medical Center, Seattle, WA, USA

J. Feng · C.R. Scott
Division of Molecular Medicine, University of Washington Medical Center, Seattle, WA, USA

Background

Serine is a nonessential amino acid that plays a critical role in the development and functioning of the central nervous system (CNS) (Furuya et al. 2000; Furuya 2008; de Koning 2006). Serine deficiency syndrome consists of a group of autosomal recessive, neurometabolic disorders due to a deficiency of one of three enzymes in the endogenous serine biosynthesis pathway: phosphoglycerate dehydrogenase (PHGDH, EC 1.1.1.95), phosphoserine transaminase (PSAT, EC 2.6.1.52), or phosphoserine phosphatase (PSPH, EC 3.1.3.3) (see Fig. 1) (Jaeken et al. 1996; Hart et al. 2007). Although the first case of phosphoserine phosphatase deficiency (OMIM #172480) was described nearly 20 years ago, only eight cases have been reported, all in children (Jaeken et al. 1997; Vincent et al. 2015). We describe a novel presentation of phosphoserine phosphatase deficiency in an adult with progressive myeloneuropathy and distal contractures of the upper extremities, expanding the currently understood phenotype. This patient had improvement of her neuropathic pain with serine supplementation.

Case Report

The patient was born to a 31-year-old gravida 4, para 4 woman at 42 weeks gestation after an uncomplicated

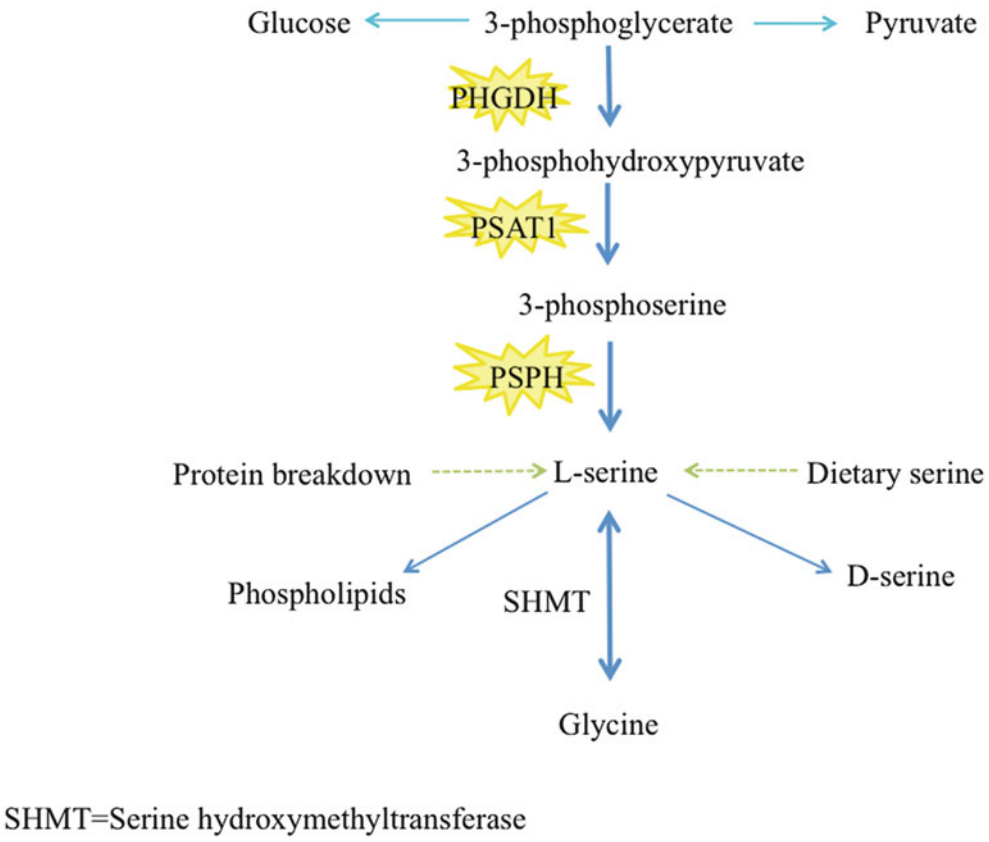

Fig. 1 Serine biosynthesis pathway

pregnancy. She weighed 4 pounds, 10 ounces at birth, 3 standard deviations (SD) below average, consistent with severe intrauterine growth restriction. The patient remained below the growth curve during childhood, though with reportedly proportionate growth. Microcephaly was never mentioned to the family and records are not available. She never had feeding difficulties. The patient met all developmental milestones until age 4 when she started performing poorly in preschool and was eventually diagnosed with absence seizures and intellectual disability. Diagnoses were confirmed with electroencephalogram (EEG) and formal neurologic testing. Absence seizures were difficult to treat, predominantly due to inconsistent medication administration, though the patient's seizures have been well controlled on ethosuximide for the past 5 years. The patient graduated from high school and held manual labor jobs until severe neuropathy prevented her from working. Her demeanor is generally described as happy, though she can be intermittently extremely irritable. She was evaluated for acute paranoia at age 26, though this was later attributed to an adverse drug reaction. Currently, the patient lives independently with her boyfriend who also has mild intellectual disability. Her mother lives across the street, manages her finances, and is involved as a caretaker.

Throughout childhood, there was no concern for fine or gross motor abnormalities. At age 19, the patient began to complain of increasing lower extremity stiffness, starting in her Achilles tendons. Gross and fine motor skills subsequently deteriorated. Her gait became progressively abnormal, and she developed bilateral foot drop at age 27. Over the next ten years, the patient required multiple surgical debridements, hyperbaric oxygen treatments, casting and therapy for complications of neuropathy including non-healing ulcers, osteomyelitis, and finger tip amputations. Stiffness progressed to involve her upper extremities at age 32, and the patient began to note contractures of her hands and fingers (see Figs. 2 and 3).

Family history is negative for growth restriction, seizures, intellectual disability, microcephaly, recurrent pregnancy losses, and neuropathy. The patient has a 42-year-old unaffected full sister and two unaffected half-brothers. She is of Polish and Northern European ancestry; her parents are not consanguineous.

The neurology service at our tertiary academic medical center was consulted during an inpatient admission for osteomyelitis. On exam, she had borderline microcephaly (occipital-frontal circumference, 52 cm, −2 SD), short stature (height, 149 cm, −2.4 SD), and obesity (weight,

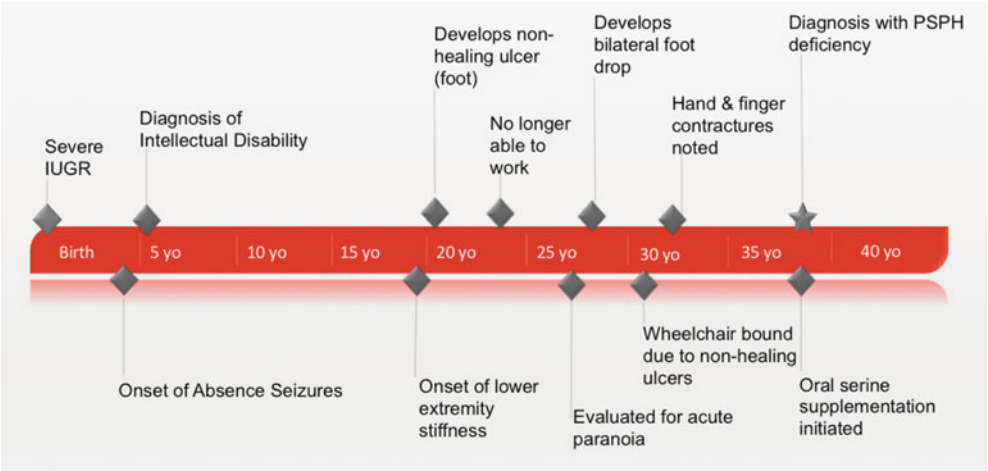

Fig. 2 Natural history timeline of one patient's experience with phosphoserine phosphatase deficiency

Fig. 3 Recent photographs (38 years old) demonstrate the patient's borderline microcephaly, anterior receding hairline, and fingertip amputations. She does not have a wide mouth as has been mentioned in two previous reports on PSPH deficiency

89 kg, BMI 40). She had a prominent widow's peak with sparse anterior hair, though this was said to be a familial trait. Upper extremities showed an increased carrying angle. Ninety-degree contractures at the distal and proximal interphalangeal (DIP, PIP) joints could be actively extended to 180°. Her hands showed bilateral muscular atrophy of the thenar eminence and intrinsic muscles as well as two left DIP joint amputations. Skin exam showed diffuse, moderately severe eczema including on her face and a right foot ulcer. Her neurologic exam was notable for an immature affect. Speech was fluent and she was able to give a limited history. Cranial nerves were intact. Strength was fully intact in bilateral proximal upper extremities and hip flexors and severely reduced in finger abduction, finger flexion, and ankle dorsiflexion. Sensory exam was notable for severely decreased temperature and vibratory sensation in a length-dependent pattern to the midleg and mid-forearm bilaterally. Deep tendon reflexes were symmetric and diffusely brisk, with the exception of Achilles tendon reflexes, which were absent. She had mild spasticity in all four extremities. There was no dysmetria. Rapid alternative movements were limited by contractures and patient understanding. The patient was able to walk short distances. Gait was antalgic, with obvious foot drop and reduced flexion in the right knee.

Her exam was concerning for a myeloneuropathy, possibly due to an inherited metabolic disorder. Electrodiagnostic study demonstrated a chronic sensory and motor axonal polyneuropathy. Brain magnetic resonance images (MRI) performed at ages 27, 32, and 38 were all normal. Glucose, vitamin B12, folate, methylmalonic acid, copper, ceruloplasmin, and zinc were all within normal range. Plasma amino acids showed a markedly low serine (31 mcmol/L, reference range 60–170) and moderately low glycine (114 mcmol/L, reference range 130–400). Other amino acids were within normal range. The patient refused lumbar puncture. In conjunction with the biochemical genetics service, we ordered sequential sequencing of 3-phoshoglycerate dehydrogenase (*PHGDH*), phosphoserine aminotransferase (*PSAT*), and phosphoserine phosphatase (*PSPH*). There were no pathogenic mutations in *PHGDH* or *PSAT*. Molecular testing revealed two novel mutations in *PSPH* (NM_004577.3): c.131T>G (p.Val44Gly) and c.421G>A (p.Gly141Ser). Val44Gly was not found in dbSNP (http://www.ncbi.nlm.nih.gov/SNP), Exome Aggregate Consortium (ExAC, http://exac.broadinstitute.org), or NHLBI Exome Sequencing Project (ESP, http://evs.gs.washington.edu/EVS) databases. Gly141Ser was not found in dbSNP. It was reported with an allele frequency of 0.02% in ESP and 0.0025% in ExAC. In silico computational tools including Align GVGD, SIFT, MutationTaster, and Polyphen2 predict Gly141Ser and Val44Gly to be pathogenic variants. Both variants are evolutionarily conserved. Direct mutational analysis in the patient's mother identified a heterozygous *PSPH*: c.131T>G (p.Val44Gly) nucleotide change. Based on our patient's phenotype, biochemical, and molecular findings, we diagnosed her with phosphoserine phosphatase deficiency. Treatment with oral serine supplementation was initiated and titrated according to plasma serine levels. She currently takes 2.5 g orally, three times a day. Laboratory-measured plasma serine levels have improved; most recent serine and glycine plasma values are 96 and 222 mcmol/L, respectively. After four months of therapeutic treatment, the patient reported improved energy levels and increased sensation in her feet. Her foot ulcer has completely healed and not recurred. She has significantly reduced the dosage of pain medication necessary for neuropathic pain control.

Discussion

Phosphoserine phosphatase deficiency has been described in just two reports, all in children (Vincent et al. 2015; Jaeken et al. 1997; Veiga-da-Cunha et al. 2004). The first described patient was an infant with a separate, unrelated diagnosis of Williams–Beuren syndrome. Apart from features typical of Williams–Beuren syndrome, he had pre- and postnatal growth deficiency, psychomotor retardation, and congenital microcephaly. He was seizure free. Serine levels in the cerebral spinal fluid (CSF) and plasma were decreased, though plasma serine normalized after meals (CSF, 18 μmol/L, control range 27–57 μmol/L; plasma, 53–80 μmol/L, normal range 70–187). The patient was started on serine supplementation at one year of life. He experienced some catch-up head growth and developmental improvements; he was lost to follow-up after age two (Jaeken et al. 1996).

A second report described seven individuals, ages 5 to 19 years, from a multiplex consanguineous Pakistani family, all homozygous for *PSPH* c.103G>A (p.Ala35Thr) pathogenic mutation (Vincent et al. 2015). All individuals presented in infancy or early childhood with severe developmental delay. All had moderate to profound intellectual disability, seizures, and hypertonia. Most had microcephaly. Plasma amino acid analysis showed low serine and moderately low glycine in individuals with reported results (serine, 26–29 μmol/L, reference 75–175 μmol/L; glycine, 102–129 μmol/L; reference 148–324 μmol/L).

Recently, a molecular study of Neu-Laxova syndrome (OMIM #256520, #616038), a typically prenatally lethal

condition characterized by profound neurodevelopmental abnormalities, found mutations in *PHGDH*, *PSAT1*, and *PSPH*. These findings suggest the most severe end of serine deficiency syndrome is incompatible with life (Acuna-Hidalgo et al. 2014). In contrast, our patient probably represents the mild end of the clinical spectrum.

PHGDH deficiency, the most common cause of serine deficiency syndrome, has been described in a single adult. *PHGDH* encodes the first enzymatic step in the serine biosynthesis pathway. Individuals with PHGDH deficiency typically present in infancy with severe neurodevelopmental abnormalities, including intractable seizures, severe intellectual disability, congenital microcephaly, and psychomotor retardation though more mild phenotypes have also been described (Jaeken et al. 1996; Tabatabaie et al. 2011). Méneret et al. describe a patient with congenital cataracts, mild psychomotor retardation, and slight cerebellar ataxia, who presented at age 31 with adult onset axonal sensorimotor polyneuropathy. He was started on serine supplementation and reported subjective improvement in his quality of life (Méneret et al. 2012).

Phosphoserine phosphatase (*PSPH*) encodes the third, final, and rate-limiting enzyme in the L-serine synthesis pathway, irreversibly hydrolyzing phosphoserine to L-serine and phosphate (Collet et al. 1997). PSPH is inhibited by L-serine, creating a pathway that is regulated by serine demand rather than supply (Collet et al. 1997). Thus, in contrast to other aminoacidopathies, there is no accumulation of a metabolite or precursor. Screening tests rely on detecting low serine concentration in CSF and/or fasting plasma (de Koning 2006). The serine level in the CSF is most clinically relevant, though invasive and not routinely available. While screening plasma amino acids is specific, sensitivity is affected by the fact that serine levels can normalize after meals (Jaeken et al. 1996). It behooves the physician with a high clinical suspicion for serine deficiency to collect the plasma samples during a fasting state and pursue CSF testing if inconclusive.

Identifying phosphoserine phosphatase deficiency in our adult patient expands the phenotype to include severe axonal neuropathy and contractures in addition to the previously described intellectual disability, epilepsy, microcephaly, and growth deficiency. This case suggests that inexpensive, basic metabolic screening can potentially identify this treatable syndrome. Fasting plasma amino acids should be considered in adult patients with atypical presentations of otherwise unexplained neuropathies and complex features, such as craniofacial deformities, concomitant myelopathy, epilepsy, and developmental delay.

Acknowledgements We would like to thank the patient and her family for their participation in this report and Dr. Angela Sun for her careful review of this manuscript.

Synopsis

This novel report of phosphoserine phosphatase deficiency in an adult expands our understanding of serine deficiency syndrome and describes an important and treatable condition for practitioners to consider when evaluating patients with unexplained metabolic neuropathy.

Compliance with Ethical Guidelines

Conflict of Interest

Heather M. Byers, Emily A. Malouf, Michael D. Weiss, Jie Feng, C. Ronald Scott, and Suman Jayadev declare that they have no conflicts of interest.

Robin L. Bennett is an author for John Wiley & Sons.

Informed Consent

This article does not contain any research studies with human or animal subjects performed by the any of the authors.

Additional informed consent for identifiable photography was obtained.

Details of the Contributions of Individual Authors

Dr. Heather Byers prepared the manuscript. Heather Byers, Robin Bennett, Emily Malouf, Michael Weiss, Jie Feng, C. Ronald Scott, and Suman Jayadev participated in the clinical care of this patient and critical review of the manuscript.

References

Acuna-Hidalgo R, Schanze D, Kariminejad A et al (2014) Neu-Laxova syndrome is a heterogeneous metabolic disorder caused by defects in enzymes of the L-serine biosynthesis pathway. Am J Hum Genet 95(3):285–93

Collet JF, Gerin I, Rider MH, Veiga-da-Cunha M, Van Schaftingen E (1997) Human L-3-phosphoserine phosphatase: sequence, expression and evidence for a phosphoenzyme intermediate. FEBS Lett 408(3):281–4

de Koning TJ (2006) Treatment with amino acids in serine deficiency disorders. J Inherit Metab Dis 29(2-3):347–51

Furuya S (2008) An essential role for de novo biosynthesis of L-serine in CNS development. Asia Pac J Clin Nutr 17(Suppl 1):312–5

Furuya S, Tabata T, Mitoma J et al (2000) L-serine and glycine serve as major astroglia-derived trophic factors for cerebellar Purkinje neurons. Proc Natl Acad Sci U S A 97(21):11528–33

Hart CE, Race V, Achouri Y et al (2007) Phosphoserine aminotransferase deficiency: a novel disorder of the serine biosynthesis pathway. Am J Hum Genet 80:931–937

Jaeken J, Detheux M, Van Maldergem L et al (1996) 3-Phosphoglycerate dehydrogenase deficiency and 3-phosphoserine phosphatase deficiency: inborn errors of serine biosynthesis. J Inherit Metab Dis 19:223–226

Jaeken J, Detheux M, Fryns JP (1997) Phosphoserine phosphatase deficiency in a patient with Williams syndrome. J Med Genet 34 (7):594–596

Méneret A, Wiame E, Marelli C, Lenglet T, Van Schaftingen E, Sedel F (2012) A serine synthesis defect presenting with a Charcot-Marie-Tooth-like polyneuropathy. Arch Neurol 69(7):908–11

Tabatabaie L, Klomp LWJ, Rubio-Gozalbo ME et al (2011) Expanding the clinical spectrum of 3-phosphoglycerate dehydrogenase deficiency. J Inherit Metab Dis 34(1):181–184

Veiga-da-Cunha M, Collet JF, Prieur B (2004) Mutations responsible for 3-phosphoserine phosphatase deficiency. Eur J Hum Genet 12 (2):163–166

Vincent JB, Jamil T, Rafiq MA et al (2015) Phosphoserine phosphatase (*PSPH*) gene mutation in an intellectual disability family from Pakistan. Clin Genet 87(3):296–8

JIMD Reports
DOI 10.1007/8904_2015_540

CASE REPORT

Erratum to: Novel Report of Phosphoserine Phosphatase Deficiency in an Adult with Myeloneuropathy and Limb Contractures

Heather M. Byers · Robin L. Bennett · Emily A. Malouf · Michael D. Weiss · Jie Feng · C. Ronald Scott · Suman Jayadev

Received: 07 August 2015 / Revised: 24 September 2015 / Accepted: 01 October 2015 / Published online: 19 February 2016

Erratum to: JIMD Reports
DOI: 10.1007/8904_2015_510

"Heather Byers is supported by NIH 5T32GM007454"

The online versions of the original chapter can be found under DOI 10.1007/8904_2015_510

H.M. Byers · R.L. Bennett · E.A. Malouf · J. Feng · C.R. Scott · S. Jayadev (✉)
Division of Medical Genetics, University of Washington Medical Center, Seattle, WA, USA
e-mail: sumie@uw.edu

M.D. Weiss · S. Jayadev
Department of Neurology, University of Washington Medical Center, Seattle, WA, USA

J. Feng · C.R. Scott
Division of Molecular Medicine, University of Washington Medical Center, Seattle, WA, USA